The electron transfers associated with the cytochrome c peroxidase of *Paracoccus denitrificans*.

Raymond Gilmour

Thesis presented for the degree of Doctor of Philosophy.
Faculty of Veterinary Medicine.
University of Edinburgh.
October 1993.

Declaration

The work presented in this thesis, is my own, unless otherwise indicated. Part of this work has been published in Gilmour, R., Goodhew, C.F., Pettigrew, G.W., Prazeres, S., Moura, I. and Moura J.J.G (1993) Biochem J. 294, 745-752, which is bound in the appendix, and Gilmour, R., Goodhew, C.F., Pettigrew, G.W., Prazeres, S., Moura, I. and Moura J.J.G (1993) Biochem J. (in press).

Raymond Gilmour.
October 1993.

Acknowledgements

I am deeply indebted to my supervisor, Dr Graham Pettigrew, for his encouragement and support over the past three years. His faith in my ability and constant enthusiasm have been, and will continue to be, a source of inspiration to me. I also wish to say thank you to Dr Celia Goodhew who has helped me with both scientific and technical problems. Her attention to detail has set me example that I hope to follow in the future. The newest member of our group, big Derm (Dermot M^{c} Ginnity) deserves a great deal of thanks for helping me both in and outwith the lab. over the past 12 months. His relaxed nature and positive outlook on life helped me enormously. I will miss the daily lunchtime ritual of swapping funny stories from our respective newspapers. Like myself, he also enjoys a nice pint of Guinness.

I would like to acknowledge Susana Praseras, Isabel Moura and Jose Moura, who invited me to work with them for a short spell in Lisbon. It was an excellent learning experience and they showed me a great deal of kindness and generosity by having me in their lab. I also thank Wilm Koppenol and Larry Hayward for their help in understanding some basic maths. Additional thanks go to Dr Paul Taylor and Dr Richard Ashley for computer programs.

I would also like to acknowledge the help of Dr David Apps for his helpful discussions throughout my PhD. Additional thanks go to Colin Warwick who has been a great help with the photography and computing. A great enthusiast who takes a keen interest in ensuring that the presentation of work is both clear and concise. Thanks also go to the secretaries for helping me with the more practical side of life, like using the fax machine! I would like to thank the lads downstairs, Jeremy, Peter, Larry, Kevin and Andy, for making coffee time good fun.

Outwith the Vet. school, my principal thanks go to my flatmates: Nick 'old man' Hocking, Stephen 'beanie' Peacock, Andy 'stan' Brickell, Ewan 'no nickname' Grant and Richard 'no hair' Jones. I thank them for all their encouragement and patience, especially during the recent months. These guys have always been there when I've needed them most and I will miss them a great deal. Additional thanks go to Debbie Eaves, Sam, and my friends from the CRAC course in Stirling.

On the home front, deepest gratitude and love goes to my mum who has supported me throughout my life. Additional thanks to my big brothers Derrick, Nick and Kevin for looking after me. I thank my very close friend Colin and his wife Alana for taking care of me whenever I am home. I also thank Colin for making me best man at his wedding. A great day. Last but certainly not least, many thanks to Marc Orr (big Orzy). A great lifelong friend with good taste in films and music.

ABSTRACT

A study of the electron transfers associated with the cytochrome c peroxidase of *Paracoccus denitrificans* has been made.The peroxidase is similar to the well-studied enzyme from *Pseudomonas aeruginosa*, although significant differences do exist. Like the *Pseudomonas* enzyme, the *Paracoccus* peroxidase contains two haem c groups, one high potential (E_m= +226mV) and one low potential ($E_m \approx$ -100mV). The high potential haem acts as a source of the second electron for hydrogen peroxide reduction and the low potential haem acts as a peroxidatic centre.

The fully oxidised form of the *Paracoccus* enzyme is inactive and does not bind added ligands. Reduction of the high potential haem (by ascorbate treatment) results in a switch of the low potential haem to a high spin state, as shown by visible and n.m.r. spectroscopy. This high spin haem of the mixed-valence enzyme is accessible to ligands and binds CN^- with a K_D of 5μM.

The *Paracoccus* enzyme is significantly different from that from *Pseudomonas* in the time course of high spin formation after reduction of the high potential haem, and in the requirement for divalent cations. Reduction with 1mM ascorbate at pH 6 is complete within 2 min and this is followed by a slow appearance of the high spin state with a half time of 10 min. This separation is also evident in e.p.r. spectra although the slow change involves an alteration in the low spin ligation at this low temperature rather than a change in spin state. The appearance of the high spin state after ascorbate-reduction is correlated with an increase in enzyme activity, suggesting that the mixed-valence, high-spin state of the enzyme is the active form.

At pH 7.5 the separation between ascorbate-reduction and spin-state change in the low potential haem is even more striking, no high spin form being obtained until 1 mM Ca^{++} is added to the mixed valence enzyme. This spectroscopic observation is also reflected in the kinetics where no enzyme activity is seen until 1mM Ca^{++} is added. The same result can be obtained at pH6 by pretreating the enzyme with EGTA prior to ascorbate-reduction. The spin state switch of the low potential haem shifts the midpoint redox potential of the high potential haem by 50mV, a further indication of

haem-haem interaction.

A comparison of the molecular weight of the enzyme under native and denaturing conditions suggests that the enzyme exists in a monomer/ dimer equilibrium. Dilution of the enzyme results in loss of some of the enzyme activity, suggesting that only the dimer is active. Reconcentration of the enzyme recovers the activity lost upon dilution. From the kinetic data, the K_D for the monomer/ dimer equilibrium is estimated at 0.6μM.

The peroxidase can receive electrons both from the acidic *Paracoccus* cytochrome c-550 and from the basic mitochondrial cytochrome c. Under conditions where the reaction is rapid, the enzyme exhibits first order kinetics with respect to mitochondrial cytochrome c, even at very high substrate concentrations. Deviation from first order is observed at slow rates with mitochondrial cytochrome c and under all conditions tested with *Paracoccus* cytochrome c550. The apparent maximal turnover of the enzyme is 62000 min^{-1} with mitochondrial cytochrome c and 85000 min^{-1} with Paracoccus c-550. The concentrations required for half-maximal activity are 3.25μM mitochondrial cytochrome c and 13μM *Paracoccus* c-550.

Although the mitochondrial and Paracoccus cytochrome donors are very different in overall charge, an examination of their crystal structures show that they both contain a high concentration of positive charge around their front face. The positive front surface in combination with a negatively charged back hemisphere gives the c-550 a large dipole moment which has been calculated as 935 Debye (compared to 342 Debye for tuna cytochrome c). This dipole moment may be important for preorientation of the cytochrome prior to its interaction with the peroxidase. Such a preorientation would allow for an increased number of fruitful collisions.

CONTENTS

Abbreviations

ATCC	American Type Culture Collection
c-550	cytochrome c-550
ccp	cytochrome c peroxidase
DAD	diaminodurol
e.p.r.	electron paramagnetic resonance spectroscopy
EGTA	Ethylene Glycol-bis-(b-aminoethyl ether)N,N,N′N′-tetraacetic acid
Eh	redox potential, mV
Em	midpoint redox potential, mV
Hepes	N-2-hydroxyethylpiperazine-N′ 2-ethanesulphonic acid
HHC	horse-heart cytochrome c
LMD	Laboratory of Microbiology, Delt
μ	dipole moment
Mes	2(-N-Morpholino)ethanesulphonic acid
n.m.r.	nuclear magnetic resonance spectroscopy
p.p.m.	parts per million
Paracoccus	*Paracoccus denitrificans*
Pseudomonas	*Pseudomonas aeuginosa*

The main aim of this project is to study the mode of action of *Paracoccus* cytochrome c peroxidase. A model is presented for the preactivation of the enzyme, a process which involves a haem-haem interaction and is dependent on divalent cations. The spectroscopic data show that the spin-state assignments for the haem groups of the *Paracoccus* enzyme are in agreement with those of Foote et al (1984) for the *Pseudomonas aeruginosa* cytochrome c peroxidase and the model proposed for the *Paracoccus* enzyme is similar to that proposed by Foote et al for the *Pseudomonas* enzyme. The electrostatic properties of the donor cytochrome, cytochrome c-550, are also investigated. The dipole moment of this protein is calculated and its possible role in ensuring fruitful collisions with the peroxidase is discussed.

CHAPTER I

INTRODUCTION

1.1 Structure and function of cytochromes c

Cytochromes c are electron transferring proteins which contain one or more covalently bound protohaem IX prosthetic groups. The covalent attachment is formed by condensation of the protohaem IX vinyl groups with two cysteine residues in the polypeptide chain. Haem attachment sites can be identified in the amino acid sequence by the motif Cys-Xaa-Yaa-Cys-His. Exceptions to this general rule can be found in some protozoan cytochromes c where a single thioether linkage is observed (for example, cytochrome c-557 of *Crithidia oncopelti* (Pettigrew, 1972)). The iron atom of the haem is normally coordinated by 5 or 6 ligands. Four of the ligands are from the 'in-plane' pyrrole ring nitrogens of the haem, with the additional, extraplanar ligands provided by the protein. The nature of the ligands from the protein determines the spectroscopic and spin-state properties of the cytochrome. An absent or weak field sixth ligand normally results in the cytochrome adopting a high-spin state (for example cytochrome c′ (Meyer & Kamen 1982). The presence of a strong field sixth ligand yields a low spin cytochrome. The properties of these two spin-states are discussed in detail in chapter 3. The cytochromes function by a reversible change in the iron oxidation state between reduced (Fe^{II}) and oxidised (Fe^{III}). One exception to this is found in the cytochrome c peroxidase of *Pseudomonas aeruginosa* where an Fe^{IV} state is observed as an intermediate in the catalytic cycle of the enzyme (Ronnberg et al 1981).

The best known cytochrome c is that found in the eukaryotic mitochondrion where it acts as a mediator between a number of soluble and membrane bound redox components (Pettigrew & Moore 1987). Although well known, this cytochrome is only one member of a large family of c-type cytochromes which can be distinguished on the basis of amino acid sequence, size, redox potential, and extraplanar haem ligands. Based on these distinguishing features, Ambler (1980), proposed a

classification system for c-type cytochromes.

Class I cytochromes c, which include the mitochondrial protein, are low-spin and have Methionyl-Histidinyl coordination. This haem coordination is characterised by a weak 695nm band in the visible spectrum of the oxidised protein (Moore & Pettigrew 1990). The haem group is attached near the N-terminal end of the protein. The midpoint redox potentials of these cytochromes c are generally high (+150 to +440mV) and so they are often found towards the oxidising end of the respiratory chain where they interact with terminal oxidases. The structure of a number of class I cytochromes are known (figure 1.1). They all have the same core structure (cytochrome fold) with any differences mainly due to the absence or presence of surface loops. Based on this size difference, the class I cytochromes c can be subdivided into large and small. Large class I cytochromes include cytochrome c-550 of *Paracoccus denitrificans* (135 amino acid residues, Timkovich et al 1976) and mitochondrial cytochromes c (103-112 residues, Moore & Pettigrew 1990). The small class I cytochromes include *Pseudomonas aeruginosa* c-551 (82 residues, Ambler 1963).

Class II cytochromes c possess a single haem c located close to the C-terminus. The mid-point oxidation-reduction potentials of these cytochromes c are in the range -10 to +150mV. The class II cytochromes are subdivided on the basis of haem spin-state. Class IIa cytochromes c are high-spin (for example cytochrome c′) and class IIb cytochromes c are low-spin (for example, cytochrome c-556). Although showing similar spectral characteristics to the class I cytochromes c, members of the class IIb can be distinguished by the red-shifted Soret and α-band of the ferrous protein.

Class III cytochromes c are characterised by having multiple haem groups with very low midpoint potentials (-100 to -300mV). The cytochromes have bishistidinyl coordination with 30-40 residues per haem. The most well-studied members of this group are the tetrahaem cytochromes c_3. These cytochromes contain 102-118 amino acids (Pettigrew & Moore 1987).

A fourth class of cytochrome c was also proposed by Ambler (1980). This group included proteins with a second prosthetic group in addition to haem c. However, an

Figure 1.1 The structure of class I cytochromes c

Ribbon drawings are shown of the structures of A. *Chlorobium limicola* cytochrome c-555, B. *Pseudomonas aeruginosa* cytochrome c-551, C. Tuna cytochrome c, D. *Rhodospirillum rubrum* cytochrome c_2, and E. *Paracoccus denitrificans* cytochrome c-550. The shaded portion of the chain of mitochondrial cytochrome c, consisting of 16 residues, is missing from the smaller cytochromes. The shaded regions of the chain of *R. rubrum* cytochrome c_2 correspond to 3- and 8-residue insertions relative to mitochondrial cytochrome c. The shaded regions in *Paracoccus* c-550 correspond to 2- and 6- residue insertions plus a 10-residue c-terminal tail. *Pseudomonas* c-551 has a single residue insertion relative to the others, indicated by the shading (reproduced from Moore & Pettigrew 1990).

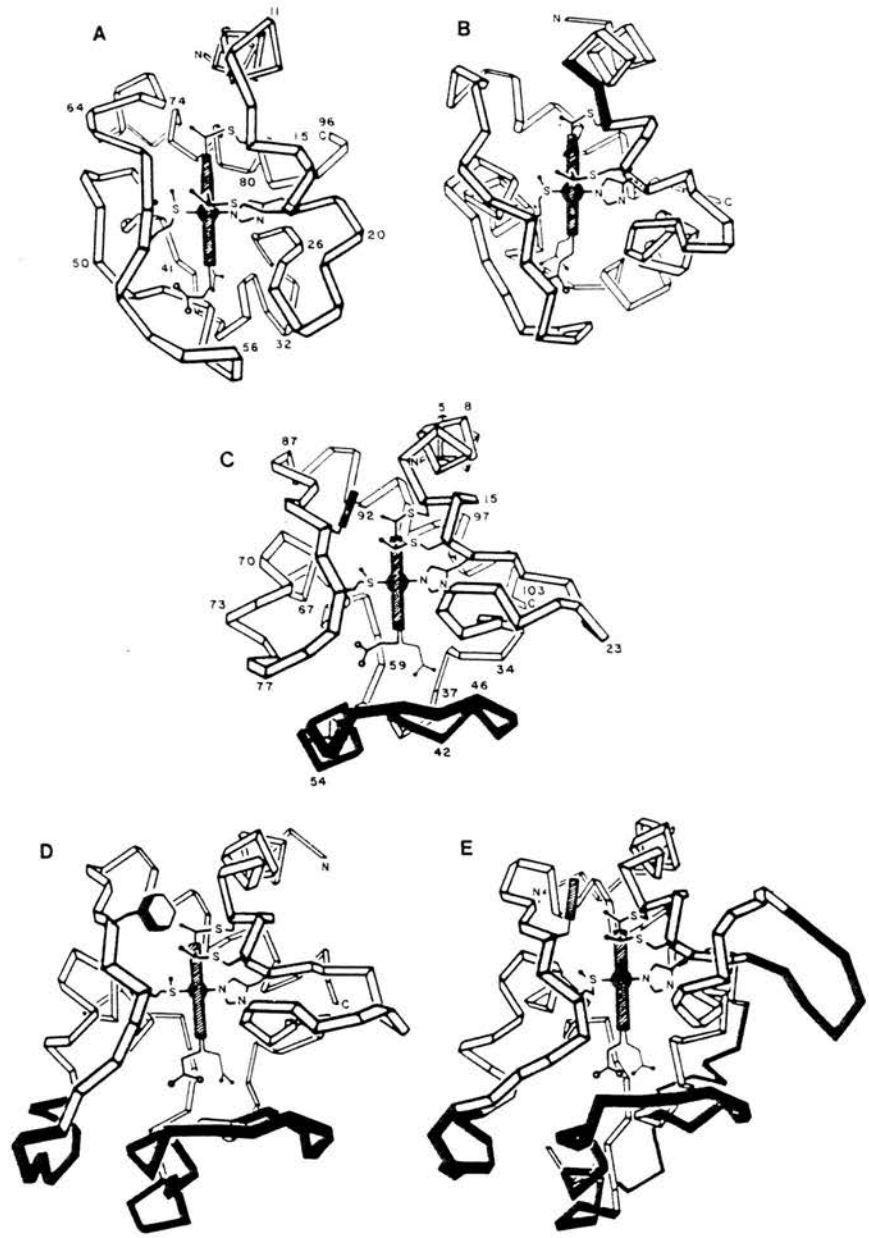
A
B
C
D
E

alternative class IV has been proposed by Pettigrew & Moore (1987). This class includes the reaction cytochrome c of *Rhodopseudomonas viridis* and structural homologues (Moore & Pettigrew 1990). A summary of the cytochrome c classification is shown in table 1.1.

Some c-type cytochromes do not fall into any of the above classes. Included in these is the bacterial cytochrome c peroxidase. This enzyme contains two haem c moieties, one high-potential and one low-potential. This enzyme will be discussed in more detail in section 1.3.2.

1.2 Electrostatic properties of mitochondrial cytochrome c

The relationship between structure and function in cytochrome c was, until recently, unclear despite a wealth of sequence information and several crystal structures. However, over the past 10-15 years, an examination of the electrostatic properties of the protein has given insight into its molecular mode of action (reviewed in Margoliash & Bosshard 1983).

Two independent approaches (kinetic and chemical) aimed at determining the site on cytochrome c which interacts with redox partners yielded very similar results. In the kinetic approach, sets of cytochromes c singly-modified at a number of specific lysine residues were prepared. Brautigan et al (1978a, 1978b) prepared and purified a number of singly modified carboxydinitrophenylated (CDNP-) cytochrome c derivatives. Although chemical isomers, ion-exchange chromatography proved successful in separating the monosubstituted derivatives. Unchanged visible spectra and only slightly altered n.m.r. spectra and redox potential (Falk, 1981) indicated that the structure of the derivatives were almost identical to the native cytochrome. In a separate study, a similar set of monosubstituted cytochromes c were prepared and purified, except in this case trifluoracetylation (TFA) and trifluoromethylphenylcarbamoylation (TFC) were used to generate the cytochrome c derivatives (Smith et al, 1977, Smith et al 1980). The modified cytochromes c were tested for their electron transfer activities with a variety of redox partners, including cytochrome oxidase (Ferguson-Miller et al, 1978, Smith et al 1977, 1980, Koppenol

Class	Features	Subdivision	Examples
I	Low spin His-Met coordination Haem near N-terminus	(a) Large	Mitochondrial cytochrome c *Paracoccus* c-550
	80-120 amino acids	(b) Small	*Pseudomonas* c-551
II	Haem near C-terminus	(a) High spin	Cytochrome c'
		(b) Low spin	Cytochrome c-556
III	Multi -haem, one haem per 30-40 amino acids Bis-histidinyl coordination	Haem content	Cytochrome c (3 haem) Cytochrome c (4 haem) Cytochrome c (8 haem)

Table 1.1 Major classes of c-type cytochromes

The three major classes of c-type cytochrome shown are based on the classification system proposed by Ambler (1980). Class IV, which includes cytochromes with prosthetic groups in addition to haem c is not shown (from Pettigrew & Moore 1987).

& Margoliash 1982), cytochrome reductase (Speck et al 1979), sulphite oxidase (Speck et al 1981) and cytochrome c peroxidase (Kang et al 1978). It was found that, irrespective of the modifying reagent involved or the redox partner used, preparations modified at one of a particular set of lysines were greatly inhibited, while substitutions at other lysines had less or no effect. This suggested that the same set of lysine residues on cytochrome c was involved in electron transfer with all redox partners tested.

Examination of the crystal structure found that the set of modified lysines which led to a major loss of electron transfer activity were all clustered around the exposed haem edge. These observations allowed maps of the interaction surface of cytochrome c to be generated. As shown in figure 1.2, the maps are all similar, irrespective of which redox partner is used in the study.

In the chemical approach an attempt was made to map the interaction surface using differential modification of lysine residues (Rieder & Bosshard 1978a, 1978b, 1980, Pettigrew 1978). In this study, the chemical reactivity of each lysine residue is compared in cytochrome c free in solution and cytochrome c in the presence of a redox partner. The surface area involved in the interaction is then deduced from the decrease in reactivity of those lysines that are shielded in the complex. This more straightforward approach yielded an interaction domain on the cytochrome c very similar to that defined by the kinetic approach.

The conclusions drawn from the above studies were that: (1) electron transfer complexes involving cytochrome c were electrostatic in nature, (2) the interaction domain on cytochrome c is very similar for each redox partner, (3) electron entry and exit occur at the same site and (4) the site of electron transfer is close to the exposed haem edge.

The group of CDNP-cytochromes c less strongly inhibited in the kinetic studies were found to be modified away from the interaction domain, i.e. at the sides and back of the protein. The reason why these modified cytochromes c should be inhibited at all only became clear after calculation of the dipole moment for the protein(Koppenol & Margoliash 1982). The asymmetric charge distribution on the protein (Dickerson 1980) results in a dipole moment of over 300 debye. Significantly,

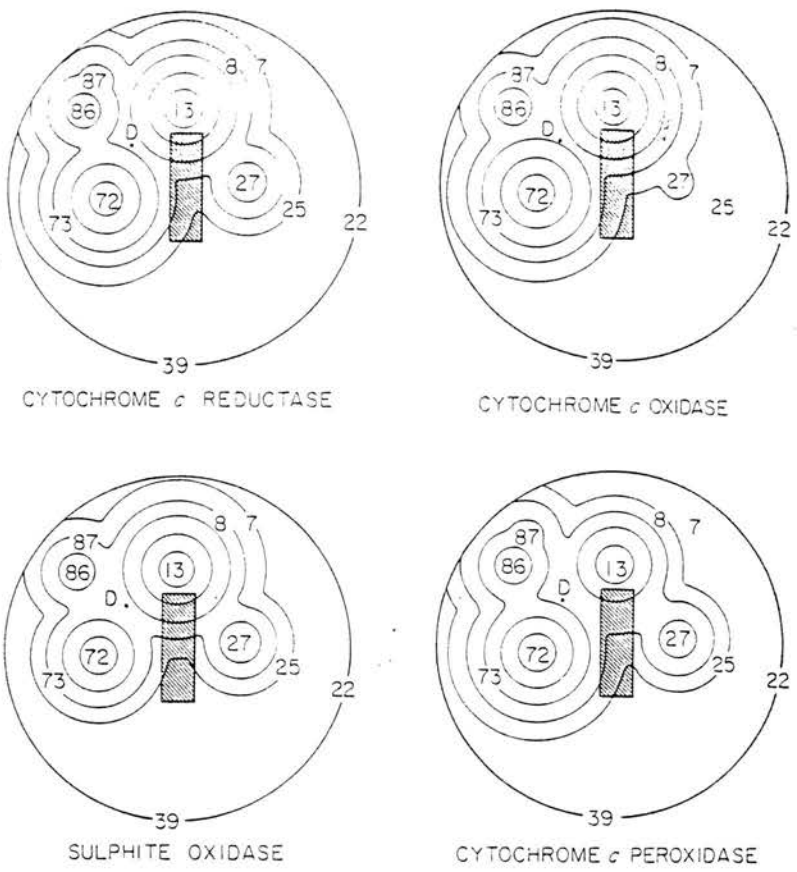

Figure 1.2 Schematic representation of the interaction surface on cytochrome c for redox partners.

The shaded rectangle represents the solvent-accessible haem edge. The number of circles around a given lysyl residue is proportional to the percentage of the inhibition of the CDNP-cytochrome c modified at that lysine which is unaccounted for by alteration in the dipole moment. The radii of these circles are multiples of an arbitrary value of 2.5Å. The numbers indicate the relative positions of the α-carbons of the residues and D is the point at which the dipole axis of the native cytochrome c crosses the protein surface (from Koppenol & Margoliash, 1982).

the positive end of the dipole axis was shown to exit the protein surface on the 'front face', close to the exposed haem edge. Koppenol & Margoliash suggested that this molecular dipole was responsible for preorientation of the cytochrome c prior to its interaction with redox partners such that the number of fruitful collisions would be increased. Examination of the CDNP-cytochromes c showed that they had modified dipole moments which had been altered through an angle θ relative to the native protein. Koppenol & Margoliash (1982) proposed that extra work (U) will be needed to rotate the abnormal dipole through the angle θ in the electric field of the redox partner (E), to achieve the orientation which allows electron transfer. This extra work will increase the activation energy, and hence decrease the rate of the reaction. Koppenol & Margoliash (1982) showed that for those cytochromes c modified away from the interaction domain, there is a linear relationship between U/E and the natural log of r (ratio of activity of modified to that of native protein) (figure 1.3). The slope of the line depends on the magnitude of the electric field such that an increase in the electric field results in an increased slope. In addition, the slope of the line gives an estimation of the electric field presented by the redox partner.

1.3 Cytochrome c peroxidases

Hydrogen peroxide is formed as a result of the incomplete reduction of oxygen (i). The toxicity of H_20_2 arises from its ability to form free radicals (ii), e.g. hydroxyl radicals, which are highly reactive and can result in cell damage or cell death (Halliwell & Gutteridge 1989). H_2O_2 may be removed by catalase in a dismutation reaction (iii) or by peroxidase in a process of reduction to water (iv).

$$O_2 + 2e^- + 2H^+ \rightarrow H_2O_2 \qquad \text{(i)}$$

$$H_2O_2 + 1e^- + 1H^+ \rightarrow {}^{\cdot}OH + H_2O \qquad \text{(ii)}$$

$$2H_2O_2 \rightarrow 2H_2O + O_2 \qquad \text{(iii)}$$

$$H_2O_2 + 2e- + 2H^+ \rightarrow 2H_2O \qquad \text{(iv)}$$

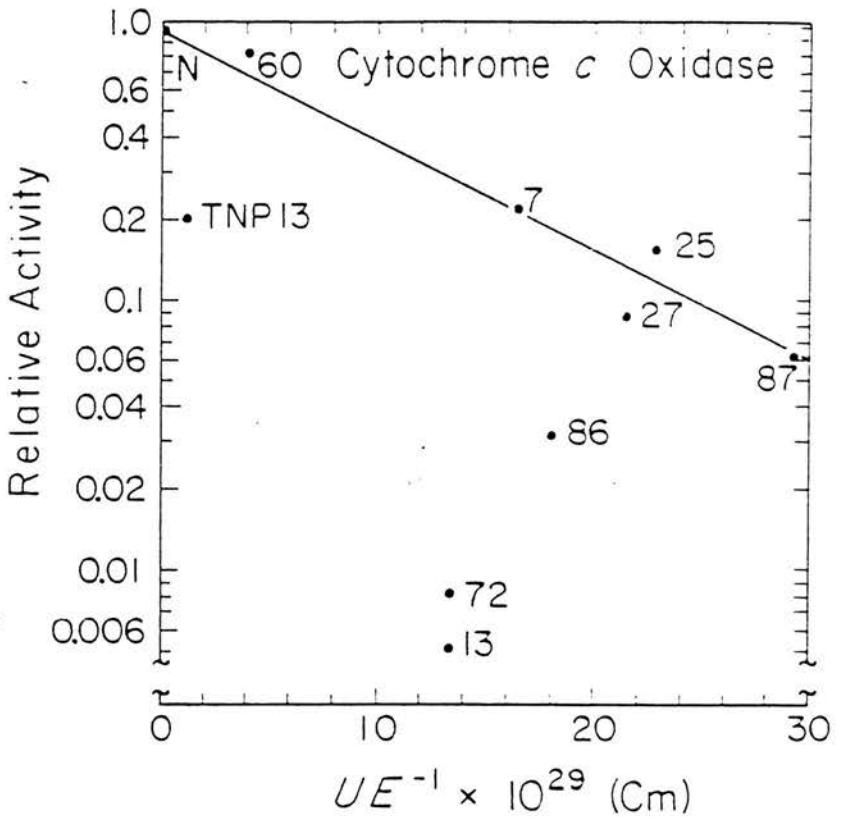

Figure 1.3 Bimolecular activities of various mono-CDNP-cytochromes c with cytochrome c oxidase.

The activities are represented as relative to native cytochrome c. The activities were determined by the stopped-flow technique. The slope represents the expected relative activities for a homogeneous field of 38.5 x 10^6 $V.m^{-1}$ (from Koppenol & Margoliash, 1982).

Cytochrome c peroxidases are enzymes which catalyse the reduction of H_2O_2 using electrons donated by cytochrome c. The two best-studied cytochrome c peroxidases are from *Saccharomyces cerevisiae* and *Pseudomonas aeruginosa*. These enzymes are discussed separately below.

1.3.1 Yeast cytochrome c peroxidase

The cytochrome c peroxidase of *Saccharomyces cerevisiae* is found exclusively in aerobically grown yeast where it is located in the mitochondrial intermembrane space (Daum et al 1982). The apoenzyme can be expressed under anaerobic conditions but oxygen is required for addition of haem to give the active enzyme. The relatively small size (35kDa) and its soluble nature have made the enzyme the focus of extensive structural, spectroscopic and kinetic studies.

The mature peroxidase contains a single, non-covalently bound protohaem IX in a polypeptide of 294 amino acid residues (Takio et al 1980, Kaput et al 1982). At room temperature the haem iron is high-spin with the sixth coordination position thought to be either unoccupied (pentacoordinated) or weakly coordinated by H_2O (hexacoordinated) (Finzel et al 1984). Hydrogen peroxide binds the b-type haem of this enzyme and removes two reducing equivalents to leave compound I which contains a ferryl (Fe^{IV}) oxene intermediate and a side chain radical (figure 1.4). Restoration of the original enzyme is achieved by two successive one electron transfers from cytochrome c. The kinetics of the peroxidation are first order with respect to ferrocytochrome c (Beetlestone 1960, Nicholls 1964). Similar first order kinetics have been observed for cytochrome oxidase and have been interpreted as due to product inhibition in which $K_I = K_m$ (Smith and Conrad 1956, Minnaert 1961). The complex formed between cytochrome c and the peroxidase is electrostatic and can be disrupted by high salt concentrations.

1.3.2 Bacterial cytochrome c peroxidases

The most extensively studied bacterial cytochrome c peroxidase is that from

(a) *Saccharomyces cerevisiae* cytochrome c peroxidase

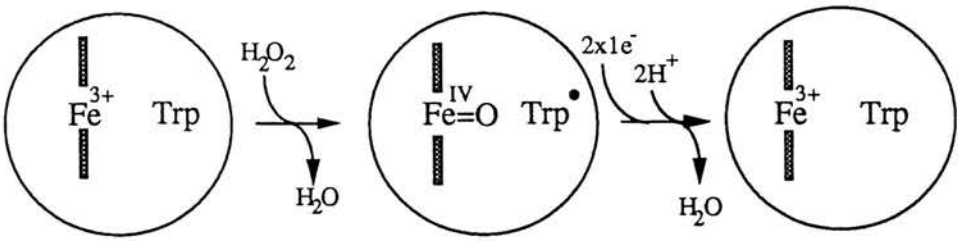

(b) *Pseudomonas aeruginosa* cytochrome c peroxidase

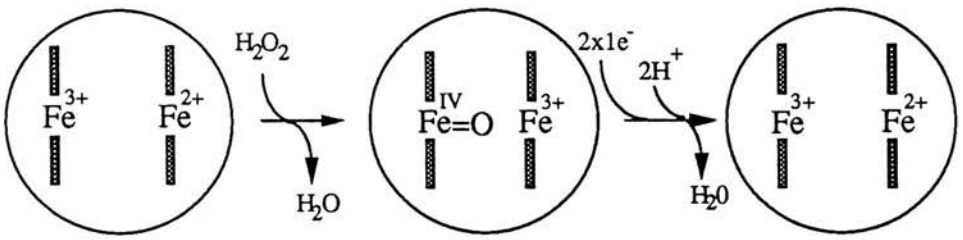

Figure 1.4 Reaction mechanisms of cytochrome c peroxidases

The reaction mechanisms for the eukaryotic (yeast, (a)) and prokaryotic (*Pseudomonas aeruginosa*, (b)) cytochrome c peroxidases are shown. The models are based on the findings of various workers, as reviewed in Pettigrew & Moore (1987). The yeast enzyme contains a single b-type haem. The side chain radical observed in the reaction intermediate is thought to be tryptophan 191 (reviewed in Bosshard 1991).The bacterial enzyme contains two c-type haems which differ in redox potential and protein ligands (see text).

Pseudomonas aeruginosa. Localisation of this enzyme within the organism has not been possible due to difficulties in spheroplasting (Goodhew & Pettigrew, unpublished results). However, by comparison with the peroxidase from *Pseudomonas stutzeri*, and c-type cytochromes in general, the enzyme is probably periplasmic in location. Expression is induced under growth conditions in which oxygen is limiting (Lenhoff & Kaplan 1956). This indicates that either more hydrogen peroxide is present under such conditions, or more likely, that some cellular constituents which only appear at low oxygen tension are highly susceptible to peroxide-induced damage. Estimations of the molecular weight of the protein have led to conflicting results. The native enzyme has been estimated at 54kDa (Ellfolk & Soininen 1971) and 77kDa (Singh & Wharton 1973), however, the amino acid sequence indicates a molecular weight of approx. 34kDa (Ronnberg et al 1989). These discrepancies probably result from the existence of a rapid monomer/dimer equilibrium.

The amino acid sequence of this protein is known, but the x-ray structure remains to be solved. The enzyme contains two haem c moieties covalently attached to a single polypeptide chain. The properties of the two haems are different with the mid-point oxidation-reduction potentials being +320mV and -330mV (Ellfolk et al, 1983). The higher potential haem acts as an electron transferring pole and can be reduced physiologically by cytochrome c-551 or azurin and non-physiologically by ascorbate. The low potential haem acts as the peroxidatic centre. The fully oxidised enzyme is unable to bind added ligands and only slowly reacts with hydrogen peroxide (Araiso et al 1980, Ronnberg et al 1981, Ellfolk et al 1984(b)). In contrast, the low-potential haem of the mixed valence enzyme will readily bind added ligands such as CN^- (Ellfolk et al 1984(b)). It is apparent that a communication exists between the two haems of this enzyme whereby reduction of the high potential haem results in the low potential haem adopting a more open conformation, available for ligand binding.

Binding of hydrogen peroxide to the active enzyme removes two reducing equivalents from the enzyme to leave the intermediate compound I (figure 1.4). This state is analogous to the compound I observed spectroscopically in other peroxidases

(Ronnberg et al 1981). In this intermediate form, one electron has been removed from the peroxidatic iron to leave a ferryl oxene derivative. The second electron is removed from the high potential haem. Restoration of the original enzyme is achieved by two successive one electron transfers into the high-potential haem. The activity of the enzyme is inhibited by high salt concentrations (Soininen & Ellfolk 1972). This is consistent with an electrostatic stabilisation of the complex between the donor and the enzyme.

Various spectroscopic studies have shown the low potential haem of the *Pseudomonas aeruginosa* peroxidase to be high spin in the mixed valence enzyme (Ellfolk et al. 1983, Ellfolk et al. 1984a, Ronnberg et al. 1980, Ellfolk et al. 1984b). Ellfolk and co-workers concluded that this haem was also high-spin in the fully oxidised enzyme (Ronnberg et al 1980, Ellfolk et al 1984b). Similarly, a study of the spin-states of a cytochrome c peroxidase from *Pseudomonas stutzeri* led Villalain and co-workers to assign the high-spin signal to the low-potential haem in both the fully oxidised and ascorbate-reduced enzyme (Villalain et al. 1984). In contrast, Foote and co-workers, using m.c.d. spectroscopy, proposed that the high spin signal of the fully oxidised enzyme of the *Pseudomonas aeruginosa* peroxidase was due to a labile methionine coordination of the high potential haem (Foote et al. 1984, Foote et al. 1985). The high spin states of both the fully oxidised and mixed-valence enzymes are temperature-dependent and convert to low spin at the very low temperatures used in e.p.r. spectroscopy (Ellfolk et al 1983).

The high-potential haem of the *Pseudomonas* peroxidase is located in the C-terminal region of the protein. This region shows faint similarity (26% identity) to *Pseudomonas aeruginosa* cytochrome c-551 and this area may form a class I domain (Ambler 1980) with a Cys-X-Y-Cys- His haem binding site and extraplanar iron coordination by His-181 and Met-254 (Ronnberg 1987b, Ronnberg et al 1989). The peroxidatic haem resides in the N-terminal part of the protein and is coordinated proximally by His-55 (Ronnberg 1987a). Ronnberg et al (1989) have proposed that His-240 is the distal ligand of the peroxidatic haem which controls the access of ligands to the haem group. The close proximity of Met-254 to His-240 may provide the link through which the high potential haem is able to alter the structure around the

low potential haem.

Recently a cytochrome c peroxidase was identified in cells of *Paracoccus denitrificans* grown under low oxygen tension (Goodhew et al 1990). The enzyme was localised to the periplasmic compartment of the bacterium, a result consistent with the proposal of Wood (1983) that soluble c-type cytochromes are periplasmic in location. The spectrum of this enzyme closely resembled that from *Pseudomonas aeruginosa* i.e. Soret bands that do not cross at the Soret (oxidised) maximum, an α-peak at 555-557nm with a shoulder at the short wavelength side, and the presence of a weak absorbance band at 630nm in the oxidised enzyme (Goodhew et al 1990). These spectral features are also observed in the cytochrome c peroxidase from *Pseudomonas stutzeri* (Villalain et al 1984). The specificity of the *Paracoccus* peroxidase for electron donors was studied (Goodhew et al 1990). The enzyme was shown to react well with both acidic *Paracoccus* cytochrome c-550 and basic mitochondrial cytochrome c. However, it was shown to react poorly with acidic *Pseudomonas* cytochrome c-551. This apparent anomaly was later resolved (Pettigrew 1991) after comparison of the mitochondrial and *Paracoccus* cytochrome c (c-550) crystal structures. This comparison showed that although acidic overall, the c-550 had a cluster of positive charge on the 'front face', close to the exposed haem edge. This same cluster of positive charge is also found on the mitochondrial cytochrome c.

1.4 The electron transport chain of *Paracoccus denitrificans*

Paracoccus denitrificans is a coccoid, non-motile bacterium found in soil, sewage or sludge (Nokhal & Schlegal 1983). The organism is gram negative and therefore contains a periplasmic compartment lying between an inner and outer membrane (figure 1.5). In recent years an increasing number of proteins involved in cellular respiration have been localised to this compartment (Anthony 1988). The periplasmic contents can be selectively released from this bacterium by spheroplast formation as described in chapter 2. This bacterium has received much attention over the past twenty years or so for two reasons: its close resemblance to the eukaryotic mitochondria and its great nutritional adaptability.

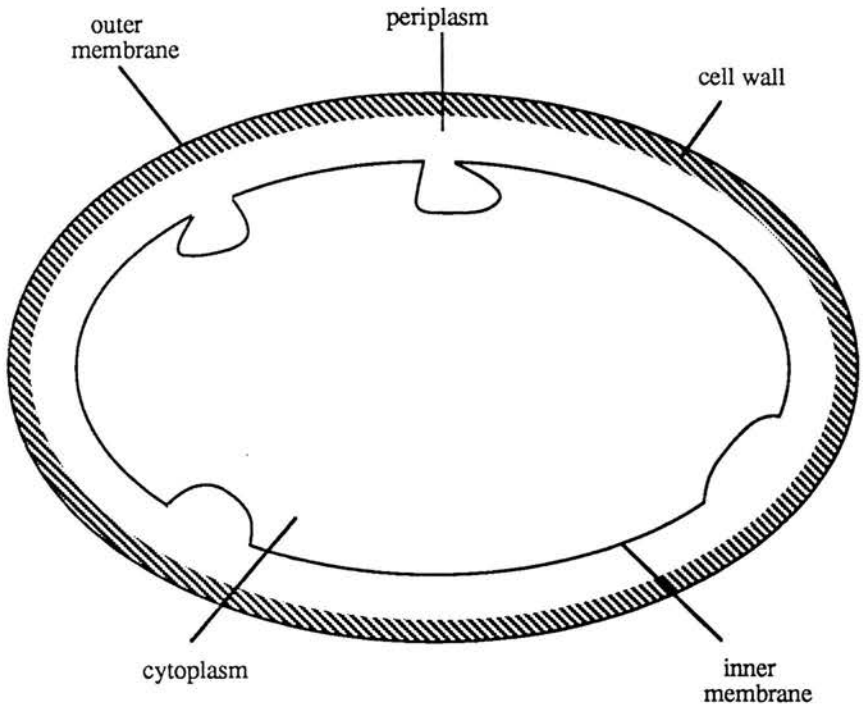

Figure 1.5 Structure of a gram negative bacterium

Gram negative bacteria contain a periplasmic compartment situated between the outer membrane and the inner (plasma) membrane. The cell wall is denoted by hatching and consists largely of peptidoglycan.

Paracoccus denitrificans is an extremely versatile bacterium which can grow and adapt to a wide variety of environmental conditions. The bacterium can grow on a variety of sugars, amino acids and alcohols as sole carbon and energy sources (van Verseveld & Stouthamer 1991). This heterotrophic growth can occur both aerobically and anaerobically. In addition, the bacterium can also grow methylotrophically with methanol, methylamine, formaldehyde or formate as the sole sources of carbon and energy (Anthony 1992). The adaptation to growth under these differing conditions is reflected in the composition of the electron transfer chain (for example, figures 1.6 and 1.7).

As shown in figure 1.6, electron transport during aerobic heterotrophic growth proceeds from NADH and succinate dehydrogenases through the bc_1 complex, to the aa_3-type cytochrome oxidase. It is doubtful whether the soluble c-550 plays a role in electron transfer between complexes III and IV since deletion of the gene encoding the protein has little effect on the growth capacity of the enzyme under these conditions (van Spanning et al, 1990). In addition, a membrane-bound cytochrome c-552 has been shown to successfully mediate electron transfer between the bc_1 complex and cytochrome oxidase (Berry & Trumpower 1985).

Anaerobic growth on heterotrophic substrates is possible if alternative electron acceptors such as nitrate, nitrite, nitrous oxide or nitric oxide are present (Stouthamer 1980) (figure 1.7). The nitrite formed in the cytoplasm by the action of nitrate reductase is transported across the plasma membrane where it is eventually reduced to nitrogen gas. As with aerobic growth on heterotrophic substrates, the role of c-550 in this process is in doubt after it was shown that mutant strains lacking the cytochrome had growth characteristics similar to that of the wild type strain (van Spanning et al 1990).

Paracoccus can also grow methylotrophically on the C_1 compounds methanol and methylamine (Anthony, 1992). Growth on methanol requires the presence of methanotrophes which release methanol as an intermediate in methane oxidation (Pettigrew & Moore 1987). Growth on methanol induces expression of methanol dehydrogenase and cytochrome c-551i, both of which are found in the periplasm (Anthony 1992). Methanol dehydrogenase oxidises methylamine to ammonia and

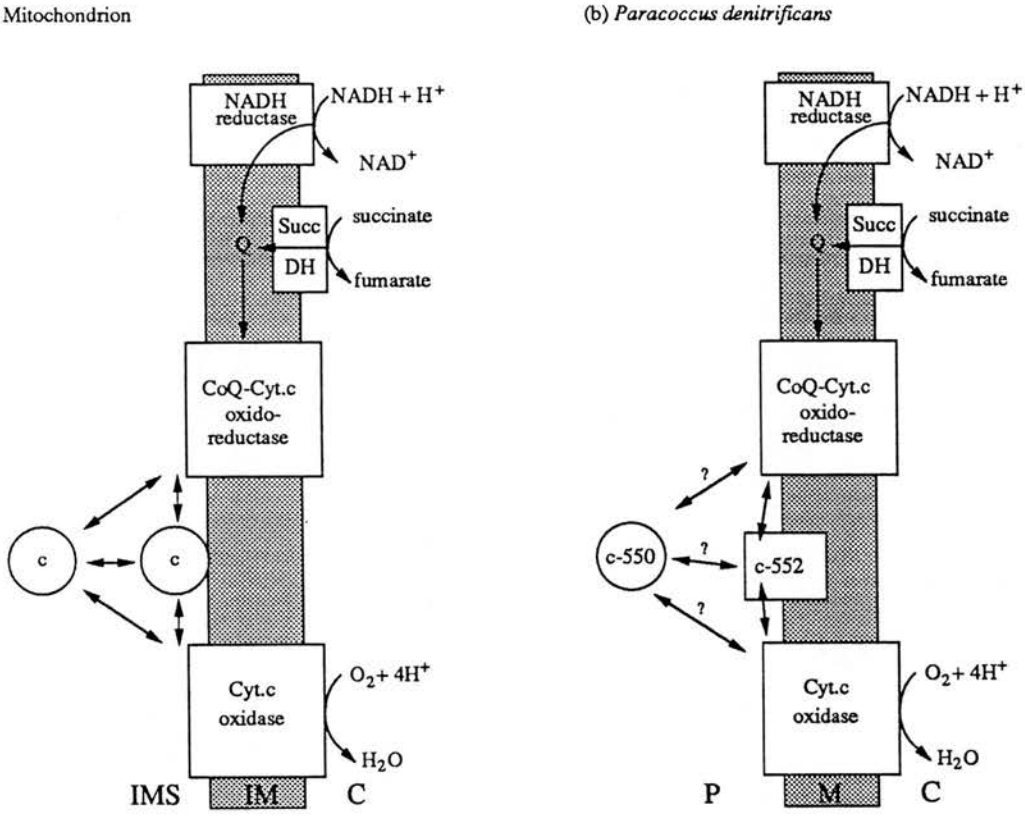

Figure 1.6 Respiratory chain of mitochondria and aerobic *Paracoccus denitrificans*

The electron transport chain of *Paracoccus denitrificans* grown aerobically on heterotrophic substrates is similar to the electron transport chain of the eukaryotic mitochondrion. Differences exist in the composition of the individual electron transport complexes, for example, the mitochondrial cytochrome c oxidase contains 13 subunits (Kadenbach et al 1983), whereas the Paracoccus enzyme contains only 3 subunits (Haltia et al 1988). The other major difference is in the electron transfer between the cytochrome c reductase and the cytochrome c oxidase. In mitochondria, this transfer is mediated by the soluble cytochrome c, however, in *Paracoccus* it is probably mediated by the membrane-bound cytochrome c-552 (Berry & Trumpower, 1985).

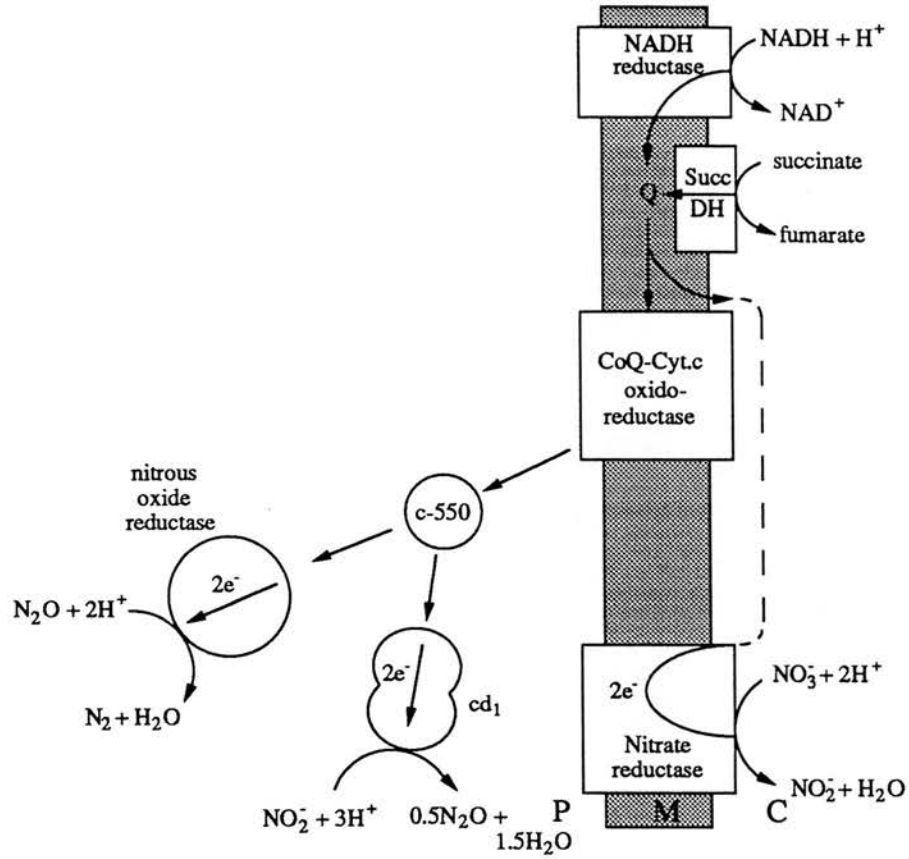

Figure 1.7 Denitrification by *Paracoccus denitrificans*

Paracoccus denitrificans synthesises alternative electron transport components when grown anaerobically in the presence of nitrate than when grown aerobically (figure 1.6). In *Paracoccus*, both NO_2^- and N_2O reduction occur at the level of cytochrome c, while NO_3^- reduction occurs at the level of coenzyme Q, independent of cytochrome c. The broken line connecting Q and nitrate reductase (Na_R) is a redox connection within the membrane.

formaldehyde and the electrons released are passed to cytochrome c-551i (Long & Anthony 1991). There appears to be no role for cytochrome c-550 in this pathway after deletion of the gene for the protein was shown to have no effect on the growth of the bacterium on methanol (van Spanning et al 1991).

Methylamine is a nitrogenous excretion product of plants and animals. Growth on this substrate requires expression of the periplasmic proteins methylamine dehydrogenase and amicyanin (Anthony 1992). Methylamine dehydrogenase oxidises methylamine to ammonia and formaldehyde with transfer of electrons to amicyanin. Amicyanin then transfers the electrons to the terminal oxidase (Husain & Davidson 1987, Gray et al 1988). As with the above growth conditions, the involvement of c-550 is in doubt since the gene can be deleted with no apparent effect (van Spanning et al 1991).

The variety of cytochromes c capable of being expressed by *Paracoccus denitrificans* was demonstrated by Bosma et al (1987). These workers studied the cytochrome c content of the periplasmic compartment from *Paracoccus denitrificans* grown under a variety of conditions. Their results indicated that different sets of c-type cytochromes were expressed depending on growth conditions. The only c-type cytochrome found to be expressed under all conditions was cytochrome c-550. The structure and function of this cytochrome forms part of the study presented in this thesis. When grown under O_2-limiting conditions, a c-type cytochrome of 45kDa was observed. This protein probably corresponds to the 45kDa cytochrome c peroxidase later identified in this organism grown under similar conditions (Goodhew et al, 1990).

When grown aerobically on heterotrophic substrates, the organisation of the respiratory chain of *Paracoccus* closely resembles that of the mitochondrion (figure 1.6). Both contain a nicotinamide nucleotide transhydrogenase, NADH and succinate dehydrogenases, iron-sulphur proteins, ubiquinone- 10, a cytochrome bc_1 complex, a small, soluble, cytochrome c and an aa_3- type cytochrome oxidase (John & Whatley 1977, van Spanning 1991). In addition, the respiratory chains of the mitochondrion and the bacterium are inhibited by a similar range of compounds including CN^-,

antimycin, and rotenone. This high level of similarity has led to suggestions that *Paracoccus denitrificans* represents the free-living ancestor of the eukaryotic mitochondrion (John & Whatley 1975). It has been proposed that the prokaryote was taken up by a protoeukaryote and during the course of its evolution its metabolism became integrated with that of the host (figure 1.8). The result of this endosymbiotic relationship would be loss of the adaptive components of the prokaryotic metabolism with retention of those components which allowed aerobic growth on heterotrophic substrates.

A comparison of the electron transfer components of three gram negative bacteria are shown in table 1.2. It will be shown in this thesis that although the electron transfer chains of *Paracoccus denitrificans* and *Pseudomonas aeruginosa* are somewhat different, the cytochrome c peroxidases in the two bacteria are similar in terms of both sequence (chapter VI) and overall mechanism (chapters II and VI).

	[a]*Ps. aeruginosa*	[b]*Pa. denitrificans*	[c]*Rb. capsulata*
Cytochrome c_8	+		
Cytochrome c_5	+		
Cytochrome c_4	+		
Cytochrome c_2		+	+
Cytochrome c_1		+	+
Cytochrome c′		+	+
Cytochrome c peroxidase	+	+	+
Cytochrome oxidases	baa_3 o	aa_3 o	aa_3 o
Azurin	+		
Amicyanin		+	
Nitrate reductase	cyt. b		

Table 1.2 Electron Transfer proteins in Three Gram -ve Bacteria

[a]*Pseudomonas aeruginosa*

[b]*Paracoccus denitrificans*

[c]*Rhodobacter capsulatus*

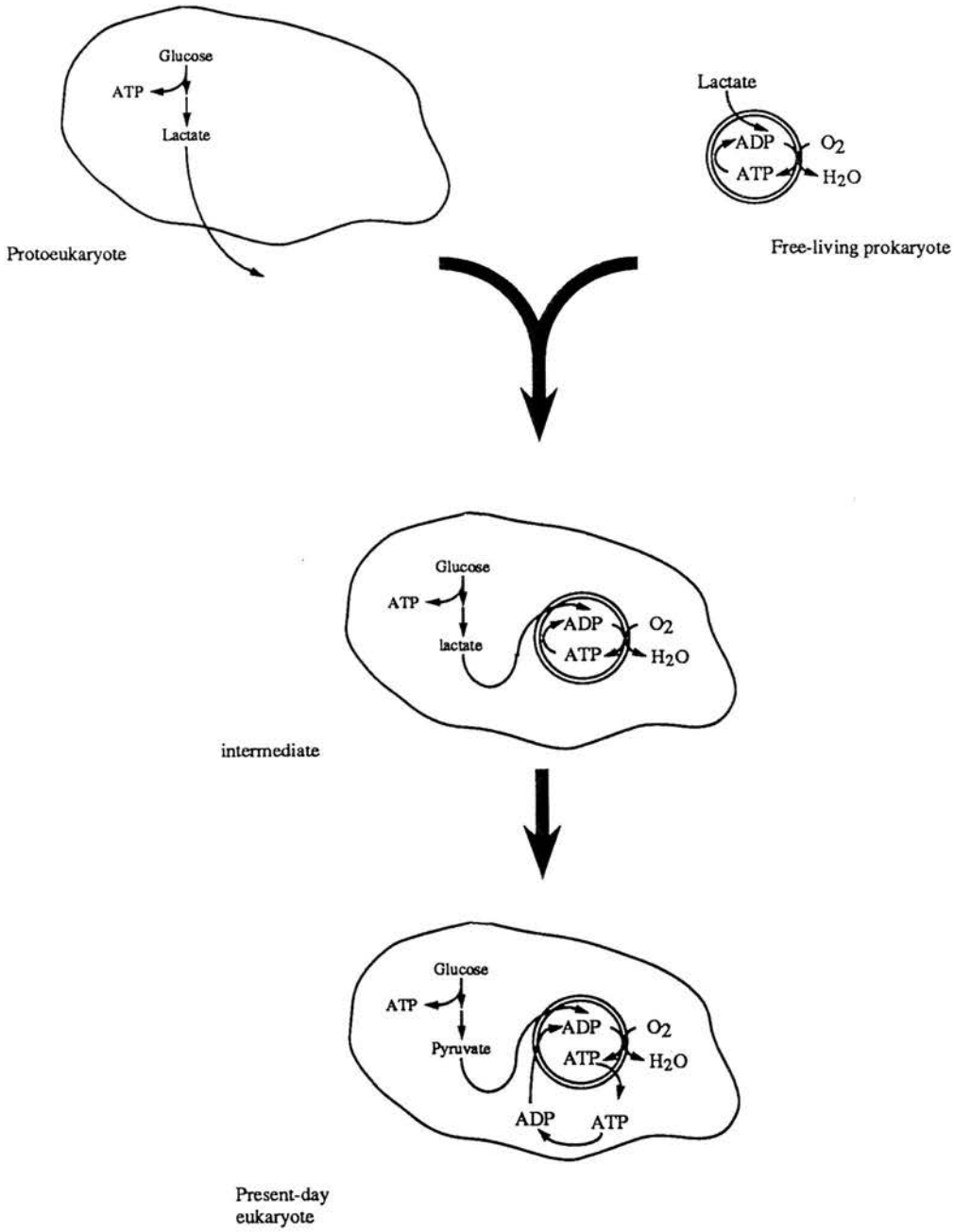

Figure 1.8 Evolution of the mitochondrion.

A hypothetical evolutionary transition from a free-living aerobic bacterium to a mitochondrion is shown. A fermenting protoeukaryote takes up a respiring bacterium to the advantage of both partners. The intermediate form is sometimes referred to as the 'pelomyxa stage', in which the free-living prokaryote is only partially integrated and may still be lost. By the acquisition of an adenine nucleotide carrier the ATP synthesising potential of the bacterium is made available to the host cell.

CHAPTER II

MATERIALS AND METHODS

2.1 Growth of cells

Paracoccus denitrificans strain LMD 52.44 was a generous gift from Professor R.P. Ambler, University of Edinburgh. The cells were grown by the method of Goodhew et al (1990), as described below. The organisms were maintained on nutrient agar plates. The plates contained 1% peptone, 1% NaCl, 0.5% yeast extract and 1.5% agar. The bacteria were grown aerobically in liquid medium containing sodium succinate (13.5 g/l), KH_2PO_4 (4 g/l), K_2HPO_4 (6 g/l), $MgSO_4$ (0.2 g/l), $CaCl_2$ (0.04 g/l), sodium molybdate (0.15 g/l), $MnSO_4$ (0.001 g/l) NH_4Cl (1.6 g/l). $FeSO_4.7H_20$ (0.005 g/l) was added from a stock solution (1.1 g/litre in 5mM citric acid). Cells were grown up from the agar plates in steps of 10ml $\rightarrow$ 100ml $\rightarrow$ 1000ml. At each step, cells were grown for 1-2 days in a Denley orbital shaker at 30°C. After growth at 1000ml, the cells were then transferred to a 10 litre volume in a New Brunswick microfermenter. During growth in the microfermenter (3 days, 30°C), the cells were sparged with air (2 litres/min). Cells were harvested at A_{600} 1.0 -1.5 in an Alfa-Laval centrifuge, then washed with 5 vol. of 10mM sodium phosphate buffer, pH 7 to remove growth media. Washed cells were then spun down (8000g for 20min), resuspended at 1 gram wet weight cells per ml 10mM sodium phosphate pH 7 and stored frozen. Cells stored in this way remained intact as judged by minimal release of cytoplasmic contents during spheroplast formation.

2.2 Purification of cytochromes

Cytochrome c peroxidase and cytochrome c-550 were purified from periplasmic extracts of the *Paracoccus* cells obtained after spheroplast formation. A flow diagram of the purification of each cytochrome is shown in figure 2.1. The purification of the

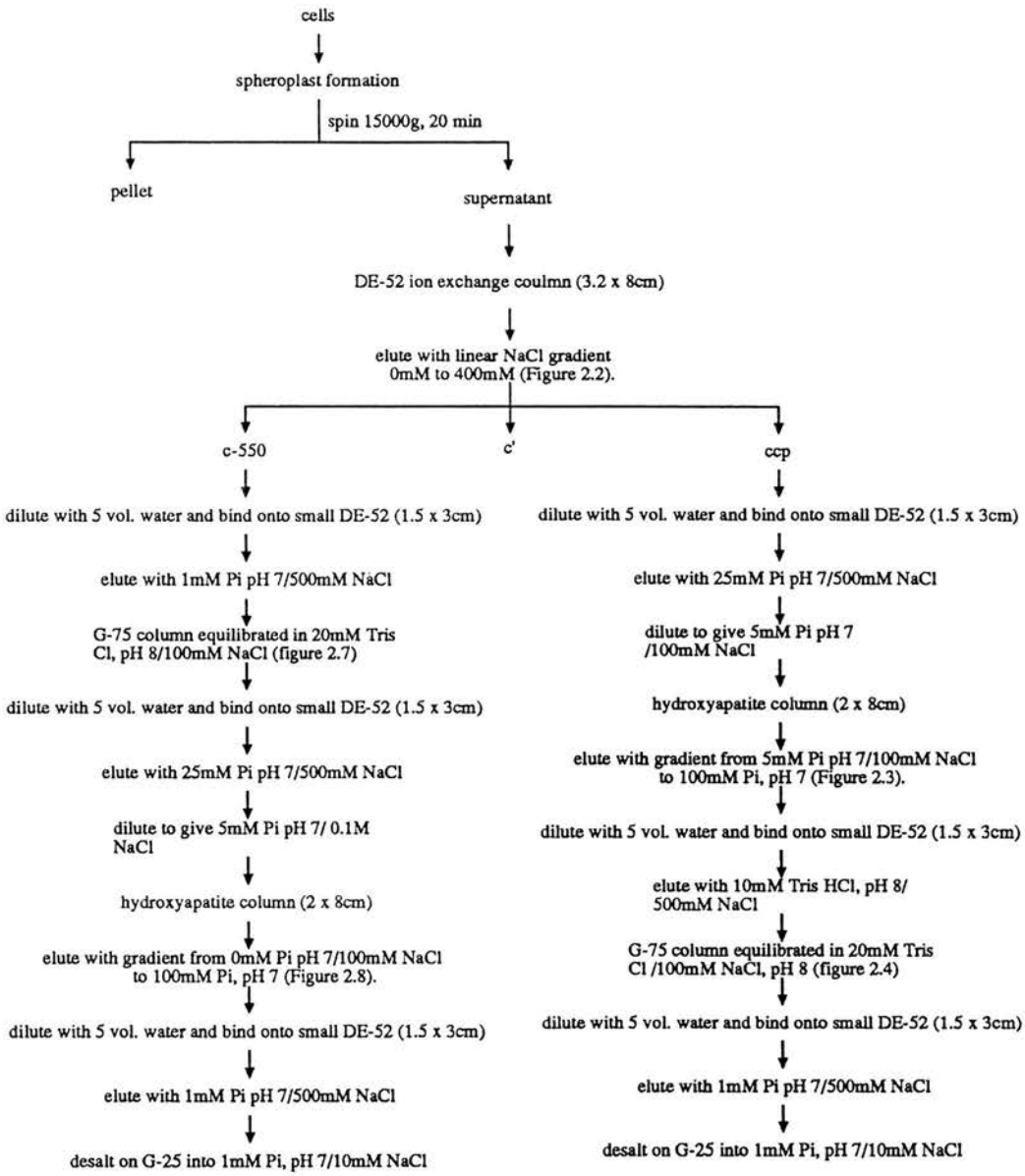

Figure 2.1 Purification of *Paracoccus* cytochromes c peroxidase and c-550.

A summary of the steps involved in the purification cytochromes c-550 and c peroxidase from *Paracoccus denitrificans* is shown.

peroxidase has previously been described (Goodhew et al (1990)).

For spheroplast formation, 1ml cell suspension was mixed with 2.5ml M sucrose, 0.2ml M tris HCl, pH 8, 0.2ml 0.1M EDTA, and 0.6ml 4mg/ ml lysozyme. This mixture was diluted by addition of 5ml of H_2O over a two minute period. Following addition of H_2O, 0.5ml $MgCl_2$ was added. The final concentrations in the spheroplast medium were : 0.25M sucrose, 20mM tris/ HCl. pH 8, 2mM EDTA, and 5mM $MgCl_2$. The cells were incubated in this solution for 30 min at 30°C before being spun down at 15000g for 15 min. The pink supernatant contains the periplasmic extract and outer membrane fragments. The pellet contains the spheroplasts.

After spheroplast formation , the periplasmic extract was applied to a DE-52 ion-exchange column (3.2 x 8cm). A linear salt gradient separated the 3 periplasmic c-type cytochromes (figure 2.2), with c-550 eluting at 190mM NaCl, c′ at 240mM NaCl, and the peroxidase at 300mM NaCl.

Peroxidase-containing fractions were pooled, diluted by 5 volumes of H_2O and adsorbed onto a small DE-52 column (1.5 x 3cm). After stripping with 25mM Pi, pH 7/0.5M NaCl, the sample was diluted to give 5mM Pi, pH 7/ 0.1M NaCl. The desalted material was then adsorbed onto a hydroxyapatite column (2 x 8cm) equilibrated in the same buffer and eluted by a linear gradient from 5mM Pi, pH 7/100mM NaCl to 100mM Pi, pH 7 (figure 2.3). Fractions containing the peroxidase were diluted by 5 vol of H_2O and re-adsorbed onto a small DE-52 column (1.5 x 3cm) and eluted with 10mM tris/HCl, pH 8, containing 500mM NaCl. The peroxidase was then applied to a G-75 molecular exclusion column (2.5 x 82cm) equilibrated in 20mM tris/HCl, pH 8 and 100mM NaCl (figure 2.4). Fractions containing pure peroxidase (as determined by SDS-PAGE) were pooled, diluted by 5 vol. of H_2O and concentrated on a small DE-52 column (1.5 x 3cm). After stripping with 1mM Pi, pH 7/0.5M NaCl, the peroxidase was desalted on G-25 into 1mM Pi, pH 7/10mM NaCl. The pure enzyme was dispensed into equal volumes in eppendorf tubes and stored at -40°C. A gel of the enzyme at each stage of the purification is shown in figure 2.5. A u.v.-visible spectrum is shown in figure 2.6.

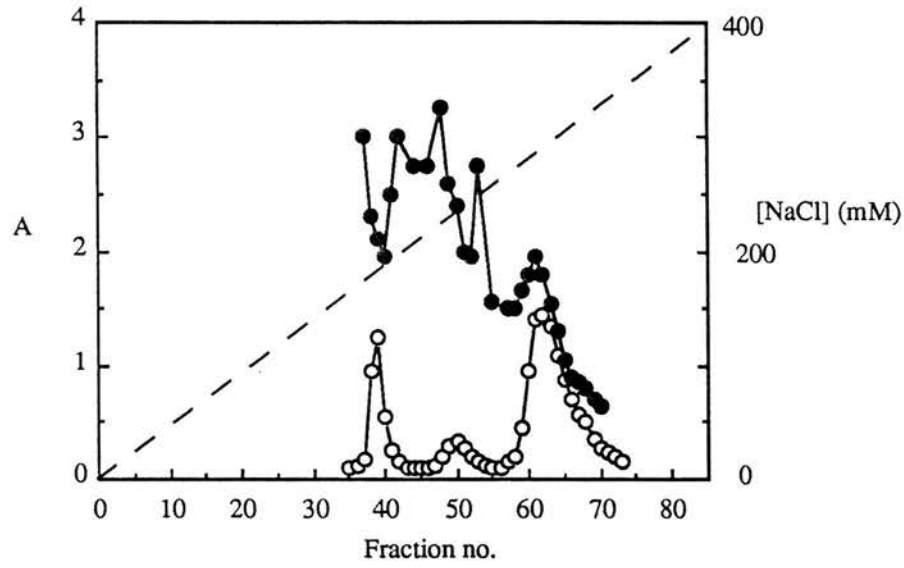

Figure 2.2 Purification of periplasmic cytochromes - Ion-exchange chromatography

A periplasmic extract was obtained as described in the text. This extract was applied to a DE-52 ion-exchange column equilibrated in 10mM tris/HCl, pH 8. Proteins were eluted using a linear salt gradient from 10mM tris/ HCl, pH 8 to 10mM tris/HCl, pH 8 and 400mM NaCl. Fractions were assayed for cytochrome content at 410nm (O-O) and protein content at 280nm (●-●).

Figure 2.3 Purification of cytochrome c peroxidase - Chromatography on hydroxyapatite

Peroxidase was prepared for hydroxyapatite as described in the text. The column was equilibrated in 5mM Pi, pH 7/ 100mM NaCl. Proteins were eluted from the column with a linear gradient from 5mM Pi, pH 7/ 100mM NaCl to 100mM Pi. Fractions were assayed for absorbance at 410nm (O-O) and 280nm (●-●).

Figure 2.4 Purification of cytochrome c peroxidase - Molecular exclusion chromatography

Cytochrome c peroxidase was prepared for gel filtration as described in text. The column was run in 20mM tris HCl, pH 8/0.1M NaCl. Fractions were assayed for absorbance at 410nm (O-O) and 280nm (●-●).

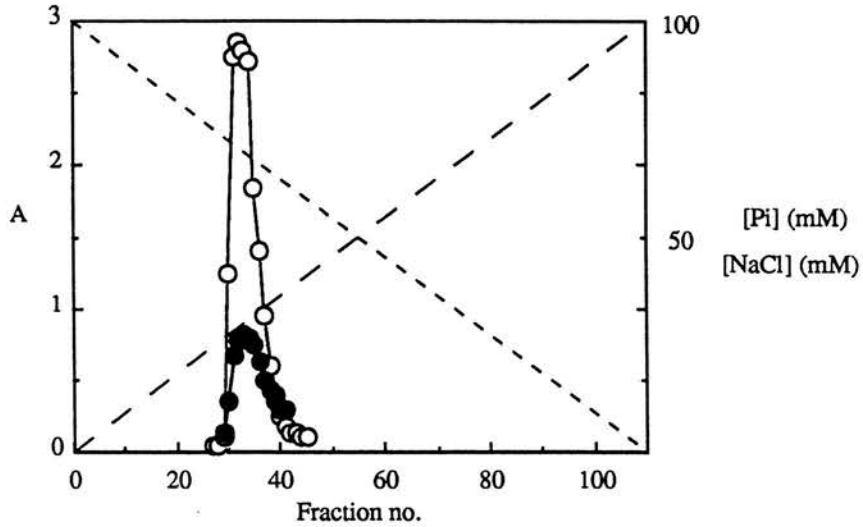
3
2
1
0
A
100
50
[Pi] (mM)
[NaCl] (mM)
0
20
40
60
80
100
Fraction no.

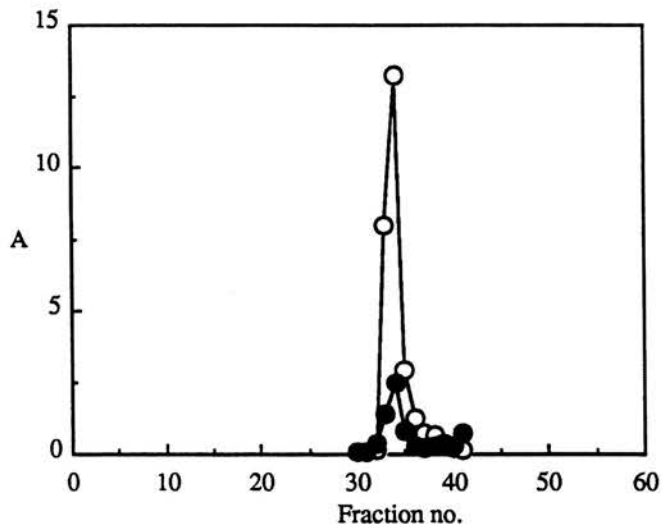
15
10
5
0
A
0
10
20
30
40
50
60
Fraction no.

Figure 2.5 Purification profile of cytochrome c peroxidase.

Samples after each stage of purification were taken for analysis by SDS-PAGE. The two periplasmic extracts shown (Pa, Pb) were combined for application onto DE-52 ion-exchange column. Apart from the periplasmic extracts (30µl), 1nmol of peroxidase was applied to the gel, as determined from visible spectroscopy. Samples were prepared for SDS-PAGE as described in Materials & Methods. The protein standards shown (lane S) are bovine serum albumin (BSA, 67000), ovalbumin (45000), carbonic anhydrase (29000), myoglobin (17000), and cytochrome c (12000). The gel was run at 180V for 4 hours and then stained with Coomassie blue.

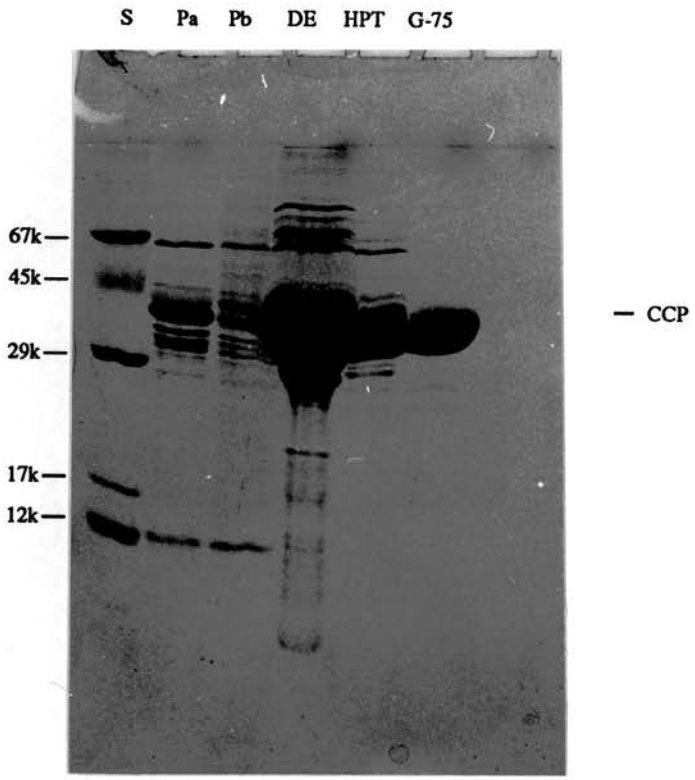
S
Pa
Pb
DE
HPT
G-75
67k
45k
29k
17k
12k
CCP

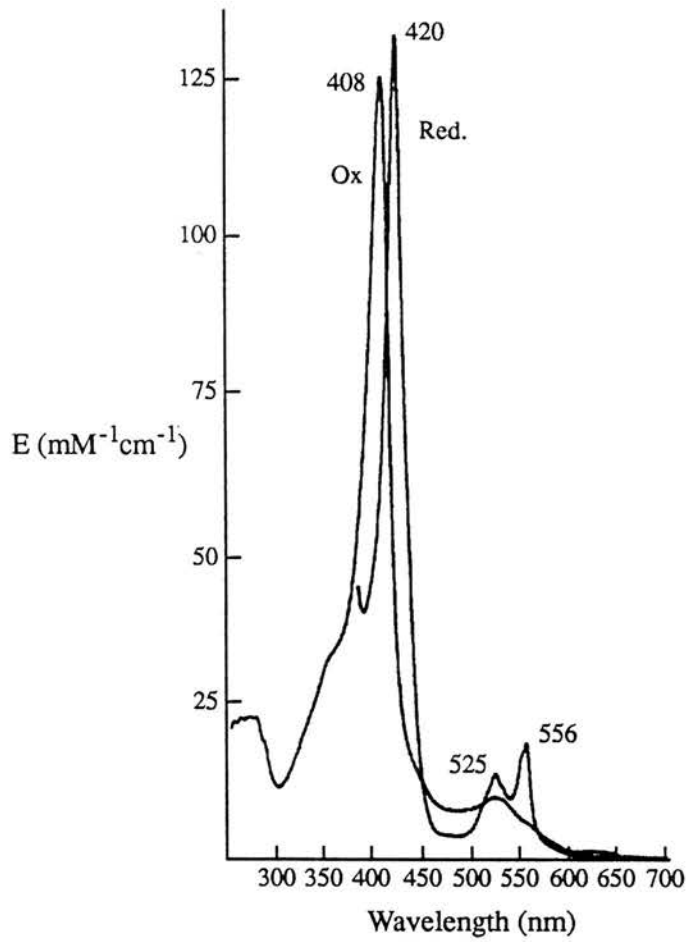

Figure 2.6 U.V.-Visible absorption spectra of *Paracoccus* cytochrome c peroxidase.

The spectra are of the final product of purification of cytochrome c peroxidase. The oxidised (ox) spectrum was obtained from an untreated sample in 0.1M-sodium phosphate buffer, pH 7. The reduced form (red) was obtained by addition of a few grains of sodium dithionite. The ordinate axis is the absorption coefficient on a per haem basis, the haem concentration being determined by the pyridine haemochrome method (section 2.4, Falk 1964).

Purification of the c-550 employs the same chromatographic steps as the peroxidase, but in a different order. (figure 2.1). After the DE-52 step (figure 2.2) the c-550 is applied to G-75 molecular exclusion chromatography (figure 2.7). After G-75, the final stage is chromatography on a hydroxyapatite column (figure 2.8). Elution from the hydroxyapatite column is by a linear gradient from 5mM Pi, pH 7/100mM NaCl to 200mM Pi, pH 7. A gel of the purified c-550 is shown in figure 2.9. A u.v.-visible spectrum is shown in figure 2.10.

2.3 Sodium Dodecyl Sulphate-Polyacrylamide gel electrophoresis (SDS-PAGE)

Electrophoresis in the presence of SDS was carried out using the buffer system of Laemmli (1970) lacking 2-mercaptoethanol, with the addition of 2mM EDTA. SDS polyacrylamide gels were as 130mm x 150mm x 1mm slabs. The separating (running) gel was 15% acrylamide and 0.4% bisacrylamide. The stacking gel was 4% acrylamide and 0.1% bisacrylamide. Electrophoresis was performed at 50V for approximately 16 hours or at 180V for 4 hours.

Samples were prepared for electrophoresis by dissolving in 62.5mM tris/HCl, pH 6.8 containing 2mM EDTA, 2% SDS and 10% glycerol. Sample denaturation was assisted by heating samples to 90°C for 2 min prior to loading onto the gel.

Gels were stained either for haem or for protein. Haem staining was by the method of Goodhew et al (1986). Gels were soaked in 1.25mM 3,3' 5,5' tetramethylbenzidine (TMBZ) in methanol / 0.25mM sodium acetate, pH 5 (30/70, v/v) for 30 min with constant shaking. H_2O_2 was then added to a final concentration of 26mM, and the shaking allowed to proceed for 15 min. After staining, the gels were washed twice in propanol / 0.25M sodium acetate, pH 5 (30/70, v/v).

Protein staining of gels was by coomassie brilliant blue R (2 g/litre) in methanol / acetic acid / water (4.5/1/4.5, v/v). Gels were stained for approx. 2 hours and then destained in methanol / acetic acid / water (3/1/6, v/v)

Gels were photographed and scanned immediately after staining. Photographs

Figure 2.7 Purification of cytochrome c-550 - Molecular exclusion chromatography

Cytochrome c-550 was prepared for gel filtration as described in text. The column was run in 20mM tris HCl, pH 8/ 0.1M NaCl. Fractions were assayed for absorbance at 410nm (O-O) and 280nm (●-●).

Figure 2.8 Purification of cytochrome c-550 - Chromatography on hydroxyapatite

Cytochrome c-550 was prepared for hydroxyapatite as described in the text. The column was equilibrated in 5mM Pi, pH 7/ 100mM NaCl. Proteins were eluted from the column with a linear gradient from 5mM Pi, pH 7/ 100mM NaCl to 200mM Pi. Fractions were assayed for absorbance at 410nm (O-O) and 280nm (●-●).

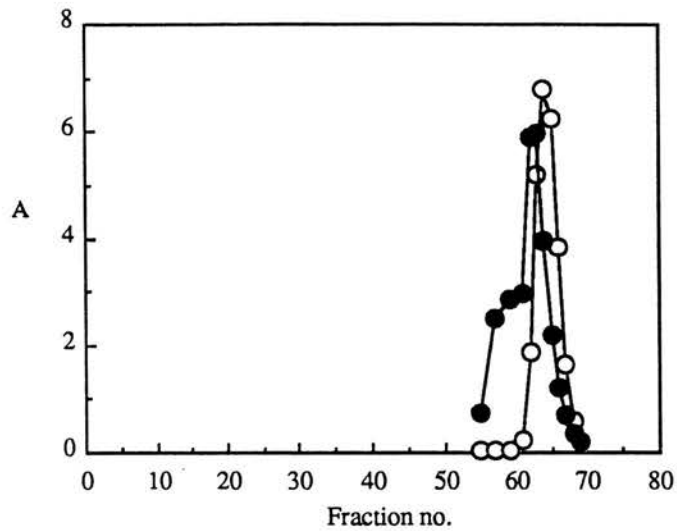
8
6
4
2
0
A
0 10 20 30 40 50 60 70 80
Fraction no.

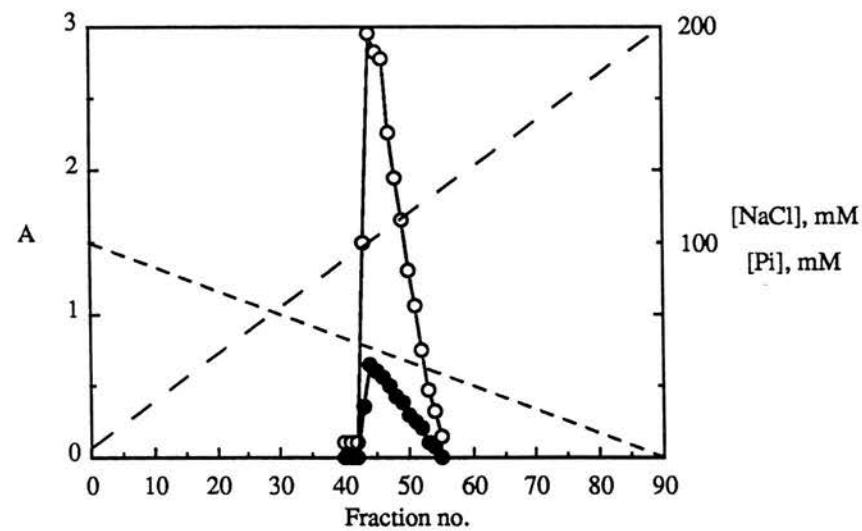
3
2
1
0
A
200
100
[NaCl], mM
[Pi], mM
0 10 20 30 40 50 60 70 80 90
Fraction no.

Figure 2.9 SDS-PAGE of pure cytochrome c-550

Cytochrome c-550 was purified as described in text. 1nmol of purified protein was subjected to SDSPAGE (lane 1). The protein standards shown (lane S) are bovine serum albumin (BSA, 67000), ovalbumin (45000), carbonic anhydrase (29000), myoglobin (17000), and cytochrome c (12000). The gel was run at 180V for 4 hours and then stained with Coomassie blue.

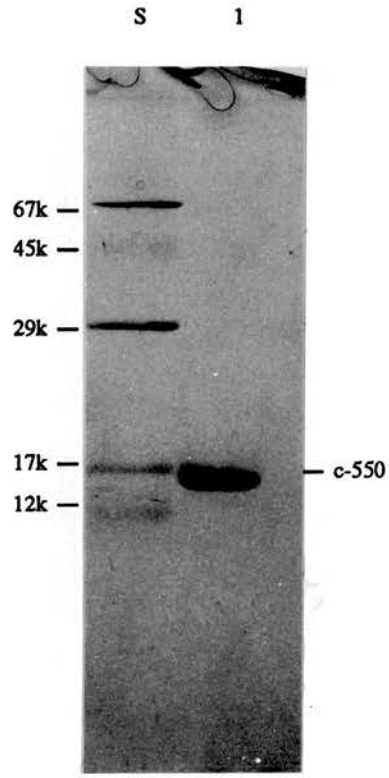
S
1
67k
45k
29k
17k
12k
c-550

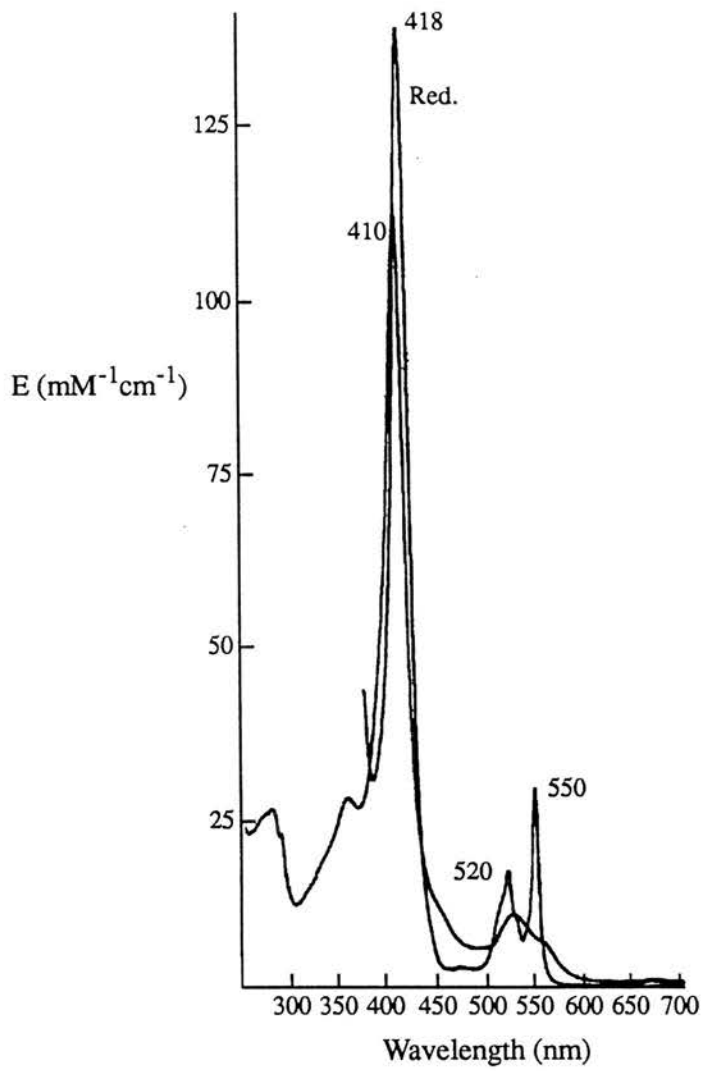

Figure 2.10 U.V.-Visible absorption spectra of Paracoccus cytochrome c-550
The spectra are of the final product of purification of cytochrome c-550. The oxidised (ox) spectrum was obtained from an untreated sample in 0.1M-sodium phosphate buffer, pH 7. The reduced form (red) was obtained by addition of a few grains of sodium dithionite. The ordinate axis is the absorption coefficient on a per haem basis, the haem concentration being determined by the pyridine haemochrome method (section 2.4, Falk 1964).

were through a yellow filter (codin A.001). Scanning was by a Shimadzu CS-930 scanner at 690nm (haem-stained gels) or 600nm (protein-stained gels).

2.4 Pyridine ferrohaemochrome

Dissolving a cytochrome in pyridine results in loss of the axial ligands which are replaced by pyridine molecules. In this way, the influence of the protein environment on the spectrum is removed and all ferrous c-type cytochromes of a given concentration will have the same absorbance at 550nm. Under these conditions, the α-peak at 550nm has an extinction co-efficient of 29.1mM^{-1} cm^{-1} (Morton 1958). A pyridine haemochrome can therefore be used to obtain an accurate concentration of haem in a sample. This can then be used to determine the extinction co-efficient of the native protein.

Pyridine ferrohaemochrome spectra were recorded in 0.15M NaOH solutions containing 2.1M pyridine. The cytochrome was reduced by addition of a few crystals of dithionite. The spectra were recorded against a NaOH-pyridine blank. For measurement of the extinction co-efficient of the native cytochrome, the same quantity of cytochrome was dissolved in 0.1M sodium phosphate buffer, pH 7 and the spectrum recorded.

2.5 pH Buffers

A mixture of Mes and Hepes (usually 5mM of each) was used to buffer the pH in all experiments other than the purification of the cytochromes (section 2.2). Mes and Hepes have pK_A's of 6.1 and 7.5 respectively (Good et al 1966). A mixture of these two buffers allowed experiments to be performed at a variety of pH values without having to alter the buffer composition.

The ionic strength, I, of the buffers was calculated from the equation :

$$I = 1/2 \Sigma m_i z_i^2$$

The summation (Σ) is taken over all the different ions in solution, multiplying the molarity, m, of each by the square of the charge, z. Mes and Hepes are zwitterions in the protonated form. Zwitterions behave as dipoles in solution rather than as electrolytes, therefore only the concentration of the base (anionic) form of the buffer and the counter ion are included in calculation of the ionic strength.

The buffers were prepared by titrating the sodium salt with HCl to the desired pH. This ensures constant ionic strength throughout the pH range used since an equivalent of zwitterion will be formed for every equivalent of Cl^- added.

2.6 N.M.R. and E.P.R. Spectroscopy.

The magnetic properties of haem groups can be studied by the use of n.m.r. and e.p.r. spectroscopies. These spectroscopies are able to separate signals from individual haem groups in a way that is not possible using conventional visible spectroscopy. E.p.r. probes the environment of a paramagnetic centre by defining the size and shape of the magnetic moment produced by the unpaired electron of the iron atom. N.m.r. probes the environment of atom nuclei such as ^{1}H which act as small bar magnets and can interact with an external magnetic field.

The e.p.r. was carried out with a Bruker ESP 380 spectrometer equipped with a continuous flow helium cryostat (Oxford Instruments Co. Oxford). The ^{1}H n.m.r. spectrum was recorded in the Fourier transform mode with a Bruker AMX300 (300MHz) spectrometer.

CHAPTER III

A Spectroscopic study of *Paracoccus denitrificans* cytochrome c peroxidase

3.1 INTRODUCTION

The most extensively studied bacterial cytochrome c peroxidase is that from *Pseudomonas aeruginosa*. A wide range of spectroscopic techniques, including optical, e.p.r., n.m.r. and m.c.d. have been applied to this enzyme (Ellfolk et al 1983, 1984a, 1984b; Foote et al 1984, 1985). These studies have shown the two haems of the enzyme to be non-equivalent in terms of redox potential, haem ligands and iron spin-states. The three redox states of the enzyme (i.e. ferric, mixed valence and ferrous), and their complexes with added ligands have been characterised from this bacterium (Ellfolk et al 1983, 1984a).

The aim of this chapter is to characterise the *Paracoccus* cytochrome c peroxidase spectroscopically. Most of the work is concerned with the preactivation of the enzyme whereby reduction of the high-potential electron transferring haem results in the low-potential peroxidatic haem adopting a more open conformation, available for ligand binding. This haem-haem interaction is studied by a number of spectroscopic techniques and is found to be dependent on both Ca^{++} ions and temperature.

3.1.1 Electronic properties of Iron

Iron is a transition metal with the electronic configuration $1s^2 2s^2 2p^6 3s^2 3p^6 3d^6 4s^2$ or $[Ar]3d^6 4s^2$, and like other transition metals, it can exist as a complex with multiple ligands. In haemoproteins, the iron is chelated by porphyrin which donates four ligands via the four pyrrole ring nitrogen atoms (figure 3.1). An additional two ligands are normally provided by the protein, thus giving the iron a coordination number of six. The two most stable oxidation states of iron in haem are ferrous (Fe(II); $[Ar]3d^6 4s^0$) and Ferric (Fe(III); $[Ar]3d^5 4s^0$).

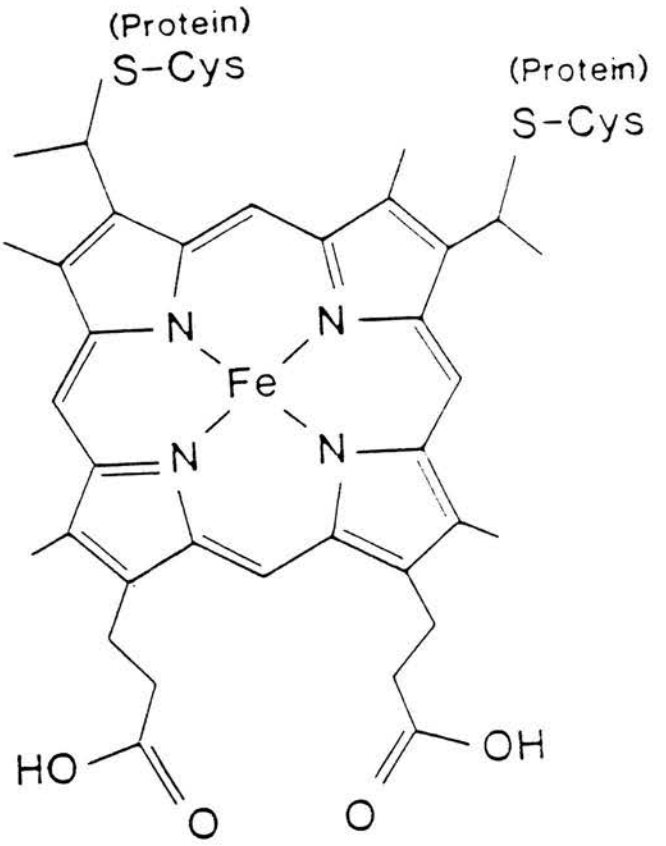

Figure 3.1 Structure of haem c.

Haem iron is bound to porphyrin by four bonds to the pyrrole ring nitrogens. The remaining, extraplanar ligands to the haem iron are provided by the protein side chains (not shown) (from Pettigrew & Moore 1987).

Iron has five 3d orbitals which are partly filled (figure 3.2). The presence of external ligands governs the distribution of electrons within these orbitals, which in turn governs the electronic properties of the iron. The effect of incoming ligands on the iron orbitals can be described in terms of crystal field theory (CFT). CFT assumes that the interaction between the metal ion and the ligands is purely electrostatic (ionic) in nature. CFT then considers the effect that the electrostatic field of the ligand has on the d orbitals of the central metal ion. In a free transition metal ion, all five d orbitals have equal orbital energies, they are degenerate (figure 3.3a). However, the energy of the d-orbitals are split by the presence of incoming ligands (figure 3.3b). Those orbitals which lie along the axes of the incoming ligands (d_{z^2}, $d_{x^2-y^2}$) are destabilised to a greater extent than those which lie between the axes of the incoming ligands (d_{xz}, d_{xy}, d_{yz}). The destabilisation is due to repulsion of the d-orbital electrons by the electrons of the incoming ligands. Thus, in a 6-coordinate transition metal complex the five 3d orbitals are split into two sets: the high energy e_g orbitals (d_{z^2}, $d_{x^2-y^2}$) and the low energy t_{2g} orbitals (d_{xz}, d_{xy}, d_{yz}). The energy difference between the two sets is known as the d orbital splitting and is given the symbol Δ_o. The magnitude of the d orbital splitting is dependent on the nature of the incoming ligands. A strong field ligand produces a large d orbital splitting in comparison to a weak field ligand.

The distribution of electrons in a transition metal complex is governed by two competing factors: (1) The magnitude of d orbital splitting (Δ_o) and (2) the energy required to pair electrons in the same orbital (P). The pairing energy is always unfavourable, but the important factor is whether the energy required to pair an electron is less than that required to promote it to a higher energy e_g orbital. If $P < \Delta_o$ then the energy required to pair the electrons is less than the energy required to promote the electron to an e_g orbital. In this case the electrons pair up in the lower energy orbitals to give a low-spin electronic configuration (figure 3.4(a)). If, on the other hand, $P > \Delta_o$ then the energy required to promote an electron to an e_g orbital is less than that required to pair the electrons in the lower energy orbitals and so the

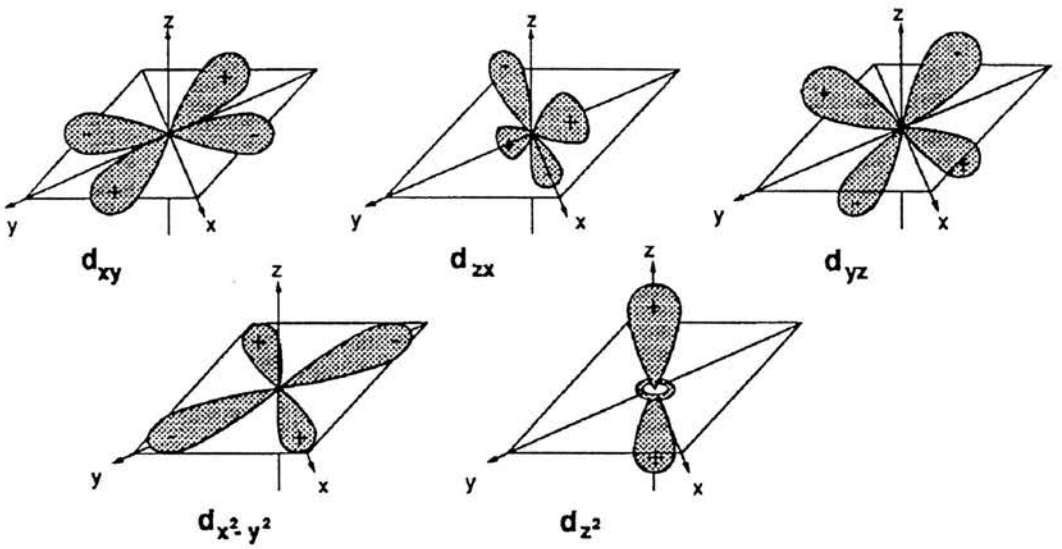

Figure 3.2 The shape and orientation of d-orbitals.

In haem-containing proteins, the haem group lies in the xy plane, with the axial ligands above and below in the z direction (from Moore & pertigrew 1990).

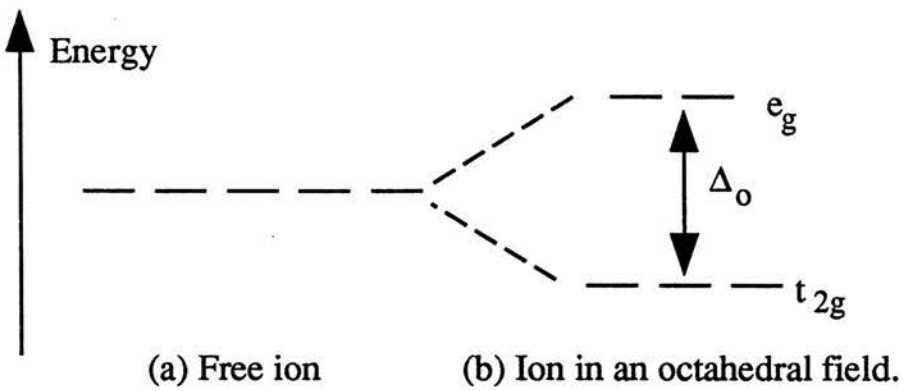

Figure 3.3 The splitting of d-orbital energies by an octahedral field.

Δ_o refers to the magnitude of the d-orbital splitting. The e_g set is made up of the $d_{x^2-y^2}$ orbital and the d_{z^2} orbital. The t_{2g} set is made up of the d_{xy}, d_{xz}, and d_{yz} orbitals.

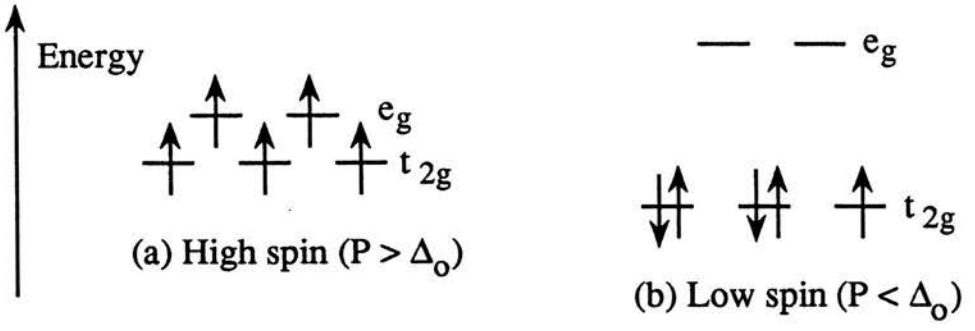

Figure 3.4 Spin-states of Fe^{III} in an octahedral field.

Each arrow represents an electron in the orbital. The presence of a weak crystal field leads to a high-spin state (a) whereas strong crystal fields result in low-spin states (b).

electrons will distribute singly amongst the 3d orbitals to give a high-spin configuration (figure 3.4(b)). low-spin configurations are seen when strong field ligands are present, whereas high-spin configurations are seen when weak field ligands are present.

In haemoproteins, both high-spin and low-spin iron is observed. Porphyrin is a strong ligand and places the iron close to its crossover point between high and low-spin (figure 3.5). The result is that relatively small energy differences between the axial ligand components of the field can cause the spin-state to change. The ligand fields of 5-coordinate haems are usually weak, and as a result the majority of low-spin haems are found to be 6-coordinate.

3.1.2 Ligand field strength

The extent of d orbital splitting in haemoproteins can be estimated from charge transfer bands in the near infrared region of the spectrum. Charge transfer transitions result from the transfer of electrons between iron orbitals and orbitals of the axial ligands. The energy of these transitions are influenced by Δ_o.

Based on CFT, one would expect increasing ligand field strength when going from poor electron donors to strong electron donors. However, this is not observed in the spectrochemical series and reflects the fact that the interaction between metal and ligand is not purely ionic, but has covalent characteristics also.

Although a spectrochemical series for haem protein ligands has been devised, it is not always possible to predict whether a ligand will be strong or weak since additional factors such as the protein environment are likely to be important. However, based a study of well-characterised haem proteins, histidine, methionine, cysteine, and lysine are generally strong field ligands whereas water, glutamate, aspartate and tyrosine are generally weak field ligands (Moore & Pettigrew, 1990).

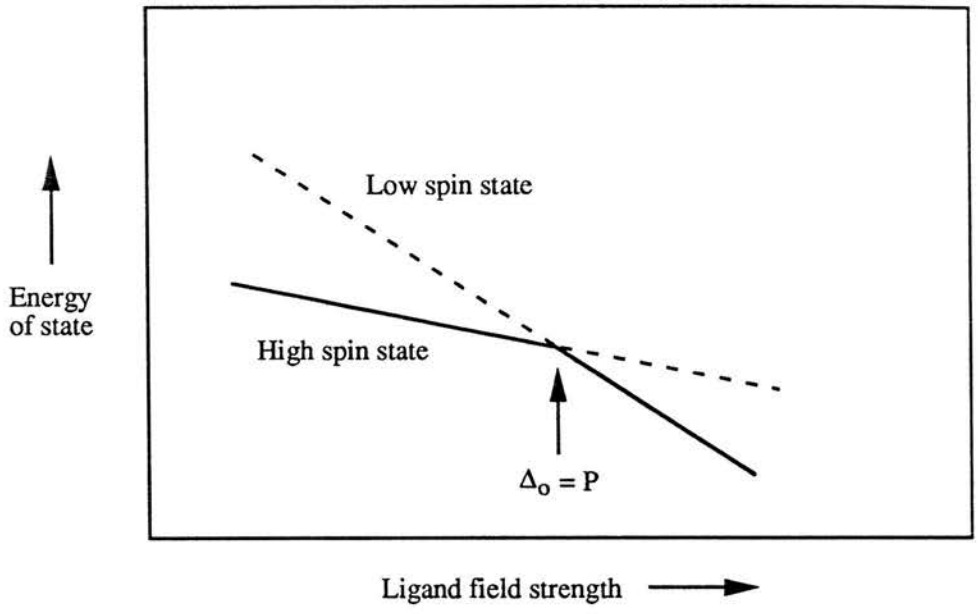

Figure 3.5 Relationship between ligand field strength and spin-state.
The electronic configuration (solid line) is dependent on the ligand field strength. Complexes in the vicinity of the crossover point may exist in a thermal equilibrium between high- and low-spin forms.

3.2 METHODS

3.2.1 Redox titrations

Reductive and oxidative titrations were performed in an anaerobic cuvette constantly flushed with argon and magnetically stirred. The cuvette contained approximately 6μM cytochrome c peroxidase in 5mM Mes/5mM Hepes (sodium salts), adjusted to pH 7.5 with HCl, and 17μM phenazine methosulphate (PMS, E_m = +60mV (Wilson, G 1978)), phenazine ethosulphate (PES, E_m = +80mV (Wilson, G 1978)), diaminodurol (DAD, E_m = +220mV (Wilson, G 1978)), 2-hydroxy-1,4-naphthoquinone (HNQ, E_m = -140mV (Wilson, G 1978)), and flavin mononucleotide (FMN, E_m = -200mV (Wilson, G 1978)) as redox mediators. Higher buffer concentrations were avoided in order to prevent Ca^{++} contamination from buffer salts. Redox mediators were present to ensure rapid equilibration between the redox electrode and the buried redox centres within the enzyme. The pH at the end of the redox titration was measured and these values are given in the figure legend. The total volume of the cuvette was 3.5ml.

The ambient redox potential (E_{obs}) was monitored by a Pt pin electrode in combination with a Ag/AgCl reference (Russell pH Ltd.) and the potential, with reference to the standard hydrogen electrode, was obtained by adding 196mV (Bates 1954).

Reductive titrations were carried out by addition of small volumes of an anaerobic sodium dithionite solution (30mM). Sodium dithionite stock solutions were prepared in anaerobic 100mM Mes/100mM Hepes (sodium salts) adjusted to pH 7.5 with HCl. Oxidative titrations were carried out using 30mM potassium ferricyanide in the same buffer.

Spectra were scanned in the region of the α and β bands using a Unicam SP1800 spectrophotometer, coupled to a chart recorder (Lloyd Instruments Graphic 1000).

3.2.2 Data analysis

The mid-point oxidation-reduction potential can be calculated using the Nernst

Equation, shown below:

$$E_h = E_m + \frac{2.3RT}{nF} \log \frac{[\text{oxidised form}]}{[\text{reduced form}]}$$

where R is the gas constant, T is the temperature, n is the number of electrons involved in the redox reaction and F is the Faraday. At 25°C, this simplifies to :

$$E_h = E_m + \frac{0.059}{n} \log \frac{[\text{oxidised form}]}{[\text{reduced form}]}$$

A plot of E_h against log ox/red gives a straight line of slope 59mV for a one electron oxidation-reduction reaction. The intercept of this line with the y-axis gives the value of the mid-point potential.

3.2.3 Calibration of redox electrode

Prior to the redox titrations, the performance of the electrode was checked using the Fe^{2+}/ Fe^{3+}-EDTA redox couple, which has a mid-point potential of +108mV at pH 5 (Kolthoff & Auerbach 1952). By measuring the ambient potential at two different ratios of oxidised and reduced, it is possible to check the electrode gives the true potential (196mV, Bates 1954) and slope.

For calibration, the electrode was placed in a stirred cuvette containing 0.125M sodium acetate pH 5, 0.5mM ferric ammonium sulphate and 10mM EDTA. This solution was made anaerobic by bubbling with N_2 for 15 min. After bubbling, an anaerobic solution of ferrous ammonium sulphate was added to give 0.2mM and the ambient potential recorded. A further addition of ferrous ammonium sulphate was then made, to give a final concentration of 0.5mM, for which the potential was recorded. A graph of E_h against log ox/red was then plotted, from which the E_m was

measured and the slope determined.

3.2.4 Visible spectroscopy

Absolute spectra were recorded either on a Varian Cary 219 or a Phillips PU8700 spectrophotometer, as detailed in the figure legends. Difference spectra were recorded on the Phillips PU8700 using the maths option to subtract spectra stored in the memory. Oxidised spectra were obtained from untreated protein samples, unless otherwise stated. Ascorbate-reduced spectra were obtained by addition of ascorbate, and the redox mediator diaminodurol (DAD) to final concentrations of 1mM and 5μM, respectively. Dithionite-reduced spectra were obtained by addition of a few crystals of solid sodium dithionite to well-buffered protein solutions, except for the redox titrations, where the dithionite was added as small volumes of a 30mM anaerobic solution, as detailed in section 3.2.1.

3.2.5 Ca^{++} titrations

Ca^{++} titrations were carried out by following the changes in the protein spectrum upon addition of Ca^{++} ions. The titrations were performed with both unbuffered and buffered $CaCl_2$ solutions. EGTA was used as a Ca^{++} buffer. For titrations in the absence of EGTA, the free calcium concentration was determined assuming the spectral change observed resulted from binding of a single calcium ion per protein molecule. The use of EGTA as a buffer allows for additions of larger concentrations of $CaCl_2$ and hence less error is involved. In addition, EGTA buffering eradicates the need to make assumptions when calculating the free Ca^{++} concentration. The theory of Ca^{++} buffering is described below.

3.2.6 Ca^{++} buffering - theory

The two most important factors in any metal ion buffer is (1) its affinity constant and (2) its selectivity against other ions.The association constant, K_A for a 1:1 Ca^{++}

buffer complex is given by

$$K_A = \frac{[Ca][L]}{[CaL]} \quad ; \quad [Ca]_T = [CaL] + [Ca]_F$$

Given the concentrations of total Ca^{++} and ligand added and knowing the value of K_A, the concentration of free Ca^{++} can be determined.

A number of potential calcium buffers exist, however, EGTA is often used since it has a high affinity constant and is highly selective towards Ca^{++} over other ions. However, a complicating factor of EGTA is that only the fully ionised form ($EGTA^{4-}$) is able to bind Ca^{++}. The pK_A values of the four ionisations of EGTA are 9.58, 8.90, 2.76, and 2.1, so at pH 7 the dominant form is $EGTAH_2^{2-}$. As a consequence of this pH dependence, the association constant decreases with decreasing pH. It is therefore necessary to calculate an apparent association constant for the pH at which the particular experiment is being carried out. This apparent association constant accounts for the fact that not all the EGTA present is available to complex with the Ca^{++}.

The apparent association constant, K_{app} is given by

$$K_{app} = K_{abs} \times \frac{1}{\alpha L}$$

where αL is a multiplication factor which takes into account the relative concentration of $EGTA^{4-}$ for a given pH and is given by

EX BIBL. UNIV. EDINBURGH

$$\alpha L = \frac{[L] + [HL] + [H_2L] + [H_3L] + [H_4L]}{[L]}$$

$$= 1 + 10^{pK_1 - pH} + 10^{pK_1 + pK_2 - 2pH} + 10^{pK_1 + pK_2 + pK_3 - 3pH} + 10^{pK_1 + pK_2 + pK_3 + pK_4 - 4pH}$$

Using this equation, the apparent association constant of EGTA for Ca^{++} is $10^{7.415}$ (M^{-1}) at pH 7.5 and $10^{4.43}$ (M^{-1}) at pH 6. Taking the reciprocal of these values, the dissociation constants are calculated as 38.5nM at pH 7.5 and 37μM at pH 6.

Example

What is the free Ca^{++} in a solution 1mM in EGTA buffered at pH 7.5 and containing 0.1mM $CaCl_2$.

$$[Ca] = \frac{[Ca\text{-}EGTA]}{[EGTA] \times K_{app}}$$

A close approximation of the free calcium concentration can be obtained using the fact that since the K_D is 38.5nM at this pH, then almost all the Ca^{++} is present as Ca^{++}-EGTA = 10^{-4}M. Therefore, the free EGTA concentration = 9×10^{-4}M. Entering these values into the above equation gives a free calcium concentration of 4.28×10^{-9} M. A more accurate free concentration can be calculated by solving the equation as a quadratic. This gives a free calcium concentration of 4.23×10^{-9} M. Routine calculations of free calcium were performed using a computer program kindly supplied by Dr Richard Ashley. This program is based on the theory described above and calculates the free calcium at any given pH.

It has been shown that $EGTAH^{3-}$ can bind Ca^{++} with an association constant of $10^{5.3}$ (Sillen and Martell 1971). However, as previously indicated by Thomas (1982), incorporation of this binding constant gives free Ca^{++} concentrations which are almost identical to those in which only Ca^{++} binding to the $EGTA^{4-}$ ($K_A = 10^{10.97}$) form is taken into account (less than 1% difference in free Ca^{++} concentrations).

3.3 RESULTS AND DISCUSSION

3.3.1 Visible spectra of oxidised and ascorbate-reduced cytochrome c peroxidase

3.3.1.1 Absolute spectra

Selected regions of the optical spectra of the oxidised and ascorbate-reduced peroxidase are shown in figure 3.6. The oxidised enzyme has a Soret maximum at 409nm and a weak absorption band at 640nm (figure 3.6(i)). The band at 640nm indicates the presence of a ferric high-spin haem (Moore & Pettigrew, 1990)). This signal is also observed in the oxidised cytochrome c peroxidase from *Pseudomonas aeruginosa*, but there is disagreement as to its origin (Ellfolk et al. 1984b, Foote et al. 1984). Treatment of the enzyme with ascorbate, and the electron mediator diaminodurol, for 2 min. yields the mixed valence enzyme, with the high-potential haem reduced and the low-potential haem oxidised. A spectrum taken two minutes after ascorbate addition (figure 3.6(ii)) shows the reduced high-potential haem Soret at 419nm with the oxidised low-potential haem Soret seen as a shoulder at 408nm. This spectrum also shows disappearance of the ferric high-spin signal at 640nm, suggesting that this signal in the oxidised enzyme arose from the high-potential haem. This assignment is in agreement with that of Foote et al. (1984) for the *Pseudomonas* enzyme. Incubation of the mixed valence enzyme at room temperature for 60 min. in the presence of 1mM $CaCl_2$ results in a gain of absorbance at 380nm with concomitant loss at 410nm, representing a blue-shift in the oxidised low-potential haem Soret (figure 3.6(iii)). This shift of the Soret in conjunction with the appearance of the 640nm band (figure 3.6(iii)) represents a low to high-spin transition in the oxidised low-potential haem.

The presence of a weak absorption band at 695nm in the fully oxidised enzyme (figure 3.7) suggests the presence of a methionyl-histidinyl coordinated haem. The band is difficult to observe because of the neighbouring high-spin absorption at 640nm and because only a portion of the Met-His haem is in a low-spin state. This weak absorption band disappears upon ascorbate-reduction (figure 3.7) suggesting it

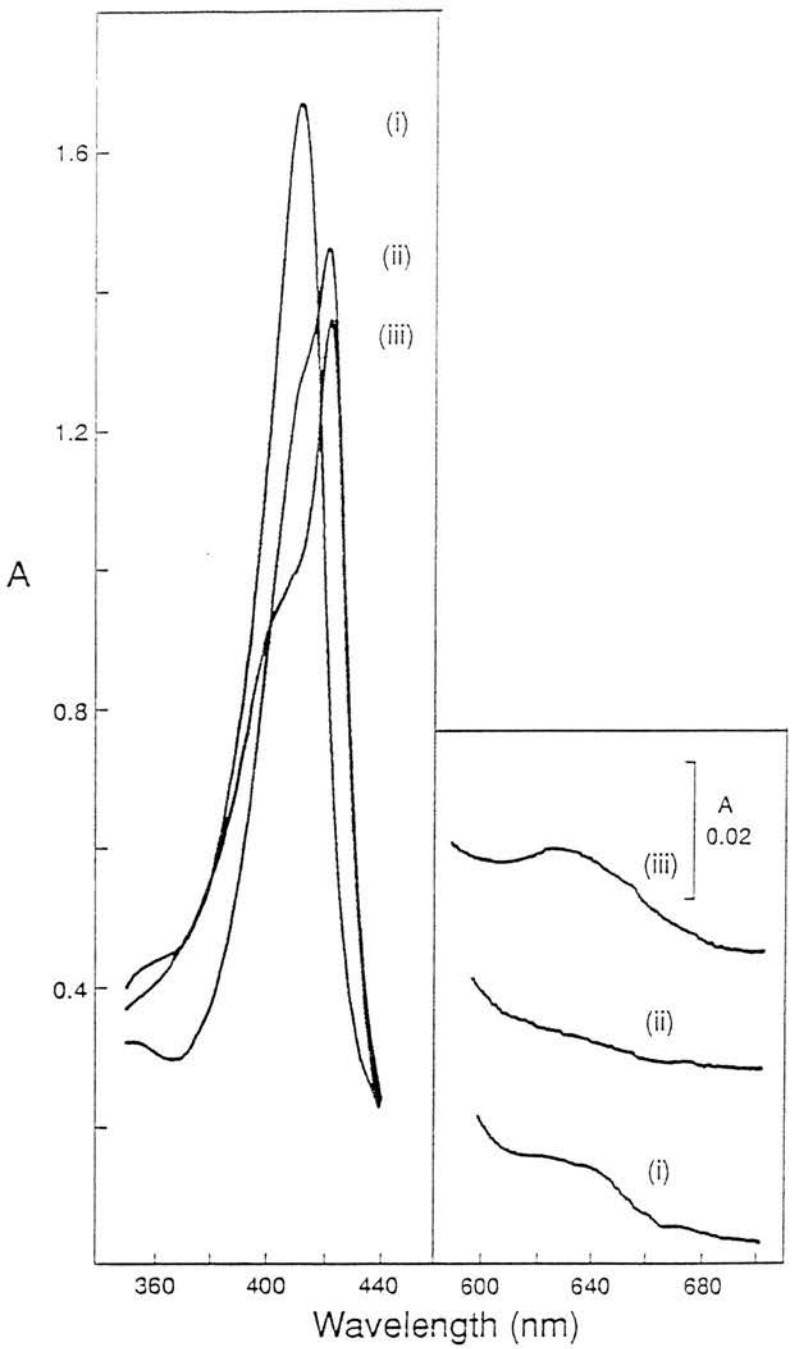

Figure 3.6 Visible absorption spectra of *Paracoccus denitrificans* cytochrome c peroxidase.

The spectrum of oxidised cytochrome c peroxidase (i) was obtained from an untreated, 8μM sample of enzyme in 5mM Mes/5mM Hepes, pH 6. Mixed valence spectra were obtained by addition of 1mM ascorbate, 5μM DAD. (ii) shows a spectrum of the peroxidase 2 min after ascorbate addition. The same sample is shown in (iii), 60 min after ascorbate addition in the presence of 1mM $CaCl_2$.

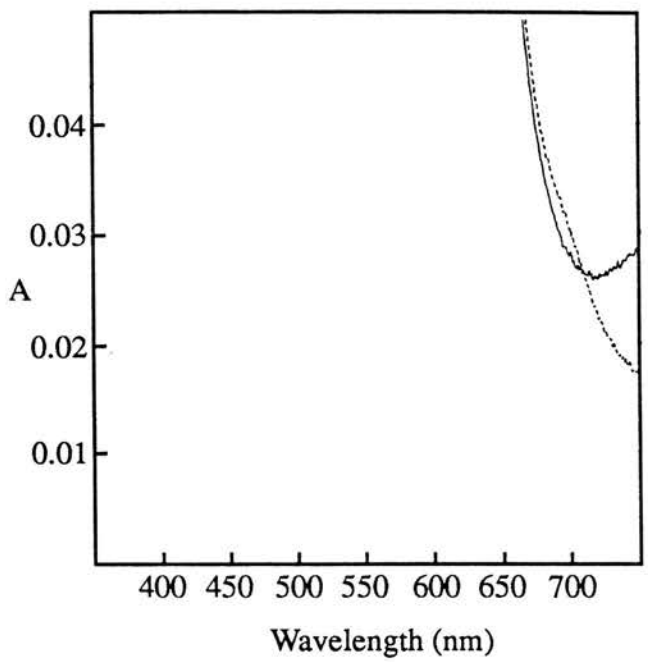

Figure 3.7 Evidence for a methionyl-histidinyl coordinated haem in cytochrome c peroxidase.

(------) shows a 60μM sample of cytochrome c peroxidase in 5mM Mes/Hepes pH 6. The shoulder at approximately 690nm indicates the presence of a Met-His haem. This shoulder disappears after ascorbate-reduction (——), suggesting it originates in the oxidised enzyme from the high-potential haem. The ascorbate-reduced spectrum was taken 2 min after addition of 2mM ascorbate, 10μM DAD.

originates in the oxidised enzyme from the high-potential, electron transferring haem. A similar 695nm signal is observed in the visible spectrum of well characterised ferric cytochromes which contain a Met-His coordinated haem (Moore & Pettigrew, 1990). The m.c.d. spectrum of *Pseudomonas aeruginosa* cytochrome c peroxidase has a trough located at 708nm (Foote et al 1984). This signal is thought to be the m.c.d. counterpart of the 695nm visible absorption band. Villalain et al (1984) have indicated the presence of a 705nm band in the visible spectrum of the fully oxidised form of *Pseudomonas stutzeri* cytochrome c peroxidase.

3.3.1.2 Difference spectra

The ascorbate reduction and spin state changes can be seen more clearly using difference spectroscopy (figure 3.8). At pH 6.0, the difference spectrum of the enzyme 2 min. after ascorbate addition versus the oxidised enzyme (figure 3.8(i)) shows characteristic features of a reduced low-spin haem with maxima at 419, 525, and 557nm. Difference spectra, recorded at various times after this, versus the enzyme 2 min. after ascorbate addition (figure 3.8(ii)), show the slow appearance of ferric high-spin signals with maxima at 380, 500, and 640nm. The level of high-spin state formed and the time for its formation varies from one enzyme preparation to the next and is probably due to different amounts of residual $CaCl_2$ already on the enzyme. Addition of 1mM $CaCl_2$ after the partial high-spin state has formed leads to an enhancement of the high-spin signals (from 1 to 2 in figure 3.8(ii)). The Ca^{++} effect is complete within 15 min. The high-spin state is temperature-sensitive and can be converted back to low-spin if the Ca^{++}-treated, ascorbate-reduced sample is cooled on ice for 20 min. (figure 3.8(iii)). Addition of Mg^{++} ions to the ascorbate-reduced, partial high-spin state of the enzyme produces the same enhancement of high-spin signals as seen by addition of Ca^{++} ions (figure 3.9). Ca^{++} addition to a Mg^{++}-treated enzyme produces no further high-spin formation, suggesting both ions act in the same way and probably at the same site. Addition of Ca^{++} ions to the fully oxidised enzyme produces no spectral effect, suggesting the low-potential haem can

Figure 3.8 The appearance of a high-spin state following ascorbate reduction of cytochrome c peroxidase.

A 4μM solution of cytochrome c peroxidase in 5mM Mes/5mM Hepes, pH 6 was reduced with 1mM ascorbate, 5μM DAD. (i) shows the difference spectrum of the enzyme 2 min after ascorbate addition minus that of the oxidised enzyme. Ascorbate reduction is complete within 2 min and is followed by the slow appearance of ferric high-spin signals. (ii) shows difference spectra with increasing time after ascorbate addition minus that of the enzyme 2 min after ascorbate addition. The high-spin state forms slowly over 30 min in the absence of added calcium and reaches an initial end-point (1). After addition of 1mM $CaCl_2$ an enhanced high-spin state (2) forms within 15 min. The high-spin formation is temperature-dependent and can be reversed by cooling on ice. (iii) shows the difference spectrum of the ascorbate-reduced high spin enzyme put on ice for 20 min minus that of the same sample at room temperature.

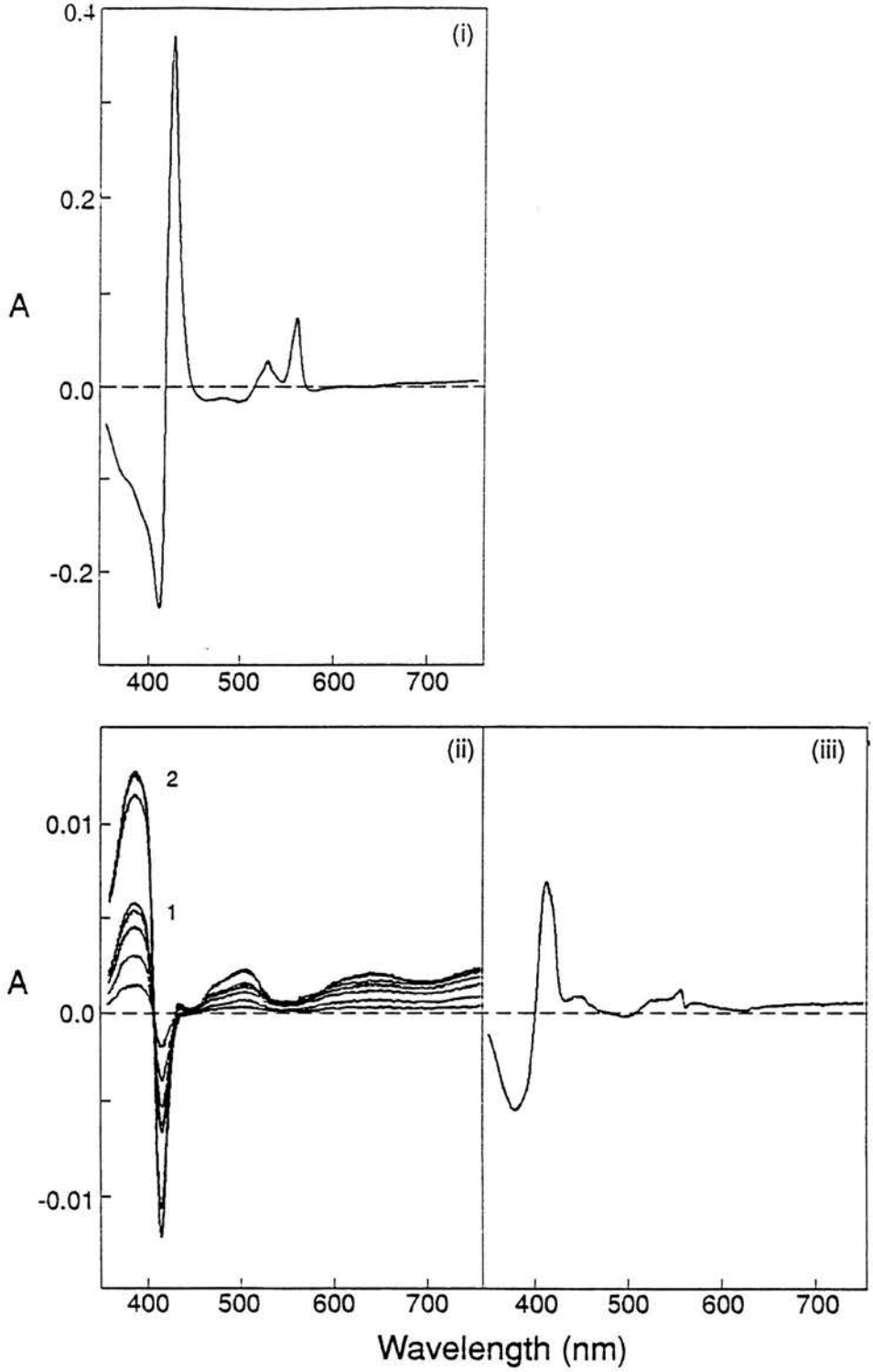
(i)
0.4
0.2
0.0
-0.2
A
400
500
600
700
(ii)
(iii)
2
1
0.01
0.0
-0.01
A
400
500
600
700
400
500
600
700
Wavelength (nm)

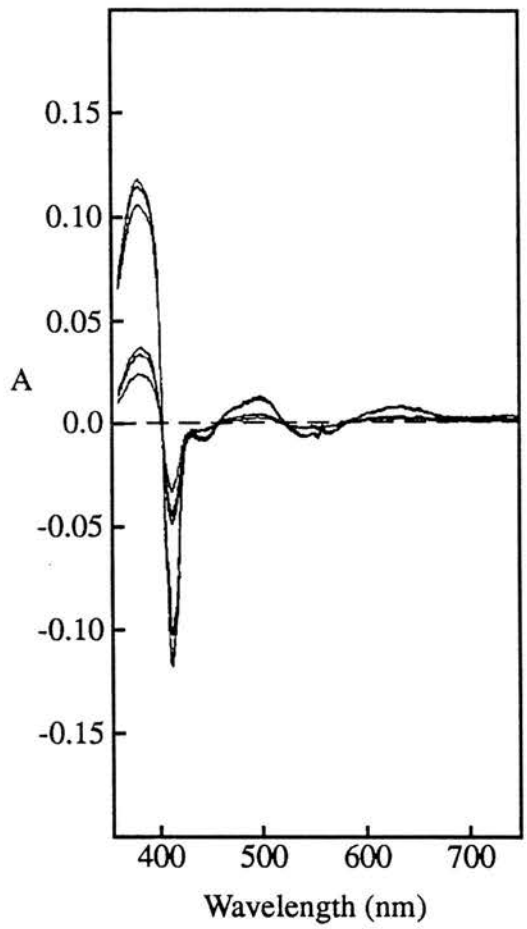

Figure 3.9 Effect of Mg^{++} ions on the ascorbate-reduced spectrum of cytochrome c peroxidase.

A 4μM sample of cytochrome c peroxidase in 5mM Mes/Hepes pH 6 was reduced with 1mM ascorbate, 5μM DAD. Reduction of the high-potential haem was complete within 2 min and this spectrum was used as a baseline to study any subsequent changes in the spectrum. The lower three spectra shown were recorded at 30, 60 and 90 min after ascorbate-reduction and show the slow formation of high spin signals. The higher three spectra were recorded 3, 7, and 14 min after addition of 1mM $Mg(NO_3)_2$.

only be converted to a high-spin state after prior reduction of the high-potential haem.

The partial high-spin state in the absence of added Ca^{++} is not observed at pH 7.5, although addition of 1mM Ca^{++} results in the full appearance of the high-spin form (figure 3.10). This observation suggests the residual Ca^{++} on the enzyme is more weakly bound at this higher pH.

3.3.1.3 Spectral characteristics of reduced low-potential haem.

Reduced low-spin c-type haems have well-structured α and β band spectra, with the α band peak normally centred around 550nm and the β peak around 525nm (Pettigrew & Moore 1987). Reduced high-spin haems, on the other hand, have a much less well-defined spectrum in this region, with no resolution of 2 separate peaks. The spin state of the peroxidatic haem can be confirmed by studying the spectrum of the reduced low-potential haem in the region of the α and β bands. Figure 3.11 shows the effect of fully reducing the enzyme after ascorbate reduction in the presence and absence of added calcium at pH 7.5.

In the absence of added Ca^{++}, the fully reduced spectrum has an α and β band at 551 and 525nm respectively (figure 3.11A(i)). The α band has a shoulder on the long wavelength side, at 557nm. The spectrum of the reduced low-potential haem can be obtained by subtracting the ascorbate-reduced spectrum from the fully reduced spectrum (figure 3.11A(ii)). This difference spectrum shows fully resolved α and β bands, indicative of a ferrous low-spin haem. The absence of a trough at 640nm shows that the low-potential haem was not high-spin in the ascorbate-reduced enzyme.

In the presence of 1mM Ca^{++}, the fully reduced spectrum has an α and β band at 557 and 525nm respectively (figure 3.11B(i)). The α band has a shoulder on the short wavelength side (551nm). A fully reduced minus ascorbate-reduced spectrum shows the reduced low-potential haem to have a fused α/β band similar to that seen in ferrous high-spin cytochromes c′ (figure 3.11B(ii)) (Meyer & Kamen 1982). The trough at 640nm suggests that this haem was also high-spin in the ascorbate-reduced enzyme. The fully reduced forms of *Pseudomonas aeruginosa and Pseudomonas*

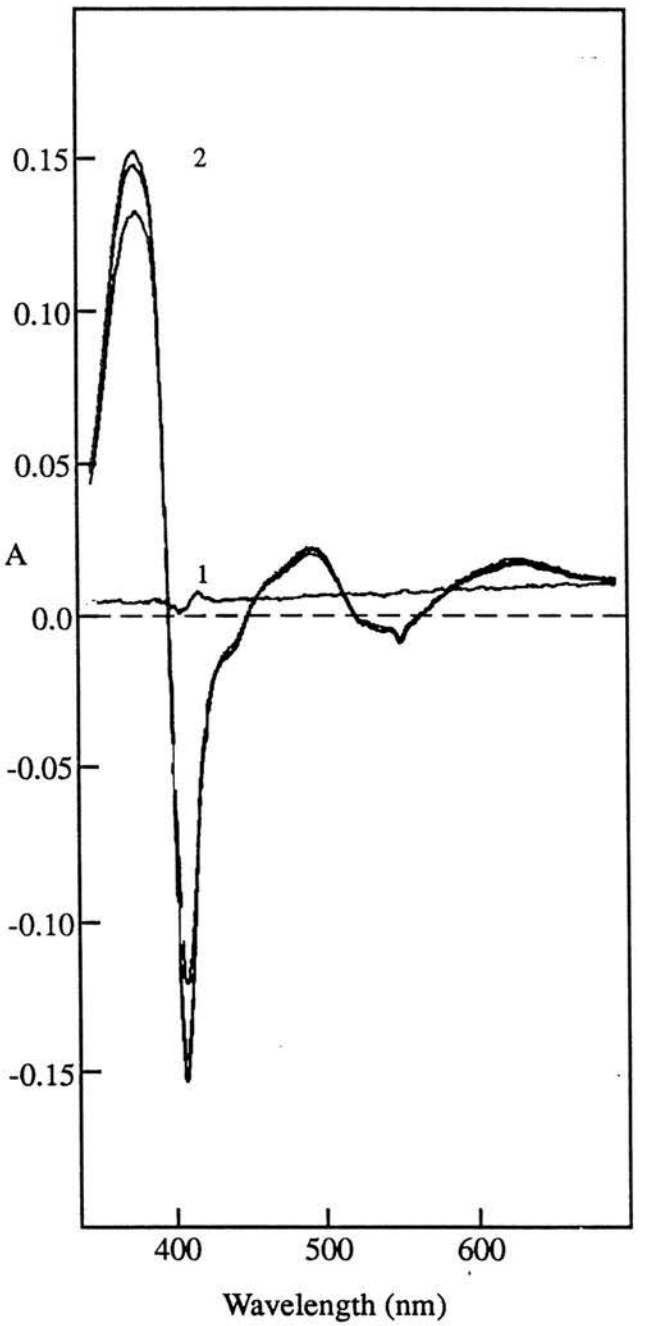

Figure 3.10 The spin-state of the peroxidatic haem of cytochrome c peroxidase at pH 7.5.

A 4μM sample of cytochrome c peroxidase in 5mM Mes, Hepes pH 7.5 was reduced with 1mM ascorbate, 5μM DAD. A spectrum taken 2 min after ascorbate addition was used as a baseline to allow formation of any subsequent high-spin signals to be observed. A spectrum taken 60 min after ascorbate-reduction (1) shows no high-spin signals have formed. Addition of 1mM $CaCl_2$ at this stage results in formation of the same high-spin signals seen at pH 6 (2). The high-spin formation is complete after 15 min.

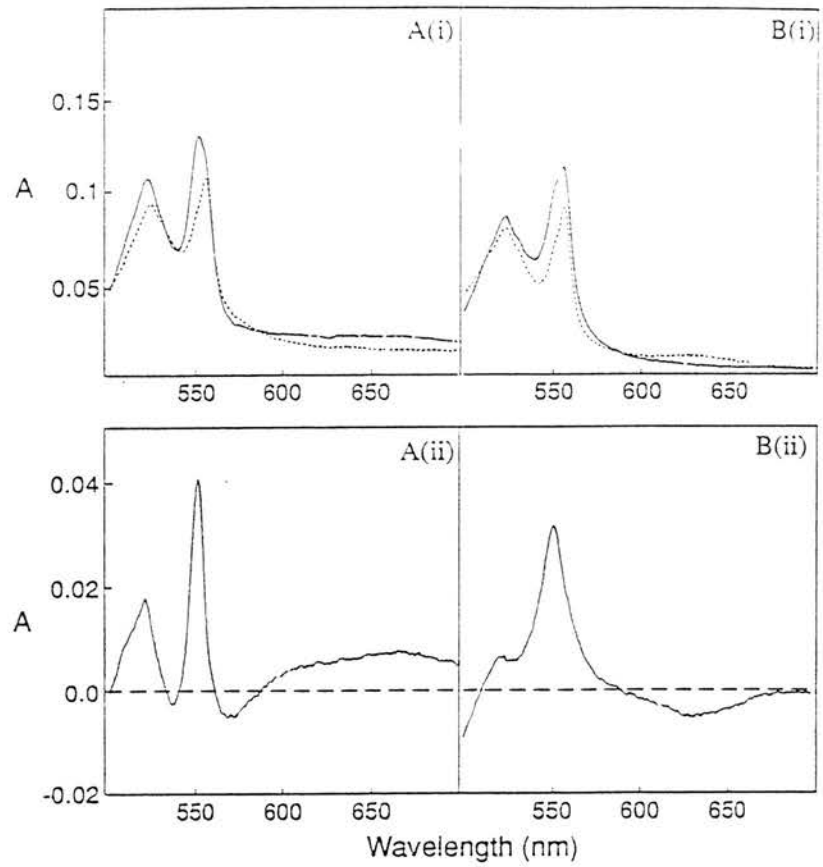

Figure 3.11 Spectral changes in the low potential haem after ascorbate reduction of cytochrome c peroxidase.

Anaerobic solutions of cytochrome c peroxidase (4μM) in 5mM Mes/5mM Hepes pH 7.5 in the absence (A) and presence (B) of 1mM $CaCl_2$ were reduced by addition of 1mM ascorbate and 5μM DAD. Under these conditions, the higher potential haem is reduced (HP_{red}) and the lower potential haem remains oxidised (LP_{ox}). This mixed valence enzyme was incubated at room temperature for 30 min to allow any spin state changes to occur. Small aliquots of a solution of anaerobic dithionite (50mM) in 100mM Mes/100mM Hepes pH 7.5 were added until full reduction of the enzyme was obtained ($LP_{red}HP_{red}$). The absolute spectra of $LP_{red}HP_{red}$ (----) and $LP_{ox}HP_{red}$ (- - - -) forms are shown in A(i) and B(i). The difference spectra (A(ii), B(ii)) of the $LP_{red}HP_{red}$ minus $LP_{ox}HP_{red}$ are the redox difference spectra of the low potential haem and gives information on its spin state.

stutzeri cytochromes c peroxidase have been shown to bind carbon monoxide, suggesting the low-potential haem remains high-spin when reduced (Foote, 1983; Villalain 1984).

These results show that the position and shape of the fully reduced α band of the *Paracoccus* peroxidase is dependent on the spin state of the low-potential haem. In the absence of Ca^{++} the fully reduced spectrum (with the low-potential haem in the low-spin state) has an α band peak at 551nm with a shoulder on the long wavelength side. In the presence of Ca^{++} (with the low-potential haem in the high-spin state) the α band peak is at 557nm with a shoulder at 551nm. A shift in the shoulder of the fully reduced α peak of *Rhodobacter capsulatus* cytochrome c peroxidase has been observed upon storage of the enzyme for one week at 4°C (Stuart Ferguson, personal communication). However it is not known whether this reflects a spin-state change in the reduced low-potential haem.

3.3.2 300 MHz ^{1}H nuclear magnetic resonance (n.m.r.) spectroscopy of cytochrome c peroxidase.

N.m.r. spectroscopy confirms the presence of a high-spin haem in the fully oxidised and mixed valence enzyme. The fully oxidised enzyme shows two groups of haem methyl resonances (figure 3.12(A)). The group of strongly downfield-shifted resonances at 58.2 (2 methyls), 55 and 51.5ppm arise from the partially high-spin, high-potential haem.The fully high-spin ferric cytochromes c′ have been shown to have very large-downfield shifted haem methyl resonances, in the region 60-90ppm (Emptage et al. 1981).The group of resonances at 33.2 and 23.8ppm arise from the low-spin, low-potential haem. The observation of a broad resonance near 90ppm, which is assigned to the ε-CH_3 group of an axial methionine, suggests that the partially haem has methionyl-histidinyl coordination (Moore 1985, Saraiva et al 1990).

A spectrum taken 60 min. after ascorbate addition shows the disappearance of the signals seen in the oxidised enzyme with a new set of resonances occurring between

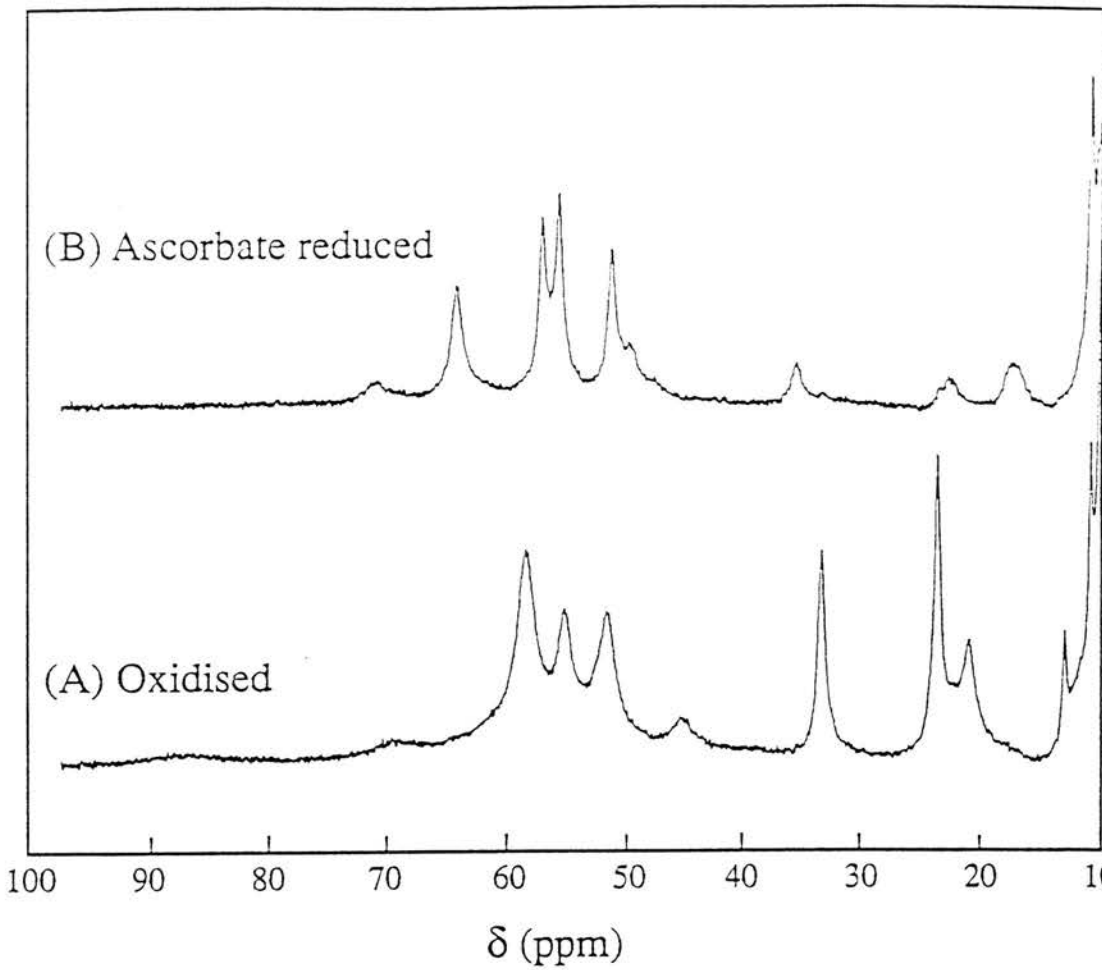

Figure 3.12 300 MHz ^{1}H n.m.r. spectroscopy of cytochrome c peroxidase. Spectra were recorded on a 1mM sample of enzyme in 10mM Mes/10mM Hepes pH 6 (99.8% ^2H_2O). T = 303K, ns = 5000. The oxidised spectrum (A) was obtained from an untreated peroxidase sample. The ascorbate-reduced spectrum (B) was obtained 60 min after addition of 5mM ascorbate/5μM DAD. Spectrum courtesy of S. Pissarra, C.T.Q.B., Portugal.

51 and 64ppm (figure 3.12(B)). The strong downfield shifts of these resonances arise from the oxidised low-potential haem in a state.

A summary of the n.m.r. data collected for bacterial cytochrome c peroxidases is shown in table 3.1.

3.3.3 Potentiometric redox titration of cytochrome c peroxidase.

Oxidative and reductive titrations were carried out in the absence and presence of Ca^{++} at pH 7.5. The respective reductive and oxidative titrations in the absence of calcium are shown in figures 3.13A(i) and 3.13A(ii). The respective reductive and oxidative titrations in the presence of calcium are shown in figures 3.14A(i) and 3.14A(ii). In both cases, because of the large separation of midpoint potential (E_m) values, the contribution of a higher potential haem could be easily separated from that of a lower potential haem, and, in each case, the individual contributions are fitted to Nernst plots with slopes of 59mV (25°C) (figures 3.13B and 3.14B).

The redox titration establishes the presence of a high-potential and low-potential haem as found in the Pseudomonad cytochrome c peroxidases (Ellfolk et al. 1983, Villalain et al. 1984). The high-potential haem has a midpoint potential of 176mV in the absence of Ca^{++} and 226mV in its presence. The latter value is consistent with an approximately isopotential electron transfer from the proposed electron donor, cytochrome c-550 (E_m= 0.25V, pH 7 (Kamen & Vernon 1955)). Non-concordance of the mid point potential of the high-potential haem in the absence and presence of Ca^{++} may reflect an influence of the spin state of the low-potential haem. When the high-potential haem is titrated in the presence of Ca^{++} the low-potential haem is high-spin, but in the absence of Ca^{++} it is low-spin.

The low-potential haem was difficult to titrate accurately, with poor reversibility of spectroscopic changes and a midpoint potential in the range -100 to -200mV. This difficulty may be due to spin state changes in this haem during the titration, perhaps as a result of alternative haem ligands being generated from dithionite. Orii & Anni (1990) have shown that H_2O_2 forms transiently during the aerobic reduction of yeast

An alternative explanation would be that Ca^{++} has a more direct effect on the redox state of the high-potential haem. The more positive E_m in the presence of Ca^{++} suggests stabilisation of the reduced form with tighter binding of Ca^{++} to this form.

Table 3.1 N.m.r. and e.p.r. data for bacterial cytochrome c peroxidases.

Organism	Oxidised				Ascorbate-reduced[c]		Spin-state Assignments				Reference
	High potential haem		Low potential haem		Low potential haem		Oxidised		Ascorbate-reduced		
	NMR[a]	EPR[b]	NMR[a]	EPR[b]	NMR[a]	EPR[b]	HP haem[d]	LP haem[e]	HP haem[d]	LP haem[e]	
Ps. aeruginosa	19.5, 21.5 ppm	g = 3.24	45-65 ppm	g = 2.93	45-65 ppm	g = 2.84	Low	High	Low	High	Ellfolk et al. 1984
		g = 3.3		g = 3.0		g = 2.85	High	Low	Low	High	Foote et al. 1984
Ps. stutzeri	22.7, 32.0 ppm	g = 3.39	55-70 ppm	g = 3.01	53-62 ppm	g = 2.94	Low	High	Low	High	Villalain et al. 1984
Pa. denitrificans	53-62 ppm	g = 3.41	24, 34.3 ppm	g = 3.0	48-61 ppm	g = 3.3	High	Low	Low	High	this study.

[a] position of resolved downfield-shifted haem methyls

[b] g max values

[c] ascorbate-reduced high potential haem is EPR invisible and, due to being much less strongly downfield shifted, is not resolved in NMR.

[d] HP haem, high-potential haem

[e] LP haem, low-potential haem

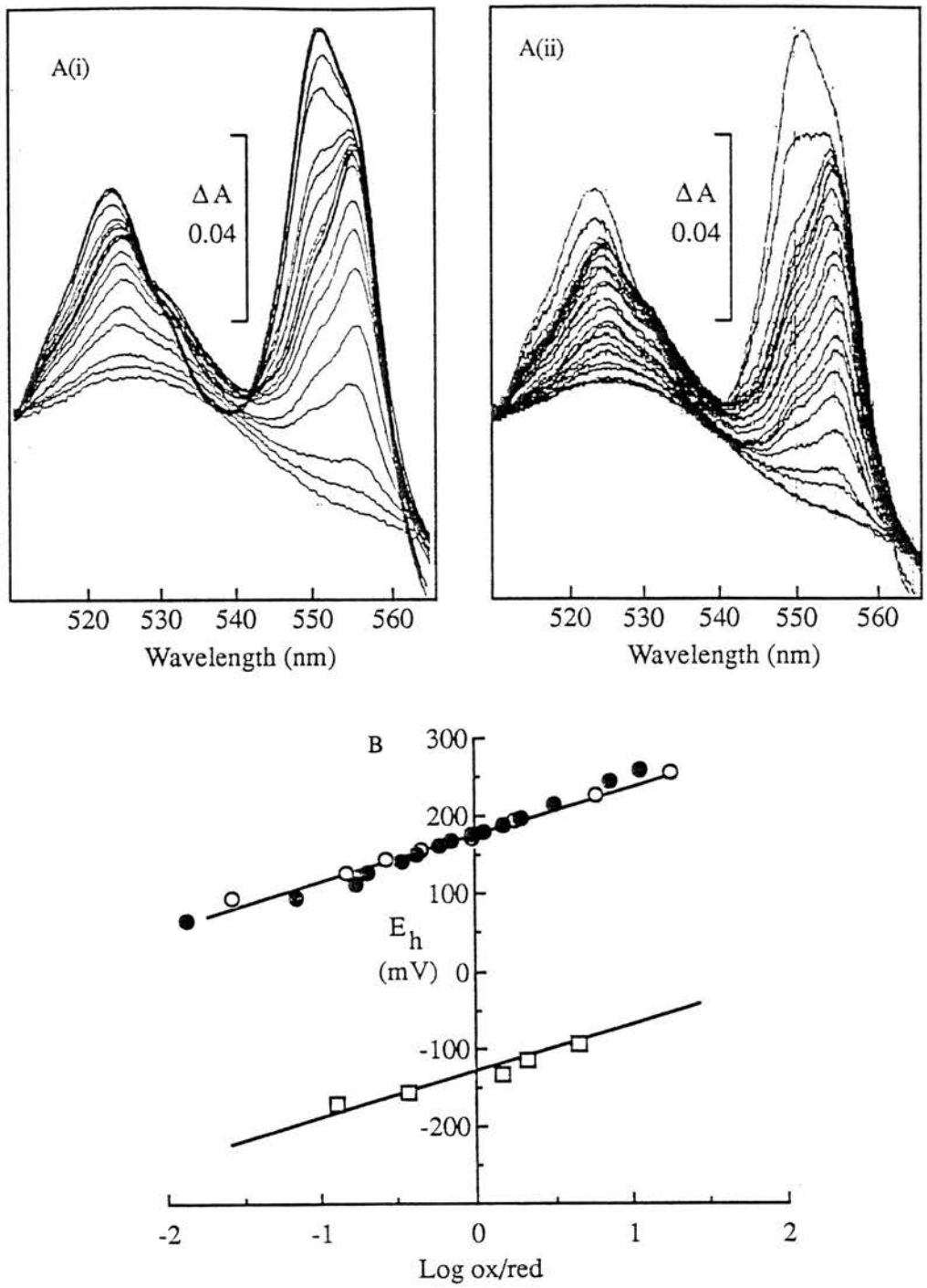

Figure 3.13 Potentiometric redox titration of cytochrome c peroxidase in the absence of Ca^{++}.

The redox titration was performed as described in Methods section 3.2.1. A(i) and A(ii) show the reductive and oxidative titrations of the peroxidase respectively, as followed in the region of the α and β bands. B is a Nernst analysis of the high and low potential components. Closed circles are for the oxidative titration. Open circles are for the reductive titration.

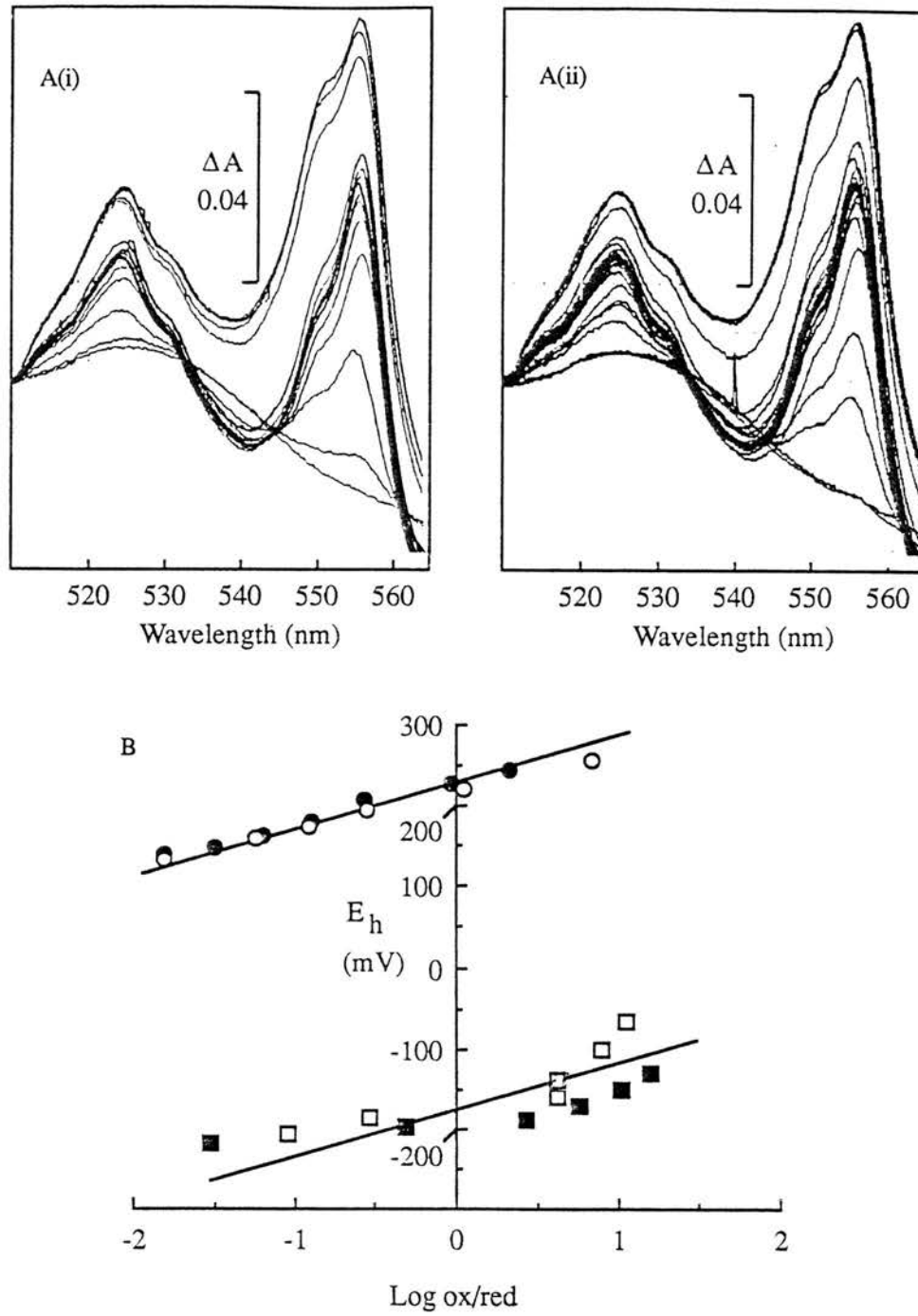

Figure 3.14 Potentiometric redox titration of cytochrome c peroxidase in the presence of Ca^{++}.

The redox titration was performed as described in Methods section 3.2.1. A(i) and A(ii) show the reductive and oxidative titrations of the peroxidase respectively, as followed in the region of the α and β bands. B is a Nernst analysis of the high and low potential components. Closed circles are for the oxidative titration. Open circles are for the reductive titration.

cytochrome c peroxidase by sodium dithionite. The presence of any peroxide during the redox titration of the *Paracoccus* peroxidase would result in binding to the low-potential haem and possible catalysis. Such reactions would be likely to interfere with the redox titration. The mid-point potential for the peroxidatic haems of other peroxidases are : *Pseudomonas aeruginosa* peroxidase, -330mV (Ellfolk et al. 1983); horseradish peroxidase, -270mV (Harbury 1957); yeast cytochrome c peroxidase, -190mV (Conroy et al. 1978)).

3.3.4 Electron paramagnetic resonance (e.p.r) spectroscopy of cytochrome c peroxidase.

The high to low-spin transition seen upon cooling the enzyme from 20 to 0°C (figure 3.8(iii)) means that when the enzyme is subjected to e.p.r. spectroscopy, carried out at 8K, very little in the way of high-spin features will be observed.The e.p.r. spectrum of the oxidised enzyme shown in figure 3.15 indicates the presence of three spectral components. The signals at g = 3.41 and g = 3.0 are indicative of two haems in a low-spin state with the signal at g = 6.0 representing a minor high-spin component.

The relative intensity of the signal at g = 3.41 compared to that at g = 3.0 is less than one. It is therefore possible that the signal at g = 6.0 represents a small proportion of the haem with g = 3.41 in a high-spin state even at very low temperature, although it does not disappear after ascorbate reduction.

Ascorbate reduction of the enzyme results in the loss of the g = 3.41 signal with initially no change in the g = 3.0 signal. From this we conclude that the g = 3.41 signal is that of the high-potential haem while the low-potential haem is represented by the g = 3.0 signal. This g = 3.0 signal disappears over a 60 min. period as new spectral features appear at g = 3.3 (82%), g = 2.9 (16%) and g = 2.79 (2%).The alteration in the e.p.r. signal represents a change in the coordination structure around the haem. It is this same slow process that at room temperature gives rise to the high-spin state of that haem.

Interestingly, an inactive form of the *Pseudomonas aeruginosa* peroxidase has

The relative intensities of the e.p.r. signals are determined using a computer program which simulates the experimentally determined spectra using the values for g_z, g_y, and g_x and integrates the resulting signals (see More et al 1990).

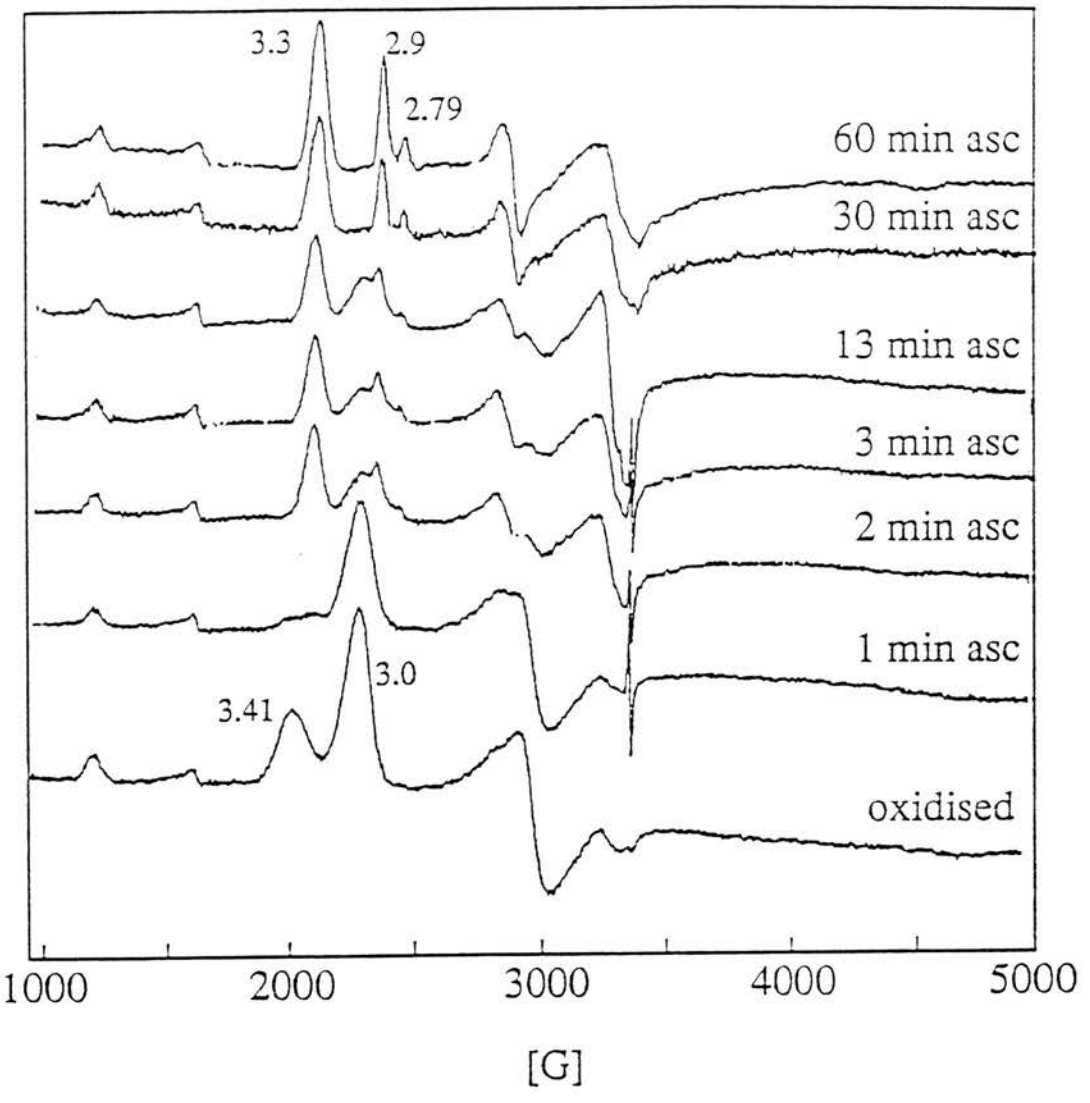

Figure 3.15 E.p.r. spectroscopy of cytochrome c peroxidase.

Spectra were recorded from a 337μM sample of enzyme in 10mM NaCl, 1mM phosphate, pH 7. Temperature: 8K, microwave frequency 9.45GHz, microwave power 2mW, modulation 10.39, gain 1.6 x 10^5. The oxidised spectrum was obtained from an untreated sample of enzyme. Ascorbate was used to obtain the mixed-valence spectrum. Spectrum recorded by S. Prazeres (C.T.Q.B., Lisbon).

been found in which no ferric high-spin state forms after ascorbate reduction (Foote et al. 1985). This inactive form has a g = 3 e.p.r. signal like the transient ascorbate-reduced form of the *Paracoccus* enzyme and may correspond in structure to this form.

A summary of e.p.r. data for the bacterial peroxidases is shown in table 3.1. The signals for the individual peroxidases are similar, except for the signal arising from the low-potential haem of the mixed valence form of the *Paracoccus* enzyme. The g-value of 3.3 is a somewhat higher value than observed for the other peroxidases.

3.3.5 Cyanide titration of cytochrome c peroxidase

No change in the spectrum of the oxidised enzyme is observed upon addition of up to 150μM cyanide (results not shown). This result indicates that the high-spin haem of the fully oxidised enzyme is not available for ligand binding, a result not surprising considering that the high-spin haem in this state is the high-potential, electron-transferring haem. The fully oxidised form of *Pseudomonas aeruginosa* peroxidase is also unable to bind cyanide unless concentrations of over 4mM are used, at which point reduction of the enzyme is also seen (Ellfolk et al. 1984a).

When the ascorbate-reduced, aged enzyme (in 1mM $CaCl_2$) is titrated with cyanide, marked spectral changes occur, representing a high to low-spin transition in the oxidised low-potential haem (figure 3.16A). The decrease in absorbance at 380nm can be used as a measure of CN^- bound to the peroxidase. The experimental data fit a theoretical saturation curve created for the titration of a single binding site per protein molecule with a dissociation constant of 5μM (figure 3.16B) which is similar to the 23μM found for the *Pseudomonas aeruginosa* peroxidase (Ellfolk et al. 1984a). The Soret band of the low-potential haem with CN^- bound is more red-shifted than would be expected for a low-spin low-potential haem. This is a result of the CN^- ligation and has also been observed in the CN^- adducts of *Pseudomonas aeruginosa* (Ellfolk et al. 1984a), horseradish (Keilin & Hartree 1951), and yeast cytochrome c peroxidases (Sievers 1978).

Figure 3.16 Cyanide titration of the ascorbate-reduced form of cytochrome c peroxidase.

A 1.76μM solution of cytochrome c peroxidase in 5mM Mes/5mM Hepes pH 6, 1mM $CaCl_2$ was reduced with 1mM ascorbate, 5μM DAD. The sample was aged for 60 min at room temperature to allow formation of the high-spin state. A cyanide titration was performed using a stock neutralised sodium cyanide solution. Selected spectra are shown at the following CN^- concentrations: 0, 0.5, 1.5, 3.5, 6.0, 10.0, 15.0, 40.0, 110.0, 150.0μM (A). The dissociation constant for CN^- binding was calculated using the decrease in absorbance at 380nm as an indicator of CN^- bound to the enzyme. (B) shows a plot of CN^--bound peroxidase versus log $[CN^-]_{free}$. The experimental points are fitted to a theoretical curve for the titration of a single binding site with a K_D of 5μM.

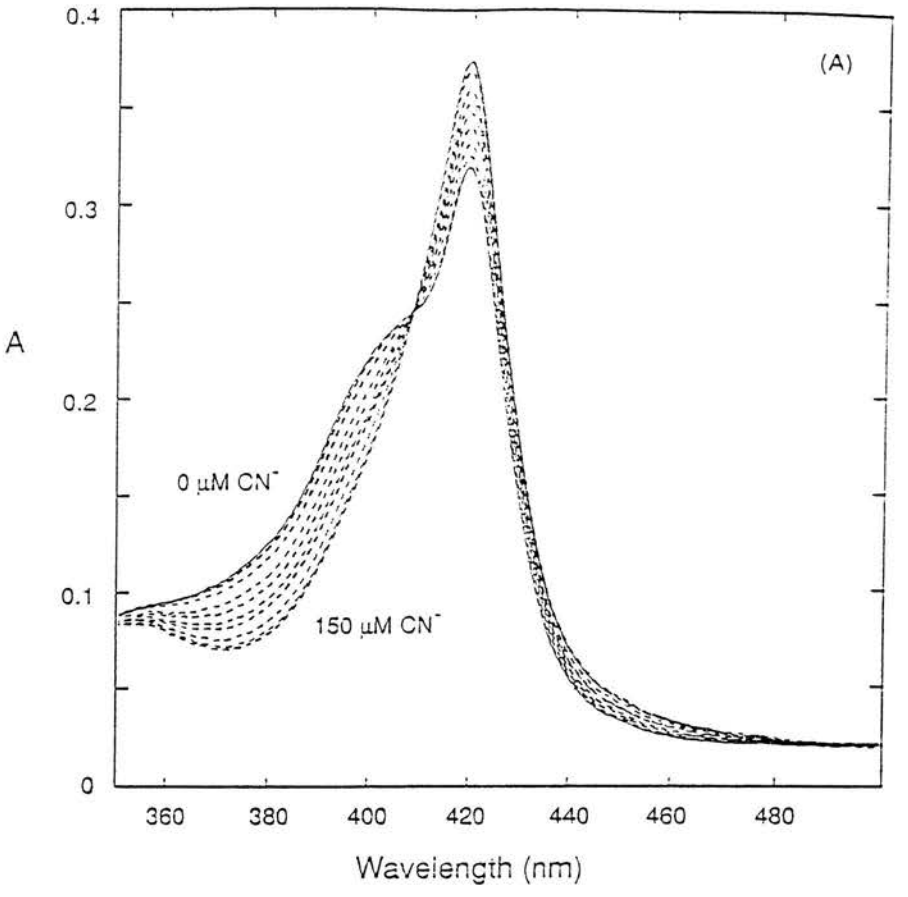
(A)
A
0.4
0.3
0.2
0.1
0
0 μM CN⁻
150 μM CN⁻
360
380
400
420
440
460
480
Wavelength (nm)

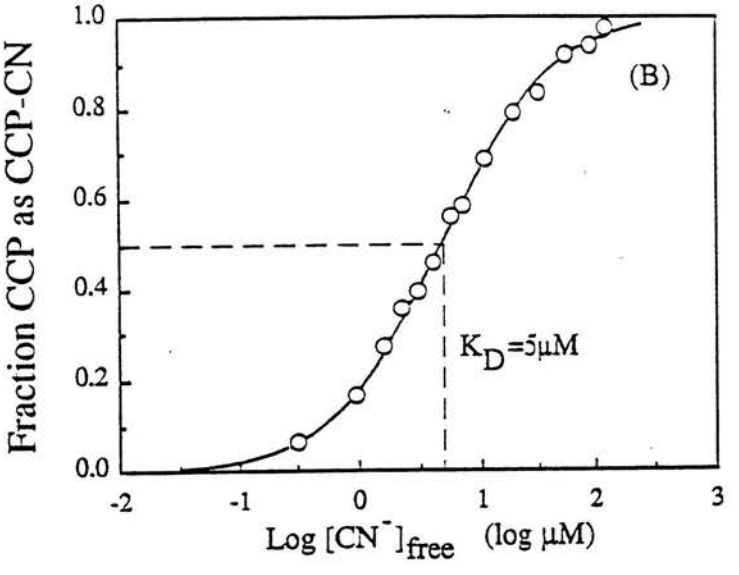
(B)
Fraction CCP as CCP-CN
1.0
0.8
0.6
0.4
0.2
0.0
K_D=5μM
-2
-1
0
1
2
3
Log [CN⁻]free (log μM)

3.3.6 Effect of EGTA on cytochrome c peroxidase spectra

3.3.6.1 Oxidised cytochrome c peroxidase.

At pH 6, EGTA treatment of the oxidised form of cytochrome c peroxidase results in shift of absorbance in the Soret region from 410nm to 400nm (figure 3.17(a)). Loss of absorbance at 380nm is also observed in some samples, although not in others. The shift in the Soret peak towards the u.v. region is interpreted as a low-spin to high-spin transition in one of the haems. Ascorbate reduction of the EGTA-treated, oxidised enzyme is complete within 2 min., however, the slow appearance of high-spin signals normally observed at this pH are no longer present (figure 3.17(b)). This suggests the EGTA has removed the residual Ca^{++} which is responsible for the slow appearance of the high-spin state.

The effect of EGTA on the oxidised enzyme at pH 7.5 is shown in figure 3.18. Although the shift in the Soret absorbance is similar to that caused by EGTA treatment at pH 6, the actual amount of absorbance shifted is much smaller. It is not known why the EGTA effect is less pronounced. It is possible that less Ca^{++} is bound at this site at higher pH. This would be consistent with the observation that no 380nm high-spin state is formed after ascorbate-reduction at this pH (figure 3.10). Loss of absorbance at 380nm is also observed. This loss may be associated with a conversion of a portion of the high-potential haem to a low-spin state.

3.3.6.2 Ascorbate-reduced cytochrome c peroxidase.

EGTA treatment of the ascorbate-reduced, aged enzyme at pH 6 produces two spectral effects which can be separated in time. The initial effect is rapid (complete within 2 min) and is similar to that seen on the oxidised enzyme, i.e. gain of absorbance at 400nm with loss at 410nm (figure 3.19(b)). This effect is interpreted as a transition to a high-spin state of the proportion of the low-potential haem that is still low-spin. The effect of EGTA on this form of the enzyme appears more pronounced than on the oxidised form. In addition, the presence of EGTA results in a shift of the α band of the reduced high-potential haem to a longer wavelength (figure 3.19(b)).

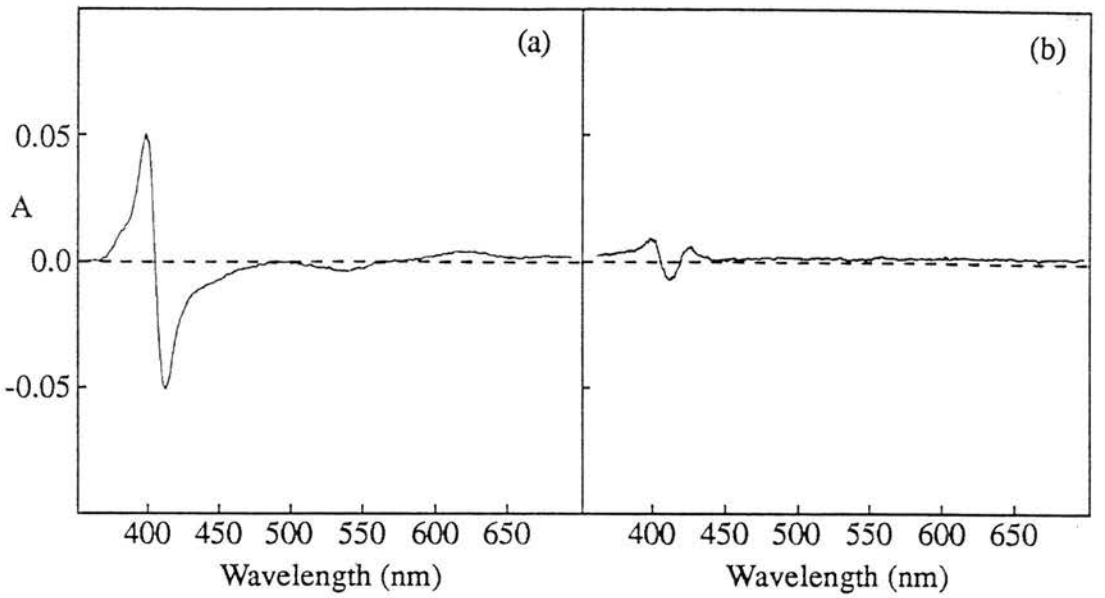

Figure 3.17 Effect of EGTA on oxidised cytochrome c peroxidase at pH 6. A 4μM solution of cytochrome c peroxidase in 5mM Mes/Hepes, pH 6 was treated with 1mM EGTA. (a) shows a spectrum of the enzyme treated with EGTA for 2 min against the untreated enzyme. The EGTA-treated, oxidised enzyme was reduced by addition of ascorbate (1mM) and DAD (5μM). The ascorbate-reduced enzyme was aged at room temperature for 30 min. (b) is a difference spectrum of the enzyme 30 min after ascorbate-reduction minus the enzyme 2 min after ascorbate-reduction and shows the absence of the high spin signals normally observed after aging at this pH (compare with figure 3.8).

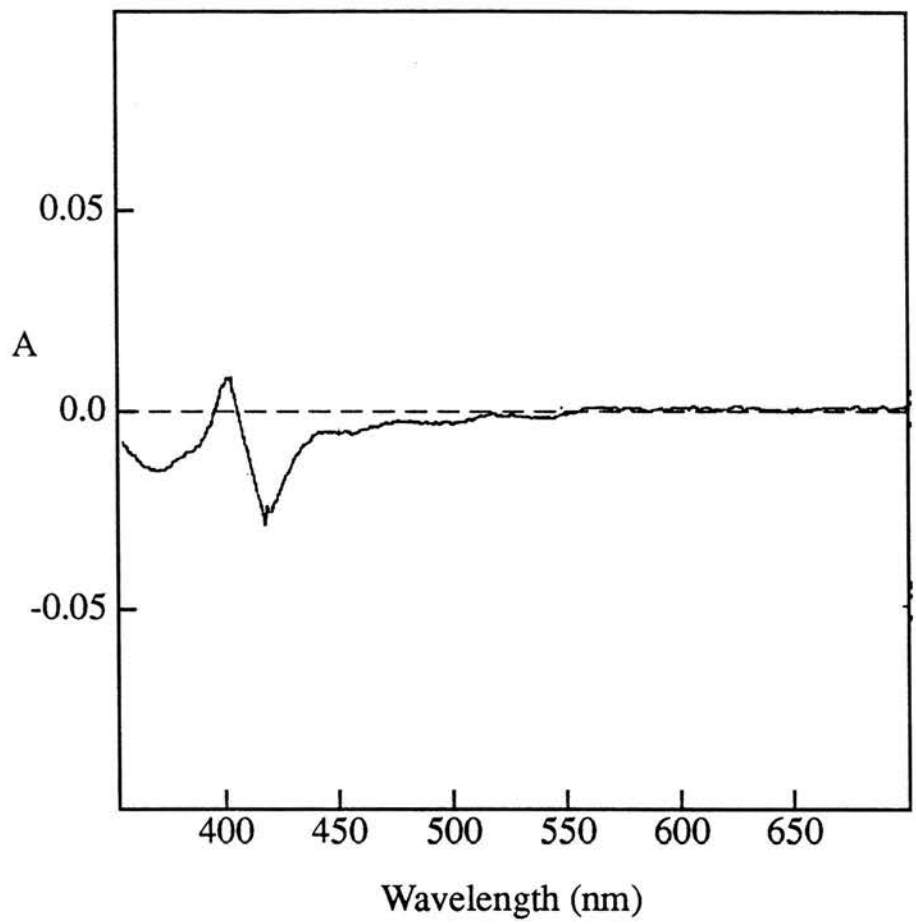

Figure 3.18 Effect of EGTA on oxidised cytochrome c peroxidase at pH 7.5. A 4μM solution of cytochrome c peroxidase in 5mM Mes/Hepes, pH 7.5 was treated with 1mM EGTA. The difference spectrum shows the enzyme treated with EGTA for 2 min against the untreated enzyme.

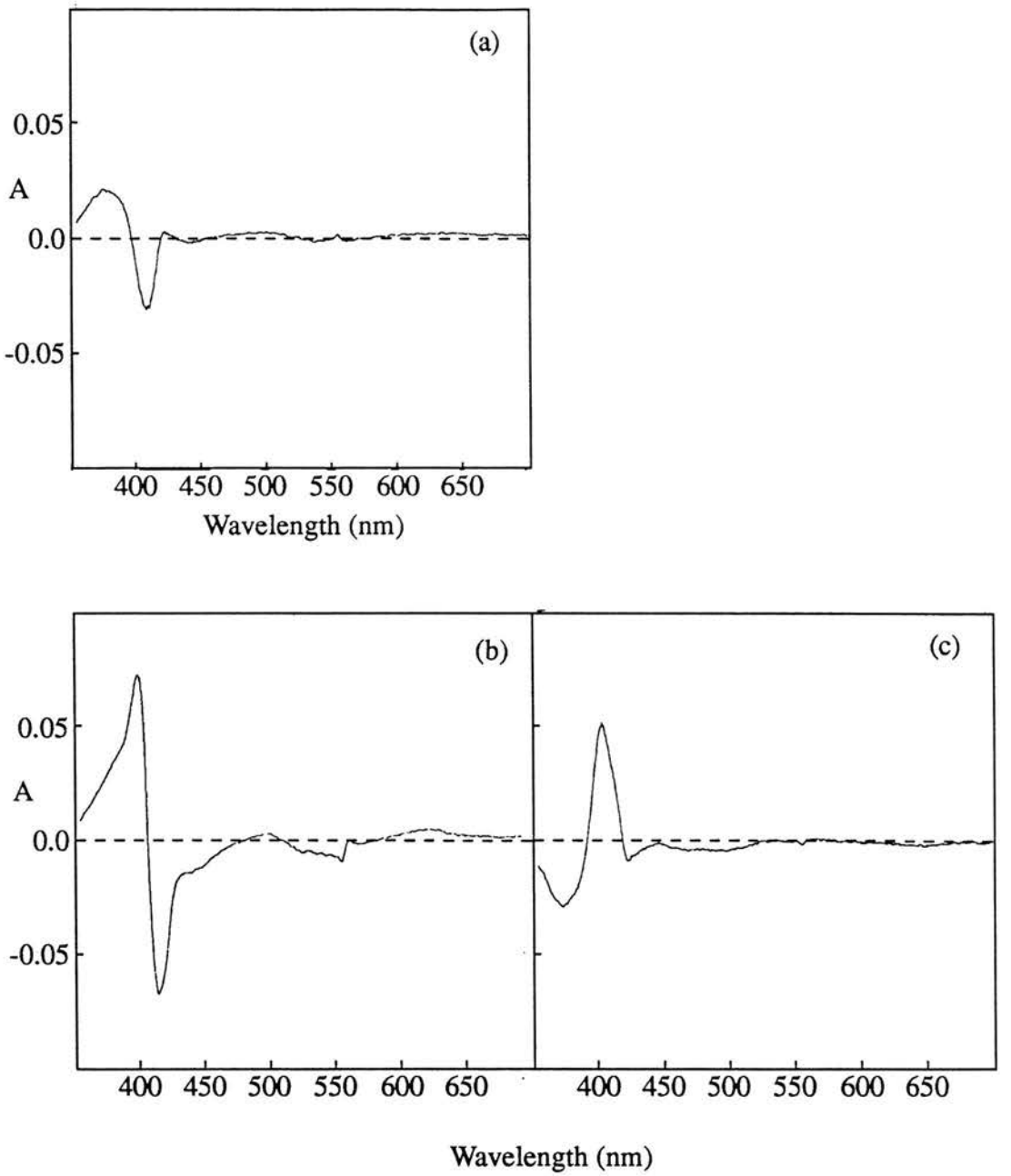

Figure 3.19 Effect of EGTA on ascorbate-reduced cytochrome c peroxidase, pH 6.

A 4μM solution of cytochrome c peroxidase in 5mM Mes/Hepes, pH 6 was reduced with 1mM ascorbate/ 5μM DAD. The sample was aged for 45 min at room temperature to allow formation of the high spin state. (a) is a difference spectrum of the enzyme 45 min after ascorbate reduction against the enzyme 2 min after ascorbate reduction. Using this spectrum as a baseline, the effect of 1mM EGTA, 2 min after addition can be seen (b). (c) is a spectrum 45 min after EGTA addition minus the spectrum 2 min after EGTA addition, and shows the slow phase of the EGTA effect, i.e. a shift of absorbance from 380nm to 400nm.

The secondary effect of the EGTA is over a much longer time scale (45 min) and involves conversion of the 380nm species formed during aging (figure 3.19(a)) to a 400nm species (figure 3.19(c)). The magnitude of the 380nm loss is almost identical to the 380nm gain during the aging process. This secondary effect of EGTA is interpreted as a conversion of the Ca^{++}-induced high-spin state to an EGTA-induced high-spin state.

The effect of EGTA on the ascorbate-reduced enzyme at pH 7.5 is biphasic. The initial, rapid effect (figure 3.20(i)) is similar to that seen at pH 6, i.e. a shift in the Soret absorbance towards the u.v. region of the spectrum with a concomitant small shift in the α band of the reduced high-potential haem to a longer wavelength. The slower EGTA effect takes place over a number of hours and is similar to the initial effect, except no α band shift is observed (figure 3.20(ii)). It is possible that at this pH two forms of the enzyme exist. One form contains Ca^{++} which can be removed rapidly with a resultant shift in the α band. In the second form, the Ca^{++} is removed much more slowly with no effect on the α band.

3.3.6.3 Summary of Ca^{++} and EGTA effects on the peroxidase.

The effects of Ca^{++} and EGTA on the peroxidase spectra suggest the enzyme binds two Ca^{++} ions. The high affinity Ca^{++}-binding site is responsible for maintaining the low-potential haem in a low-spin state. This site is normally filled, since addition of Ca^{++} produces no spectral change associated with this site. Removal of this Ca^{++} by EGTA treatment converts the low-potential haem to a 400nm high-spin form. The lower affinity Ca^{++} binding site is only partially filled at pH 6 and is unfilled at pH 7.5. Binding of Ca^{++} to this site promotes formation of the 380nm high-spin state.

A model for the effects of Ca^{++} and EGTA on the enzyme is shown in figure 3.21. It should be noted that this model takes no account of the biphasic effect of

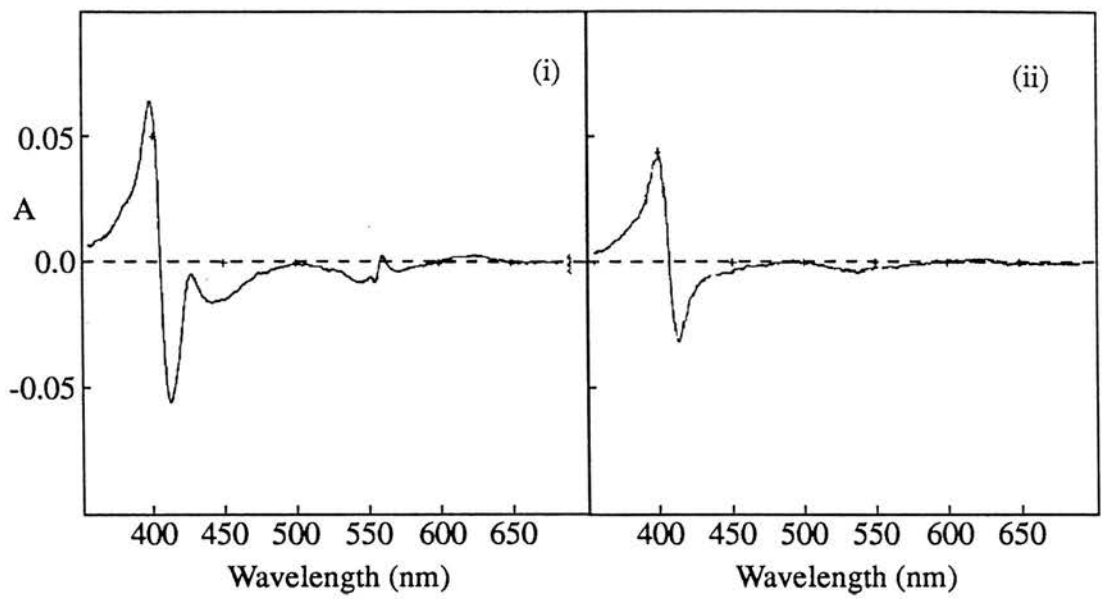

Figure 3.20 Effect of EGTA on ascorbate-reduced cytochrome c peroxidase, pH 7.5.

A 4μM solution of cytochrome c peroxidase in 5mM Mes/Hepes, pH 7.5 was reduced with 1mM ascorbate, 5μM DAD. 1mM EGTA was added 30 min after ascorbate reduction. (i) is a difference spectrum of the enzyme 2 min after EGTA addition minus the nonEGTA-treated enzyme. After EGTA addition the enzyme was incubated at room temperature and any further changes in the spectrum followed. (ii) is a difference spectrum of the enzyme 90 min after EGTA addition versus the enzyme 2 min after EGTA addition.

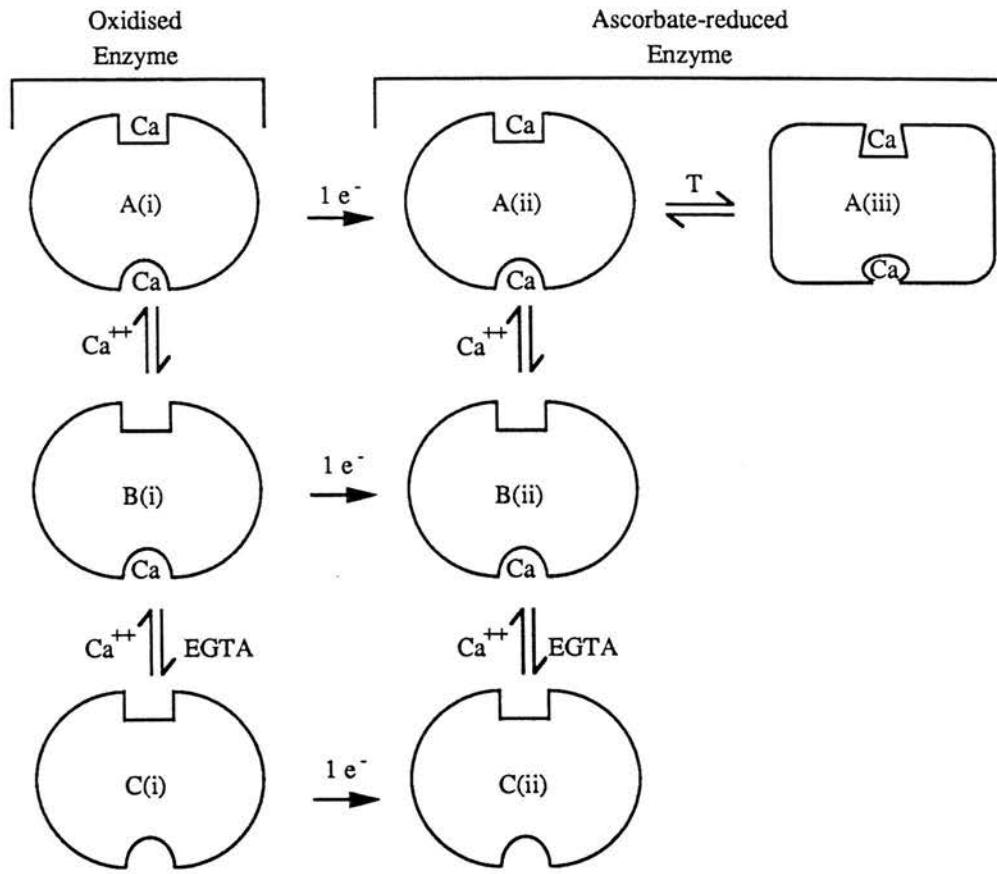

Figure 3.21 Model of Ca^{++} binding to *Paracoccus* cytochrome c peroxidase.

The enzyme is shown to have two Ca^{++} binding sites. The oxidised enzyme exists in equilibrium between forms A(i) and B(i) at pH 6, but is found entirely as form B(i) at pH 7.5. Addition of Ca^{++} at this stage, to convert all the enzyme to the A(i) form has no effect on the spectrum of the peroxidase. Removal of all the Ca^{++} by EGTA treatment results in a conversion of one haem from a low spin 410nm species to a high spin 400nm species, to yield form C(i). The ascorbate-reduced enzyme at pH 6 exists in equilibrium between forms A(ii) and B(ii). Conversion of the B(ii) form to A(ii) is associated with gain of a high spin 380nm signal and loss of a low spin 410nm signal. Removal of Ca^{++} from the ascorbate-reduced form by EGTA yields form C(ii) which is characterised by appearance of a 400nm high spin signal. At pH 7.5 the ascorbate-reduced enzyme exists entirely as form B(ii). This form can be converted to A(ii) by addition of Ca^{++} ions, with gain of a high spin 380nm signal and loss of a low spin 410nm signal. Alternatively, B(ii) can be converted to C(ii) by EGTA treatment. A reduction in temperature can convert the fully active form A(ii) into the form A(iii) which contains the bound Ca^{++} but has no 380nm band. This form exists when the enzyme is studied under the low temperatures used in e.p.r. spectroscopy (see figure 3.15).

EGTA on the ascorbate-reduced enzyme at pH 7.5.

3.3.7 Calcium titration of cytochrome c peroxidase.

3.3.7.1. Unbuffered calcium (absence of EGTA).

3.3.7.1.1 Oxidised cytochrome c peroxidase.

Since addition of calcium to the oxidised enzyme produces no spectral effect, this form of the enzyme cannot be titrated when using spectroscopy as a measure of bound calcium.

3.3.7.1.2 Ascorbate-reduced cytochrome c peroxidase.

The high-spin, 380nm band of the ascorbate-reduced peroxidase at pH 7.5 was titrated with calcium. Since no high-spin state forms after ascorbate-reduction at this pH, any calcium which is in the solution can be ignored as insignificant.

The spectra collected during the titration are shown in figure 3.22A. The data points from the titration are fitted to a theoretical saturation curve for the titration of a single binding site per protein molecule with a K_D of 75μM (figure 3.22B). Although the latter points fit reasonably well to the curve, the points corresponding to lower Ca^{++} concentrations fall below the line, suggesting there is less bound Ca^{++} at these lower concentrations than would be expected for this K_D. One possible explanation is that the rate of high-spin formation is dependent on the Ca^{++} concentration, such that the high-spin state formed by the lower Ca^{++} concentrations has not reached an endpoint over the 30 min time gap between Ca^{++} addition and scanning of the spectrum. A comparison of the time dependence of high-spin formation for a low (75μM) (figure 3.23(i)) and a high (500μM) (figure 3.23(ii)) Ca^{++} concentration confirms that the time required for the high-spin formation by 75μM Ca^{++} is longer (not complete after the 30 min) than that required by 500μM Ca^{++}. In addition,

Figure 3.22 Ca^{++} titration of ascorbate-reduced cytochrome c peroxidase, pH 7.5.

A 4μM solution of cytochrome c peroxidase in 5mM Mes/Hepes, pH 7.5 was reduced with 1mM ascorbate/ 5μM DAD. The 380nm band was titrated with $CaCl_2$ from a 100mM stock. The spectra were scanned 30 min after addition of each aliquot of Ca^{++} (a). The spectra are represented as difference spectra of the ascorbate-reduced + Ca^{++} enzyme minus the ascorbate-reduced enzyme. The temperature was kept constant at 25°C. The spectra shown correspond to the following Ca^{++} concentrations : 0μM, 50μM, 100μM, 125μM,150μM, 200μM, 300μM, 500μM, 1000μM, 2000μM. The increase in absorbance at 380nm can be used to estimate the dissociation constant for Ca^{++} binding to the enzyme. The data were fitted to a theoretical saturation curve created for the titration of a single binding site per protein molecule with a K_D of 75μM.

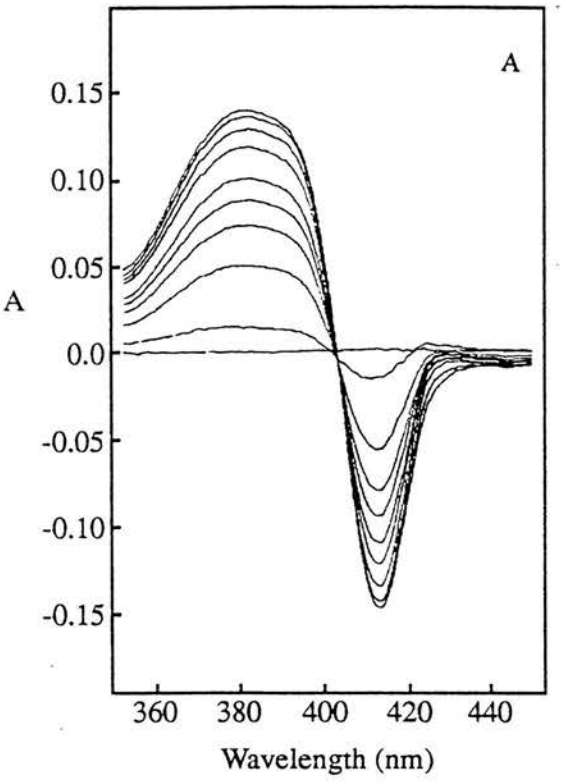
A
0.15
0.10
0.05
A
0.0
-0.05
-0.10
-0.15
360
380
400
420
440
Wavelength (nm)

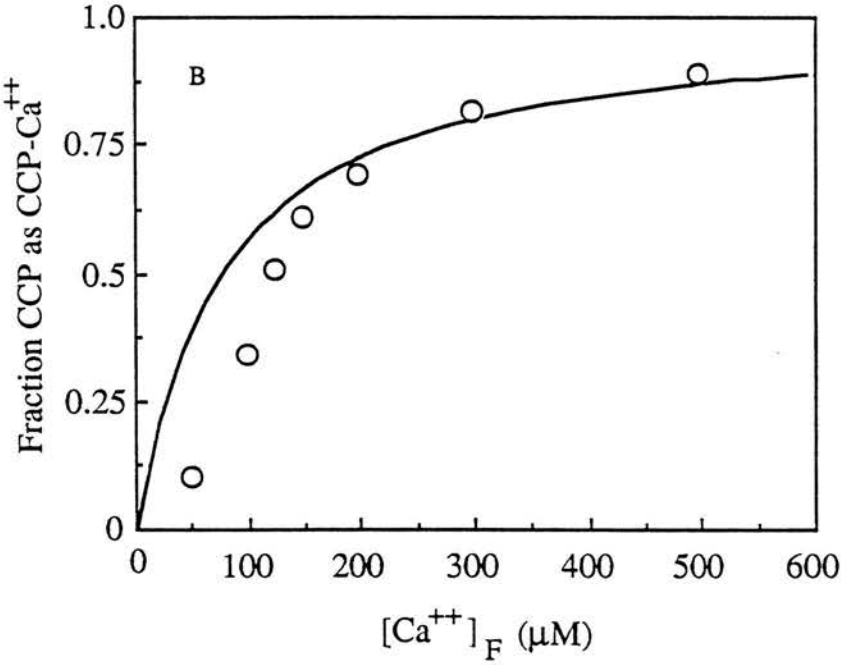
B
1.0
0.75
0.5
0.25
0
Fraction CCP as CCP-Ca++
0
100
200
300
400
500
600
[Ca++]F (μM)

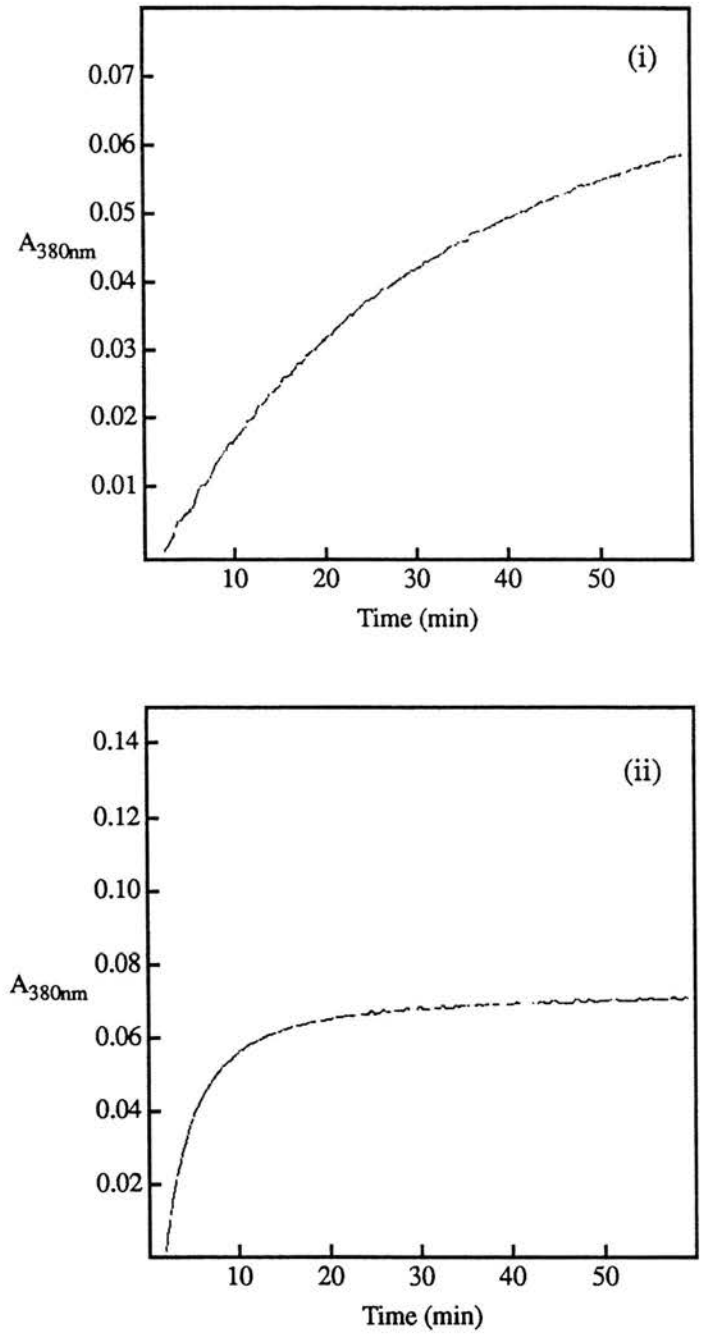

Figure 3.23 Rate of high spin formation in ascorbate-reduced cytochrome c peroxidase, pH 7.5.

The rate of high spin formation at two different Ca^{++} concentrations was measured by following the rate of increase in absorbance at 380nm. (i) shows the rate of high spin formation in an ascorbate-reduced sample treated with 75μM Ca^{++} and (ii) shows the rate of high spin formation in an ascorbate-reduced sample treated with 500μM Ca^{++}.

extrapolating the progress curve for the 75μM Ca^{++} yields the same endpoint as that for the 500μM Ca^{++}. This suggests the K_D is certainly lower than that estimated from this experiment and that the plot of figure 3.22B must be ignored as unreliable. The excessively long time required for the effects of the low Ca^{++} concentrations to reach an end point (>60 min) makes this titration unfeasible. The only conclusion which can be drawn is that the K_D is significantly less than 75μM.

A Ca^{++} titration of the ascorbate-reduced enzyme at pH 6 is complicated by two factors. Firstly, the majority of the high-spin state forms before any addition of Ca^{++} is made. This means when the data are fitted to a theoretical saturation curve, only the latter part of the curve will contain any experimental points. Any deviation in the early part of the curve will not be observed. The second complicating factor is that, like pH 7.5, the effects produced by Ca^{++} addition take up to two hours to complete. This very slow formation of the high-spin state makes determination of the end-point for each Ca^{++} addition very difficult to determine with any confidence.

3.3.7.2 EGTA-Buffered calcium

The use of EGTA as a calcium buffer facilitated the calcium titrations by removing all the residual Ca^{++} on the enzyme. This allowed titrations of the oxidised enzyme and a full titration of the ascorbate-reduced enzyme at pH 6. In all titrations carried out in the presence of EGTA, the rate of high-spin formation was observed to be more rapid than when the titrations were carried out in its absence. Although the more rapid attainment of equilibrium is desirable, it should be noted that the enzyme may not be in the same form when titrated with Ca^{++} in the presence of EGTA and when titrated with Ca^{++} in the absence of EGTA. It is unclear why EGTA should enhance the rate of Ca^{++} binding to the enzyme.

3.3.7.2.1 Oxidised cytochrome c peroxidase.

The EGTA-treated oxidised enzyme at pH 6 (figure 3.24A(i)) was titrated with Ca^{++} as shown in figure 3.24A(ii). The data fit reasonably well to a theoretical saturation curve for a single binding site with a K_D of 0.44μM (figure 3.24B(i)). The points corresponding to the higher Ca^{++} concentrations are seen to deviate slightly from the theoretical curve. A deviation of this type would be observed if the end-point of the titration has been underestimated. An underestimate of the true endpoint may occur as a result of dilution by Ca^{++} additions during the titration. Although it is difficult to see, the last spectrum in figure 3.24A(ii) is slightly downward shifted, possibly as a result of dilution by the Ca^{++} addition. If the end-point is adjusted upwards slightly to $A_{412nm} = 0.055$, the data fit very well onto a saturation curve with a K_D of 0.5μM (figure 3.24B(ii)).

3.3.7.2.2 Ascorbate-reduced cytochrome c peroxidase.

Figure 3.25 shows a Ca^{++} titration of a sample of ascorbate-reduced enzyme at pH 6 which had been previously treated with EGTA in the oxidised form. The titration has two phases which overlap (figure 3.25A). The initial phase, at low Ca^{++} concentarations, is the reverse of the rapid EGTA effect seen on the ascorbate-reduced enzyme at this pH (figure 3.19(b)). The spectral signals corresponding to this initial phase become contaminated early in the titration by signals from the second phase (figure 3.25A)). The signals from the second phase correspond to the appearance of the 380nm band normally seen when Ca^{++} is added to the ascorbate-reduced enzyme.The overlap suggests the strength of Ca^{++} binding at each site is of the same order of magnitude. It is assumed that the two phases are more separated at pH 7.5, since the ascorbate-reduced enzyme at this pH has one site filled and one site empty.

It is not possible to plot a saturation curve for the first phase of the titration since the spectra become contaminated very early in the titration by the second phase effects. However since the 380nm change absorbance is due almost entirely to the second phase, it is possible to plot a saturation curve for the data at this wavelength.

Figure 3.24 Ca^{++} Titration of EGTA-treated, oxidised cytochrome c peroxidase, pH 6.

A 4μM solution of cytochrome c peroxidase in 5mM Mes/ Hepes pH 6 was treated with 5mM EGTA (pH6). A(i) shows the spectrum of the EGTA-treated oxidised enzyme versus the untreated oxidised enzyme. The EGTA-treated enzyme was titrated with Ca^{++}, with the spectrum recorded 30 min after each Ca^{++} addition (A(ii)). Each spectrum is represented as a difference spectrum, from which the EGTA-treated, oxidised spectrum has been subtracted. The spectra correspond to free Ca^{++} concentrations of : 47nM, 189nM, 385nM, 675nM, 1167nM, 1570nM, and 8600nM. The data from the titration were fitted to two theoretical saturation curves for the titration of a single binding site per protein molecule. B(i) shows the data fitted to a theoretical curve with a K_D of 0.44μM. The experimental data points were plotted using the endpoint for the titration (ΔA_{412nm}) as 0.05. (see text). In B(ii) the data points were calculated assuming an endpoint for the titration (ΔA_{412nm}) of 0.055 (see text) and are plotted onto a theoretical saturation curve corresponding to a K_D of 0.5μM.

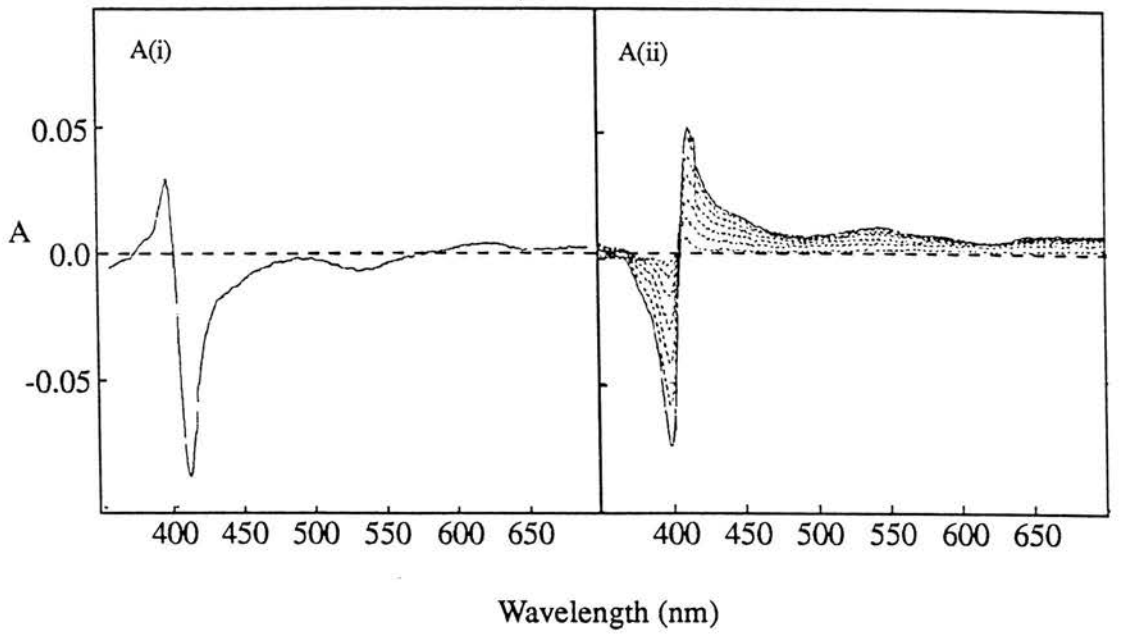
A(i)
A(ii)
0.05
A
0.0
-0.05
400 450 500 550 600 650
400 450 500 550 600 650
Wavelength (nm)

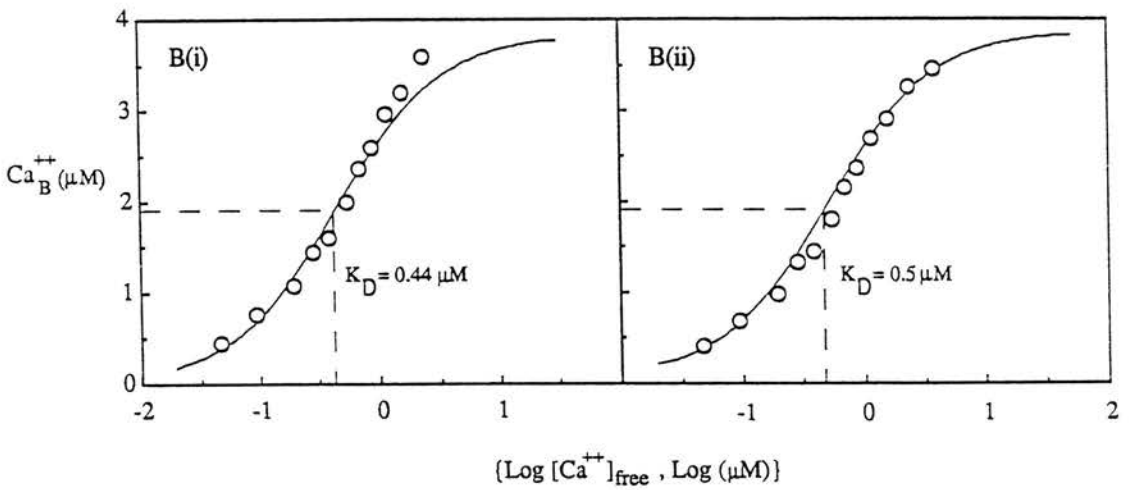
B(i)
B(ii)
Ca^{++}_{B} (μM)
4
3
2
1
0
K_D = 0.44 μM
K_D = 0.5 μM
-2 -1 0 1
-1 0 1 2
{Log $[Ca^{++}]_{free}$, Log (μM)}

Figure 3.25 Ca^{++} titration of EGTA-treated, ascorbate-reduced cytochrome c peroxidase, pH 6.

A 4μM solution of oxidised cytochrome c peroxidase in 5mM Mes/Hepes pH 6 was treated with 5mM EGTA, and then reduced with 1mM ascorbate/ 5μM DAD. This reduced form of the enzyme was titrated with Ca^{++}, with the spectra scanned 30 min after each Ca^{++} addition. The spectra shown (A) are represented as difference spectra for the various Ca^{++} concentrations, from which the ascorbate-reduced spectrum (with no added Ca^{++}) has been subtracted. The spectra are for free Ca^{++} concentrations of : 94nM, 283.6nM, 523.18nM, 765.84nM, 1560nM, 3710nM, and 6752nM. The absorbance at 380nm was used to determine the K_D for the second phase of the titration (see text). The experimental points are fitted to a theoretical curve for the titration of a single binding site with a K_D of 1.3μM (B).

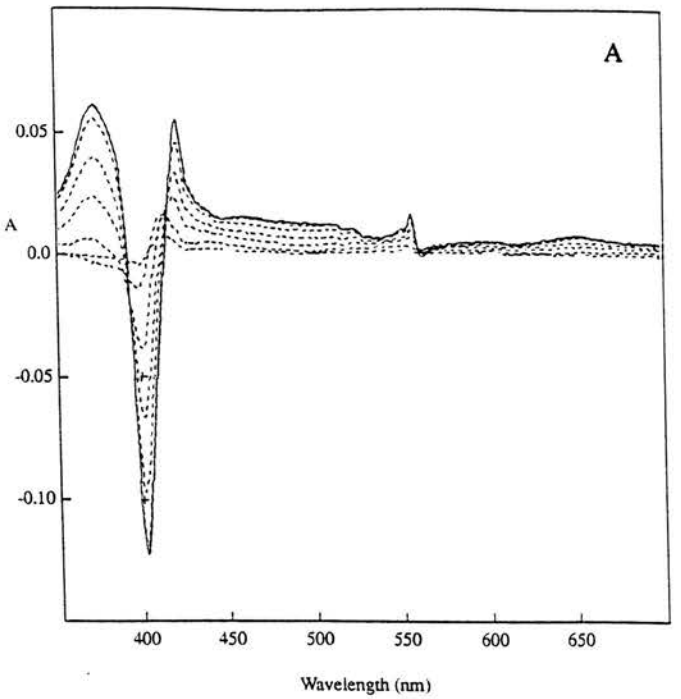
A
0.05
A
0.0
-0.05
-0.10
400
450
500
550
600
650
Wavelength (nm)

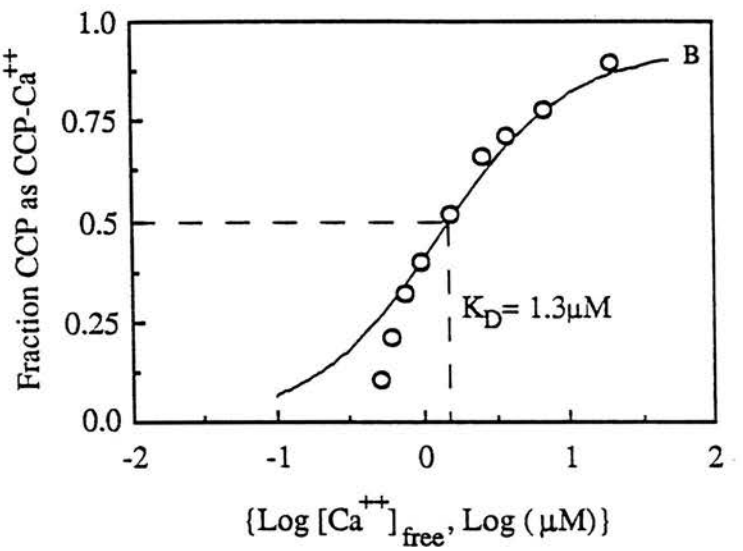
B
1.0
0.75
0.5
0.25
0.0
-2
-1
0
1
2
K_D= 1.3μM
Fraction CCP as CCP-Ca^{++}
{Log [Ca^{++}]$_{free}$, Log (μM)}

The data fit reasonably well to a theoretical saturation curve for a single binding site per protein molecule with a K_D of 1.3μM (figure 3.25B)

3.3.7.2.3 pH changes during Ca^{++} titrations

A study of the pH effects on binding of Ca^{++} to EGTA has indicated that H^+s are released upon Ca^{++} chelation. This is not surprising since Ca^{++} can only bind to the fully ionised form ($EGTA^{4-}$) yet at pH 7 most EGTA is present as the di-protonated form ($EGTAH_2^{2-}$). Ca^{++} buffering around this pH therefore results in displacement of two H^+s for every Ca^{++} ion bound. As a result, the Ca^{++} titrations shown in figures 3.24 and 3.25 are flawed as the pH is gradually decreasing as more Ca^{++} is added. In the titration of figure 3.24, a total of 0.947mM Ca^{++} was added. If all the Ca^{++} binds to EGTA then 1.894mM H^+s would be released. According to the Henderson-Haselbach equation, the pH would drop from 6 at the start of the experiment to 5.24 at the end. This has been confirmed by pH measurements. In the experiment of figure 3.25, the total Ca^{++} added was 0.775mM, resulting in a drop in pH from 6 to 5.47. Although these pH effects do exist in the experiments, Ca^{++} titrations in which the pH was kept constant produce similar K_D values to the ones calculated in this study (Pettigrew, personal communication)

3.4 Conclusion

The cytochrome c peroxidase of *Paracoccus denitrificans* is a dihaem c-type cytochrome with a high and low-potential haems. The haems of the fully oxidised enzyme are unavailable for ligand binding even though the high-potential haem is at least partly high-spin. Ascorbate reduction of the enzyme results in the rapid conversion of the high-potential haem from high-spin to low-spin followed by a slow conversion of the low-potential haem from low-spin to high-spin. The high-spin formation in the low-potential haem is temperature-dependent and enhanced by the

presence of divalent cations. The high-spin low-potential haem will readily bind added ligands.

The spin state change seen in the high-potential haem when it becomes reduced may play a pivotal role in the haem-haem interaction in this enzyme. The stronger association of the methionine ligand to the reduced high-potential haem may be linked through the protein to the movement of a histidine away from the low-potential haem, ensuring the substrate will only bind when the enzyme has the reducing power available to carry out the reaction. A model for the proposed activation of the enzyme is shown in figure 3.26. The reaction cycle at the lower part of the diagram is based upon the model proposed for the *Pseudomonas* peroxidase (Ellfolk et al. 1983).

Figure 3.26 Model of action for cytochrome c peroxidase of *Paracoccus denitrificans*

The diagram represents the cytochrome c peroxidase as a two domain dihaem enzyme. We propose that the smaller domain is formed by a class I cytochrome c sequence with Methionine/ histidine coordination of one haem. This is based on the amino acid sequence of the *Pseudomonas aeruginosa* enzyme (Ellfolk et al 1991) and the same class I features are present in the amino acid sequence of the enzyme from *Paracoccus denitrificans* (Goodhew e al, unpublished results). In addition, the oxidised form has a weak absorption band at 695nm indicative of methionine coordination (Moore & Pettigrew 1990).

Class I cytochromes tend to have positive redox potentials (Pettigrew & Moore 1987) and we propose that this domain accepts the incoming electron to the oxidised enzyme (A). An intermediate mixed-valence state (B(i)) is formed in which the low potential oxidised haem remains low spin. Reduction of that haem with dithionite results in a low spin bis-Fe^{II} enzyme (B(ii)). In a slow phase, enhanced by Ca^{++} the intermediate state (B(i)) is converted to a form (C(i)) which contains a high spin low potential Fe^{III} haem. A channel indicates ligand access to this haem. When this species (C(i)) is reduced with dithionite, a high spin Fe^{II} haem is observed (C(ii)). The enzyme cycle at the bottom of the diagram has not been studied directly in the present paper and is based on the model of Ellfolk et al (1983) for the *Pseudomonas* enzyme. It shows the reduction of H_2O_2 using one electron from the methionine/ histidine haem and a second from the Fe^{III} of the peroxidatic centre. (Ellfolk et al 1983).

Although the amino acid sequence strongly suggests a methionine/histidine coordination for the high potential domain, the coordination of the peroxidatic haem is speculative. The distal ligand to the peroxidatic haem (L) is thought to be either a histidine or lysine (Ellfolk et al. 1991). It should be noted that the evidence for the high potential domain being the methionine/histidine haem is slight, and is based on the knowledge that the class I cytochromes tend to have positive potentials (Pettigrew & Moore 1987). However if the methionine is weakly bound, this haem could conceivably be low potential with the bis-histidine haem, high potential. Thus an alternative model would have an electron entering the bis-histidine haem as a high potential haem, followed by a fast switch in haem potentials so that the methionine/histidine haem becomes reduced by internal electron transfer. Such a model would retain the bis-histidine haem as the peroxidatic centre.

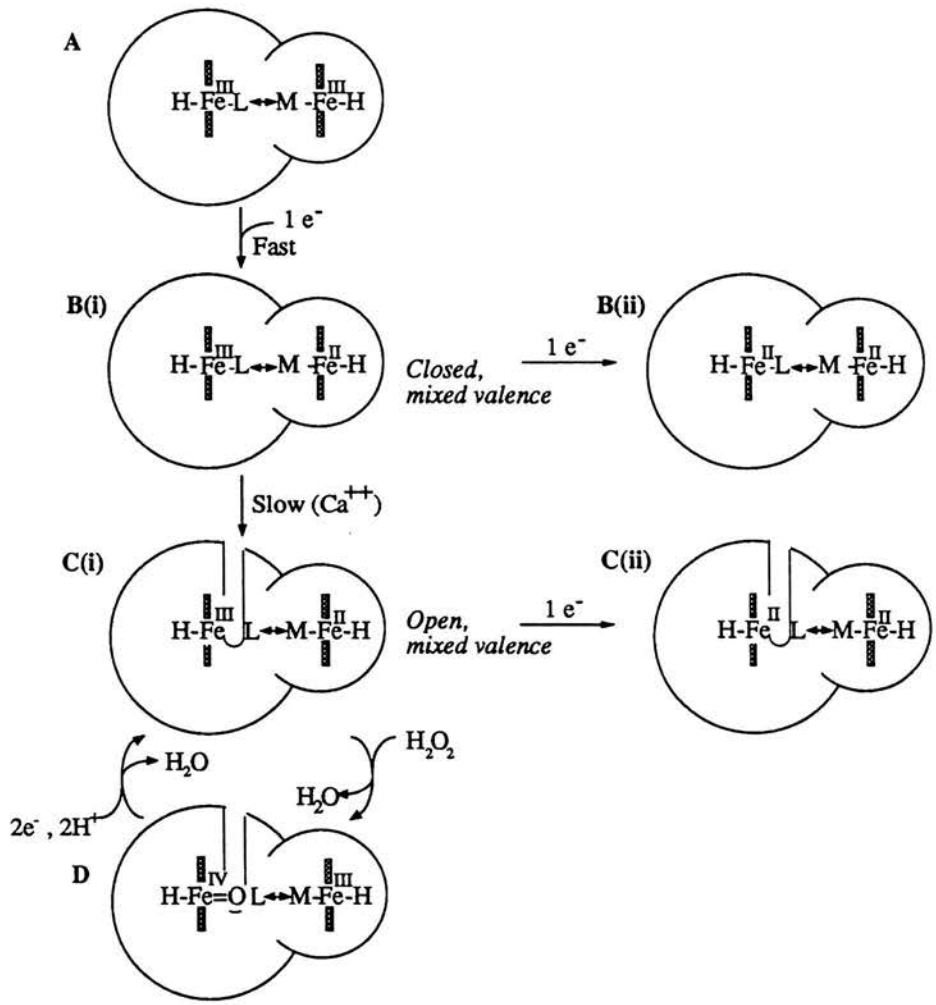
A
H-Fe-L↔M-Fe-H
1 e⁻
Fast
B(i)
H-Fe-L↔M-Fe-H
Closed,
mixed valence
1 e⁻
B(ii)
H-Fe-L↔M-Fe-H
Slow (Ca++)
C(i)
H-Fe L↔M-Fe-H
Open,
mixed valence
1 e⁻
C(ii)
H-Fe L↔M-Fe-H
H2O
2e⁻ , 2H+
H2O2
H2O
D
H-Fe=O L↔M-Fe-H

CHAPTER IV

The kinetics of the oxidation of cytochrome c by *Paracoccus* cytochrome c peroxidase

4.1 INTRODUCTION

The previous chapter suggests that the ascorbate-reduced high-spin form of the peroxidase is the active form. In order to confirm this it is necessary to study the kinetics of the peroxidase reaction. A study of the kinetics also allows comparisons to be made with the other well-characterised cytochrome c peroxidases and with cytochrome c oxidase, an enzyme which also receives electrons from a soluble class I ferrocytochrome donor.

The results presented in this chapter show that :

(i) As predicted from spectroscopic studies, the most active form of the enzyme is that in which the high potential haem is reduced and the low potential haem is oxidised and high spin.

(ii) The enzyme exists in a monomer/ dimer equilibrium in which only the dimer is active.

(iii) The enzyme does not obey conventional Michaelis-Menten kinetics with respect to substrate concentration dependence of activity.

(iv) The enzyme can receive electrons from both horse heart cytochrome c and *Paracoccus denitrificans* c-550, with a higher maximal velocity being obtained when the bacterial donor is used.

4.2 RESULTS

4.2.1 The assay of cytochrome c peroxidase

The *Paracoccus denitrificans* cytochrome c peroxidase will accept electrons from both mitochondrial cytochrome c and *Paracoccus* cytochrome c-550 (Goodhew et al, 1990) (Figure 4.1a). The activity of the enzyme is assayed by recording the decrease in absorbance of the α-band of the ferrocytochrome c at 550nm (Figure 4.1b). The reaction can be initiated either by addition of the enzyme to a cuvette containing ferrocytochrome c and hydrogen peroxide, or, by addition of hydrogen peroxide to a cuvette containing ferrocytochrome c and enzyme. These two starting methods can give very different activities (described below). The cuvette is continuously stirred using a magnetic flea so that the reaction can be monitored immediately after any additions.

The reaction is first order towards horse heart cytochrome c under conditions where the reaction is rapid. Under these conditions, the initial velocity can be calculated by determination of the first order rate constant (k) (Figure 4.1c) and use of the relationship, $v = k[C_f]$. When the reaction with horse heart cytochrome c is slow, and under all conditions with *Paracoccus* cytochrome c-550, the reaction does not follow first order kinetics (Figure 4.2). In some of these cases, the initial velocity is determined from the gradient of the progress curve.

4.2.2 The effect of ascorbate reduction and Ca^{++} on enzyme activity

From the spectroscopy results (chapter III) it is known that the high potential haem can be reduced by ascorbate, and this reduction leads to a conversion of the low potential haem to a high spin state. The level of high spin formed is influenced by the pH and the presence of Ca^{++} ions.

The enzyme, after purification, is in the fully oxidised state and is relatively inactive at pH 6 with a turnover number of 1920 min^{-1} (Table 4.1). In contrast, if the enzyme is treated with ascorbate and diaminodurol and left at room temperature for 45 min, the activity is enhanced 15-fold to give a turnover number of 30000

Fig. 1(a)

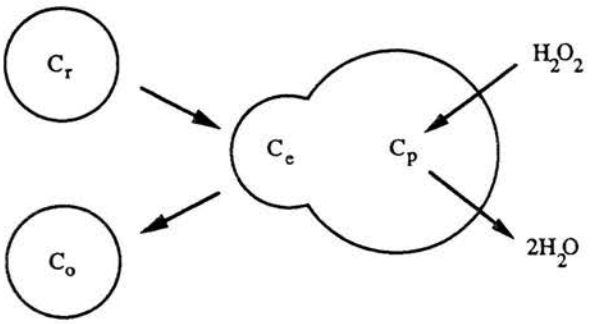

Fig. 1(b)

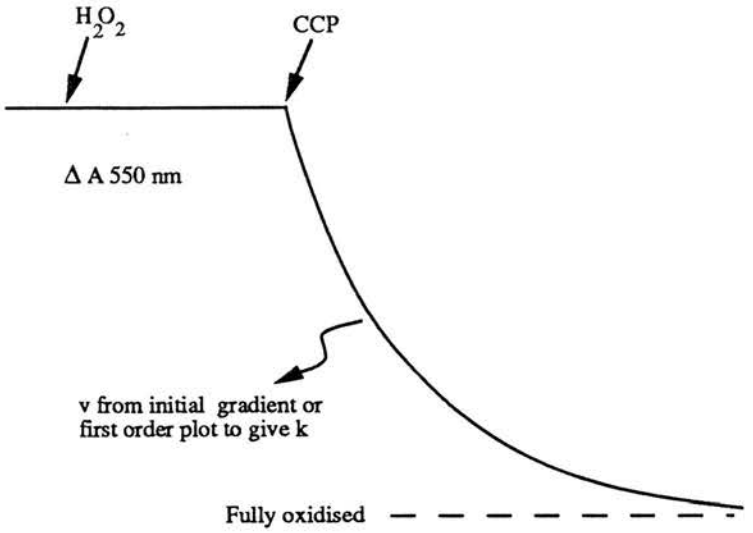

Fig. 1(c)

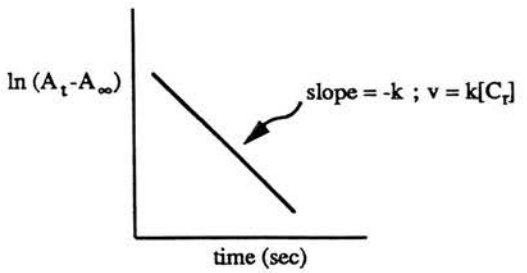

Figure 4.1 The nature of the assay

Cytochrome c peroxidase catalyses the oxidation of ferrocytochrome c by hydrogen peroxide (a). The enzyme is assayed by following the decrease in absorbance of the α band of ferrocytochrome c (b). The reaction is non-linear, even at very high concentrations of cytochrome c. The initial velocity is obtained either from the initial gradient or from the first order rate constant (c).

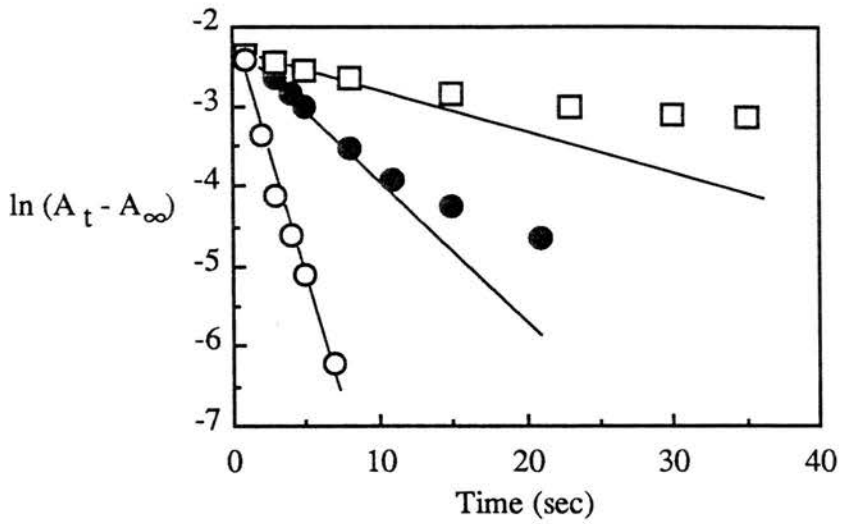

Figure 4.2 Deviation from first order kinetics in *Paracoccus* cytochrome c peroxidase

Semilogarithmic plots for the progress curves are shown for 3 concentrations of peroxidase. The ascorbate-reduced peroxidase stock (2μM) was in 5mM Mes/ 5mM Hepes pH 6, 1mM ascorbate, 5μM DAD and 1mM $CaCl_2$. Assays were initiated with the enzyme to a cuvette containing 5mM Mes/ 5mM Hepes pH 6, 10mM NaCl, 1mM $CaCl_2$, 7μM horse heart ferrocytochrome c and 18μM hydrogen peroxide. The enzyme was assayed at final concentrations of 5.33nM (O), 1.33 (●), and 0.33nM (□).

	Enzyme Pretreatment	Turnover Nos. (min^{-1})	
		Enzyme Start	Peroxide Start (40 sec preincubation)
1. pH 6	oxidised, minus Ca^{++}	1920	3900
	Asc/DAD, 45min	30000	14500
	Asc/DAD, 45min + Ca^{++}, 15min	57000	41000
2. pH 7.5	oxidised, minus Ca^{++}	0	0
	Asc/DAD, 45min	0	0
	Asc/DAD, 45min + Ca^{++}, 15min	24900	18450

Table 4.1 The activity of cytochrome c peroxidase

The activity of the enzyme assayed under various conditions is shown. The peroxidase stock was 2μM in 5mM Mes/ 5mM Hepes pH 6. The enzyme was assayed at a final concentration of 1nM in a cuvette containing 5mM Mes/ 5mM Hepes pH 6, 10mM NaCl, 7μM horse heart ferrocytochrome c and 18μM hydrogen peroxide. Reduction of the peroxidase stock was by ascorbate/DAD (1mM/5μM). $CaCl_2$ addition was to a final concentration of 1mM. Assays were initiated either by the enzyme or by hydrogen peroxide after a 40 sec preincubation of the enzyme with the ferrocytochrome c in the assay cuvette. 1mM $CaCl_2$ was present in the assay mix when the Ca^{++}-activated enzyme was assayed.

min^{-1}. A further 2-fold enhancement of activity is observed if the ascorbate-reduced, aged enzyme is treated with 1mM $CaCl_2$ for 15 min.

These increases in activity of the enzyme at pH 6 are found to be correlated with the appearance of the high spin state of the lower potential haem (Figure 4.3). Activity and the proportion of enzyme in the high spin state increase in parallel after reduction of the high-potential haem and reach a stable level after 45 min. Addition of 1mM $CaCl_2$ at this stage results in the further enhancement of both the activity and the proportion of the high spin form. This result indicates that the mixed-valence high spin form of the enzyme is the active form and that Ca^{++} promotes this state. Since the spectroscopic changes in the first phase of activation prior to Ca^{++} addition are identical to those after Ca^{++} addition, the first phase of activation is probably due to residual divalent cations already bound to the enzyme at this pH.

Addition of 1mM Ca^{++} to the oxidised enzyme results in a 4-fold increase in activity to give a turnover number of 4095 min^{-1} (Table 4.2). No change in the visible spectrum of the enzyme is observed during this activation. Ascorbate reduction of the Ca^{++}-activated oxidised enzyme yields the fully active enzyme within the 2 min required for reduction of the high potential haem Turnover number = 31500 min^{-1}). This result suggests that the haem-haem communication within the enzyme, whereby reduction of the high potential haem results in a spin state change in the low potential haem, can be a fast process provided the enzyme is fully saturated with Ca^{++} ions prior to reduction.

At pH 7.5, no high spin formation is observed at the low potential haem after reduction of its high potential counterpart (chapter III, Gilmour et al. 1993). Correlated with this is a complete inactivity of the enzyme at this pH in both the oxidised and ascorbate-reduced state (Table 4.1). Addition of 1mM Ca^{++} to the mixed valence enzyme results in formation of the same level of high spin as observed at pH 6 and a high level of activity (50% that at pH 6). The lower activity at pH 7.5 must be

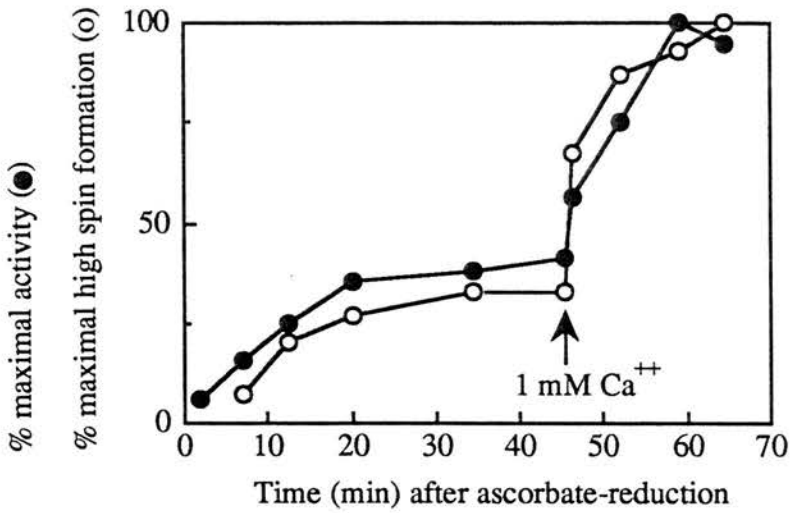

Figure 4.3 Enzyme activation after ascorbate-reduction.

Peroxidase stock was 2μM in 5mM Mes/ 5mM Hepes pH 6. Assays were initiated with the enzyme (final concentration, 1nM), to a cuvette containing 5mM Mes/ 5mM Hepes pH 6, 10mM NaCl, 7μM horse heart ferrocytochrome c and 18μM hydrogen peroxide. Reduction of the peroxidase stock was by ascorbate/DAD (1mM/5μM). High spin formation in the peroxidase stock was followed spectrophotometrically by the increase in absorbance at 380nm. Ca^{++} activation was by $CaCl_2$ to a final concentration of 1mM. 1mM $CaCl_2$ was present in the assay mix when the Ca^{++}-activated enzyme was assayed.

Enzyme pretreatment	Turnover number
oxidised, minus Ca^{++}	900 min^{-1}
oxidised, + Ca^{++}	4095 min^{-1}
+ Asc/DAD, 2 min	31500 min^{-1}

Table 4.2 Activation of the oxidised peroxidase by calcium

The peroxidase stock was 2μM in 5mM Mes/ 5mM Hepes pH 6. Assays were initiated with the enzyme (final concentration, 1.33nM), to a cuvette containing 5mM Mes/ 5mM Hepes pH 6, 10mM NaCl, 7μM horse heart ferrocytochrome c and 18μM hydrogen peroxide. Ca^{++} activation was by $CaCl_2$ to a final concentration of 1mM. Reduction of the peroxidase stock was by ascorbate/DAD (1mM/5μM). High spin formation in the peroxidase stock was followed spectrophotometrically by the increase in absorbance at 380nm.

due to influences other than the level of high-spin.

A pH titration shows a gradual loss of enzyme activity with increasing pH between 5.5 and 8.5 (figure 4.4). The results in this titration are consistent with the difference in activities shown above at pH 6 and pH 7.5. Since the ionic strength of the buffers used does not vary with pH (chapter II, section 2.5), then the loss of activity cannot be related to ionic strength.

4.2.3 The effect of dilution on peroxidase activity

The high activity of the enzyme requires that it be diluted from the purified concentrated stock prior to the assay. However, after dilution the enzyme loses a proportion of its activity over a 45 min period (figure 4.5). The loss of activity increases with increasing dilution.

We propose that the enzyme exists in a monomer/ dimer equilibrium in which only the dimer is active. Dilution of the enzyme shifts the equilibrium towards the monomer and therefore activity is lost. Evidence for this monomer/ dimer equilibrium comes from the behaviour of the peroxidase in molecular exclusion chromatography. The enzyme has a minimum relative molecular mass (from amino acid sequence) of 36,160 (Goodhew et al, unpublished results). However, it elutes from a Sephadex G-75 column, run under non-denaturing conditions, with a relative molecular mass of approx. 65,000. This figure is intermediate between that of a monomer and a dimer and suggests that the enzyme exists in a rapid monomer/ dimer equilibrium (Andrews 1964). Further evidence for the presence of an equilibrium in which only the dimer is active comes from the effect on activity of reconcentration of the enzyme (Table 4.3). Over 60% of the activity lost on dilution is recovered by reconcentration. The inability to recover the remaining 40% of the original activity may be due to enzyme damage during the reconcentration process.

It is apparent from Table 4.1 that the ascorbate-reduced enzyme is more active when the reaction is started with the enzyme rather than with hydrogen peroxide. This is consistent with loss of activity over the 40 sec preincubation period as a result of dilution of the enzyme in the cuvette. The enzyme is normally assayed at a final concentration in the cuvette of 1nM, taken from a diluted stock of 2μM.

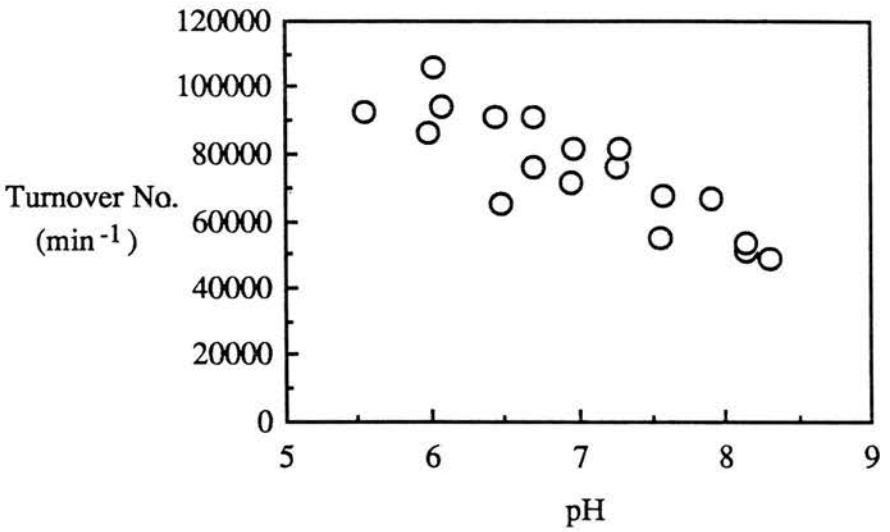

Figure 4.4 pH titration of peroxidase activity

The peroxidase stock (2μM) was reduced in 5mM Mes/ 5mM Hepes pH 6, 1mM ascorbate, 5μM DAD and 1mM $CaCl_2$. Assays were initiated with the enzyme (final concentration, 0.67nM), to a cuvette containing 5mM Mes/ 5mM Hepes pH 5.5-8.5, 10mM NaCl, 1mM $CaCl_2$, 7μM horse heart ferrocytochrome c and 18μM hydrogen peroxide

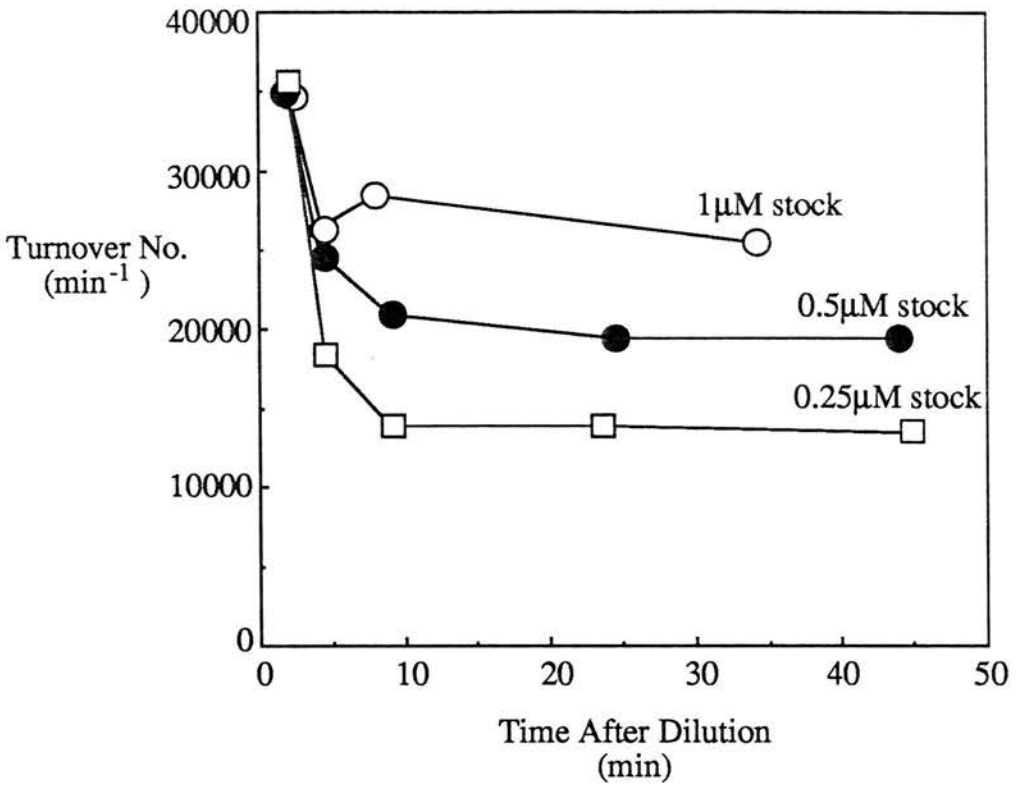

Figure 4.5 Effect of dilution on enzyme activity.

Samples from a 100μM peroxidase stock in 5mM Mes/ 5mM Hepes pH 6, 1mM $CaCl_2$ were diluted in the same buffer to 1.0μM, 0.5μM, and 0.25μM. Samples of each diluted stock concentration were assayed (1nM final concentration) at various times after dilution in a cuvette containing 5mM Mes/ 5mM Hepes pH 6, 10mM NaCl, 1mM $CaCl_2$, 7μM horse heart ferrocytochrome c and 18μM hydrogen peroxide. Assays were initiated by hydrogen peroxide addition following a 40 sec preincubation of the enzyme with the ferrocytochrome c in the assay cuvette.

conditions	comments	Turnover No. (min)
4μM stock		23000
4μM → 0.267μM	Dilution (x15)	
2.5 min	Time after dilution	13000
8.5 min		9000
15.5 min		8000
22 min		7900
34 min		7300
45 min		6300
0.267μM → 4μM	Reconcentration (x15)	16500

Table 4.3 Reconcentration of cytochrome c peroxidase.

A 4μM oxidised sample of peroxidase in 5mM Mes/ 5mM Hepes pH 6, 1mM $CaCl_2$ was assayed and then diluted to 0.267μM in the same buffer. The activity was recorded at various times after dilution. After a stable activity had been reached, the enzyme was reconcentrated back to 4μM in an Amicon centriprep-10 concentrator. The enzyme was assayed at a final concentration of 4nM in a cuvette containing 5mM Mes/ 5mM Hepes pH 6, 10mM NaCl, 1mM $CaCl_2$, 7μM horse heart ferrocytochrome c and 18μM hydrogen peroxide. The assays were initiated with hydrogen peroxide, following a 40 sec preincubation of the enzyme with ferrocytochrome c.

It is important to note that the loss of activity on dilution probably also occurs with the oxidised enzyme when assayed by starting the reaction with hydrogen peroxide. However, over the 40 sec preincubation, the activation caused by reduction of the high potential haem masks the loss of activity caused by dilution. If the preincubation is extended beyond 40 sec, a gradual loss of activity results from the dilution effect (Figure 4.6).

Ideally, the dilution effect should be studied on the ascorbate-reduced enzyme, since this is the active form. However, dilution of this form of the peroxidase results in oxidation of the enzyme, even though the dilution is into ascorbate/DAD. The oxidation results in a greater loss of activity than would be observed if monomerisation of an active dimer was the only effect. The oxidation is probably due to the presence of H_2O_2, since the addition of a small amount of catalase to the dilution buffer prior to addition of the ascorbate-reduced enzyme prevents oxidation. The H_2O_2 probably originates from the reaction of ascorbate with O_2, a process which has been shown to generate free radicals (Halliwell & Gutteridge 1989).

Studying the effects of reconcentration of the ascorbate-reduced enzyme would be of limited value since the catalase (relative molecular mass approx. 250,000 (Bergmeyer 1974)) would also be concentrated. A high concentration of catalase would compete with the peroxidase for H_2O_2 in the assay mix.

The loss of activity on dilution explains the deviation from first order seen in the assay when the reaction is slow (Figure 4.2). The monomerisation of the active dimer in the reaction cuvette results in a gradual decrease in the concentration of the active sites as the reaction proceeds. This decrease in concentration is reflected in a gradual decrease in the gradient of the first order plot (Figure 4.2).

4.2.4 Effect of EGTA on peroxidase activity

The importance of Ca^{++} in promoting the active form of the enzyme is confirmed by studies with EGTA. Treatment of the oxidised enzyme with EGTA almost fully abolishes activity (turnover number 285 min^{-1}, figure 4.7). Ascorbate reduction of the EGTA-treated, oxidised enzyme does not result in any activation of the enzyme

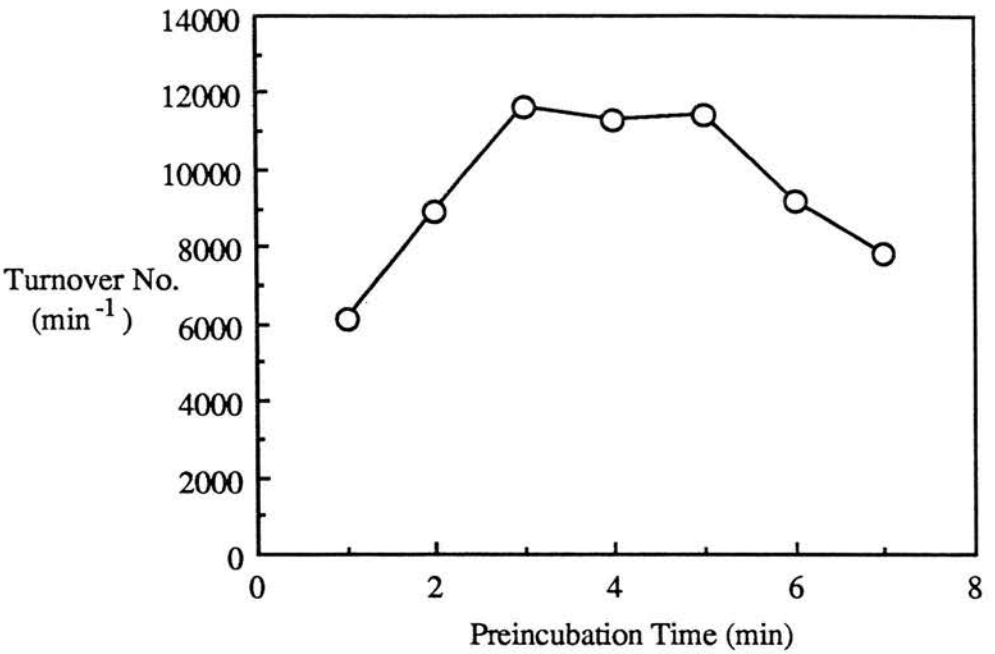

Figure 4.6 Effect of preincubation on enzyme activity

A 6μM stock of oxidised cytochrome c peroxidase in 5mM Mes/ 5mM Hepes pH 6 was assayed at a final concentration of 6nM. The assay mix contained 5mM Mes/ 5mM Hepes pH 6, 10mM NaCl, 7μM horse heart ferrocytochrome c and 18μM hydrogen peroxide.The assays were initiated with hydrogen peroxide, following a preincubation of the enzyme with ferrocytochrome c. The preincubation times varied in the manner shown in the results.

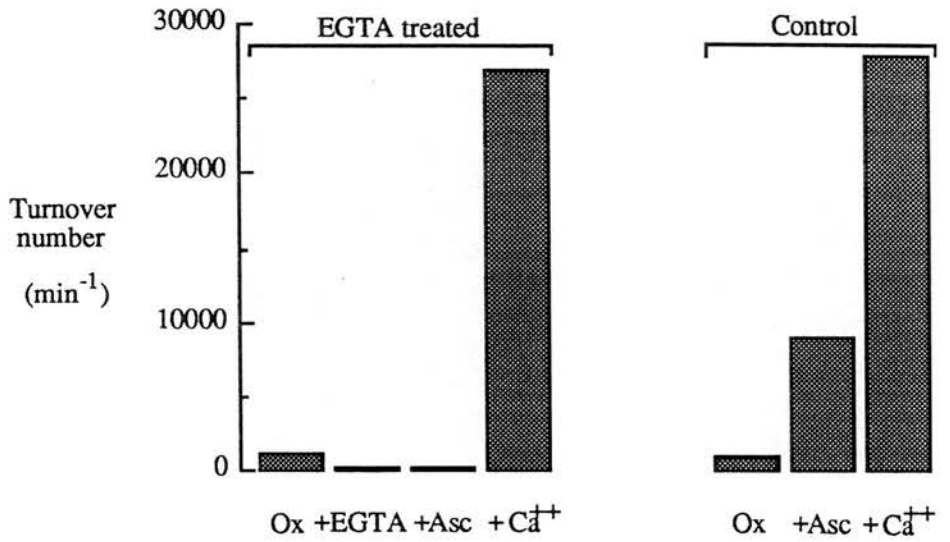

Figure 4.7 The effect of EGTA on the oxidised enzyme

Cytochrome c peroxidase (2μM) in 5mM Mes, 5mM Hepes pH 6.2 was treated with EGTA (1 mM). The enzyme was then reduced with ascorbate (1mM) and DAD (5μM). Finally Ca^{++} was added to 2mM along with 2mM NaOH. A control solution was not treated with EGTA. Assays were performed as described in Figure 4.3.

(turnover number 128 min^{-1}). Associated with this inactivity is an absence of any high-spin formation. This result is in contrast to the non-EGTA treated control where ascorbate reduction results in formation of a 380nm high spin band with an associated 10-fold activation of the enzyme activity to give a turnover number of 9000 min^{-1} (figure 4.7). Addition of a 1mM excess of Ca^{++} to the ascorbate-reduced, EGTA-treated enzyme results in activation of the enzyme (turnover number 27000 min^{-1}) to the level seen in the Ca^{++}-activated control (turnover number 27900 min^{-1}). The EGTA effect is therefore reversible by Ca^{++} at this pH with no long-term damage to the enzyme.

In the experiment of figure 4.8, the enzyme shows 84% of full activity after reduction with ascorbate in the absence of added Ca^{++}. EGTA causes complete loss of this activity with a half-time of approximately 60 min. Complete loss of the 380nm band associated with the high spin state is also observed. Addition of Ca^{++} to give a 1mM excess over the EGTA results in activation of the enzyme activity (turnover number 30000 min^{-1}) to a level similar to that seen in the control (figure 4.8). It is important to note that the 'rapid' EGTA effect on the enzyme seen in visible spectroscopy (chapter III, Figure 3.19(b)) is not associated with any change in enzyme activity. This suggests that only the Ca^{++} ion associated with 380nm formation is required for activity of the enzyme.

4.2.5 CN^- titration of cytochrome c peroxidase activity

When the ascorbate-reduced, aged enzyme (in 1mM $CaCl_2$) is titrated with CN^-, the enzyme activity is inhibited. The CN^- concentration required for half-inhibition of the peroxidase activity is slightly higher than the K_D for CN^- binding calculated from the spectroscopic titration (figure 4.9). The higher concentration required may be a result of competition in the assay mix between

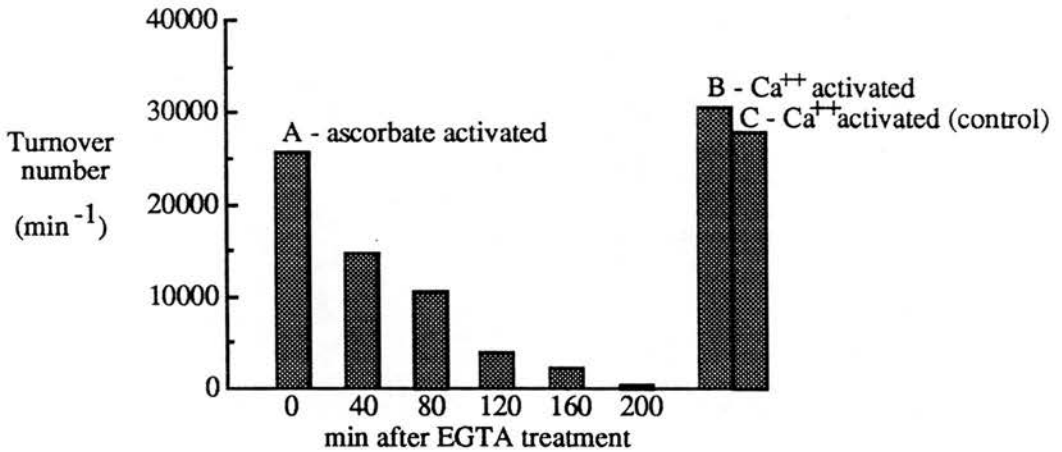

Figure 4.8 The effect of EGTA on the enzyme after reduction with ascorbate Cytochrome c peroxidase (2μM) in 5mM Mes, 5mM Hepes pH 6.3 was reduced with 1mM ascorbate, 5μM DAD. After 45 min, EGTA was added to 1mM and samples were removed for assay of activity at time intervals. Finally $CaCl_2$ was added to 2mM along with 2mM NaOH (to neutralise H^+ released from the EGTA as Ca^{++} binds). A control solution was reduced with ascorbate and treated with Ca^{++} without EGTA addition. Assays were performed as described in Figure 4.3.

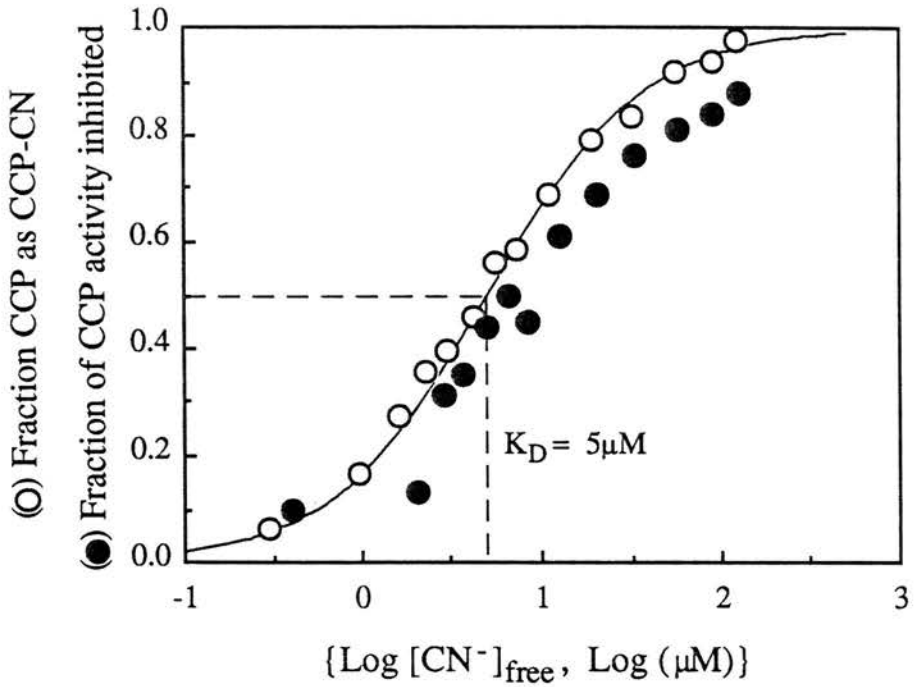

Figure 4.9 Titration of peroxidase activity by CN^-.

A 1.76μM solution of cytochrome c peroxidase in 5mM Mes/5mM Hepes pH 6, 1mM $CaCl_2$ was reduced with 1mM ascorbate, 5μM DAD. The sample was aged for 60 min at room temperature to allow formation of the high-spin state. A cyanide titration was performed using a stock neutralised sodium cyanide solution. The enzyme was assayed after each addition of cyanide. Assays were initiated with the enzyme (final concentration, 1nM), to a cuvette containing 5mM Mes/ 5mM Hepes pH 6, 10mM NaCl, 1mM $CaCl_2$, 7μM horse heart ferrocytochrome c and 18μM hydrogen peroxide. The assay cuvette also contained cyanide to the same concentration as in the stock enzyme solution. A plot of fraction of activity inhibited versus log $[CN^-]_{free}$ is shown (●). The titration was also followed spectrophotometrically (see spectroscopy chapter section 3.3.5) and the data calculated from the Δ380nm absorbance is shown as a comparison (O).

CN^- and H_2O_2 for the low potential haem. A K_I of 7μM has been determined for the inhibition of *Pseudomonas aeruginosa* peroxidase by CN^- (Soininen & Ellfolk 1973). This value is slightly lower than the K_D of 23μM determined by n.m.r. spectroscopy. (Ellfolk et al 1984a).

4.2.6 Substrate dependence of cytochrome c peroxidase activity

4.2.6.1 Horse heart ferrocytochrome c as substrate

The oxidation of ferrocytochrome c is first order, even at high concentrations of substrate (figure 4.10a). The first order rate constant obtained from these plots decreases with increasing ferrocytochrome c concentration (figure 4.10a).

Although the reaction does not show zero order kinetics, a plot of initial velocity against substrate concentration does produce a 'saturation' effect typical of Michaelis-Menten kinetics (figure 4.10b). The theoretical curve shown is for a maximum turnover number of 62000 min^{-1} and a substrate concentration which gives half-maximal turnover of 3.3μM. A comparison with results of substrate dependence for other cytochrome c peroxidases is shown in table 4.4.

4.2.6.2 *Paracoccus denitrificans* ferrocytochrome c-550 as substrate.

Semilogarithmic plots of the progress curves of the oxidation of *Paracoccus* cytochrome c-550 are non-linear indicating that the reaction deviates from first order kinetics as the oxidation progresses (figure 4.11a). The initial, linear portions of the plots are less strongly influenced by substrate concentration than is the case for horse cytochrome c. These initial portions were used to estimate rate constants and hence initial velocities. As observed with horse cytochrome c these calculated velocities fit a saturation curve (figure 4.11b) in this case with a maximum turnover number of 85000 min^{-1} and a substrate concentration which gives half maximum turnover number of 13μM. A comparison with results of substrate dependence for other cytochrome c peroxidases is shown in table 4.4.

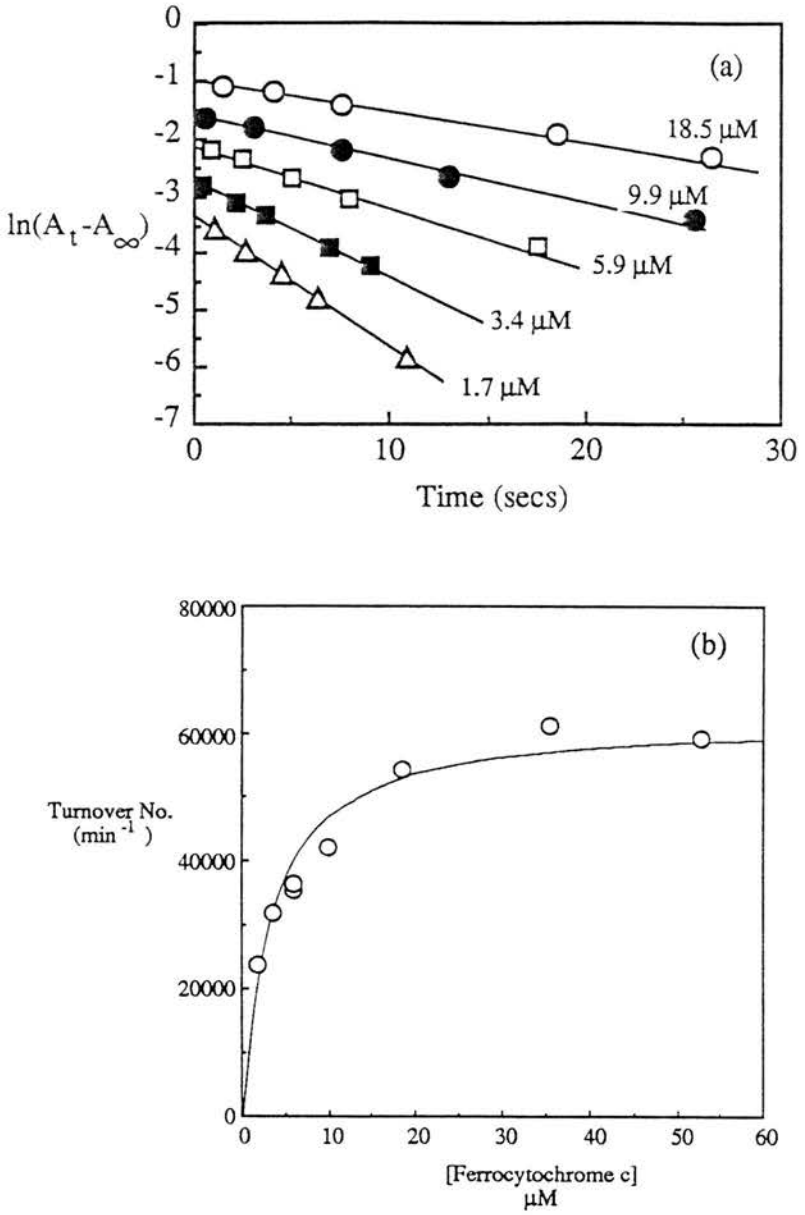

Figure 4.10 Effect of horse heart ferrocytochrome c concentration on peroxidase activity.

Assays were performed on ascorbate-reduced, Ca^{++}-activated peroxidase. The peroxidase stock was 2μM in 5mM Mes/ 5mM Hepes pH 6, 1mM ascorbate/5μM DAD, 1mM $CaCl_2$. Assays were initiated with the enzyme (final concentration, 1nM), to a cuvette containing 5mM Mes/ 5mM Hepes pH 6, 10mM NaCl, horse heart ferrocytochrome c and 100μM hydrogen peroxide. The enzyme was assayed with ferrocytochrome c concentrations of 1.7μM, 3.375μM, 5.9μM, 5.93μM, 9.875μM, 18.5μM, 35.25μM and 52.75μM. Initial velocities were calculated from first order plots (a). Turnover numbers were determined by dividing the initial velocity by the enzyme concentration.

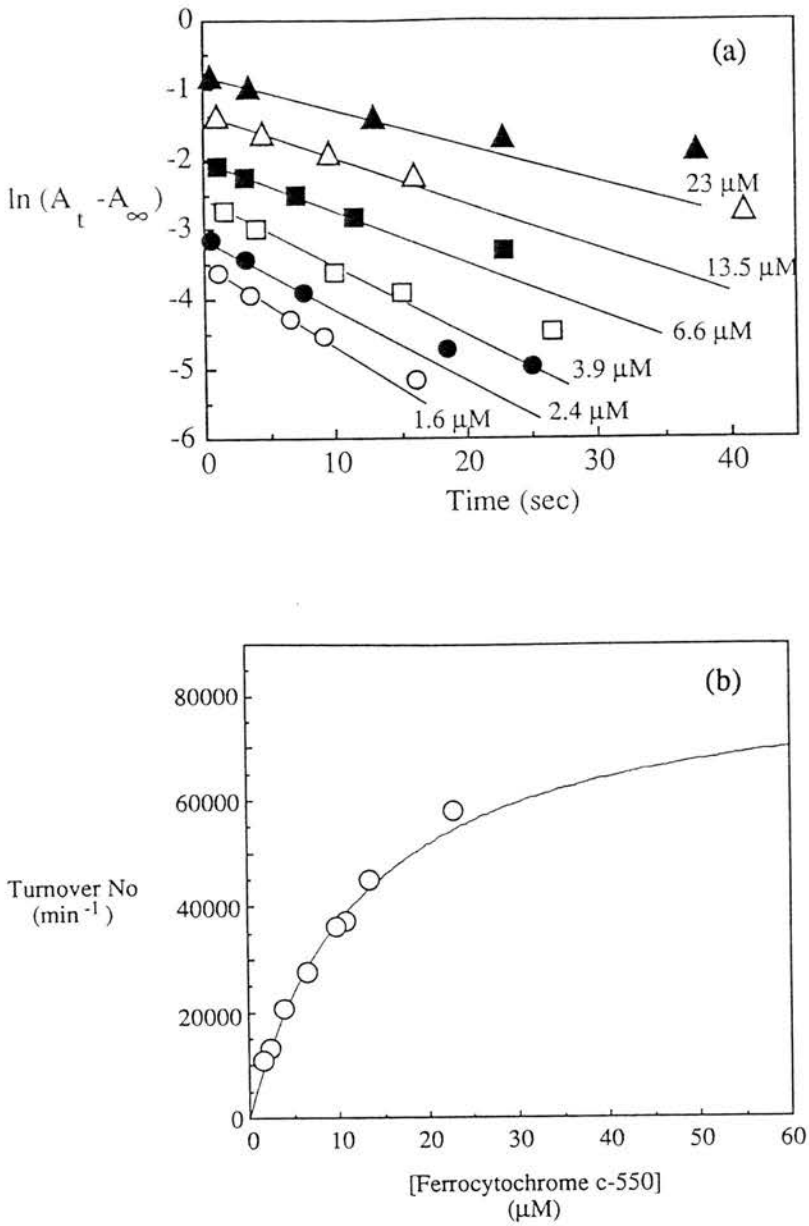

Figure 4.11 Effect of *Paracoccus denitrificans* ferrocytochrome c550 concentration on peroxidase activity.

Assays were performed on ascorbate-reduced, Ca^{++}-activated peroxidase. The peroxidase stock was 2µM in 5mM Mes/ 5mM Hepes pH 6, 1mM ascorbate/5µM DAD, 1mM $CaCl_2$. Assays were initiated with the enzyme (final concentration, 1nM), to a cuvette containing 5mM Mes/ 5mM Hepes pH 6, 10mM NaCl, *Paracoccus denitrificans* ferrocytochrome c-550 and 100µM hydrogen peroxide. The enzyme was assayed with ferrocytochrome c550 concentrations of 1.59µM, 2.35µM, 3.9µM, 10µM, 10.7µM, 13.5µM and 23µM. Initial velocities were calculated from first order plots (a). Turnover numbers were determined by dividing the initial velocity by the enzyme concentration.

Table 4. Kinetic Parameters for Cytochrome c Peroxidases

organism	electron donor/conc	Turnover No.	K_m	Ref.
Saccharomyces cerevisiae	Y-cyt.c[g] / saturated	14000 s^{-1}	25μM	a
Pseudomonas aeruginosa	c-551 / saturated	710 s^{-1}	91μM	b
	c-551/ 12μM	90 s^{-1}		c
Pseudomonas stutzeri	c-551/ 16μM	0.38 s^{-1}		d
Pseudomonas perfectomarinus (22K proteolytic fragment of cyt. c-552)	c-551/ 16μM	30 s^{-1}		e
Paracoccus denitrificans	HHC[h] / saturated	1040 s^{-1}	3.25μM	f
	c-550 / saturated	1400 s^{-1}	13μM	f

[a] Yonetani & Ray (1966).

[b] Soininen & Ellfolk (1972)

[c] Foote et al (1983)

[d] Villalain et al (1983)

[e] Den Ariaz et al (1989)

[f] This study

[g] *Saccharomyces cerevisiae* cytochrome c

[h] Horse-heart cytochrome c

4.3 DISCUSSION

4.3.1 The activation of the enzyme

The relative inactivity of the oxidised enzyme is due to the fact that, in this state, the enzyme has neither the reducing equivalents for peroxide reduction nor an accessible site for the peroxide to bind. The activity observed when the reaction is initiated by hydrogen peroxide is due to a small amount of high spin formation occurring in the assay cuvette following reduction of the enzyme by the ferrocytochrome c. When the oxidised enzyme is used to start the reaction, a lag effect is normally observed (figure 4.12). This lag effect was also observed with the *Pseudomonas aeruginosa* peroxidase (Ronnberg & Ellfolk 1978) and is probably due to time taken for activation of a portion of the enzyme.

Reduction of the high potential haem is followed by a slow switch in the low potential haem to a high spin state, making it available for ligand binding. The active enzyme formed has both the necessary reducing equivalents for the reaction and an available binding site for the hydrogen peroxide. Addition of 1mM Ca^{++} enhances the level of high spin in the low potential haem and therefore increases the concentration of sites available for peroxide binding.

The haem-haem communication which exists within this enzyme may be a form of protection to ensure hydrogen peroxide only binds when the enzyme has the necessary reducing equivalents for the reaction. If hydrogen peroxide were able to bind to the peroxidatic haem in a fully oxidised enzyme, the single electron transfer that would follow may result in formation of the highly reactive hydroxyl radical. This aspect of 'design' is also seen in cytochrome oxidase which will only bind oxygen when it contains four transferable electrons (Palmer et al. 1976). Cytochrome oxidase is also isolated in a relatively inactive oxidised form which becomes fully active (the pulsed form) after reduction and turnover (Antonini et al. 1985).

4.3.2 The monomer/ dimer equilibrium and dilution of the enzyme

The enzyme gradually loses activity with time after dilution from stock

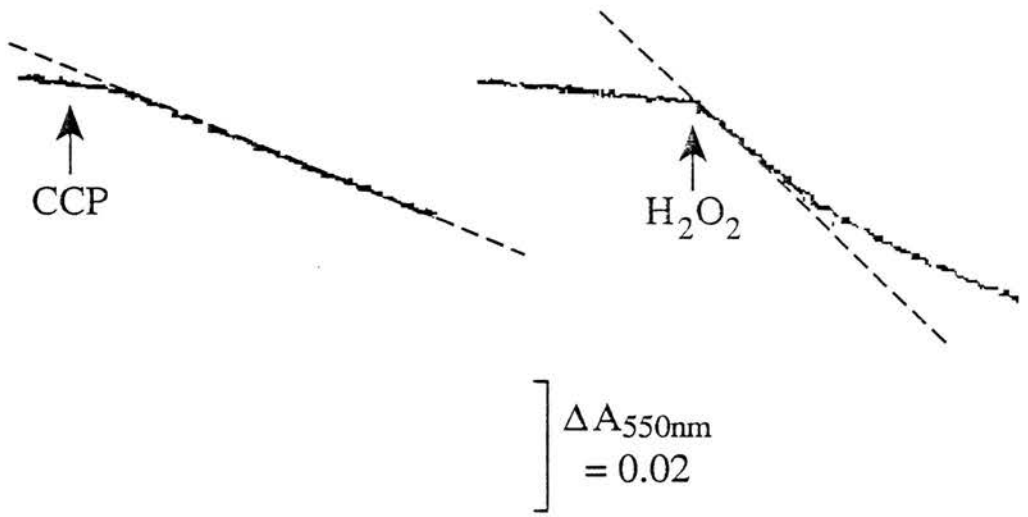

Figure 4.12 The lag phase during peroxidase assays.

The peroxidase stock was 2μM in 5mM Mes/ 5mM Hepes pH 6. Assays were performed with the peroxidase at a final concentration of 1.33nm in a cuvette containing 5mM Mes/ 5mM Hepes pH 6, 10mM NaCl, 7μM horse heart ferrocytochrome c and 18μM hydrogen peroxide. (A) Assay initiated with peroxidase. (B) Assay initiated with hydrogen peroxide following a 40 sec preincubation of the enzyme with ferrocytochrome c.

concentrated solutions to concentrations that are appropriate for assay. We propose that this is due to a monomer/ dimer equilibrium in which only the dimer is active. An alternative explanation is that a small cofactor is diluted. However, firstly, such a loss should not be reversed by reconcentration of the enzyme by filtration and secondly, it would be expected that simply lowering the concentration of a cofactor, free in solution, should have an immediate, rather than a time-dependent effect. The data in figure 4.5 can be used to provide a rough estimate for the dissociation constant for the monomer/ dimer equilibrium. Extrapolation of the curves back to zero time gives an activity of approx. 45000 min^{-1}. If we assume that this represents the activity of the dimer, we can calculate the concentration of the dimer present at various dilutions after equilibrium has been reestablished. For example, for the dilution to 0.5μM enzyme -

Activity = 19250 min^{-1} (from figure 4.5)

Therefore enzyme present as dimer - (19250/45000) x 0.5μM = 0.21μM

Therefore [dimer] = 0.105μM

Therefore [monomer] = 0.29μM

K_D = [monomer]^2/[dimer] = 0.8μM

Similar K_D values are obtained for the other dilutions.

4.3.3 First order kinetics and substrate dependence

Smith & Conrad (1956) showed that the kinetics of oxidation of cytochrome c by cytochrome oxidase were characterised by (a) a first order reaction even at very high substrate concentration, (b) first order rate constants which decreased with increasing [ferrocytochrome c] and (c) saturation. These features are shared by the kinetics of the oxidation of horse cytochrome c by the *Paracoccus* cytochrome c peroxidase suggesting that the nature of the reaction is similar in the two systems. Minnaert (1961) considered a number of models which reconciled the apparent anomaly of first order kinetics and the hyperbolic relationship between initial velocity and substrate

concentration. Of these, model IV, which involves binding of equal strength of the oxidised and reduced cytochrome c to the oxidase has received most experimental support.

The kinetics of oxidation of *Paracoccus* cytochrome c-550 deviated from first order and the rate constant was largely unaffected by substrate concentration. Bolgiano et al (1988) observed a similar lack of dependence of k on substrate concentration for the interaction of cytochrome c-550 with *Paracoccus* cytochrome c oxidase. Interestingly, addition of poly(L) lysine resulted in enhanced rates with a k dependence similar to that seen for mitochondrial cytochromes c. *Paracoccus denitrificans* cytochrome c-550 has a very asymmetric charge distribution (Bolgiano et al. 1988; Pettigrew, 1991) with a positively charged 'front' face and a strongly negatively charged back surface (see chapter V). It is possible that polylysine binds to the negative back surface of the cytochrome c-550 conferring similar electrostatic properties to those shown by mitochondrial cytochromes c.

4.3.4 The physiological activity of the enzyme

The requirement for divalent cations will be satisfied in the living cell by the environment of the periplasm. Mg^{++} is an important structural component of the surface layers of gram negative bacteria (Costerton et al. 1974) and chelation of this ion by EDTA forms part of the protocol for spheroplast formation (Goodhew et al 1990). It is probable that this procedure partly inactivates the peroxidase by removal of intrinsic Ca^{++} or Mg^{++}. The very low turnover number of the cytochrome c peroxidase from *Pseudomonas stutzeri* (table 4.4; Villalain et al 1984) may be due to non-optimised assay conditions and is unlikely to be a true reflection of the kinetic competence of the enzyme from this organism. It would be of interest to determine whether the enzyme from this source shows the Ca^{++} dependent activation found in the *Paracoccus* enzyme. From the yield of enzyme after purification and assuming a figure of 20% for the periplasmic volume (Stock et al. 1977), a physiological concentration in the periplasm of approximately 200μM can be calculated. Our estimate of the K_D for the monomer-dimer equilibrium is 0.8μM and clearly the

enzyme should exist as the active dimer under physiological conditions.

On the basis of similar calculations, the physiological concentration of the cytochrome c-550 may be approximately 100μM which implies that the enzyme can work near V_{max} if the steady state level of reduction of the cytochrome c-550 is high and hydrogen peroxide is present. However such arguments are complicated by the fact that competitors in the use of cytochrome c-550 may exist in the periplasm and that the electron transfers may be localised on the cell membrane rather than dispersed through the periplasmic volume.

CHAPTER V

The dipole moment of *Paracoccus denitrificans* cytochrome c-550

5.1 INTRODUCTION

Mitochondrial cytochrome c is the soluble mediator of electron transfer between the membrane-embedded complexes III (cytochrome bc_1) and IV (cytochrome c oxidase). In addition, it also interacts with soluble enzymes such as cytochrome c peroxidase and sulphite oxidase. A component defining these interactions is undoubtedly electrostatic and the electrostatic properties of cytochrome c have become an area of increasing research over the last 15 years.

A ring of lysine residues surrounds the exposed haem edge of cytochrome c. In the presence of redox partners these lysines are protected from modification by lysine-specific reagents. This observation has led to the suggestion that electron transfer in this protein takes place via the exposed haem edge. The presence of a complementary ring of negative charges found on redox partners indicates that the complexes formed involving cytochrome c are stabilised by electrostatic interactions.

The presence of an excess of negative charge on the back surface of cytochrome c gives it an asymmetric distribution of charge. Koppenol & Margoliash (1982) have shown that this asymmetry of charge results in a dipole moment of over 300 debye. The positive end of the dipole vector exits the protein close to the centre of the interaction domain. This observation led Koppenol & Margoliash (1982) to suggest the dipole is responsible for preorientation of the cytochrome prior to its interaction with redox partners. This suggestion gained experimental support when it was shown that modification of residues at the back of the protein, away from the interaction surface, resulted in lower rates of electron transfer. The modified cytochrome c molecules were shown to have dipoles which were altered in both magnitude and direction (Koppenol & Margoliash 1982).

The counterpart of cytochrome c in *Paracoccus denitrificans* is cytochrome c-550 (Scholes et al 1971). The specific role of cytochrome c-550 is unclear, although it has been shown to donate electrons to the membrane-bound cytochrome oxidase and to soluble enzymes such as cytochrome c peroxidase (Bolgiano et al 1988, kinetics chapter section 4.2.6.2). The electrostatic properties of c-550 have not been studied in any detail and very little is known about the nature of its interaction with redox partners.

This chapter shows that the c-550 has a large molecular dipole which may be responsible for preorientation of the cytochrome prior to interaction with redox partners. In addition, evidence is presented to show that interactions involving the c-550 are stabilised via electrostatic forces.

5.2 METHODS

5.2.1 Calculation of dipole moment

A molecule contains a permanent electric dipole moment (μ) if its centre of positive charge does not coincide with its centre of negative charge. Dipole moments were calculated both manually and by the use of the 'sybyl' program on the Evans and Sutherland computer. Manual calculations used the equation of Koppenol & Margoliash (1982), which is described below.

The dipole moment of a molecule is given by :

$$\mu = \Sigma\, q_i\, r_{oi} \qquad \text{(i)}$$

in which r_{oi} is a vector from a fixed point (origin, o) to the charge q_i. Σ represents the sum of q_i multiplied by r_{oi}. As with all vectors, the dipole moment is defined in terms of both a direction and a magnitude.

Using the centre of mass as the origin for the dipole, Koppenol & Margoliash (1982), extended this general equation to give :

An alternative approach to studying the preorientation of electron transfer proteins has been to compute the electrostatic potential fields around the interacting proteins. This method is often used to find the best fit for two interacting electron transfer proteins. This has been done for the interaction of flavodoxin with cytochrome c (Matthew et al 1983). The results showed that the proteins have complimentary asymmetric electric fields. The cytochrome c has a positive electric field close to the exposed haem edge and the flavodoxin has a negative electric field close to the FMN prosthetic group. These complimentary asymmetric electric fields are thought to orient the proteins to facilitate a direct approach of the two prosthetic groups. When studying the role of charge distribution in preorientation, the dipole calculation has the advantage of providing a numerical value which represents the extent of asymmetry of charge. This value can then be used to determine whether a correlation exists between the magnitude of the dipole and the rates of electron transfer.

Computer calculations of the dipole moment were performed on the Evans and Sutherland computer within a software package known as SYBYL, produced by Tripos Associates.

$$\mu = (pr_P - nr_N)\, e \qquad \text{(ii)}$$

in which p and n are the number of positive and negative charges respectively and e is the electronic charge (1.602×10^{-19}C). r_P and r_N are vectors from the centre of mass to the centres of positive and negative charge respectively (figure 5.1). The subtraction of these vectors (after weighting each vector by the number of each type of charge) gives a dipole vector with the origin at the centre of mass. The direction of the dipole is given by the coordinates x, y and z. The magnitude is calculated by summing the square of each coordinate and taking the square-root of the total.

The vectors r_P and r_N can be calculated by initially determining the centres of charge and then subtracting the centre of mass. The centres of charge are calculated by summing the coordinates of each charge position (weighted by the magnitude of the charge) and then dividing by the total number of charges.

$$\text{centre of charge} = \frac{\begin{bmatrix} \Sigma q_i x_i \\ \Sigma q_i y_i \\ \Sigma q_i z_i \end{bmatrix}}{\Sigma q_i}$$

The centre of mass is calculated in the same way as the centre of charge, with charges being replaced by atoms and charge magnitude replaced by mass of the atoms. A computer program, written by Dr Paul Taylor, was used to calculate the centre of mass.

For the dipole calculations it was assumed that all lysines and arginines carry a charge of +1 and all glutamates and aspartates carry a charge of -1. No charges were assigned to the pyrrole ring nitrogens (2 negative) or to the iron (2 or 3 positive), therefore, the calculations apply best to the reduced forms of the cytochromes. The propionic acid groups of the haem were assumed to be ionised and were given a

$$\vec{\mu} = (p\vec{r}_P - n\vec{r}_N)\, e$$

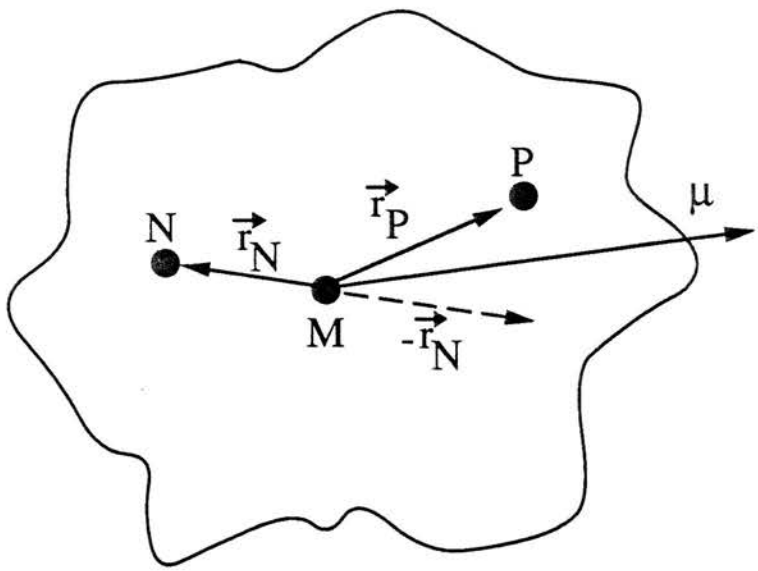

$$\vec{\mu} = \begin{bmatrix} x \\ y \\ z \end{bmatrix} \quad ; \quad \text{magnitude} = \sqrt{x^2+y^2+z^2}$$

Figure 5.1 Calculation of dipole moment

The dipole moment is a measure of charge separation within a molecule. P and N represent the centres of positive and negative charge respectively. The magnitude of the vectors r_P and r_N are scaled by the number of positive and negative charges respectively. The subtraction of nr_N from pr_P gives the dipole moment. The dipole has a direction (x, y, z) and a magnitude.

charge of -1. Given the experimental evidence (reviewed in Moore & Pettigrew 1990), this assumption appears valid for at least one propionic acid group (inner, HP-7), however, it is less clear whether the other acid group is ionised. In order to allow comparison with the results of Koppenol et al (1991), it was assumed, with due acknowledgement of the uncertainty, that both propionates are ionised.

The influence of the electric field created by α-helices (Wada et al, 1976), was taken into account. Hol et al (1978) has shown that the field, caused by the near-perfect alignment of small peptide bond dipoles in an α-helix, can be approximated by placing a charge of +1/2e at the NH_2-terminal end and -1/2e at the COOH-terminal end of the helix. The longer α-helices have larger dipole moments even though all helices are assigned the same end charges. As described by Koppenol & Margoliash (1982), the position of the +1/2e charges were calculated by taking the mean of the coordinates of the first three α-carbons of the α-helix and the -1/2e charges were calculated by taking the mean of the coordinates of the last three peptide carbonyl oxygens.

All other bond dipoles were assumed to have random orientations and were ignored. Calculations which take into account all bond dipoles yield similar results to those which use the method described above (Koppenol et al 1991).

Calculations using 'sybyl' had to be performed on protein coordinates centred around (0,0,0) since the program would use only these coordinates for the origin of the dipole. Slight discrepancies exist between calculations done on 'sybyl' and those done manually. These discrepancies arise because 'sybyl' centres molecules on a geometric basis with no weighting for the mass of each atom. However, since the proteins being studied here are globular, and because the mass of most of the atoms in these particular proteins (carbon, oxygen and nitrogen) are all similar, the unweighted centre differs only slightly from the weighted centre. Weighted and unweighted centre of mass calculations differed by less than 0.01Å and the corresponding difference in dipole moment for tuna cytochrome c is only 1.6 debye.

5.2.2 Calculation of angle between dipole vector and haem plane

The haem plane can be approximately defined by the coordinates of the four pyrrole ring nitrogen atoms.

Calculation of the angle between the dipole vector and the haem plane first requires calculation of the vector perpendicular (normal) to the haem plane (figure 5.2). The normal to the plane is calculated by taking the vector (cross) product of any two vectors lying in the plane. For example, the normal to the plane which contains the points A, B, and C can be obtained by calculating the cross product of the vectors AB and AC (figure 5.2).

After determination of the vector perpendicular to the haem, the angle between the dipole vector and the 'normal' vector can be calculated using the equation below :

$$\cos\theta = \frac{N \cdot \mu}{|N|\,|\mu|}$$

$N \cdot \mu$ is the scalar (dot) product between the dipole vector and the vector normal to the haem plane. $|N|$ and $|\mu|$ are the magnitudes of the vectors (figure 5.2).

5.3 RESULTS

5.3.1 Dipole moment of tuna cytochrome c

The tuna cytochrome c dipole moment is calculated in figure 5.3. The value of this dipole has previously been published (Koppenol and Margoliash, 1991) and is used in this study simply as a comparison to the *Paracoccus* c-550 dipole. The value of 342.17 debye obtained in this study is similar to the value of 353 Debye obtained by Koppenol & Margoliash (1991). The small difference in the magnitude probably arises from the use of slightly different coordinate sets. The dipole calculation by Koppenol & Margoliash used the coordinates of the structure refined to 2Å by Takano et al (1977). However the coordinates used in this study were generated from a 1.5Å

(i) Calculation of normal to haem plane

Points A, B, and C lie in the haem plane.

Vector perpendicular (normal) to haem plane given by vector product of vectors AB and AC.

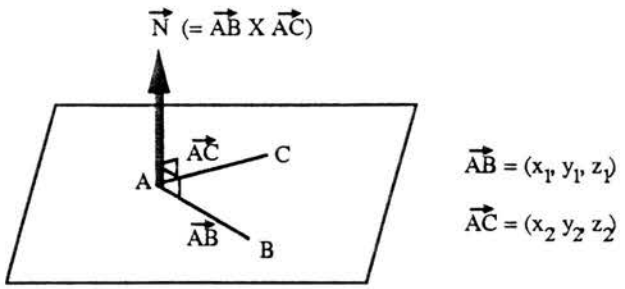

Vector Product :

$$\vec{N} = \begin{bmatrix} x_N \\ y_N \\ z_N \end{bmatrix} = \begin{matrix} y_1 z_2 - z_1 y_2 \\ x_1 z_2 - z_1 x_2 \\ x_1 y_2 - y_1 x_2 \end{matrix}$$

(ii) Calculation of angle between dipole vector and normal to haem plane

$$\cos\theta = \frac{\vec{N} \cdot \vec{\mu}}{|N|\,|\mu|}$$

$\vec{N} \cdot \vec{\mu}$ = scalar (dot) product between vectors N and μ.

$= x_N x_\mu + y_N y_\mu + z_N z_\mu$

$| \; |$ = Magnitude of vector

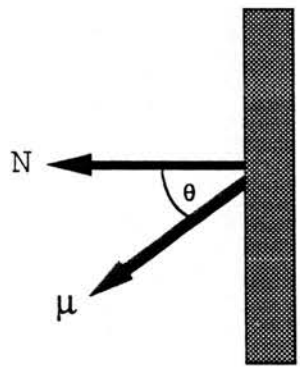

Figure 5.2 Angle of dipole to haem plane.

The angle to the haem plane is determined by calculating the dot product of the dipole vector and the vector perpendicular to the haem plane. The haem plane is illustrated as a parallelogram in the upper part of the diagram and is shown perpendicular to the plane of the paper in the lower part of the diagram.

Centre of Positive Charge (c.o.p.)

residue	Number[a]	atom[b]	x	y	z	charge
Lys	5	NZ	-11.060	-9.404	9.866	+1
Lys	7	NZ	-5.713	-14.882	23.536	+1
Lys	8	NZ	-8.324	-15.049	10.724	+1
Lys	13	NZ	0.355	-16.745	7.272	+1
Lys	25	NZ	9.987	-24.562	29.674	+1
Lys	27	NZ	5.396	-24.952	23.330	+1
Arg	38	NH1	12.964	-10.616	22.670	+1
Lys	39	NZ	22.622	-2.110	23.478	+1
Lys	53	NZ	25.778	-13.769	20.596	+1
Lys	55	NZ	19.227	-5.380	8.580	+1
Lys	72	NZ	15.701	-14.678	1.687	+1
Lys	73	NZ	15.055	-6.651	0.226	+1
Lys	79	NZ	19.758	-20.423	19.003	+1
Lys	86	NZ	8.799	-13.625	1.984	+1
Lys	87	NZ	-3.253	-12.646	0.564	+1
Lys	88	NZ	0.181	-0.547	3.936	+1
Arg	91	NH1	5.070	-6.281	5.262	+1
Lys	99	NZ	1.632	0.647	18.091	+1
α-Helix 1			-6.679	-7.716	16.630	+1/2
α-Helix 2			24.219	-13.732	15.027	+1/2
α-Helix 3			7.990	-0.961	14.358	+1/2
α-Helix 4			-1.260	-7.562	6.311	+1/2

$$\text{c.o.p.} = \begin{bmatrix} \sum q_i x_i \\ \sum q_i y_i \\ \sum q_i z_i \end{bmatrix} \Big/ \sum q_i = \begin{bmatrix} 146.31 \\ -226.659 \\ 256.642 \end{bmatrix} \Big/ 20 = \begin{bmatrix} 7.316 \\ -11.333 \\ 12.832 \end{bmatrix}$$

Figure 5.3 Tuna cytochrome c dipole moment

[a] refers to residue number. [b] refers to atom type. The cytochrome contains four stretches of α-helix, from reidues 2 to 14, 49 to 55, 60 to 70 and 88 to 103. The coordinates were obtained from the Brookhaven protein data bank file 5CYT.pdb and correspond to the crystal structure refined to 1.5Å by Takano & Dickerson (1981). The atom labelled OXT refers to the c-terminal α-carboxyl group.

centre of negative charge (c.o.n.)

residue	number[a]	atom[b]	x	y	z	charge
Asp	2	OD1	-9.153	-5.274	12.025	-1
Glu	21	OE1	3.074	-16.537	26.661	-1
Glu	44	OE1	18.941	-12.437	33.053	-1
Asp	50	OD1	26.590	-15.14	13.703	-1
Asp	62	OD1	10.137	0.856	9.611	-1
Glu	66	OE1	12.918	-2.204	6.729	-1
Glu	69	OE1	7.200	-7.790	1.191	-1
Glu	90	OE1	-1.011	-14.463	8.096	-1
Asp	93	OD1	-5.190	-6.831	11.271	-1
Ser	103	OXT	2.605	-4.402	29.538	-1
propionate 1		O1A	14.967	-10.656	20.704	-1
propionate 2		O1B	19.073	-15.784	17.033	-1
α-Helix 1			3.640	-19.938	14.484	-1/2
α-Helix 2			23.318	-5.630	14.532	-1/2
α-Helix 3			9.760	-11.473	5.899	-1/2
α-Helix 4			3.100	-7.276	26.817	-1/2

$$\text{c.o.n.} = \begin{bmatrix} \sum q_i x_i \\ \sum q_i y_i \\ \sum q_i z_i \end{bmatrix} \Big/ \sum q_i = \begin{bmatrix} 120.060 \\ -132.821 \\ 220.481 \end{bmatrix} \Big/ 14 = \begin{bmatrix} 8.576 \\ -9.487 \\ 15.749 \end{bmatrix}$$

Figure 5.3 (continued) Tuna cytochrome c dipole moment

Calcualtion of dipole moment

$$\vec{r}_P = \text{c.o.p.} - \text{c.o.m.} = \begin{bmatrix} 7.316 \\ -11.333 \\ 12.832 \end{bmatrix} - \begin{bmatrix} 8.962 \\ -11.323 \\ 16.101 \end{bmatrix} = \begin{bmatrix} -1.646 \\ -0.01 \\ -3.269 \end{bmatrix}$$

$$\vec{r}_N = \text{c.o.n.} - \text{c.o.m.} = \begin{bmatrix} 8.576 \\ -9.487 \\ 15.749 \end{bmatrix} - \begin{bmatrix} 8.962 \\ -11.323 \\ 16.101 \end{bmatrix} = \begin{bmatrix} -0.386 \\ 1.836 \\ -0.352 \end{bmatrix}$$

$$\vec{\mu} = (p\vec{r}_P - n\vec{r}_N)\, e = \begin{bmatrix} -4.408 \times 10^{-18} \\ -4.15 \times 10^{-18} \\ -9.684 \times 10^{-18} \end{bmatrix} \text{ Coulomb. Angstrom}$$

$$= \begin{bmatrix} -132.066 \\ -124.329 \\ -290.145 \end{bmatrix} \text{ Debye}$$

$$\text{magnitude} = \sqrt{x^2 + y^2 + z^2}$$

$$= 342.17 \text{ Debye}$$

Figure 5.3 (continued) Tuna cytochrome c dipole moment

refinement carried out by Takano et al in 1981.

The angle of the dipole vector with the haem plane is calculated in figure 5.4. The result of 36^{o} is similar to the published value of 38^{o} by Koppenol et al (1991). The asymmetry of charge on the protein and the resultant dipole vector are shown in figure 5.5. A front face view shows the dipole vector emerging from the protein close to the left side of the haem plane. A view of the left-hand side of the cytochrome indicates that the dipole vector exits the protein close to pyrrole ring 2, the exposed edge of the haem.

5.3.2 Dipole moment of *Paracoccus denitrificans* cytochrome c-550

Calculation of the dipole moment of *Paracoccus* cytochrome c-550 is complicated by a number of factors. The original amino acid sequence, on which the structure was partly based, was found to contain a number of errors. In addition, the sequence of the c-550 from the strain used in this study (LMD 52.44) is different from the sequence of the c-550 from the strain (LMD 22.21) used for the crystal structure determination. Both of these factors will be discussed in relation to the dipole moment.

The amino acid sequence of c-550 was originally published by Timkovich et al (1976) and later revised by Ambler et al (1981) and van Spanning et al (1990) . Timkovich et al (1976) established the c-550 sequence by a combination of standard chemical techniques and interpretation of a 2.5Å resolution electron density map. Due to 'chemical difficulties', the sequence of the c-terminal 10 residues was based solely on the electron density map. However this region was the least well-defined portion of the density map, and as a result, the assignment of the c-terminal sequence was considered tentative. Due to this tentative assignment, the residues from 122 to 134 in the crystal structure, are labelled as unknown and have no side-chain coordinates. The lack of definition in the c-terminus of the density map is the result of a tail which consists of a relatively unstructured extended chain following on from the final α-helix.

Since the original work of Timkovich et al (1976) two additional, independent,

(i) Calculation of normal to haem plane

Pyrrole ring nitrogens :

					x	y	z
NA	11.389	-14.101	16.130	AB =	-2.42	-1.153	-1.084
NB	8.969	-15.254	15.046				
NC	10.305	-17.805	14.889	AC =	1.336	-2.551	-0.157

Vector perpendicular (normal) to haem plane given by vector product of vectors AB and AC.

Vector Product :

$$\vec{N} = \begin{bmatrix} x_N \\ y_N \\ z_N \end{bmatrix} = \begin{matrix} y_1 z_2 - z_1 y_2 \\ x_1 z_2 - z_1 x_2 \\ x_1 y_2 - y_1 x_2 \end{matrix} = \begin{bmatrix} -2.584 \\ -1.828 \\ 7.714 \end{bmatrix} \text{ Å}$$

(ii) Calculation of angle between dipole vector and normal to haem plane

$$\cos\theta = \frac{\vec{N}\cdot\vec{\mu}}{|N||\mu|}$$

$$\mu = \begin{bmatrix} -132.066 \\ -124.329 \\ -290.145 \end{bmatrix} \text{ debye} = \begin{bmatrix} -27.516 \\ -25.904 \\ -60.452 \end{bmatrix} \text{ Å}$$

$\vec{N}\cdot\vec{\mu}$ = scalar (dot) product between vectors N and μ.

$= x_N x_\mu + y_N y_\mu + z_N z_\mu$

$= -347.843$

$|N||\mu| = 8.338 \times 71.292$

$= 594.435$

$$\cos\theta = \frac{\vec{N}\cdot\vec{\mu}}{|N||\mu|} = \frac{-347.873}{594.435} = -0.585$$

$\Rightarrow \theta = 126^\circ$

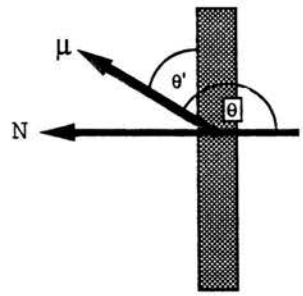

(iii) angle between dipole vector and haem plane,

$\theta' = 126 - 90$

$= 36^\circ$

Figure 5.4 Angle of tuna cytochrome c dipole to haem plane

The angle was calculated as illustated in figure 5.2. The pyrrole ring nitrogens (NA, NB, and NC) were used to estimate the haem plane. The haem group is shown as a shaded rectangle and is perpendicular to the plane of the paper.

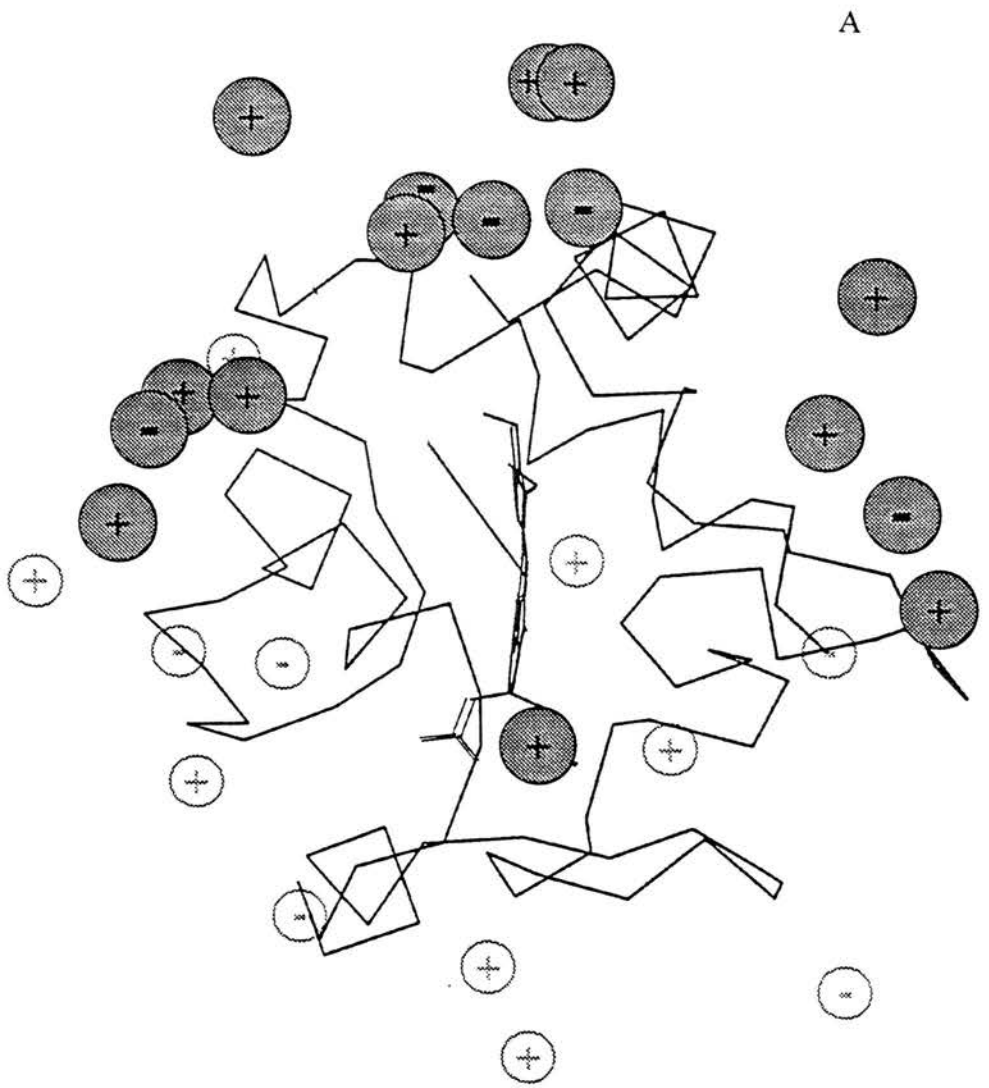

Figure 5.5 Charge distribution and associated dipole moment of tuna cytochrome c.

An α-carbon trace of tuna cytochrome c is shown. An identical trace containing side chains of the charged residues was used to place the charges in space. The protein is divided into back and front by a plane drawn through the centre of mass, perpendicular with the plane of the haem. In the front face view (a), the charges on the front half of the protein are shown as large, filled circles. The charges on the back half are shown as smaller, unfilled circles. The dipole vector is shown as a line originating at the centre of mass. In the left side view (b), the charges are shown as equally sized, filled circles. In this view, the dipole vector is in the plane of the paper with the plane dividing the protein in half perpendicular to the plane of the paper.

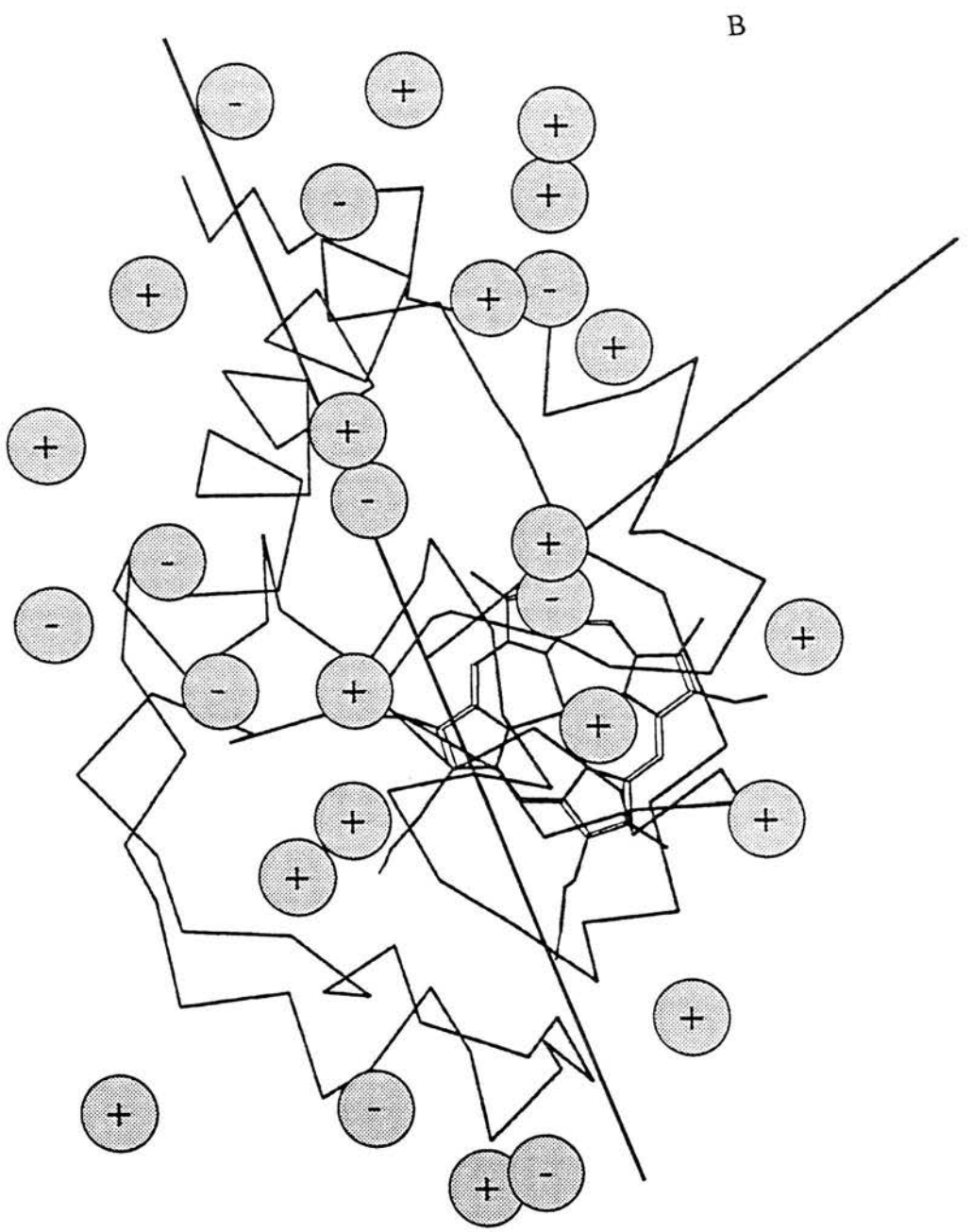

Figure 5.5 (continued) Charge distribution and associated dipole moment of tuna cytochrome c.

publications have shown the sequence to contain a number of errors (Ambler et al (1981), van Spanning et al (1990)). Ambler et al (1981), reexamined both the protein sequence and the x-ray structure and identified a number of discrepancies in the original results of Timkovich et al (1976). Isolation and sequencing of the gene encoding cytochrome c-550 (van Spanning et al (1990)) gave confirmation of the discrepancies found by Ambler et al (1981). Figure 5.6 compares the c-550 sequence of Timkovich et al (1976) with the amino acid sequence deduced from the gene by van Spanning et al (1990). The amino acid sequence deduced from the gene is identical to the reexamined protein sequence of Ambler et al (1981), except at the c-terminus where the gene sequence indicates an additional seven residues. The composition of the amino acid sequence deduced from the gene agrees well with the amino acid composition of Scholes et al (1971). This suggests the mature protein does indeed contain the extra residues at the c-terminus. In addition, the sequence work of Timkovich et al (1976) also proposed additional c-terminal residues over those found by Ambler et al (1981), although they were not individually identified (figure 5.6).

In order to calculate a dipole moment for cytochrome c-550 the revised sequence has to be fitted to the crystal structure. The following information was taken into account when calculating the dipole : (1) Lys 87 in the Timkovich sequence is deleted in the revised data. (2) Asparagine 74 was reassigned as an aspartate. (3) Aspartates 117 and 118 of the Timkovich sequence were reassigned as an asparagine and serine respectively. (4) An aspartate was assigned to position 124 (Gly) of the Timkovich sequence. (5) Glutamates were assigned to positions 126 (Ala), 130 (Gly), and 132 (Asx) of the Timkovich sequence. These changes result in the loss of positive charge at 87 and negative charge at 117 and 118. Negative charge is gained at 74, 124, 126, 130, and 132. The negative charge required at asparagine 74 was placed on the carbonyl oxygen (OD1) atom. Since there are no side chain atomic co-ordinates for 124, 126, 130, and 132, the charge was placed at the α-carbon atoms. Placing the charge on the α-carbon introduces error to the dipole, but this is likely to be small. The calculation of the dipole moment for the revised sequence is shown in figure 5.7. The dipole moment of 935 debye is considerably larger than that of tuna cytochrome

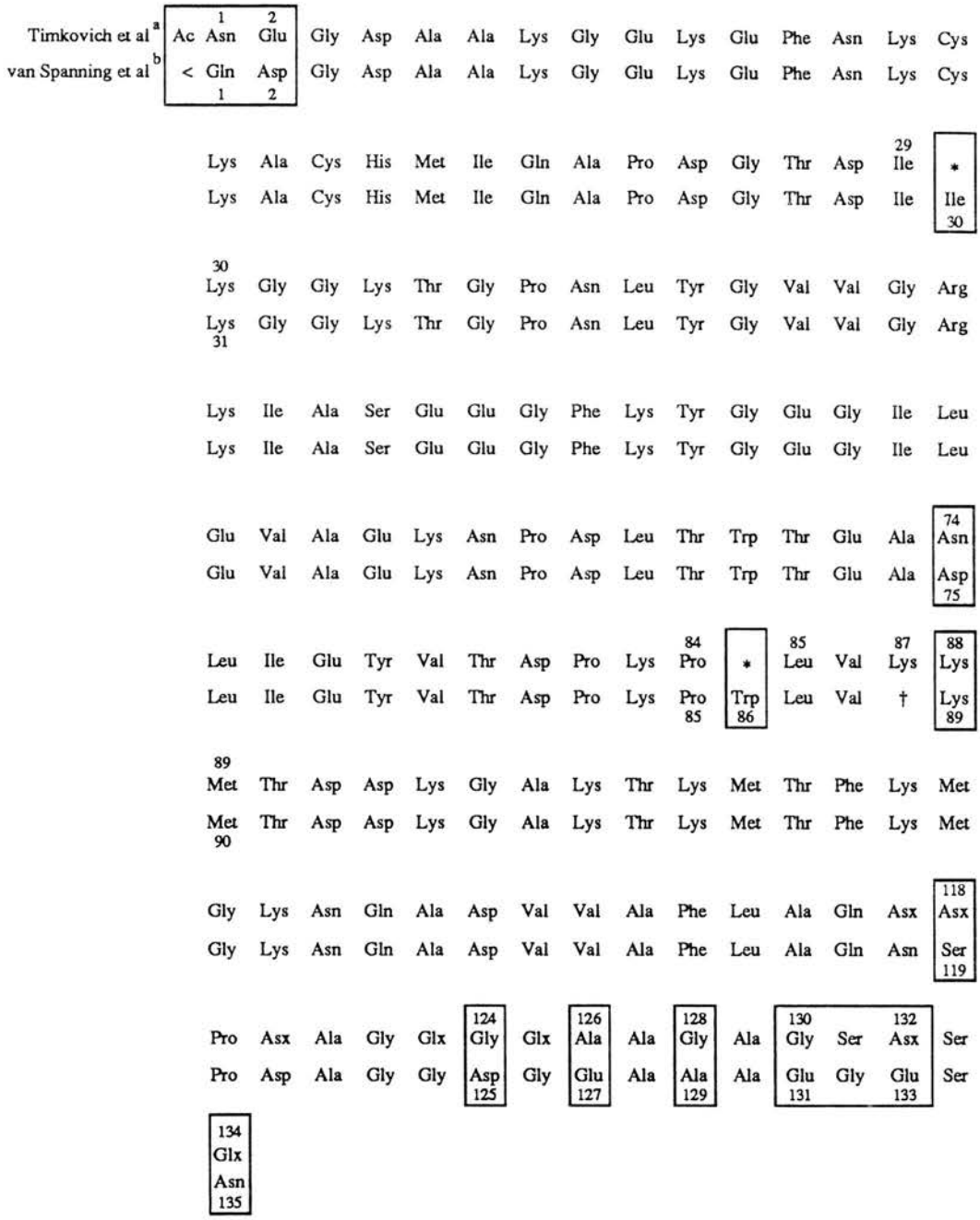

Figure 5.6 *Paracoccus denitrificans* cytochrome c-550 sequence comparison. The c-550 sequence obtained from the protein by Timkovich et al[a] (1976) is compared with the sequence deduced from the gene by van Spanning et al[b] (1990). * refers to residues not identified by Timkovich et al. The amino acid sequence deduced from the gene indicates only one lysine between Val 88 and Met 90. The second lysine was assigned by Timkovich on the basis of extra electron density in this region over that which corresponded to the sequence. However, this extra density arises as a result of the inability of Timkovich et al to identify a tryptophan residue in the sequence at position 85.

(i) Centre of Positive Charge (c.o.p.)

residue	Number[a]		atom[b]	x	y	z	charge
Lys	7[c]	7[d]	NZ	-9.684	30.379	15.123	+1
Lys	10	10	NZ	-8.899	27.995	9.572	+1
Lys	14	14	NZ	-1.296	36.207	9.460	+1
Lys	16	16	NZ	2.878	27.142	-0.166	+1
Lys	30	31	NZ	1.501	22.718	1.523	+1
Lys	33	34	NZ	10.841	25.424	-1.667	+1
Arg	44	45	NH1	17.400	25.478	13.396	+1
Lys	45	46	NZ	25.576	26.423	18.464	+1
Lys	53	54	NZ	26.028	31.834	5.274	+1
Lys	64	65	NZ	32.660	36.824	19.934	+1
Lys	83	84	NZ	19.556	47.106	13.097	+1
Lys	88	89	NZ	16.094	40.370	24.488	+1
Lys	93	94	NZ	22.710	49.335	21.448	+1
Lys	96	97	NZ	27.034	43.456	6.982	+1
Lys	98	99	NZ	22.744	35.153	3.966	+1
Lys	102	103	NZ	10.570	46.071	12.124	+1
Lys	105	106	NZ	-6.143	40.619	13.809	+1
α-Helix	1			-3.325	26.962	14.560	+1/2
α-Helix	2			24.895	37.582	10.479	+1/2
α-Helix	3			10.743	31.556	22.294	+1/2
α-Helix	4			1.867	34.754	18.595	+1/2

$$\text{c.o.p.} = \begin{bmatrix} \Sigma q_i x_i \\ \Sigma q_i y_i \\ \Sigma q_i z_i \end{bmatrix} \Big/ \Sigma q_i = \begin{bmatrix} 226.660 \\ 657.961 \\ 219.791 \end{bmatrix} \Big/ 19 = \begin{bmatrix} 11.929 \\ 34.630 \\ 11.570 \end{bmatrix}$$

Figure 5.7 *Paracoccus* cytochrome c-550 dipole moment.

The c-550 dipole moment is calculated using the 'revised' sequence of van Spanning et al (1990). The coordinates were obtained from the Brookhaven protein data bank (file 155C.pdb) and refer to the crystal structure of Timkovich & Dickerson (1976). [a] refers to residue number. [b] refers to atom type. [c] refers to the sequence numbers of the residues in the crystal structure. [d] refers to the corresponding sequence numbers in the van Spanning sequence.[e, f, g, h and i] are referred to as 'unknown' residues in the crystal structure, but are identified in the 'revised' sequence as Asp, Glu, Glu, Glu, and Asn respectively. The four stretches of a-helix are from residues 5 to 12, 55 to 64, 72 to 80, and 106 to 119.

(ii) Centre of Negative Charge (c.o.n.)

residue	Number[a]		atom[b]	x	y	z	charge
Glu	2[c]	2[d]	OE1	-7.355	32.995	23.615	-1
Asp	4	4	OD1	-6.793	27.869	18.043	-1
Glu	9	9	OE1	-2.953	23.574	8.706	-1
Glu	11	11	OE1	-3.348	34.692	11.494	-1
Asp	25	25	OD1	10.210	11.786	5.089	-1
Asp	28	28	OD1	6.927	17.428	7.028	-1
Glu	49	50	OE1	18.612	24.736	6.892	-1
Glu	50	51	OE1	26.431	20.156	5.579	-1
Glu	56	57	OE1	30.727	39.332	7.868	-1
Glu	60	61	OE1	32.326	37.585	15.886	-1
Glu	63	64	OE1	32.423	32.107	15.841	-1
Asp	67	68	OD1	25.429	28.943	27.258	-1
Glu	72	73	OE1	7.508	25.187	22.678	-1
Asp	74	75	OD1	14.907	34.140	23.291	-1
Glu	77	78	OE1	13.270	39.748	23.510	-1
Asp	81	82	OD1	11.089	45.640	15.150	-1
Asp	91	92	OD1	24.994	42.887	24.412	-1
Asp	92	93	OD1	26.974	43.528	15.063	-1
Asp	109	110	OD1	-3.434	32.392	17.625	-1
Asp	120	121	OD1	13.886	15.024	18.101	-1
UNK[e]	124	125	Cα	12.538	18.219	29.033	-1
UNK[f]	126	127	Cα	20.023	19.143	28.338	-1
UNK[g]	130	131	Cα	17.947	30.815	30.614	-1
UNK[h]	132	133	Cα	18.722	28.185	26.360	-1
UNK[i]	134	135	OXT	20.433	22.579	24.367	-1
propionate	1		O1A	18.771	29.654	12.353	-1
propionate	2		O1D	21.098	36.276	9.941	-1
α-Helix	1			3.349	31.302	7.276	-1/2
α-Helix	2			28.197	32.179	21.304	-1/2
α-Helix	3			9.439	39.609	14.861	-1/2
α-Helix	4			9.524	18.417	17.733	-1/2

$$\text{c.o.n.} = \begin{bmatrix} \Sigma q_i x_i \\ \Sigma q_i y_i \\ \Sigma q_i z_i \end{bmatrix} \Big/ \Sigma q_i = \begin{bmatrix} 426.637 \\ 855.372 \\ 504.727 \end{bmatrix} \Big/ 29 = \begin{bmatrix} 14.712 \\ 29.496 \\ 17.404 \end{bmatrix}$$

Figure 5.7 (continued) ***Paracoccus*** **cytochrome c-550 dipole moment.**

(iii) Calculation of dipole moment

$$r_P = \text{c.o.p.} - \text{c.o.m.} = \begin{bmatrix} 11.929 \\ 34.630 \\ 11.570 \end{bmatrix} - \begin{bmatrix} 12.952 \\ 30.739 \\ 14.025 \end{bmatrix} = \begin{bmatrix} -1.023 \\ 3.891 \\ -2.455 \end{bmatrix}$$

$$r_N = \text{c.o.n.} - \text{c.o.m.} = \begin{bmatrix} 14.712 \\ 29.496 \\ 17.404 \end{bmatrix} - \begin{bmatrix} 12.952 \\ 30.739 \\ 14.025 \end{bmatrix} = \begin{bmatrix} 1.760 \\ -1.243 \\ 3.379 \end{bmatrix}$$

$$\mu = (pr_P - nr_N).e = \begin{bmatrix} -1.129 \times 10^{-17} \\ 1.762 \times 10^{-17} \\ -2.317 \times 10^{-17} \end{bmatrix} \text{ Coulomb.Angstrom}$$

$$= \begin{bmatrix} -338.261 \\ 527.840 \\ -694.194 \end{bmatrix} \text{ Debye}$$

$$\text{Magnitude} = 935.383 \text{ Debye}$$

Figure 5.7 (continued) ***Paracoccus*** **cytochrome c-550 dipole moment.**

c. The angle of the dipole vector to the haem is 12°. Although this angle is smaller than that of the tuna cytochrome, the dipole vector still exits the protein at the front surface close to the exposed haem edge. Similar acute angles have been observed for some mitochondrial cytochromes c, for example, the fruit fly (*Drosophila melanogaster*, 11°) and the white cabbage butterfly (*Pieris brassica*, 12°) (Koppenol et al 1991).

The charge distribution and dipole vector for the c-550 are shown in figure 5.8. The figure shows the high concentration of negative charge on the back of the protein with the front surface containing an excess of positive charge. A front face view (figure 5.8A) shows that, like tuna cytochrome c, the dipole vector exits the protein at the upper left side of the haem. The view from the left-side shows the dipole vector exits very close to pyrrole ring II, the proposed site of electron transfer in cytochromes (Pettigrew & Moore 1987). This result indicates that although the dipole angle to the haem plane is more acute in this case, the dipole still exits the protein through the electron transferring face, close to the exposed haem edge.

Two of the most commonly studied strains of *Paracoccus denitrificans* are LMD 22.21 and LMD 52.44. The history of these strains is outlined in figure 5.9 (personal communication to Richard Ambler from Laboratory of Microbiology, Delft). Strain ATCC 13543, which is derived from LMD 22.21, was the original strain of *Micrococcus denitrificans* (Davis et al 1969). It was c-550 obtained from this strain that Scholes et al (1971) used for amino acid analysis and Timkovich et al (1976) and Ambler et al (1981) used for amino acid sequence and structure studies. A comparison of the amino acid compositions from the three studies is shown in table 5.1. As expected, the compositions are all very similar.

The gene encoding cytochrome c-550 isolated by van Spanning et al (1990) was from the *Paracoccus* strain Pd 1235. This strain corresponds to NCIB 8944 (Rob van Spanning, personal communication to Graham Pettigrew), a sub-culture of LMD 52.44 (figure 5.9). Since the amino acid sequence deduced from the gene from this strain is identical in the matching regions to the protein sequence from LMD 22.21, then it would appear that the c-550 proteins of the two strains are identical.

Figure 5.8 Charge distribution and associated dipole moment of *Paracoccus* cytochrome c-550.

An α-carbon trace of cytochrome c-550 is shown. An identical trace containing side chains of the charged residues was used to place the charges in space. The protein is divided into back and front by a plane drawn through the centre of mass, perpendicular to the plane of the haem. In the front face view (a), the charges on the front half of the protein are shown as large, filled circles. The charges on the back half are shown as smaller, unfilled circles. The dipole vector is shown as a line originating at the centre of mass. The angle of the dipole vector to the haem plane is 12^{o}. In the view of the left side view, the charges are shown as equally sized, filled circles. The dipole vector is in the plane of the paper with the plane dividing the protein in half pependicular to the plane of the paper.

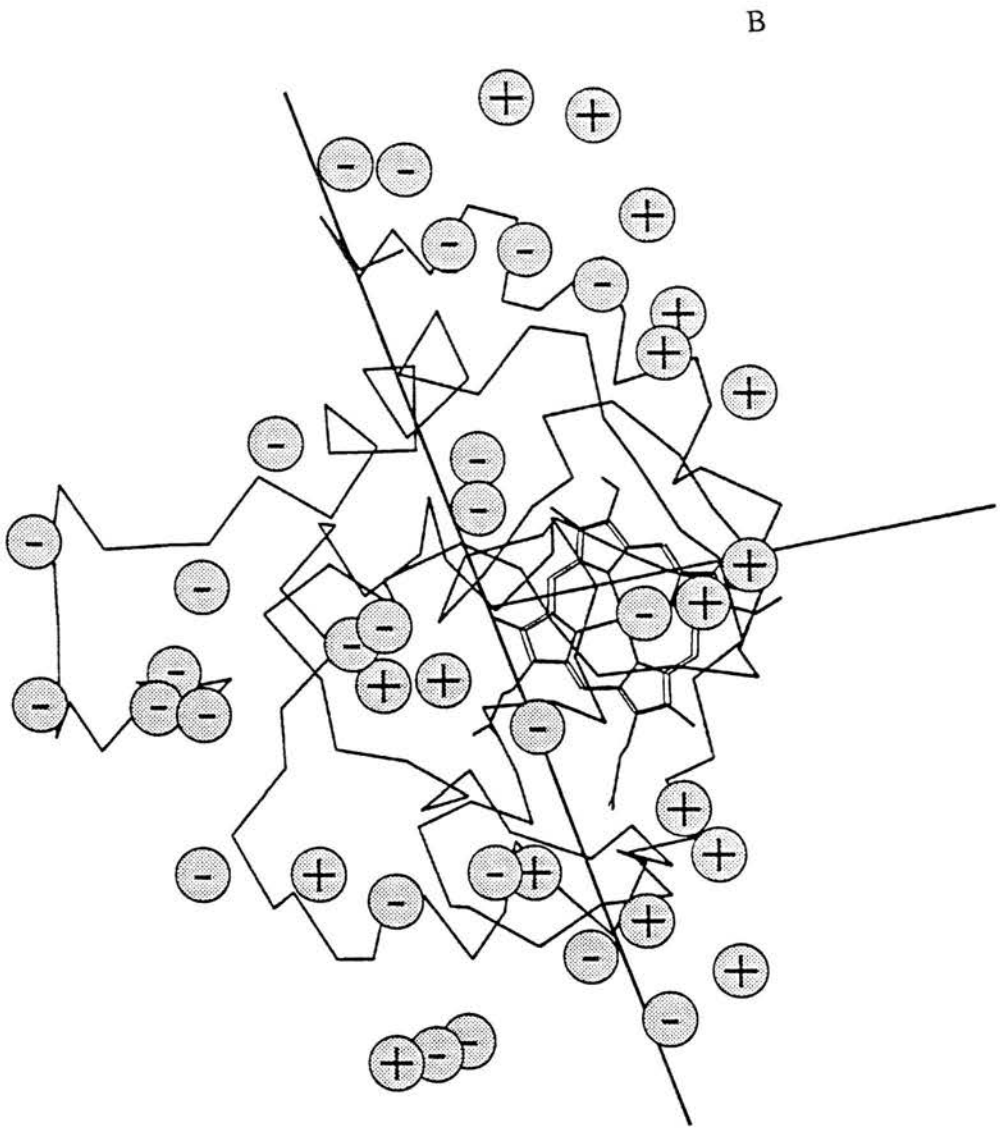

Figure 5.8 (continued) Charge distribution and associated dipole moment of *Paracoccus* cytochrome c-550.

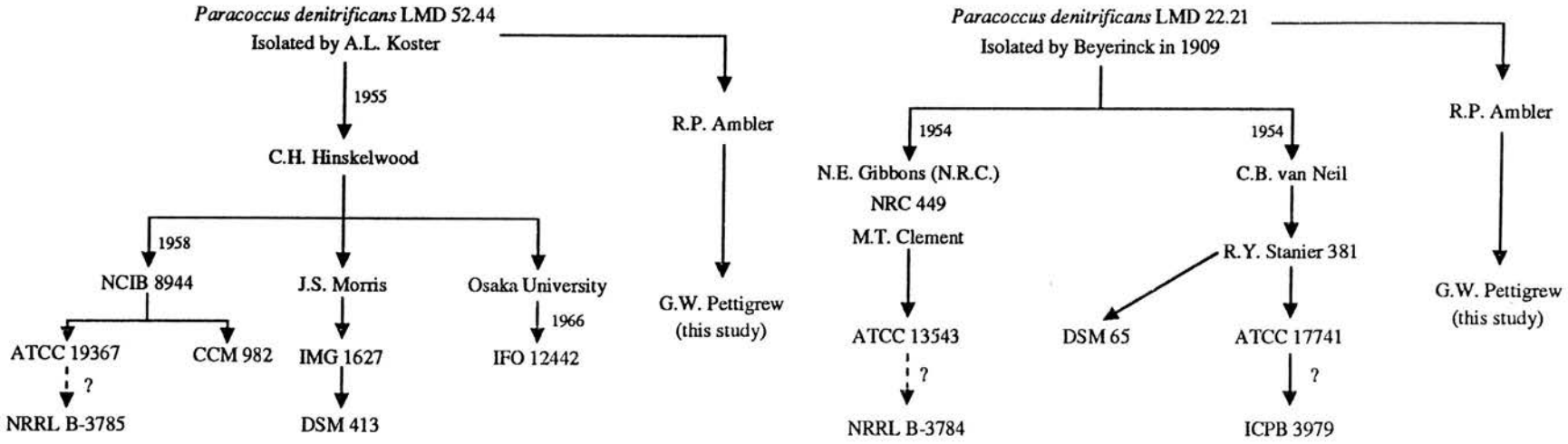

Figure 5.9 History of *Paracoccus* strains LMD 22.21 and LMD 52.44.

The two strains shown of the bacterium were originally deposited at the Laboratory of Microbiology, Delft.

Samples of the bacteria have since been distributed to various sources as shown.

However, amino acid compositions of cytochromes c-550 from *Paracoccus* strains LMD 22.21 and LMD 52.44 obtained in our laboratory are shown in table 5.1 (Pettigrew, unpublished results). The results shown indicate the proteins isolated from the two strains are not identical. The c-550 composition from LMD 22.21 agrees well with the c-550 compositions of Scholes et al (1971) and Ambler et al (1981) from ATCC 13543. This result is expected since ATCC 13543 is derived from LMD 22.21 (figure 11). However, the amino acid composition of c-550 from LMD 52.44 (Pettigrew, unpublished results), is different from the composition of the cytochromes c-550 from the other strains (table 5.1). The difference is most striking when the values for Gly, Ala and Met are compared. The c-550 from the LMD 52.44 strain contains more alanine and less glycine and methionine than is found in the c-550 from NCIB 8944 and LMD 22.21. This result is surprising since figure 5.9 indicates that NCIB 8944, used by van Spanning, and LMD 52.44, used in our laboratory, both derive from the same original isolate.

A comparison of periplasmic extracts of *Paracoccus* strains LMD 52.44 and LMD 22.21 indicates little difference in the behaviour of the cytochromes c-550 on SDS-PAGE (figure 5.10). Some of the other cytochromes do however run rather differently in the two strains. For example, cytochrome c′ from 22.21 has a greater mobility than that from 52.44. Extracts of plasma membranes from the two strains also show differences on SDS-PAGE. In addition, a comparison of the cytoplasmic extracts, which were obtained after spheroplast formation, shows that the 22.21 strain is contaminated by periplasmic cytochromes. This suggests that the two strains do not spheroplast equally well under the conditions used. It would be of great interest to repeat the above study but with *Paracoccus* strains NCIB 8944 and ATCC 13543 included in the comparison.

A recent study has shown that the sequence of a cytochrome c-550 purified from *Thiosphaera pantotropha* is very similar to the sequence of the c-550 from *Paracoccus* NCIB 8944 (Samyn et al 1993). *Thiosphaera pantotropha* is a facultative anaerobe and is considered to be a close relative of *Paracoccus denitrificans* (Woese 1987). Indeed, recently, after the 16s rRNA sequences from the two bacteria were

Table 5.1 Amino acid compositions of selected cytochromes c-550.

[a] Scholes et al (1971). Strain LMD 22.21.

[b] Ambler et al (1971). Strain LMD 22.21. Composition obtained from sequence.

[c] Pettigrew (unpublished results). Strains LMD 22.21 and LMD 52.44.

[d] van Spanning et al (1990). Strain NCIB 8944.Composition obtained from sequence.

[e] Samyn et al (1993). Composition obtained from sequence.

Compositions obtained by Pettigrew were from 3nmol samples of c-550 hydrolysed in 6M HCl, 0.1% phenol *in vacuo*, dried over sodium hydroxide pellets and analysed for amino acids using the Locarte amino acid analyser. The values are for 20h hydrolysis except for the figures for valine, isoleucine and leucine which were determined after 70h hydolysis. Figures are expressed as mole per mole haem determined by the pyridine ferrohaemochrome method using E_{550} = $29.1 mM^{-1}cm^{-1}$ (Morton 1958). Cysteine and tryptophan were not determined.

	Paracoccus denitrificans					*Thiosphaera Pantotropha*
	c-550					c-550
	Scholes[a]	Ambler[b]	Pettigrew[c]	v Spanning[d]	Pettigrew[c]	Samyn[e]
	22.21	22.21	22.21	8944	52.44	
Asp	18.3	17	19.4	18	17.4	17
Thr	7.6	8	8.0	8	6.3	7
Ser	3.1	2	4.0	3	3.0	3
Glu	16.4	14	17.5	16	15.3	16
Pro	7.7	6	6.6	6	6.4	7
Gly	17.1	16	17.0	17	13.0	14
Ala	15.3	14	15.1	15	17.4	19
Cys	(2)	2	(2)	2	(2)	2
Val	6.7	7	6.8	7	7.1	10
Met	4.1	4	3.8	4	1.0	2
Ile	5.8	6	5.1	6	4.5	4
Leu	6.2	6	6.0	6	6.6	7
Tyr	3.0	3	2.9	3	2.9	3
Phe	4.2	4	4.0	4	3.5	4
His	0.9	1	1.3	1	1.0	1
Lys	16.2	16	15.1	16	14.6	15
Arg	1.1	1	1.0	1	0.6	1
Trp		2		2		2

Figure 5.10 A comparison of *Paracoccus* strains LMD 52.44 and LMD 22.21 by SDSPAGE.

30µl of cytoplasmic, periplasmic and membrane fractions were subjected to SDSPAGE as described in materials and methods. The periplasmic fraction was obtained by spheroplasting as described in materials and methods. The spheroplasts formed were then lysed osmotically by addition of 20 vols of 20mM tris pH 8 (4°C) and spun at 15000g for 20 min to separate the cytoplasmic (supernatant) and membrane fractions. The gel was stained for haem as described in materials and methods. This gel photograph is provided courtesy of Dr Celia Goodhew who performed the experiment.

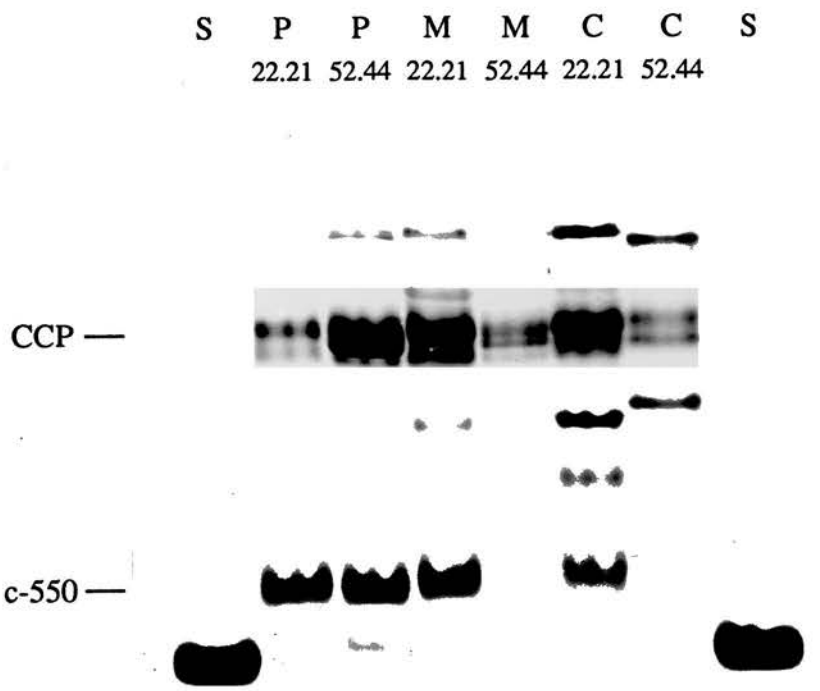
S
P
22.21
P
52.44
M
22.21
M
52.44
C
22.21
C
52.44
S
CCP
c-550

found to be identical, Ludwig et al (1993) proposed *Thiosphaera pantotropha* be reclassified as *Paracoccus denitrificans*. Table 5.1 shows the close similarity in c-550 composition between *T. pantotropha* and *Paracoccus* NCIB 8944. However, even more striking, is the similarity between the cytochromes c-550 of *T. pantotropha* and our own *Paracoccus* LMD 52.44.

Figure 5.11 shows a comparison of the sequences of cytochromes c-550 from *Paracoccus denitrificans* NCIB 8944 (van Spanning et al 1990), *Thiosphaera pantotropha* (Samyn et al, 1993), and *Paracoccus denitrificans* LMD 52.44 (partial sequence Goodhew & Pettigrew, unpublished results). As observed by Samyn et al (1993), the *T. pantotropha* c-550 sequence is very similar to the *P. denitrificans* NCIB 8944 sequence. Of the 134 residues in the *T. pantotropha* sequence, there are only 19 amino acid changes plus one additional amino acid in the *P. denitrificans* NCIB 8944 sequence. The overall sequence identity is 85.9%. (Samyn et al, 1993). The partial sequence of *Paracoccus* LMD 52.44 c-550 fits almost exactly to the corresponding regions in the *T. pantotropha* sequence. Of the approx. 70% of sequence available for *Paracoccus* LMD 52.44, only one amino acid difference exists with *T. pantotropha*. If the same level of similarity were retained over the remaining 30%, which, given the similarity in the compositions (table 5.1), is likely, then a sequence identity of over 98% would be observed. If this proves to be the case, then the sequence identity between *T. pantotropha* and *P. denitrificans* LMD 52.44 will be by far the highest observed between class I c-type cytochromes of apparently different genera (Moore & Pettigrew, 1990).

Both the cytochrome c peroxidase and cytochrome c-550 being used in our laboratory for kinetic studies derive from strain LMD 52.44. In order to interpret future experimental results in terms of the dipole moment (see discussion) it is necessary to calculate the dipole for this protein. Since neither the structure nor the complete sequence of the protein are available, two assumptions must be made in order to calculate the dipole. The first assumption is that the unknown 30% of the LMD 52.44 c-550 is identical in sequence to the corresponding regions of *T. pantotropha* c-550. Given the match of the two sequences in the regions which are known, it is likely that this level of similarity exists throughout the complete

Figure 5.11 Sequence comparison of selected cytochromes c-550

The c-550 sequence from *Paracoccus* strain NCIB 8944[a] is from van Spanning et al (1990). The sequence from *Thiosphaera pantotropha*[b] is from Samyn et al (1993). The sequence from *Paracoccus* strain LMD 52.44[c] is from Goodhew et al (unpublished results). The sequence from the strain LMD 52.44 is not complete. The regions of known sequence are underlined. The regions of unknown sequence are in brackets and have been assigned residues identical to the *Thiosphaera* c-550 (see text).

```
                2
NCIB8944[a] <Gln Asp Gly Asp Ala Ala Lys Gly Glu Lys Glu Phe Asn Lys Cys
Th.pant.[b] <Gln Glu Gly Asp Ala Ala Lys Gly Glu Lys Glu Phe Asn Lys Cys
LMD52.44[c](<Gln Glu Gly)Asp Ala Ala Lys Gly Glu Lys Glu Phe Asn Lys Cys

                                21                                  30
Lys Ala Cys His Met Ile Gln Ala Pro Asp Gly Thr Asp Ile Ile
Lys Ala Cys His Met Val Gln Ala Pro Asp Gly Thr Asp Ile Val
Lys Ala Cys His Met Val Gln Ala Pro Asp Gly Thr Asp Ile Val

Lys Gly Gly Lys Thr Gly Pro Asn Leu Tyr Gly Val Val Gly Arg
Lys Gly Gly Lys Thr Gly Pro Asn Leu Tyr Gly Val Val Gly Arg
Lys Gly Gly Lys Thr Gly Pro Asn Leu Tyr Gly(Val Val Gly Arg

                                                    57
Lys Ile Ala Ser Glu Glu Gly Phe Lys Tyr Gly Glu Gly Ile Leu
Lys Ile Ala Ser Glu Glu Gly Phe Lys Tyr Gly Asp Gly Ile Leu
Lys)Ile Ala Ser Glu Glu Gly Phe Lys Tyr Gly Asp Gly Ile Leu

                                            70
Glu Val Ala Glu Lys Asn Pro Asp Leu Thr Trp Thr Glu Ala Asp
Glu Val Ala Glu Lys Asn Pro Asp Leu Val Trp Thr Glu Ala Asp
Glu Val Ala Glu Lys Asn Pro Asp(Leu Val Trp Thr Glu Ala Asp)

                                                  88  89  90
Leu Ile Glu Tyr Val Thr Asp Pro Lys Pro Trp Leu Val Lys Met
Leu Ile Glu Tyr Val Thr Asp Pro Lys Pro Trp Leu Val Glu Lys
Leu Ile Glu Tyr Val Thr Asp Pro Lys Pro Trp Leu Ile Glu Lys
                                                  88

    92      94  95                                    104
Thr Asp Asp Lys Gly Ala Lys Thr Lys Met Thr Phe Lys Met Gly
Thr Gly Asp Ser Ala Ala Lys Thr Lys Met Thr Phe Lys Leu Gly
Thr Gly Asp Ser(Ala Ala Lys Thr Lys Met Thr Phe Lys Leu Gly

Lys Asn Gln Ala Asp Val Val Ala Phe Leu Ala Gln Asn Ser Pro
Lys Asn Gln Ala Asp Val Val Ala Phe Leu Ala Gln Asn Ser Pro
Lys Asn Gln Ala Asp Val Val Ala Phe)Leu Ala Gln Asn Ser Pro

            124     126     128                             135
Asp Ala Gly Gly Asp Gly Glu Ala Ala Ala Glu Gly Glu Ser Asn
Asp Ala Gly Ala Glu Ala  *  Ala Pro Ala Glu Asp Ala Ala Asp
Asp Ala Gly Ala Glu Ala  *  Ala Pro Ala Glu Asp Ala Ala Asp
            124     126     127                             134
```

sequences. In addition, in the unknown regions of the LMD 52.44 sequence, the *T. pantotropha* sequence differs only in three residues from the c-550 from NCIB 8944 (figure 5.12). If one includes the sequence of c-550 from *Thiobacillus versutus* (Ubbink et al 1992) in the comparison then the total number of residue differences between the three sequences is only four (figure 5.12). This suggests these are not regions of high variability. In fact, if one takes account of only the charged residues, then there is only one residue difference between the sequences in these regions and even that can be considered conservative (i.e. Glu for Asp). The evidence therefore indicates that it is valid to assume that the unknown regions of LMD 52.44 c-550 are identical in sequence to the corresponding regions of *T. pantotropha.* The unknown regions of the LMD 52.44 c-550 sequence can therefore be accounted for in the dipole calculation by using the *T. pantotropha* sequence.

The second assumption required to be made is that the crystal structure of c-550 from *Paracoccus* LMD 22.21 (Timkovich & Dickerson, 1976) is an accurate representation of the structure of *Paracoccus* LMD 52.44 c-550. In this way, the coordinates of LMD 22.21 c-550 can be used to place charge on a deduced LMD 52.44 c-550 structure. The differences between the c-550 sequence from strain NCIB 8944 and the deduced c-550 sequence from LMD 52.44 are shown in table 5.2 (note : the c-550 from strain NCIB 8944 is identical to that from LMD 22.21). We propose that these changes may be accommodated in the LMD 22.21 c-550 x-ray structure if they fit the following requirements : (1) Conservative, (2) in the c-terminal tail, or (3) in a surface loop. A conservative change would be considered as one which does little to alter the charge or the bulk of the residue in the original sequence. From table 5.2, I would consider the following changes to be conservative : residues 2 (Asp → Glu), 57 (Asp → Glu), 125 (Glu → Asp) and 104 (Met → Leu). A change in the c-terminal tail would do little to alter the overall structure of the protein since this region is thought to be 'floppy' and does not interact with the rest of the molecule (Timkovich & Dickerson 1976). The c-terminal tail is formed from residues 120 onwards and table 5.2 indicates that almost 50% of the sequence differences are in this region. *Paracoccus* cytochrome c-550 can be distinguished from mitochondrial cytochromes c by the presence of surface loops (figure 5.13, Timkovich & Dickerson 1976). It may

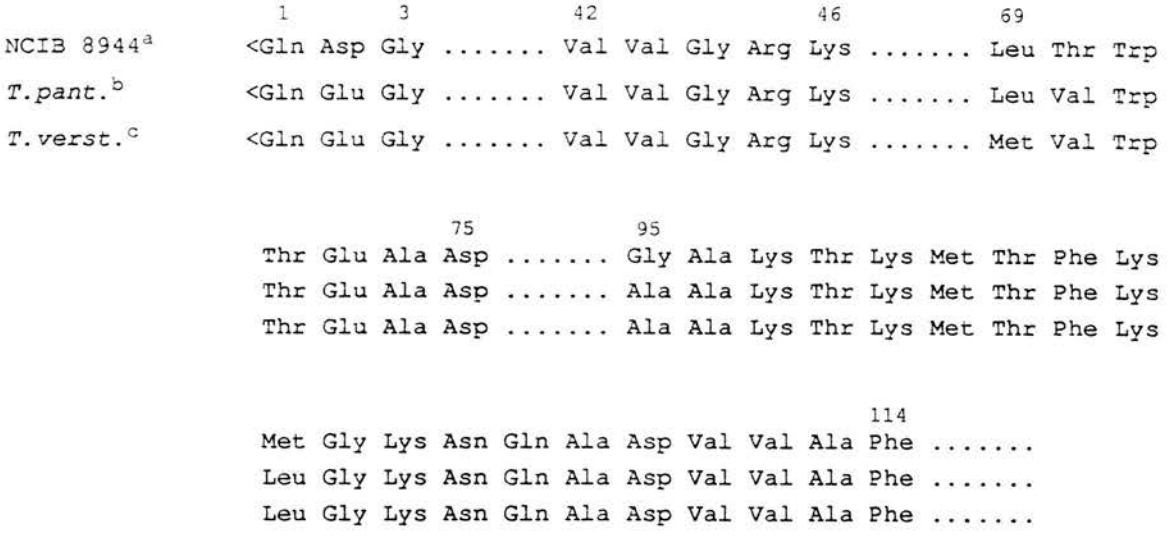

Figure 5.12 A comparison of cytochrome c-550 sequences in selected regions. The unknown regions of the c-550 sequence of *Paracoccus* LMD 52.44 are compared for cytochromes c-550 from Paracoccus NCIB 8944[a] (van Spanning et al 1990), *Thiosphaera pantotropha*[b] (Samyn et al) and *Thiobacillus versutus*[c] (Ubbink et al 1992).

residue no.	NCIB 8944	LMD 52.44	comments
2	Asp	Glu	conservative
21	Ile	Val	Loop 1
30	Ile	Val	loop 1
57	Glu	Asp	conservative
88	Val	Ile	Loop 2
89	Lys	Glu	Loop 2
90	Met	Lys	Loop 2
92	Asp	Gly	Loop 2
94	Lys	Ser	Loop 2
95	Gly	Ala	Loop 2
104	Met	Leu	conservative
124	Gly	Ala	c-terminal tail
125	Asp	Glu	c-terminal tail
126	Gly	Ala	c-terminal tail
129	Ala	Pro	c-terminal tail
132	Gly	Asp	c-terminal tail
133	Glu	Ala	c-terminal tail
134	Ser	Ala	c-terminal tail
135	Asn	Asp	c-terminal tail

Table 5.2 Sequences differences between cytochromes c-550 from *Paracoccus* strains NCIB 8944 and LMD 52.44.

The sequence differences between the c-550 from *Paracoccus* NCIB 8944 (van Spanning et al 1990) and the 'deduced' sequence from *Paracoccus* LMD 52.44 (Goodhew et al unpublished data) are shown. Comments made refer to the nature of the residue change or to which part of the structure the change occurs in (see text).

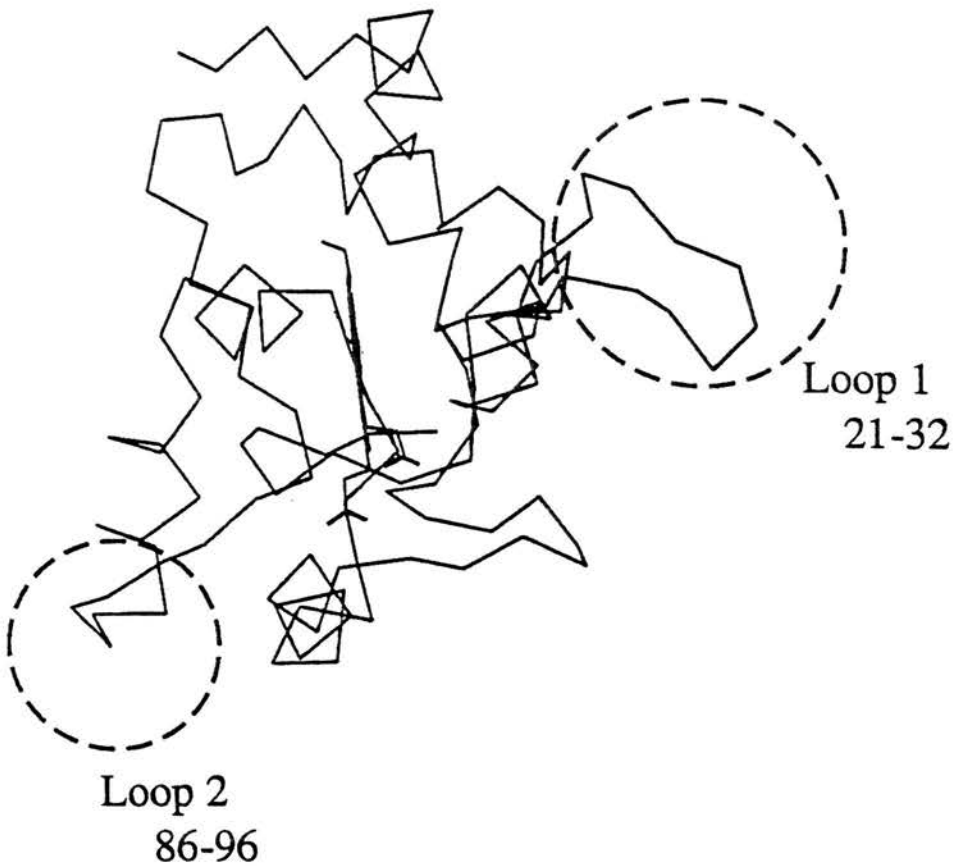

Figure 5.13 Structure of *Paracoccus denitrificans* cytochrome c-550

An α-carbon trace of Paracoccus c-550 is shown. The protein consists of a compact 'core' structure with loops on the surface. The two surface loops shown cover the amino acid stretches 21 to 32 and 86 to 96. It is our proposal that these loops can accommodate amino acid changes, additions or deletions without affecting the overall structure.

be proposed that alterations to residues within these surface loops could be accommodated within the loop itself without any alteration in the overall structure of the protein. Residue changes which occur in the surface loops are shown in table 5.2. In summary, all of the differences between the c-550 sequences appears to be either conservative or in regions which will probably have the least effect on the overall structure. I therefore consider it valid to use the coordinates of the 22.21 structure in order to calculate a dipole moment for the deduced sequence of LMD 52.44 c-550.

Taking due account of the assumptions made, an estimate of the dipole moment of the c-550 of *Paracoccus* LMD 52.44 is calculated in figure 5.14. The value of 879 debye is slightly smaller than that for *Paracoccus* LMD 22.21. The angle to the haem is 5^{o}. The asymmetric charge distribution and dipole vector associated with the protein are shown in figure 5.15. As with the Paracoccus LMD 22.21 dipole, the vector emerges from the protein on the 'front face' close to the exposed haem edge.

A summary of the data for the dipole calculations on tuna cytochrome c and *Paracoccus* cytochrome c-550 is shown in table 5.3. From the table it can be seen that the influence of α-helices on the magnitude of the dipole is small, as previously observed by Koppenol et al (1991).

5.3.3 Ionic strength dependence of peroxidase activity

The *Paracoccus* peroxidase shows a marked ionic strength dependence of activity towards both horse heart cytochrome c and *Paracoccus* c-550 (figure 5.16). This dependence of activity on ionic strength suggests the interaction between the donor cytochrome and the enzyme is electrostatic. The loss of activity at low ionic strength is possibly due to an increased affinity of the donor for the enzyme. Formation of a tightly bound complex may delay the release of the donor after electron transfer has occurred. Under these conditions, the overall rate of the reaction is controlled by the rate of dissociation of the ferricytochrome c from the enzyme (i.e. the 'off' rate). Loss of activity at high ionic strength results from the disruption of the electrostatic interactions by the presence of other ions (i.e. Na^{+} and Cl^{-}). The Na^{+} and Cl^{-} ions will effectively neutralise the charges on the donor and enzyme and therefore decrease

(i) Centre of Positive Charge (c.o.p.)

residue	Number[a]		atom[b]	x	y	z	charge
Lys	7[c]	7[d]	NZ	-9.684	30.379	15.123	+1
Lys	10	10	NZ	-8.899	27.995	9.572	+1
Lys	14	14	NZ	-1.296	36.207	9.460	+1
Lys	16	16	NZ	2.878	27.142	-0.166	+1
Lys	30	31	NZ	1.501	22.718	1.523	+1
Lys	33	34	NZ	10.841	25.424	-1.667	+1
Arg	44	45	NH1	17.400	25.478	13.396	+1
Lys	45	46	NZ	25.576	26.423	18.464	+1
Lys	53	54	NZ	26.028	31.834	5.274	+1
Lys	64	65	NZ	32.660	36.824	19.934	+1
Lys	83	84	NZ	19.556	47.106	13.097	+1
Lys	89	90	CE	19.757	38.099	24.465	+1
Lys	96	97	NZ	27.034	43.456	6.982	+1
Lys	98	99	NZ	22.744	35.153	3.966	+1
Lys	102	103	NZ	10.570	46.071	12.124	+1
Lys	105	106	NZ	-6.143	40.619	13.809	+1
α-Helix 1				-3.325	26.962	14.560	+1/2
α-Helix 2				24.895	37.582	10.479	+1/2
α-Helix 3				10.743	31.556	22.294	+1/2
α-Helix 4				1.867	34.754	18.595	+1/2

$$\text{c.o.p.} = \begin{bmatrix} \Sigma q_i x_i \\ \Sigma q_i y_i \\ \Sigma q_i z_i \end{bmatrix} \Big/ \Sigma q_i = \begin{bmatrix} 207.613 \\ 606.354 \\ 198.320 \end{bmatrix} \Big/ 18 = \begin{bmatrix} 11.534 \\ 33.690 \\ 11.018 \end{bmatrix}$$

Figure 5.14 *Paracoccus* LMD 52.44 cytochrome c-550 dipole moment.
The c-550 dipole moment is calculated using the partial sequence of Goodhew et al (unpublished results), with the unknown regions assumed to be identical to the c-550 from *Thiosphaera pantotropha* (Samyn et al, 1993, see text). The coordinates were obtained from the Brookhaven protein data bank (file 155C.pdb) and refer to the crystal structure of Timkovich & Dickerson (1976). [a]refers to residue number. [b]refers to atom type. [c]refers to the sequence numbers of the residues in the crystal structure. [d]refers to the corresponding sequence numbers in the LMD 52.44 c-550 sequence. The four streches of a-helix are from residues 5 to 12, 55 to 64, 72 to 80, and 106 to 119.

(ii) Centre of Negative Charge (c.o.n.)

residue	Number[a]		atom[b]	x	y	z	charge
Glu	2[c]	2[d]	OE1	-7.355	32.995	23.615	-1
Asp	4	4	OD1	-6.793	27.869	18.043	-1
Glu	9	9	OE1	-2.953	23.574	8.706	-1
Glu	11	11	OE1	-3.348	34.692	11.494	-1
Asp	25	25	OD1	10.210	11.786	5.089	-1
Asp	28	28	OD1	6.927	17.428	7.028	-1
Glu	49	50	OE1	18.612	24.736	6.892	-1
Glu	50	51	OE1	26.431	20.156	5.579	-1
Glu	56	57	CG	28.952	38.293	9.155	-1
Glu	60	61	OE1	32.326	37.585	15.886	-1
Glu	63	64	OE1	32.423	32.107	15.841	-1
Asp	67	68	OD1	25.429	28.943	27.258	-1
Glu	72	73	OE1	7.508	25.187	22.678	-1
Asp	74	75	OD1	14.907	34.140	23.291	-1
Glu	77	78	OE1	13.270	39.748	23.510	-1
Asp	81	82	OD1	11.089	45.640	15.150	-1
Glu	88	89	CD	17.642	41.972	23.419	-1
Asp	92	93	OD1	26.974	43.528	15.063	-1
Asp	109	110	OD1	-3.434	32.392	17.625	-1
Asp	120	121	OD1	13.886	15.024	18.101	-1
UNK[e]	124	125	Cα	12.538	18.219	29.033	-1
UNK[f]	130	131	Cα	17.947	30.815	30.614	-1
UNK[g]	131	132	Cα	16.934	31.474	27.011	-1
UNK[h]	134	135	Cα	18.067	22.543	24.827	-1
UNK[i]	134	135	OXT	20.433	22.579	24.367	-1
propionate	1		O1A	18.771	29.654	12.353	-1
propionate	2		O1D	21.098	36.276	9.941	-1
α-Helix	1			3.349	31.302	7.276	-1/2
α-Helix	2			28.197	32.179	21.304	-1/2
α-Helix	3			9.439	39.609	14.861	-1/2
α-Helix	4			9.524	18.417	17.733	-1/2

$$\text{c.o.n.} = \begin{bmatrix} \Sigma q_i x_i \\ \Sigma q_i y_i \\ \Sigma q_i z_i \end{bmatrix} \Big/ \Sigma q_i = \begin{bmatrix} 413.766 \\ 860.108 \\ 502.156 \end{bmatrix} \Big/ 29 = \begin{bmatrix} 14.268 \\ 29.659 \\ 17.316 \end{bmatrix}$$

Figure 5.14 (continued) ***Paracoccus*** **LMD 52.44 cytochrome c-550 dipole moment.**

(iii) Calculation of dipole moment

$$r_P = \text{c.o.p.} - \text{c.o.m.} = \begin{bmatrix} 11.534 \\ 33.690 \\ 11.018 \end{bmatrix} - \begin{bmatrix} 12.952 \\ 30.739 \\ 14.025 \end{bmatrix} = \begin{bmatrix} -1.418 \\ 2.951 \\ -3.007 \end{bmatrix}$$

$$r_N = \text{c.o.n.} - \text{c.o.m.} = \begin{bmatrix} 14.268 \\ 29.659 \\ 17.316 \end{bmatrix} - \begin{bmatrix} 12.952 \\ 30.739 \\ 14.025 \end{bmatrix} = \begin{bmatrix} 1.316 \\ -1.080 \\ 3.291 \end{bmatrix}$$

$$\mu = (pr_P - nr_N).e = \begin{bmatrix} -1.020 \times 10^{-17} \\ 1.352 \times 10^{-17} \\ -2.396 \times 10^{-17} \end{bmatrix} \text{ Coulomb.Angstrom}$$

$$= \begin{bmatrix} -305.592 \\ 405.059 \\ -717.842 \end{bmatrix} \text{ Debye}$$

$$\text{Magnitude} = 879.065 \text{ Debye}$$

Figure 5.14 (continued) ***Paracoccus*** **LMD 52.44 cytochrome c-550 dipole moment.**

A

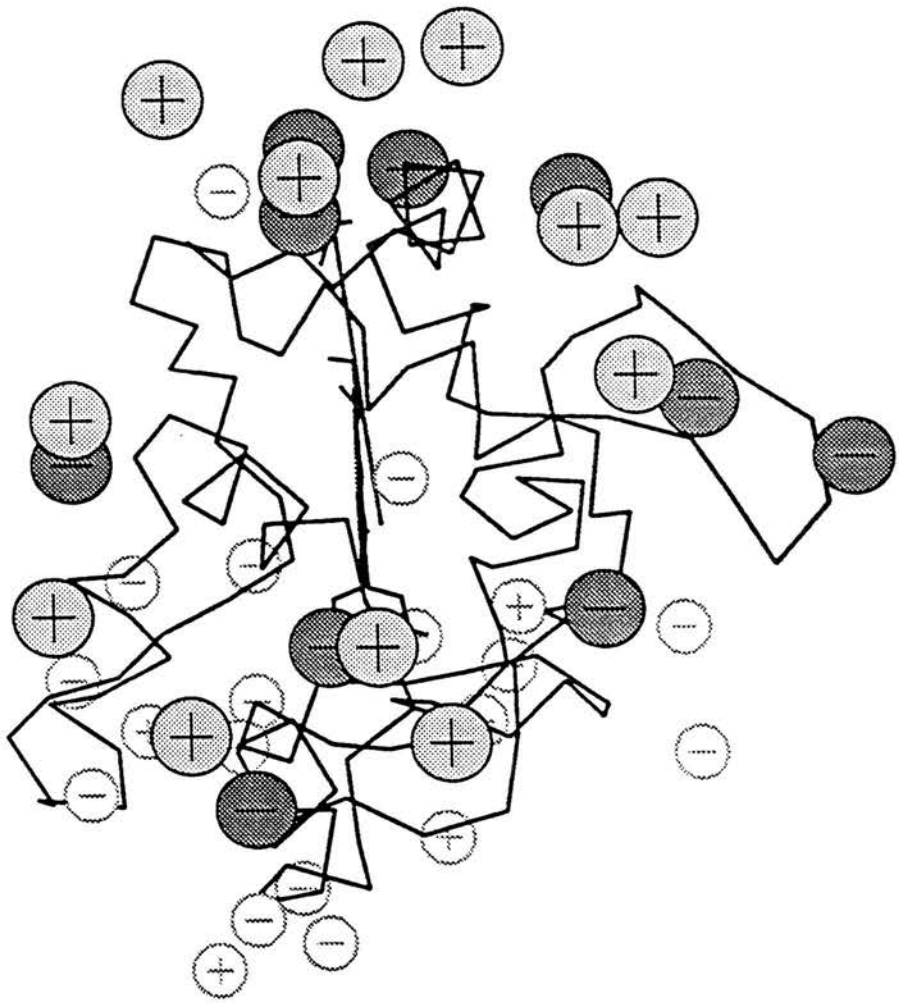

Figure 5.15 Charge distribution and associated dipole moment of *Paracoccus* LMD 52.44 cytochrome c-550.

An α-carbon trace of cytochrome c-550 from *Paracoccus* LMD 22.21 is shown. The sequence of the c-550 from *Paracoccus* LMD 52.44 has been fitted to this structure (see text) and the charge distribution was placed in space as described in figure 5.8. The protein was divided into back and front halves as described in figure 5.8. In the front face view (a), the charges on the front half of the protein are shown as large, filled circles. The charges on the back half are shown as smaller, unfilled circles. The dipole vector is shown as an arrow originating at the centre of mass. In the view of the left side view (b), the charges are shown as equally sized, filled circles. The dipole vector is in the plane of the paper with the plane dividing the protein in half perpendicular to the plane of the paper.

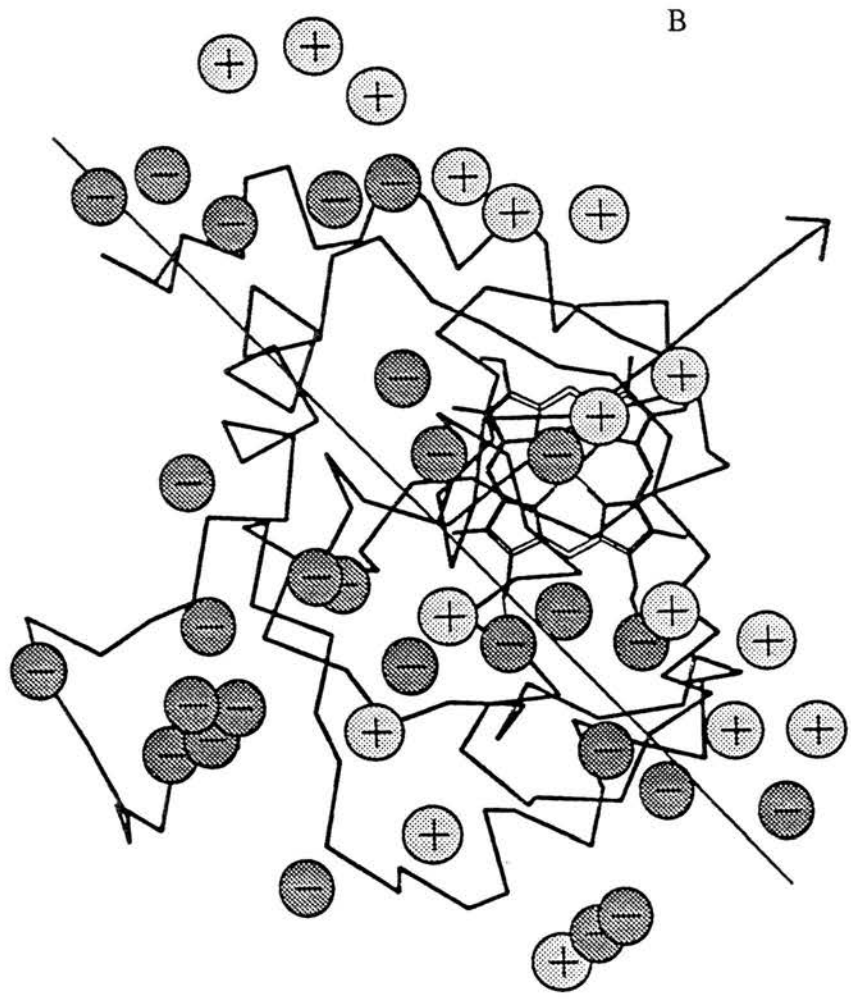

Figure 5.15 (continued) Charge distribution and associated dipole moment of *Paracoccus* LMD 52.44 cytochrome c-550.

Cytochrome	Conditions	Net Charge	Dipole	Angle to Haem
Tuna cytochrome c	no α-helices	+6 (18+, 12-)	325.238	34°
	α-helices	+6 (20+, 14-)	342.170	36°
Paracoccus LMD 22.21 cytochrome c-550	no α-helices	-10 (17+, 27-)	918.100	10°
	α-helices	-10 (19+, 29-)	935.383	12°
Paracoccus LMD 52.44 cytochrome c-550	no α-helices	-11(16+, 27-)	865.522	3°
	α-helices	-11(18+, 29-)	879.065	5°

Table 5.3 Dipole moments of tuna cytochrome c and Parcoccus c-550

The dipole moments and angles to the haem were calculated as described in the text and in figures 5.1 and 5.2.

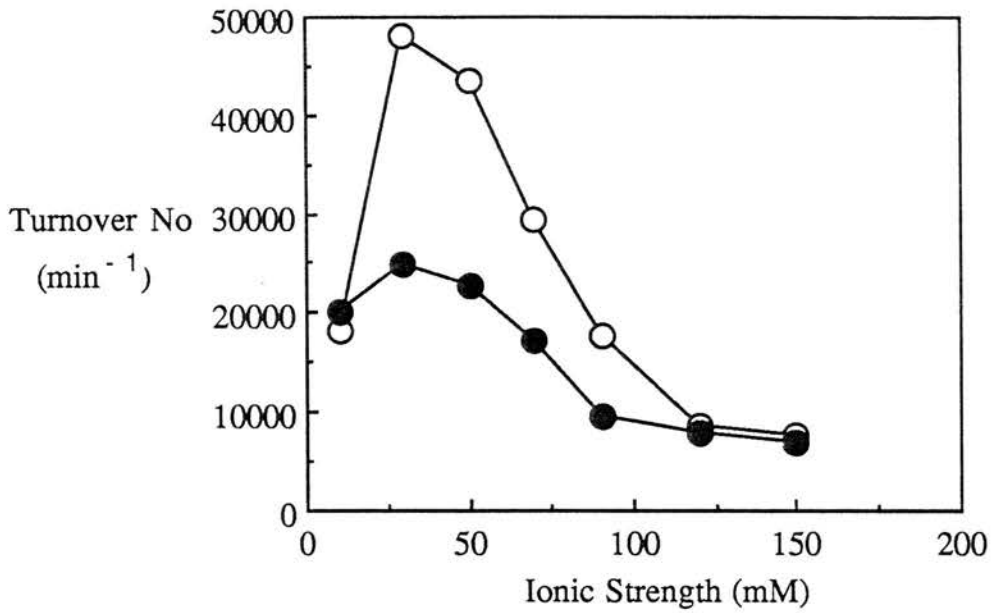

Figure 5.16 Ionic strength dependence of peroxidase activity.

Assays were performed on ascorbate-reduced, Ca^{++}-activated peroxidase. The peroxidase stock was 2μM in 5mM Mes/ 5mM Hepes pH 6, 1mM ascorbate/5μM DAD, 1mM $CaCl_2$. Assays were initiated with the enzyme (final concentration, 1nM), to a cuvette containing 5mM Mes/ 5mM Hepes pH 6, 7μM ferrocytochrome c and 18μM hydrogen peroxide. Both *Paracoccus* c-550 (O-O) and horse heart cytochrome c (O-O) were used as substrates. The ionic strength was varied by addition of NaCl and calculated as described in materials and methods (chapter II).

the strength of their charge-charge interaction. Under these conditions, the rate of the reaction is controlled by the rate at which the donor and enzyme collide productively (i.e. the 'on' rate).

5.4 DISCUSSION

5.4.1 The role of the molecular dipole

The dipole moment of *Paracoccus* cytochrome c-550 is almost 3-times that of tuna and other mitochondrial cytochromes c (Koppenol et al 1991). This large moment exists due to a pronounced asymmetric charge distribution in which a strongly positive 'front face' is present despite the protein being highly acidic (pI 4.5, (Timkovich & Dickerson 1976) (see figure 5.15). The observation that the charge distribution on c-550 may lead to a very large molecular dipole has been made previously by both Bolgiano et al (1988) and Pettigrew (1991), although no attempt was made to quantify it.

The dipole vector of cytochrome c-550 exits the protein surface close to pyrrole ring II of the haem edge. This vector orientation has also been observed for mitochondrial cytochromes c (compare figures 5.5 and 5.8, Koppenol et al (1991)). Pyrrole ring II is the most exposed region of the haem and is widely regarded to be the site of electron entry and exit in cytochromes (reviewed in Pettigrew & Moore 1987)

The observations made on cytochrome c-550 by this study provide support for the proposal of Koppenol & Margoliash (1982), that the molecular dipole is responsible for preorientation of the cytochrome prior to interaction. Koppenol & Margoliash suggested that when the cytochrome experienced the negative electric field of a redox partner it would, as a result of the molecular dipole, rotate such that the haem edge would point towards the redox partner. In this way, the number of fruitful collisions would be increased. This process of preorientation helps explain why electron transfer rates are so high between redox proteins when the surface area of the protein occupied by the exposed haem edge is less than 1% (Stellwagen, 1978).

The suggestion of a larger dipole moment on c-550 compared to mitochondrial cytochromes c led Pettigrew (1991) to suggest a more specialised role for the bacterial protein. Mitochondrial cytochrome c is involved in two types of electron transfer interactions. It diffuses laterally along the inner membrane to transfer electrons between complex III and cytochrome oxidase, and it also diffuses free in the inter membrane space to interact with soluble enzymes (see figure 5.17). The presence of a membrane-bound cytochrome c-552 in *Paracoccus* (Berry & Trumpower (1985)), which can transfer electrons from complex III to cytochrome oxidase, suggests that the c-550 may have the more straightforward role of mediating electron transfer between membrane bound and soluble periplasmic enzymes, such as cytochrome c peroxidase (see figure 5.17).

It is possible that the magnitude of the mitochondrial cytochrome c dipole moment is constrained by the presence of large amounts of cardiolipin in the inner membrane (Krebs et al 1979). Cardiolipin is a negatively charged phospholipid and when present in high concentrations, is likely to generate a large negative electric field. In the inner mitochondrial membrane, cardiolipin accounts for 25% of the total phospholipid content (Krebs et al 1979). It may be that if the cytochrome c had a very large dipole moment it could become permanently stuck onto the membrane with the front face concealed by the phospholipid bilayer. The much lower concentration of cardiolipin in the plasma membrane of *Paracoccus denitrificans* (3%, Wilkinson et al 1972) might prevent restrictions on the magnitude of the dipole, therefore resulting in much larger values and faster rates of electron transfer in solution.

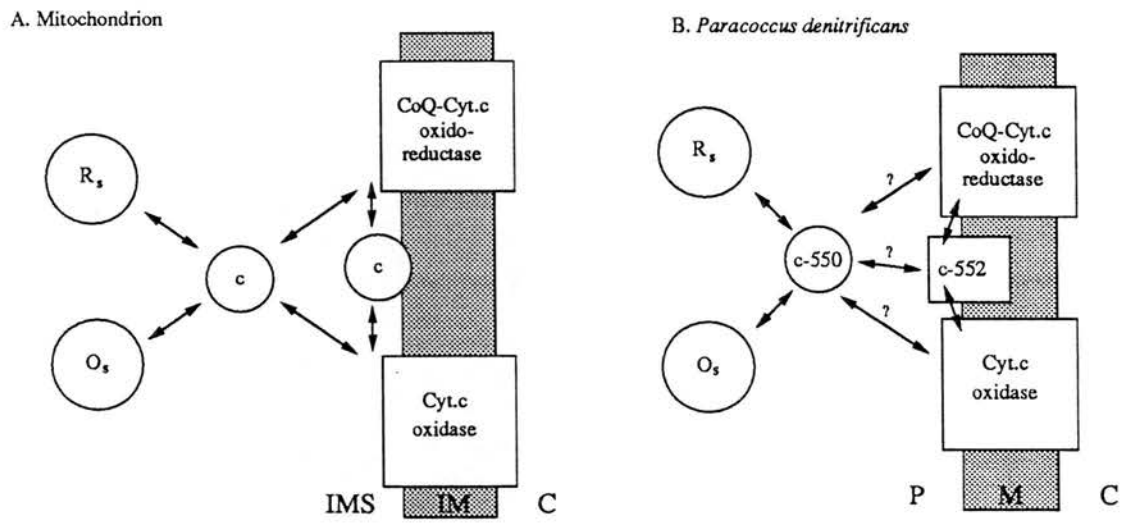

Figure 5.17 Role of cytochrome c in electron transport.

A comparison is shown of the role of mitochondrial cytochrome c with the proposed role of *Paracoccus* c-550. The role of cytochrome c involves both lateral diffusion along the inner membrane and diffusion free in solution. The proposed role for Paracoccus c-550 involves only diffusion free in solution. R_S refers to soluble reductases. O_S refers to soluble oxidases. Examples of R_S are sulphite oxidase in mitochondria and amicyanin in *Paracoccus*. Examples of O_S are yeast cytochrome c peroxidase in mitochondria and cytochrome c peroxidase in *Paracoccus*.

CHAPTER VI

DISCUSSION

This thesis has investigated the electron transfer events associated with the cytochrome c peroxidase of *Paracoccus denitrificans*. The results show that the peroxidase is similar to the well-studied enzyme from *Pseudomonas aeruginosa*, although important differences do exist. The enzyme contains two c-type haems. The higher potential haem has a mid-point potential of +226mV and is coordinated by methionine and histidine. The lower potential haem has a midpoint potential in the region of -100mV and is probably coordinated by two histidine residues. The fully oxidised enzyme is inactive and will not bind added ligands. A haem haem interaction exists within the enzyme whereby reduction of the high potential haem results in the low potential haem adopting a more open conformation, available for ligand binding. A model for the function of *Paracoccus* cytochrome c peroxidase is shown in figure 6.1. This model is based on the results of spectroscopic and kinetic experiments. The donor to the peroxidase, cytochrome c-550, has a pronounced asymmetry of charge resulting in a molecular dipole of 879 debye. The dipole vector is shown to exit the protein close to the exposed haem edge and may preorientate the protein prior to its interaction with the peroxidase. Such a preorientation would enhance the number of successful collisions between the c-550 and the peroxidase.

6.1 The role of haem-haem communication in *Paracoccus* cytochrome c peroxidase

The fully oxidised form of *Paracoccus* cytochrome c peroxidase is relatively inactive and does not bind added ligands (e.g. CN^-). Reduction of the high potential haem by ascorbate, to give the mixed valence form of the enzyme, results in a conversion of the low potential haem to a high spin state. The high spin state of the low potential haem is stabilised by divalent cations and can bind CN^- with a K_D of

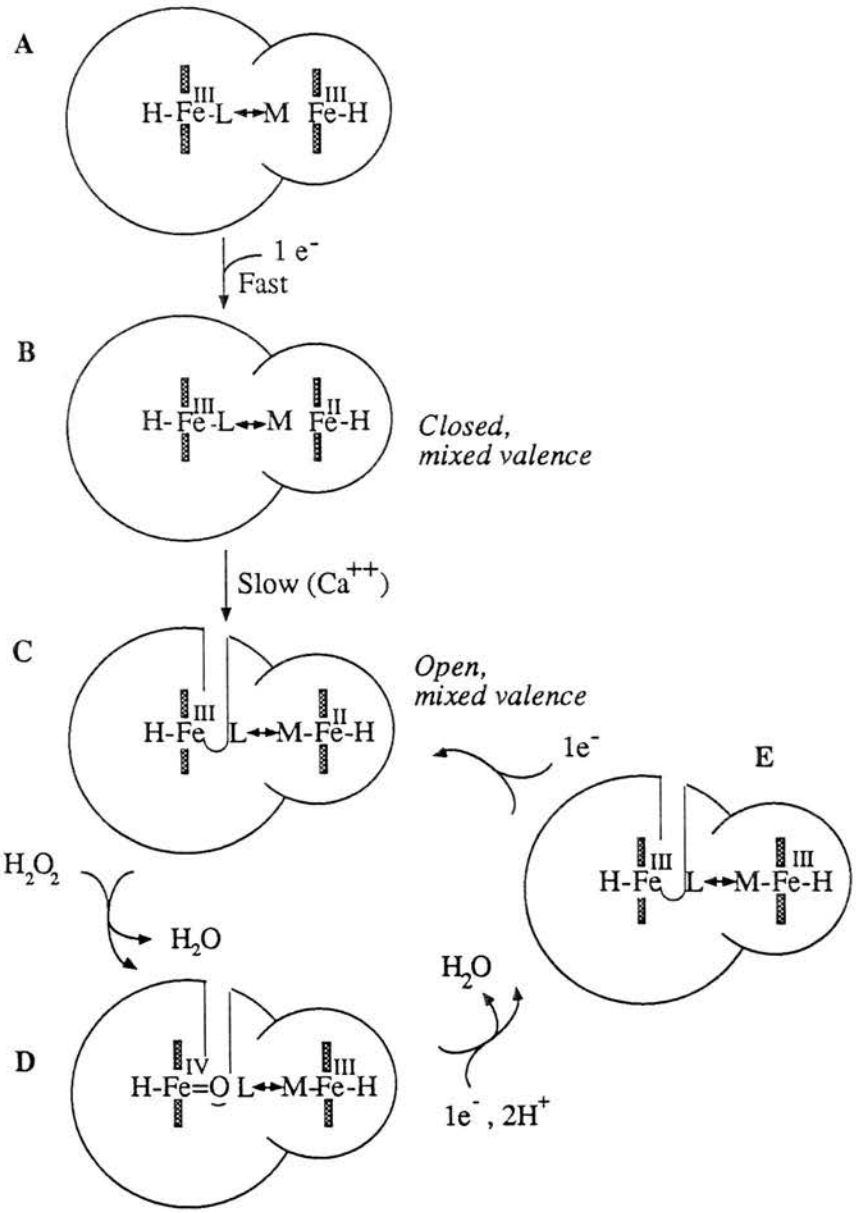

Figure 6.1 Model of action of *Paracoccus denitrificans* cytochrome c peroxidase
This model draws on both the spectroscopic results of chapter III and the kinetic results presented in chapter IV. The oxidised enzyme is inactive and reduction at the high-potential haem is required before the reaction can be catalysed. We believe that two forms of the oxidised enzyme may exist. When a supply of electrons are available the oxidised form E may exist. In this form the low potential haem remains high spin. Such an arrangement would by-pass the need for opening of the haem crevice (a slow process) after every turnover of the enzyme. In the absence of an electron supply, the oxidised form E would relax to the 'protected' form A.

5μM. Formation of the high spin state is associated with an increase in enzyme activity, with the mixed valence high spin enzyme in Ca^{++} around 30 times more active than the oxidised enzyme. Removal of Ca^{++} by EGTA treatment results in loss of the active high-spin state. The high-spin state is temperature-dependent and can be converted to low-spin lowering the temperature of the sample to 0°C.

The conclusion from these observations is that the two haems of the peroxidase interact such that reduction of the high potential haem converts the low potential haem to a high spin state. Communication between the two haems requires the presence of divalent cations.

In the cytochrome c peroxidase of *Pseudomonas aeruginosa* a haem-haem communication has also been observed, however the precise nature of this interaction has been disputed (Ellfolk et al 1983, Foote et al 1985). Ellfolk et al (1983, 1984a) have suggested that reduction of the high potential haem results in a conversion of the low potential haem from a 'closed' high spin state which is inaccessible to added ligands, to an 'open' high spin state which is accessible. An alternative model has been proposed by Foote et al (1984,1985) who suggested that reduction of the high potential haem converts the low potential haem from a low spin to a high spin state. This high spin state is then available for ligand binding. This proposal is in agreement with our results for the *Paracoccus* enzyme.

Irrespective of which model for the *Pseudomonas* enzyme proves to be correct, the two bacterial peroxidases share the same feature whereby binding of the substrate is prevented until the enzyme has the full complement of electrons to complete the reaction.

The well-studied enzyme, cytochrome c oxidase contains a mechanism similar to the bacterial peroxidases in that O_2 cannot bind until the enzyme has the reducing power necessary to complete its full reduction (Antonini et al 1985, Brunori & Wilson 1981). A model for the action of cytochrome oxidase is shown in figure 6.2. The enzyme contains four redox centres, 2 a-type haems (a and a_3) and 2 Cu atoms (Cu_A and Cu_B). Haem a_3 acts as the ligand binding site for oxygen. In the fully oxidised

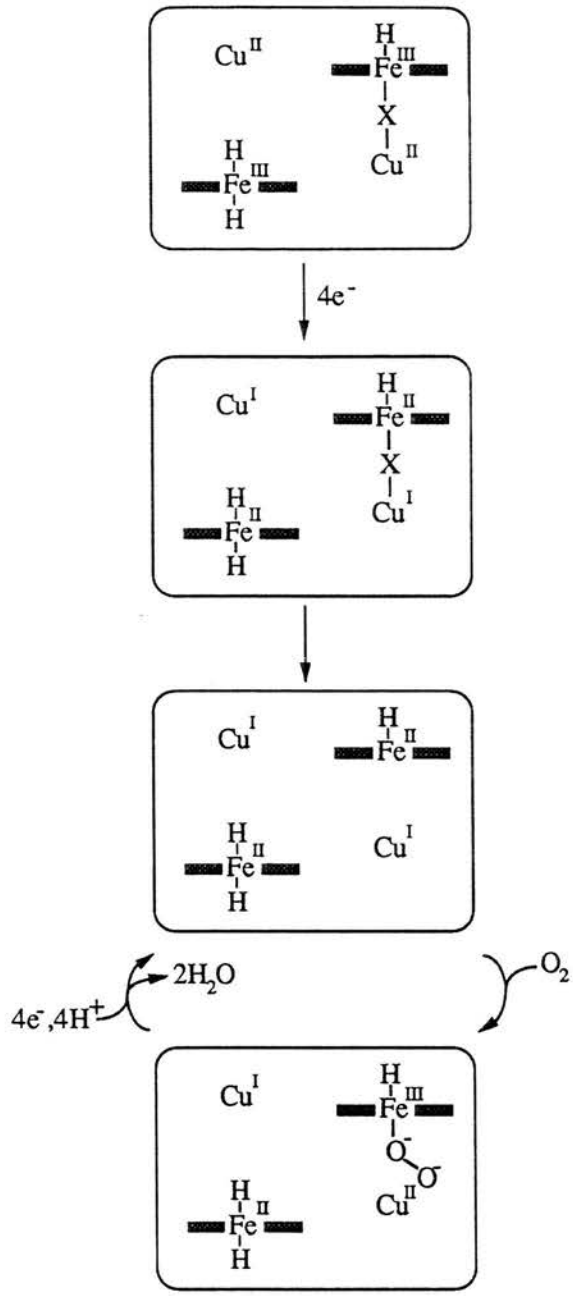

Figure 6.2 Mechanism of action of cytochrome c oxidase.

X is an unknown bridging ligand shared by haem a_3 and Cu_B. The fully oxidised form of the enzyme is inactive and cannot bind O_2. The substrate can only bind after the enzyme becomes fully reduced. The reaction cytochrome oxidase is coupled to proton pumping across a membrane (not shown).

enzyme (resting), the haem a_3 is low spin with the sixth coordination site occupied by an unknown ligand (X). This unknown ligand is termed the bridging ligand because it coordinates to both the haem a_3 and the Cu_B at the reaction centre. The fully oxidised form of the enzyme is unable to bind oxygen since the haem a_3 is oxidised and its coordination sites are fully occupied. The oxygen is only able to bind to the enzyme after it has become fully reduced and the haem a_3 is high spin (figure 6.2).

The role of haem haem communication within these enzymes may be one of protection. The complete reduction of hydrogen peroxide to H_2O is a two electron reaction. However, partial reduction of H_2O_2 yields the highly reactive intermediate, the hydroxyl radical. Free radicals have been implicated in the damage of proteins and cells (Halliwell & Gutteridge 1989). It is possible that in order to avoid such an intermediate forming the enzyme prevents the substrate binding until it has the necessary reducing power to complete the reaction.

$$H_2O_2 + 2e^- + 2H^+ \rightarrow 2H_2O$$

$$H_2O_2 + 1e^- + 1H^+ \rightarrow {}^{\cdot}OH + H_2O$$

The same protection mechanism would also have a role in cytochrome oxidase since the partial reduction of O_2 can also lead to formation of highly reactive intermediates:

$$O_2 \underset{e}{\uparrow\rightarrow} O_2^{\cdot-} \underset{e}{\uparrow\rightarrow} H_2O_2 \underset{e}{\uparrow\rightarrow} {}^{\cdot}OH \underset{e}{\uparrow\rightarrow} H_2O$$

It would appear that the yeast cytochrome c peroxidase has no protection mechanism against free radical formation. A model for the yeast enzyme is shown in figure 6.3. Unlike the bacterial peroxidases, the H_2O_2 binds to the oxidised form of this enzyme. Binding of the substrate results in removal of two reducing equivalents from the enzyme to leave a ferryl oxene (Fe^{4+}=O) intermediate and a side-chain

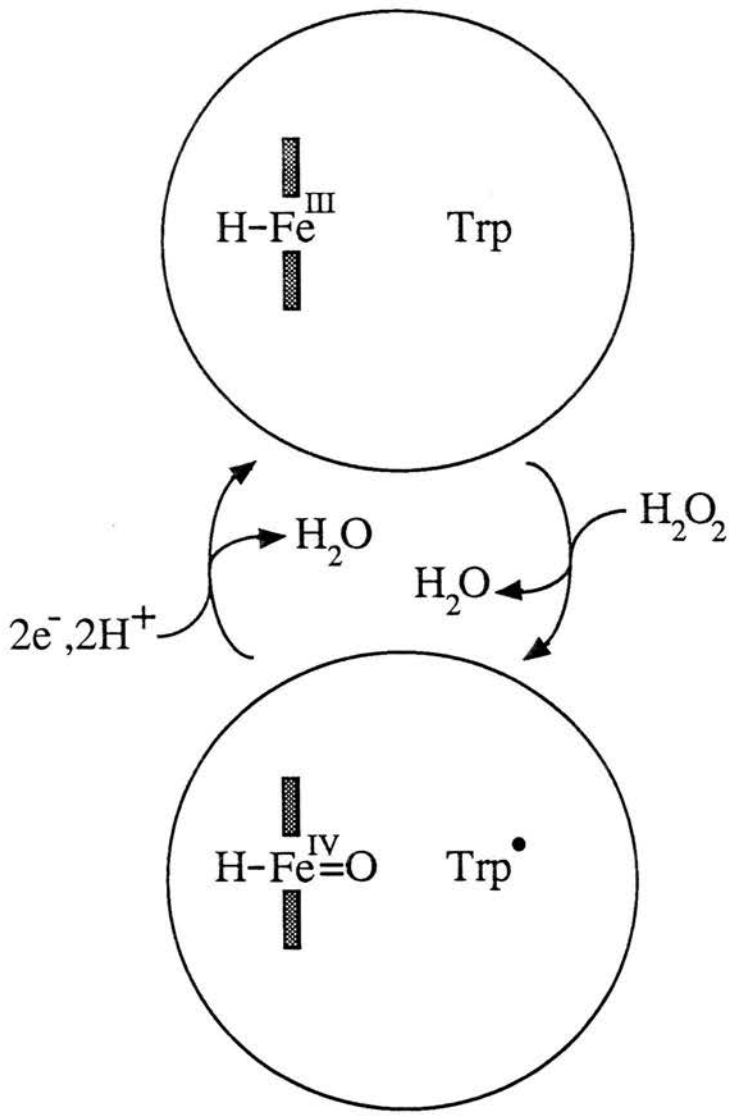

Figure 6.3 Mechanism of action of yeast cytochrome c peroxidase.
The yeast enzyme contains a single b-type haem and is found in the intermembrane space of the mitochondrion. H_2O_2 reacts with the oxidised form of the enzyme to generate the intermediate, compound I (reviewed in Bosshard et al 1991), in which Fe^{IV} and a tryptophan radical are formed. Restoration of the original enzyme is achieved by two successive one electron transfers from cytochrome c.

radical (reviewed in Bosshard et al 1991). Restoration of the original enzyme is achieved by two successive one electron transfers from ferrocytochrome c. It is possible that formation of a free radical intermediate by this enzyme could lead to enzyme damage or destruction. Indeed, it has been shown that, in the absence of electron input from cytochrome c, a number of hydrophobic residues become destroyed after reaction of the enzyme with hydrogen peroxide (Coulson & Yonetani 1972). Prolonged treatment of oxidised *Pseudomonas aeruginosa* peroxidase leads to inhibition of enzyme activity (Araiso et al 1980). It is possible in this case that small amounts of peroxide are able to bind to the enzyme over a long time period and become partially reduced. The reactive intermediates then formed may destroy the enzyme.

6.2 The structural basis for haem haem communication

The high potential haem of *Pseudomonas aeruginosa* cytochrome c peroxidase is thought to have Met-His coordination with the low potential haem having bis-His or His-Lys coordination (Ronnberg 1987a, Ronnberg 1987b, Ellfolk et al 1991). The presence of a weak absorption band at 695nm which disappears upon ascorbate-reduction (chapter III, figure 3.7) suggests a similar arrangement (at least for the high potential haem) in the *Paracoccus* cytochrome c peroxidase.

The sequence of the *Pseudomonas aeruginosa* cytochrome c peroxidase is known (Ronnberg et al 1989). The high-potential, electron transferring haem is thought to reside in the C-terminal region with coordination from His-181 and Met-254 (Ronnberg 1987b). The low potential haem is in the N-terminal end and is coordinated proximally by His-55 (Ronnberg 1987a). The distal ligand to the peroxidatic haem is still unknown. His-240 was originally suggested as the likely candidate (Ronnberg et al 1989), however, comparison of this region of the sequence with the sequence of tuna cytochrome c indicated that Lys-118 in the peroxidase would occupy the position of the distal ligand (Met 80) in the tuna cytochrome (Ellfolk et al 1991). The sequence of the *Paracoccus denitrificans* peroxidase has recently been established (Goodhew & van Beeuman, unpublished results) (figure

6.4). A comparison of the two sequences shows that His-240 is conserved whereas Lys-118 in the *Pseudomonas* sequence is an alanine in the *Paracoccus* sequence. The C-terminal region of the *Pseudomonas* sequence shows faint similarity (26% identity) to *Pseudomonas* cytochrome c-551 and probably forms a class I structure with the Met-His coordinated high-potential haem (Ronnberg 1987) (figure 6.4). Similar features are found in the peroxidase sequences from *Paracoccus denitrificans* and *Rhodobacter capsulatus* and are summarised in figure 6.5.

In the fully oxidised form of the *Paracoccus* peroxidase the high-potential haem has some high spin character. Reduction of this haem converts the iron to a fully low spin state. Our model for haem-haem communication (figure 6.1) proposes that the movement of this methionine ligand closer to the haem iron is linked to movement of the distal ligand of the peroxidatic haem away from the iron. The close proximity of Met-254 and His-240 is consistent with a model whereby movement of the methionine influences the position of the histidine. In fact, in *Pseudomonas* cytochrome c-551, the residue (Gly 51) corresponding to His-240 in the peroxidase sequence lies close to the back of the methionine ligand at the left hand side of the molecule (figure 6.6).

The validity of the above model requires confirmation of His-240 as the distal ligand to the peroxidatic haem. Work is presently underway to identify the distal ligand of the peroxidatic haem by chemical modification of the protein in the oxidised and ascorbate-reduced states (D. M^{c} Ginnity, personal communication). This approach is working on the hypothesis that the distal ligand will be bound to the peroxidatic haem iron in the fully oxidised enzyme and will therefore be unavailable for modification. Reduction of the high-potential haem will however result in movement of the histidine off the haem iron, thus making it available for modification.

The link proposed to exist between the methionine of the high potential haem and the distal ligand of the low potential haem requires the presence of divalent cations. Although the crystal structure is not available, it may be possible to gain insight into the position of the ions by examination of the protein sequence (figure 6.4). The

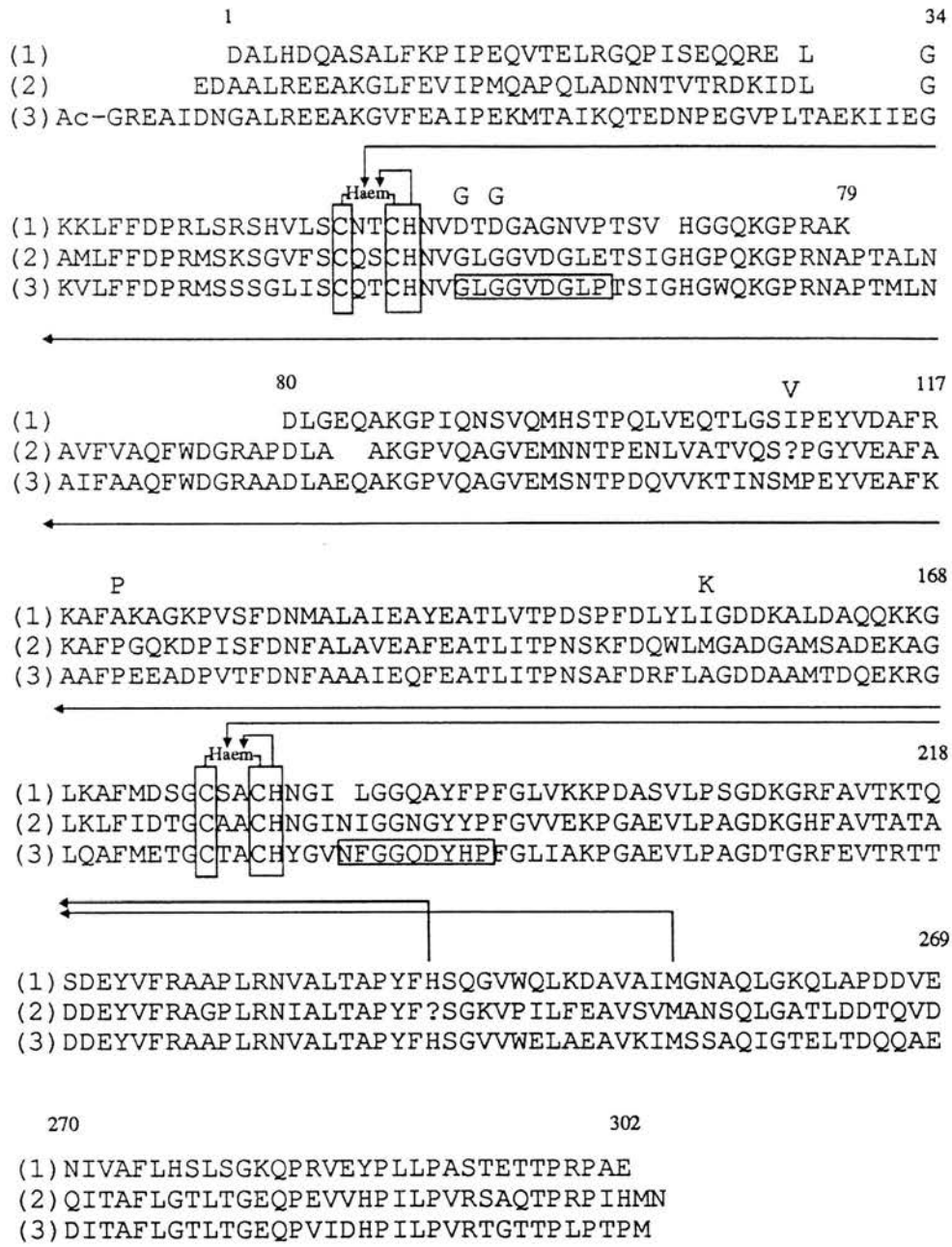

Figure 6.4 Amino acid sequences of bacterial cytochrome c peroxidases. The amino acid sequences are shown for the cytochrome c peroxidases from (1) *Pseudomonas aeruginosa* (Ronnberg et al 1989), (2) *Rhodobacter capsulatus* (van Beeuman, unpublished results), and (3) *Paracoccus denitrificans* (Goodhew & van Beeuman, unpublished results). Haem binding sites are boxed, with the proposed haem ligands indicated by an arrow to the haem. The possible Ca^{++} binding sequences in the Paracoccus peroxidase are boxed.

	Rb. capsulatus	*Ps. aeruginosa*
Pa. denitrificans	65% (213/328)	53% (168/316)
Rb. capsulatus		51% (163/318)

Figure 6.4 (continued) Overall pairwise sequence identity.
Gaps and N and C-terminal extensions were counted as one comparison.

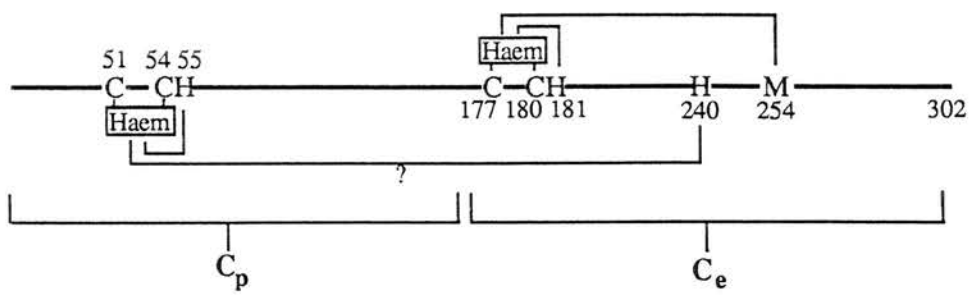

Figure 6.5 Features of the amino acid sequence of bacterial cytochrome c peroxidases

The haem binding sites and proposed haem ligands are conserved amongst the bacterial peroxidase sequences, except for position 240 which has not been identified in the sequence from Rhodobacter capsulatus. The C-terminal region of the enzyme is proposed to form a class I electron transferring domain (C_e), with a Met-His coordinated haem. C_p refers to the peroxidatic domain which contains the low potential haem with possible distal coordination by His-240 (see text). The sequence is numbered as in the *Pseudomonas aeruginosa* sequence.

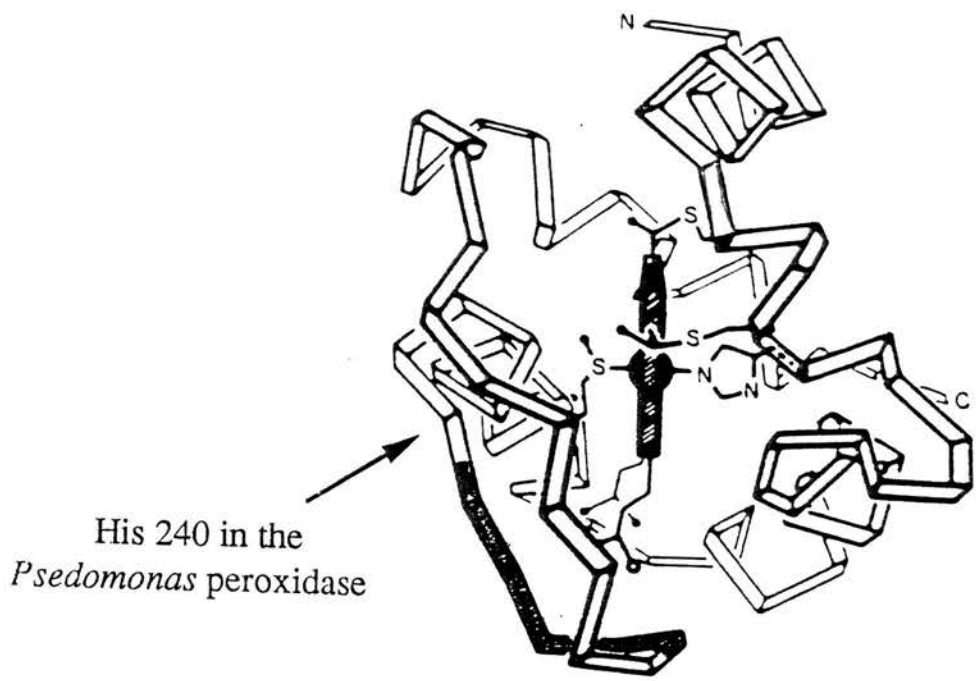

Figure 6.6 Structure of *Pseudomonas aeruginosa* cytochrome c-551.
The shaded region of the structure represents those residues which are identical in the *Pseudomonas* cytochrome c peroxidase sequence. The arrow points to Gly 51, which corresponds to His-240 in the peroxidase sequence.

crystal structure of alkaline protease from *Pseudomonas aeruginosa* has recently been published (Baumann et al 1993). The protein is shown to contain a parallel β-roll motif stabilised by Ca^{++} ions. The loops connecting consecutive turns of the β-roll contain the consensus sequence GGXGXDXUX, in which X is any amino acid residue and U is a large hydrophobic, preferably leucine. Each GGXGXD motif forms two half-sites for Ca^{++} binding. Thus, each Ca^{++} ion is bound between a pair of loops in the β-roll. The first loop contributes main chain carbonyls of G2 and G4 and one carboxyl oxygen of D6. The second loop contributes carbonyls of G1′, G3′, as well as a carboxyl oxygen of D6′ (figure 6.7). An examination of the *Paracoccus* peroxidase sequence (figure 6.4) shows two stretches of sequence that are similar to the consensus sequence from alkaline protease (Neil Saunders, personal communication) :

	G G X G X D X U X	consensus
(72)	G L G G V D G L P (80)	stretch 1
(218)	N F G G Q D Y H P (226)	stretch 2

The first stretch is from residues 72 to 80 and follows almost immediately on from the low potential haem binding site (figure 6.4). It is a match in all but the second G. The second stretch, from 218 to 226 is less similar to the consensus sequence than the first, but like the first, it follows almost immediately on from a haem attachment site, in this case, the high potential haem (figure 6.4). If these two stretches formed a Ca^{++} binding site then the two haem groups of the enzyme would lie very close to each other, with a Ca^{++} ion possibly lying between them.

An alternative model for Ca^{++} binding would be that only the stretch following the low potential haem can bind Ca^{++} and that it forms a binding site with the same stretch from another peroxidase molecule. In this model Ca^{++} would be stabilising the

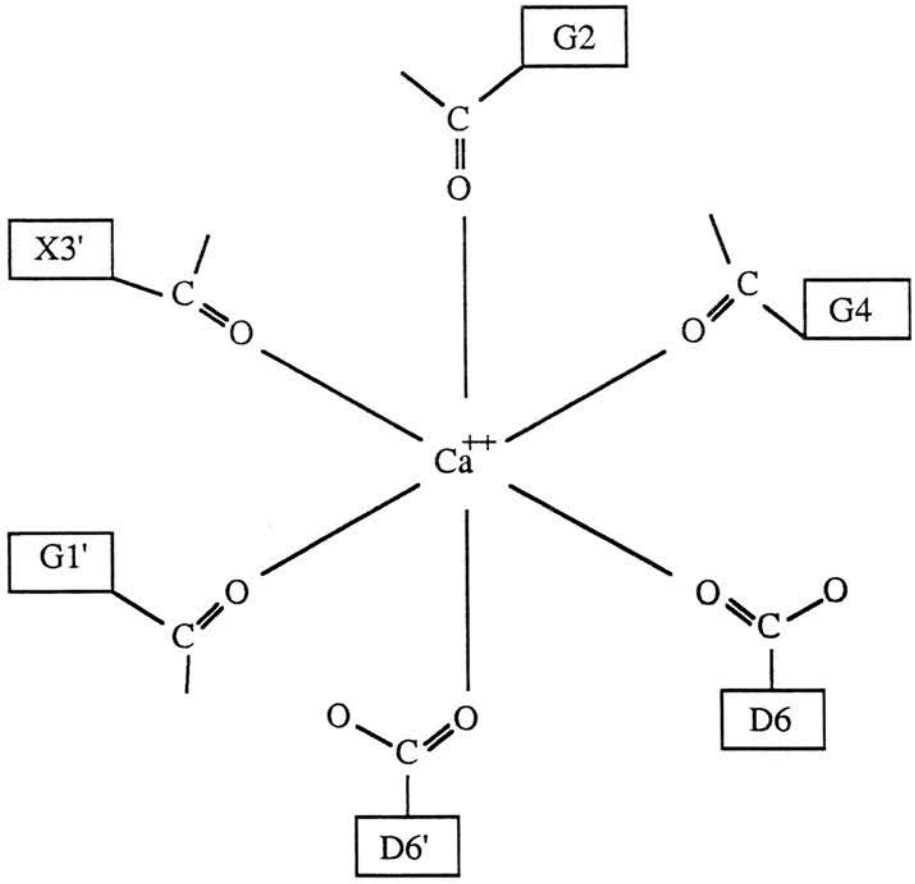

Figure 6.7 Octahedral Ca^{++} ion coordination in *Pseudomonas aeruginosa* alkaline protease.

Ca^{++} ion coordination in *Pseudomonas* alkaline protease is by the GGXGXD sequence motif. G2, G4 and D6 belong to successive residues in one sequence motif, and G1′, X3′ and D6′ belong to another sequence motif elsewhere in the sequence. (Figure adapted from Baumann et al 1993).

active dimer of the enzyme (see chapter IV, section 4.2.3).

The requirement for Ca^{++} by this enzyme has not been observed for the other bacterial cytochrome c peroxidases studied. However, it is possible that these enzymes do contain tightly bound Ca^{++} ions that are not lost during purification and therefore show no apparent requirement for the ion. A comparison of the peroxidase sequences shown in figure 6.4 indicates that the *Pseudomonas aeruginosa* sequence does not contain any regions of similarity to the Ca^{++} binding consensus sequence found in alkaline protease. The peroxidase from *Rhodobacter capsulatus* does however contain the postulated Ca^{++} binding sequence seen after the low potential haem. It would be of interest to study the Ca^{++} dependence of activity in this enzyme.

The crystal structure of yeast cytochrome c peroxidase is known and shows no associated divalent cations. However, a number of 'non-cytochrome c' peroxidases have been shown to contain bound Ca^{++} (table 6.1). Horseradish peroxidase contains 2 mols of bound Ca^{++} ions per mol of protein (Haschke & Friedhoff 1979, Shiro et al 1986). Removal of the Ca^{++} by guanidine HCl/EGTA treatment results in a 50% decrease in activity. Correlated with this loss of activity is a switch in the spin-state of the haem iron from a high-spin state to a state intermediate between high and low spin. Ca^{++} removal from HRP also results in a shift in the n.m.r. signal of the proximal histidyl NH of the ferrous protein (Shiro et al 1986). In addition, the pK_A of the distal histidine is lowered by two pH units. These observations indicate that Ca^{++} is required to maintain the structural integrity of the haem environment. In addition Ca^{++} ions have also been shown to be important in the folding of newly synthesized horseradish peroxidase. Expression of a synthetic gene for horseradish peroxidase in *E. coli* by Smith et al (1990) resulted in formation of insoluble enzyme in inclusion bodies. Solubilisation and recovery of active enzyme was shown to be critically dependent on the presence of Ca^{++} ions.

Peroxidase	Source	Electron Donor	Ca^{++} [a]	comments	Reference
Cytochrome c	*Paracoccus denitrificans*	cytochrome c-550	2[b]	Ca^{++} stabilises high-spin state of peroxidatic haem	This study
	Pseudomonas aeruginosa	cytochrome c-551	?[c]		
	yeast	mitochondrial cytochorome c	0[d]		Finzel et al 1984
Horseradish	horseradish	variety of aromatic molecules	2[e]	Ca^{++} maintains structure of haem enviroment and is required for folding of the enzyme	Haschke & Friedhoff 1979 Shiro et al 1986
Lignin	white rot fungus	lignin	2[d]	Ca^{++} ions lie close to haem crevice	Poulos et al 1993
Myeloperoxidase	canine netrophil cells	chloride ion	1[d]	Ca^{++} lies close to distal histidine of haem iron	Zeng & Fenna 1992
	bovine neutrophile cells	chloride ion	1[e]		Booth et al 1989
Lactoperoxidase	milk	thiocyanate	1[e]		Booth et al 1989

Table 6.1 Presence of Ca^{++} ions in peroxidase enzymes.

[a] Ca^{++} expressed as mol/ mol protein

[b] Two separate spectral effects observed upon EGTA treatment lead us to conclude at least two Ca^{++} binding sites are present

[c] No study yet published on Ca^{++} dependence in this enzyme

[d] Ca^{++} determined form x-ray structure

[e] Ca^{++} determined form atomic emission spectrometry

The crystal structure of lignin peroxidase indicates the presence of 2 bound Ca^{++} ions (Poulos et al 1993). One Ca^{++} ion lies very close to the proximal histidine ligand of the haem iron. In fact, one of the Ca^{++} ligands is Ser 177 which immediately follows the proximal histidine (His 176). In addition, one of the ligands to the second Ca^{++} ion is Asp 48, which immediately follows the distal histidine (His 47). The crystal structure of another peroxidase, myeloperoxidase, shows the presence of bound Ca^{++} ions (Zeng & Fenna 1992). This enzyme contains 2 identical domains linked via a disulphide bridge. Each domain contains a bound Ca^{++} ion. Asp 96, which is situated adjacent to the distal histidine ligand to the haem iron (His 95), is a ligand to one of the Ca^{++} ions. The fact that the Ca^{++} ions in these enzymes lie so close to the haem suggests they play a major role in defining the structural environment in the haem crevice. It would be interesting to study the effects of Ca^{++} removal on the structure and kinetics of these enzymes. A summary of the properties of the peroxidases is shown in table 6.1. Form the above, it would appear that the involvement of Ca^{++} runs through almost the entire peroxidase family. It is not clear whether the Ca^{++} participates directly in the reduction of H_2O_2, but it certainly ensures that the structure of the haem environment is optimised for the reaction.

In summary, *Paracoccus denitrificans* cytochrome c peroxidase contains 2 c-type haems. A protection mechanism exists within the enzyme against free radical formation whereby the substrate can only bind when the enzyme has the reducing power necessary to complete the reaction. The active form of the enzyme is the mixed valence state, in which the high-potential haem is reduced and the low potential haem is oxidised and high-spin. The high spin state of the low potential haem is stabilised by divalent cations which may bind very close to the haem groups. A more thorough understanding of the haem-haem communication and the role of Ca^{++} will become clear when the crystal structure is established.

6.3 The dipole moment of cytochrome c-550

The asymmetric distribution of charge on cytochrome c-550 results in a dipole moment of 879 debye. The magnitude of this dipole is considerably larger than that of mitochondrial cytochromes c (Koppenol & Margoliash, 1982; Koppenol et al 1991). The positive end of the dipole axis exits the protein close to the exposed edge of the haem on the 'front face'.

Chemical modification (Ferguson-Miller et al 1978, Pettigrew 1978, Rieder & Bosshard 1980) and n.m.r. (Keller & Wuthrich 1978) studies have indicated that electron transfer takes place at or close to the exposed haem edge. However, the surface area of the haem group accessible to the solvent forms only 0.6% of the total surface area of the protein (Stellwagen 1978). If a similar percentage applied to redox partners of cytochrome c, then a complex formed by random collision would only have a small chance of being in the proper orientation for electron transfer. However, direct measurements of electron transfer between cytochrome c and its redox partners show that it occurs at rates close to the diffusion-limit. Koppenol & Margoliash (1982) suggest that this apparent paradox can be solved by a model involving preorientation prior to collision such that the front face of the cytochrome c faces towards the redox partner. The mechanism of preorientation was proposed to be through the action on the dipole of the negative electric potential field of the redox partner, orientating the cytochrome c in such a way that the positive end of the dipole faced towards the redox partner. We propose a similar preorientation of cytochrome c-550 occurs as it approaches the cytochrome c peroxidase (figure 6.8). The peroxidase is a highly acidic protein and we would therefore expect it to generate a negative potential field which rotates the c-550 such that the positive end of the dipole faces towards it.

In order to test their proposal of preorientation, Koppenol & Margoliash (1982) studied the kinetics of chemically modified cytochrome c populations. Brautigan et al (1978a, 1978b) generated a number of cytochrome c molecules modified at specific

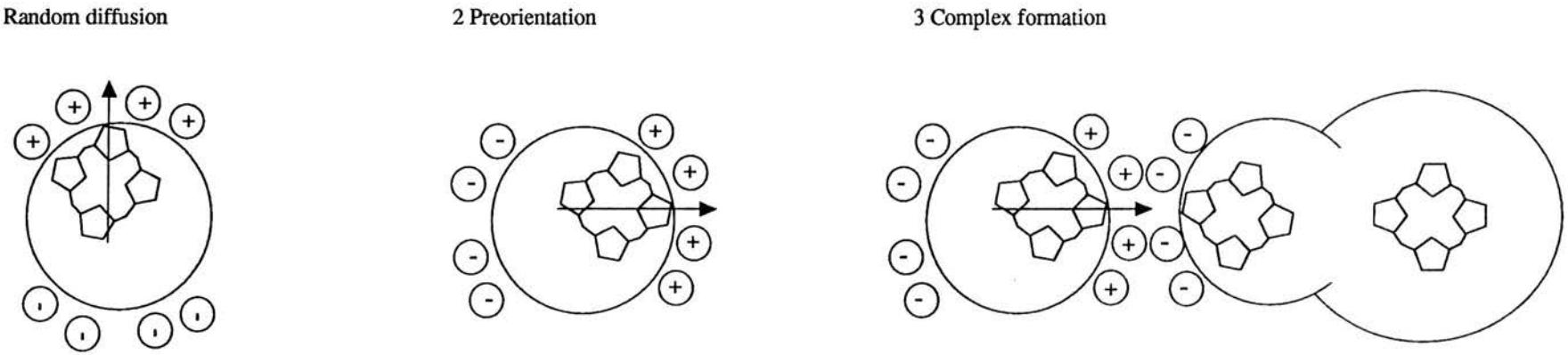

Figure 6.8 Complex formation by cytochrome c-550 of *Paracoccus denitrificans*.

The cytochrome c-550 is represented as a spherical monohaem protein. The dipole moment of the c-550 is represented by an arrow. The cytochrome c peroxidase is represented as a dihaem, two domain enzyme. The smaller domain includes the high potential haem which accepts electrons from the c-550. The larger domain includes the peroxidatic centre where the peroxide binds to the low potential haem. We propose that the c-550 preorientates prior to its interaction with the peroxidase. The preorientation occurs as a result of the influence of the negative electric field of the peroxidase on the dipole of the c-550.

lysine residues by carboxydinitrophenylation (CDNP). Using ion-exchange chromatography, these workers were able to purify populations of mono CDNP-cytochrome c molecules, with each population representing a different modified lysine residue. Koppenol & Margoliash (1982) calculated the dipole moment for each population of modified cytochrome c and studied their kinetics of electron transfer with various redox partners. The results of their study indicated a reciprocal relationship between the activity (relative to the unmodified cytochrome) and the work required to orientate the cytochrome against its dipole to allow electron transfer. Although each modified cytochrome was less efficient at electron transfer than the native protein, the results fell into two distinct categories, with one set of modified cytochromes much more inhibited than the other. The group showing the poorer reactivity were found to be those with a lysine modified at the 'front face'. These lysine residues are involved in stabilisation of electron transfer complexes through specific interactions with acidic residues on redox partners (reviewed in Pettigrew & Moore 1987). The loss of activity of cytochromes in this group could therefore not be interpreted as due to alteration of the dipole alone. The group of less strongly inhibited CDNP-cytochromes were found to be modified away from the front face. the inhibition of electron transfer by theses proteins was thought solely to be due to alteration of the dipole. Koppenol & Margoliash (1982) concluded that this dipole did indeed play a role in enhancement of electron transfer reactions by preorientation of the cytochrome.

The work presented in this thesis lays the foundation for a thorough study of the role of the dipole moment of c-550 in electron transfer reactions. A true test of the importance of the dipole will only come about by altering its magnitude and direction and studying the resultant effects on the ability of the protein to transfer electrons. We believe that the larger dipole on c-550 will allow us to make greater alterations of both the magnitude and direction than was possible with mitochondrial cytochrome c.

Work at present is aimed towards alteration of the dipole by removal of the c-terminal tail. Such a modification would be an advantage over lysine modification since the c-terminal tail is at the back of the protein, away from the electron transfer

site.The crystal structure suggests this tail hangs out at the back of the protein and does not interact with the main chain structure (chapter V, figure 5.8(b)). It was envisaged that this tail would be accessible to protease treatment and could be clipped off without affecting the core structure of the protein. Initial studies suggest subtilisin will be a useful enzyme for this cleavage. A recent digest of native c-550 using this protease yielded a peptide corresponding to the c-terminal nine residues, indicating the subtilisin cleaved at the Glu (125) - Ala (126) bond (Pettigrew, unpublished results). Cleavage of this tail removes three negative charges from the protein, resulting in an altered dipole of 707.843 (20% lower than native cytochrome (879). The visible spectrum and midpoint potential of this modified cytochrome is identical to the native c-550, indicating the overall structure of the protein is unchanged. Work is in progress to obtain a large scale preparation of this modified c-550 which can be tested for electron transfer ability.

Additional experiments to study the role of the dipole will include preparation of singly modified c-550 molecules like those used for study of cytochrome c by Koppenol & Margoliash (1982). It may be that modification of acidic residues will prove more useful than modification of lysines as the latter are congregated on the front face and may be involved in specific interactions. It is likely that the c-550 molecules will be modified at acidic residues rather than basic ones. Modification of negative residues is possible via reaction of the cytochrome with EDC and glycinemethyl ester. EDC cross-links the glycine methyl ester to negatively charged residues. The result is a conversion of the negative charge to a zero charge. Pilot experiments have shown that at least four acidics are available for modification.

REFERENCES

Ambler, R.P. (1963). Biochem. J. 89, 349-378.

Ambler, R.P. (1980) The structure and classification of cytochromes c. In : Robinson, A. B., Kaplan, N.O., (eds). From cyclotrons to cytochromes. Academic Press, London New York pp 263-279.

Ambler, R.P., Meyer, T.E., Kamen, M.D., Schichman, S.A. and Sawyer, L. (1981) J. Mol. Biol. 147, 351-356.

Andrews, P. (1964) Biochem. J. 91, 222-233

Anthony, C. (1988) In : Bacterial energy transduction. Academic Press, London, pp151-183.

Anthony, C. (1992) Biochim. Biophys. Acta. 1099, 1-15.

Antonini, G., Brunori, M., Colosimo A., Malatesta F. and Sarti, P. (1985) J. Inorg. Biochem. 23, 289-293.

Arasio, T., Ronnberg, M., Dunford, H.B. and Ellfolk. N. (1980) FEBS Lett. 118, 99-102.

Bates, R.G. (1954) Electrometric pH determination p208, Wiley New York.

Baumann, U., Shan, W., Flaherty, K.M. and McKay, D.B. (1993) EMBO J. 12, 3357-3364.

Beetlestone, J. (1960) Arch. Biochem. Biophys. 89, 35-40.

Berry, E.A. and Trumpower, B.L. (1985) J. Biol. Chem. 260, 2458-2467.

Bolgiano, B., Smith L. and Davies H.C. (1988) Biochim Biophys Acta 933, 341-350

Booth, K.S., Kimura, S.H., Lee, C., Ikeda-Siato, M. and Caughey, W.S. (1989) Biochem. Biophys. Res. Commun. 160, 897-902.

Bosma, G., Braster, M., Stouthamer, A.H. and van Verseveld, H.W. (1987) Eur. J. Biochem. 165, 665-670.

Bosshard, H.R., Anni, M. andYonetani T (1991) Yeast cytochrome c peroxidase. In: Everse J, Everse KE, Grisham MB (Eds), Peroxidases in Chemistry and Biology, Volume II. CRC Press, Boca Raton, p 51-84

Brautigan, D.L., Ferguson-Miller, S. and Margoliash, E. (1978a) J. Biol. Chem. 253, 130-139.

Brautigan, D.L., Ferguson-Miller, S. Tarr, G.E., and Margoliash, E. (1978b) J. Biol. Chem. 253, 140-148.

Brunori, M. and Wilson, M.T. (1982) Trends Biochem. Sci. 7, 295-299.

Conroy, C.W., Tyma, P., Daum, P.H. and Erman, J.E. (1978) Biochim Biophys. Acta. 537, 62-69.

Costerton, J.W., Ingram, J.M.and Cheng, K-J. (1974) Bacteriol. Reviews 38, 87-110

Coulson, A.F.W. and Yonetani, T. (1972) Biochem. Biophys. Res. Commun. 49, 391-398.

Daum, G., Bohni, P.C. and Schatz, G. (1982) J. Biol. Chem. 257, 13028- 13033

Davis, D.H., Doudoroff, M., Stanier, R.Y. and Mandel, M. (1969) Int. J. Syst. Bacteriol. 19, 375-390.

Den Ariaz, C.M., Liu, M.Y., Payne, W.J., LeGall, J., Marquez, L., Dunford, H.B., Van Beeumen, J. (1989) Arch Biochem Biophys 270, 114-125

Dickerson, R.E. (1980) Sci. Am. 242, 136-153.

Ellfolk, N. and Soininen, R. (1970) Acta Chem. Scand. 24, 2126-2136.

Ellfolk, N. and Soininen, R. (1971) Acta Chem. Scand. 25, 1535-1540.

Ellfolk, N., Ronnberg, M. and Osterlund, K. (1991) Biochim. Biophys. Acta. 1080, 68-77.

Ellfolk, N., Ronnberg, M., Aasa, R., Andreasson, L.-E. and Vanngard, T. (1983) Biochim Biophys. Acta. 743, 23-30.

Ellfolk, N., Ronnberg, M., Aasa, R., Andreasson, L.-E. and Vanngard, T. (1984a) Biochim Biophys. Acta.. 784, 62-67.

Ellfolk, N., Ronnberg, M., Aasa, R., Vanngard, T. and Ångstrom, J. (1984b) Biochim Biophys. Acta. 791, 9-14.

Emptage, M. H., Xavier, A.V., Wood, J. M., Alsaadi, B. M., Moore, G. R., Pitt, R. C., Williams, R. J. P., Ambler, R. P. and Bartsch, R. G. (1981) Biochemistry 20, 58-64.

Falk, J.E. (1964) Porphyrins and Metalloporphyrins, p 240, Elsevier, Amsterdam.

Falk, K.E., Jovall, P.A. and Angstrom, J. (1981) Biochem. J. 193, 1021-1024.

Falk, J.E. (1964) Porphyrins and Metalloporphyrins, p 240, Elsevier, Amsterdam.

Ferguson-Miller, S., Brautigan, D.L. and Margoliash, E. (1978) J. Biol. Chem. 253, 149-159.

Finzel, B.C., Poulos, T.L. and Kraut, T. (1984) J. Biol. Chem. 259, 13027-13036.

Foote, N., Thomson, A.C., Barber, D. and Greenwood, C. (1983) Biochem J 209, 701-707.

Foote, N., Peterson, J., Gadsby, P. M. A., Greenwood, C. and Thomson, A. J. (1984) Biochem. J. 223, 369-378.

Foote, N., Peterson, J., Gadsby, P. M. A., Greenwood, C. and Thomson, A. J. (1985) Biochem. J. 230, 227-237.

Gilmour, R., Goodhew, C.F., Pettigrew, G.W., Prazeres, S., Moura, I. and Moura J.J.G (1993) Biochem J. 294, 745-752.

Good, N.E., Winget, G.D., Winter, W., Connolly, T.N., Izawa, S. and Singh, R.M.M. (1966) Biochemistry 5, 467-477.

Goodhew, C.F., Wilson, I.B.H., Hunter, D.J.B., Pettigrew, G.W. (1990) Biochem J 271, 707-712.

Goodhew, C.F., Brown, K.R. and Pettigrew, G.W. (1986) Biochim Biophys. Acta. 852, 288-294.

Gray, K.A., Davidson, V.L. and Knaff, D.B. (1988) J. Biol. Chem. 263, 13987-13990.

Halliwell, B. and Gutteridge, J.M.C. (1989) Free radicals in biology and medicine, Oxford science publications.

Haltia, T., Puustinen, A. and Finel, M. (1988) Eur. J. Biochem. 172, 543-546.

Harbury, H.A. (1957) J. Biol. Chem. 225, 1009-1023.

Haschke, R.H. and Friedhoff, J.M. (1979) Biochem. Biophys. Res. Commun. 80, 1039-1042.

Husain, M. and Davidson, V.L. (1987) J. Bacteriol. 169, 1712-1717.

John, P and Whatley, F.R. (1975) Nature (London) 254, 495-498.

John, P and Whatley, F.R. (1977) Biochim Biophys. Acta. 463, 129-153.

Kadenbach, B, Ungibauer, M., Jarausch, J., Buge, U. and Kuhn-Nentwig, L.

(1983) Trends Biochem. Sci. 8, 398-400.

Kamen, M.D. and Vernon, L.P. (1955) Biochim. Biophys. Acta. 17, 10-22.

Kang, C.H., Brautigan, D.L., Osheroff, N. and Margoliash, E. (1978) J. Biol. Chem. 253, 6502-6510.

Kaput, J., Glotz, S. and Blobel, G. (1982) J Biol Chem 257, 15054 - 15058

Keilin, D. and Hartree, E.F. (1951) Biochem. J. 49, 88-104.

Keller, R.M. and Wuthrich, K. (1978) Biochem. Biophys. Res. Commun. 83, 1132-1139.

Kolthoff, I.M. and Auerbach, C. (1952) J. Am. Chem. Soc. 74, 1452-1456.

Konig, B.W., Osheroff, N., Wilms, J., Muijsers, A.O., Dekker, H.L. and Margoliash, E. (1980) FEBS Lett, 111, 395-398.

Koppenol, W.H. and Margoliash, E. (1982) J. Biol. Chem. 257, 4426-4437.

Koppenol, W.H., Rush, J.D., Mills, J.D. and Margoliash, E. (1991) Mol. Biol. Evol. 8, 545-558.

Krebs, J.J.R., Hauser, H . and Garafoli, E. (1979) J. Biol. Chem. 254, 5308-5316.

Laemmli, U.K. (1970) Nature 227, 680-685.

Lenhoff, H.N. and Kaplan N.O. (1956) J. Biol. Chem. 220, 967-982.

Long, A.R. and Anthony, C. (1991) J. Gen. Microbiol. 137, 415-425.

Ludwig, W., Mittenhuber, G. and Friedrich, C.G. (1993) Int. J. Sys. Bacteriol. 43, 363-367.

Margoliash, E. and Bosshard, H.R. (1983) Trends Biochem. Sci. 8, 316-320.

Meyer, T.E. and Kamen, M.D. (1982) Adv. Protein Chem. 35, 105-212.

Minnaert, K. (1961) The kinetics of Cytochrome c Oxidase Biochim Biophys. Acta. 50, 23-34.

Moore, G.E. and Pettigrew G.W. (1990) Cytochromes c - Evolutionary, Structural and Physicochemical Aspects, Springer-Verlag, Heidelberg.

Moore, G.R. (1985) Biochim Biophys. Acta. 829, 425-429.

Morton, R.K. (1958) Rev. Pure Appl. Chem. 8, 161-220.

Nicholls, P. (1964) Arch. Biochem. Biophys. 106, 25-48.

Nokhal, T.H. and Schlegel, H.G. (1983) Int. J. Syst. Bacteriol. 33, 26-37.

Palmer, G., Babcock, G.T. and Vickery, L.E. (1976) Proc Nat Acad Sci USA 76,

3320-3324

Pettigrew, G.W. and Moore, G.E. (1987) Cytochromes c - Biological Aspects, Springer-Verlag, Heidelberg.

Pettigrew, G.W. (1972) FEBS Lett. 22, 64-66.

Pettigrew, G.W. (1978) FEBS Lett. 86, 14-16.

Pettigrew, G.W. (1991) Biochim Biophys. Acta. 1058, 25-27.

Poulos TL, Edwards SL, Wariishi H, Gold MH (1993) J Biol Chem 268, 4429-4440

Poulos, T.L., Edwards, S.L., Wariishi, H. and Gold, M.H. (1993) J. Biol. Chem. 268, 4429-4440.

Rieder, R. and Bosshard, H.R. (1978a) J. Biol. Chem. 253, 6045-6053.

Rieder, R. and Bosshard, H.R. (1978b) FEBS Lett. 92, 223-226.

Rieder, R. and Bosshard, H.R. (1980) J. Biol. Chem. 255, 4732-4739.

Ronnberg, M., and Ellfolk, N. (1978) Biochim Biophys Acta 504, 60-66

Ronnberg, M. (1987a) Biochim Biophys Acta 912, 82-86.

Ronnberg, M. (1987b) Biochim Biophys Acta 916, 112-118.

Ronnberg, M., Araiso, T., Ellfolk, N and Dunford, H.B. (1981) Arch. Bichem. Biophys. 207, 197-204.

Ronnberg, M., Kalkinnen, N.and Ellfolk, N. (1989) FEBS Lett 250, 175-178.

Ronnberg, M., Osterlund, K. and Ellfolk. N. (1980) Biochim Biophys. Acta. 626, 23-30.

Samyn, B, Berks, B.C., Page, M.L.D., Ferguson, S.J. and van Beeumen, J.J. (1993) Eur. J. Biochem. in press.

Saraiva, L.M., Liu., M.Y., Payne, W.J., LeGall, J., Moura, J.J.G. and Moura, I. (1990) Eur. J. Biochem. 189, 333-341.

Scholes, P.B., McLain, G. and Smith, L. Biochemistry 10, 2072-2075.

Shiro, Y., Kurono, M., and Morishima, I. (1986) J Biol Chem 261, 9382-9390.

Sievers, G. (1978) Biochim Biophys. Acta. 536, 212-225.

Singh, J. and Wharton, D.C. (1973) Biochim Biophys Acta. 292, 391-401.

Smith, L. and Conrad, H. (1956) Arch Biochem Biophys. 63, 403-413

Smith, A.T., Santama, N., Dacey, S., Edwards, M., Bray, R.C., Thorneley, R.N.F. and Burke, J.F. (1990) J. Biol. Chem. 265, 13335-13343.

Smith, H.T., Staudenmeyer, N. and Millet, F. (1977) Biochemistry 16, 4971-4974.

Smith, M.B., Stonehuerner, J., Ahmed, A.J., Staudenmeyer, N. and Millet, F. (1980) Biochim Biophys Acta. 592, 303-313.

Soininen, R. and Ellfolk N. (1972) Acta Chem Scand 26, 861-872

Soininen, R., Sojonen, H. and Ellfolk, N. (1970) Acta Chem Scand 24, 2314-2320

Soininen, R. and Ellfolk, N. (1973) Acta Chem. Scand. 27, 35-46.

Soininen, R., Sojonen, H. and Ellfolk, N. (1970) Acta Chem. Scand. 24, 2314-2320.

Speck, S. H., Ferguson-Miller, S. Osheroff, N. and Margoliash, E. (1979) Proc. Natl. Acad. Sci. USA 76, 155-159.

Speck, S. H., Koppenol, W.H., Dethmers, J.K., Osheroff, N., Margoliash, E. and Rajagopalan, K.V. (1981) J. Biol. Chem. 256, 7394-7400.

Stellwagen, E. (1978) Nature (London) 275, 73-74.

Stock JB, Rauch B, Roseman S (1977) J Biol Chem 252, 7850-7861.

Takano, T. and Dickerson, R.E. (1981) J. Mol. Biol.153,

Takano, T., Trus, B.L., Mandel, N., Mandel, G., Kallai, O.B., Swanson, R. and Dickerson, R.E. (1977) J. Biol. Chem. 252, 776-785.

Takio, K., Titani, K., Ericsson, L.H. and Yonetani, T. (1980) Arch. Biochem. Biophys. 203, 615-629.

Timkovich, R. and Dickerson, R.E. (1976) J Biol. Chem. 251, 4033-4046.

Timkovich, R., Dickerson, R.E and Margoliash, E (1976) J Biol. Chem. 251, 2197-2206.

Ubbink, M., van Beeumen, J. and Canters, G.W. (1992) J. Bacteriol. 174, 3707-3714.

van Spanning, R.J.M. (1991) PhD Thesis. University of Amsterdam, Holland.

van Spanning, R.J.M., Wansell, C.W., Harms, N. Oltmann, L.F. and Stouthamer, A.H. (1990) J. Bacteriol. 172, 986-996.

van Spanning, R.J.M., Wansell, C.W., Reijnders, W.N.M., Harms, N., Ras, J., Oltmann, L.F. and Stouthamer, A.H. (1991) J. Bacteriol. 173, 6962-6970.

van Verseveld, H.W. and Stouthamer, A.H. (1991) The genus *Paracoccus*. In : The Prokaryotes

2nd edition (Barlows, A., Truper, H.G., Dworkin, M., Harder, W. and Schleifer, K.H. eds) Springer Verlag, New York.

Villalain, J., Moura, I., Liu, M. C., Payne, W. J., LeGall, J., Xavier, A.V. and Moura, J. J. G. (1984) Eur. J. Biochem. 141, 305-312.

Wada, A. (1976) Adv. Biophys. 9, 1-63.

Wilkinson, B.J., Morman, M.R. and White, D.C. (1972) J. Bacteriol. 112, 1288-1294.

Williams, R. J. P., Ambler, R. P. and Bartsch, R. G. (1981) Biochemistry 20, 58-64.

Wilson, G.S. (1978) Meth. Enzymol. LIV, 396-409.

Woese, C.R. (1987) Microbiol. Rev. 51, 221-271.

Wood P.M. (1983) FEBS Lett. 164, 223-226.

Yonetani T. and Ray G.S. (1966) J Biol Chem 241, 700-706

Zeng, J. and Fenna, R.E. (1992) J. Mol. Biol. 226, 185-207. 226, 185-207.

Matthew, J.B., Weber, P.C., Salemme, F.R. and Richards, F.M. (1983) Nature 301, 169-170.

More, C., Gayda, J.P. and Bertrand, P. (1990) J. Mag. Res. 90, 486-499.

Sillen, L.G. and Martell, A.E. (1971) Special publication No. 25. The chemical society, London.

Thomas M.V. (1982) Techniques in Calcium Research - Biological Techniques Series, Academic Press.

APPENDIX

Spectroscopic characterization of cytochrome *c* peroxidase from *Paracoccus denitrificans*

Raymond GILMOUR,* Celia F. GOODHEW,* Graham W. PETTIGREW,*§ Susana PRAZERES,†‡ Isabel MOURA†‡ and José J. G. MOURA‡

*Department of Preclinical Veterinary Sciences, Royal (Dick) School of Veterinary Studies, University of Edinburgh, Summerhall, Edinburgh EH9 1QH, Scotland, U.K., †Centro de Tecnologia Quîmica e Biologica, Rua da Quinta Grande 6, Apartado 127, 2780 Oeiras, Portugal, and ‡Departamento de Quimica, Faculdade de Ciencias e Tecnologia, Universidade Nova de Lisboa, 2825 Monte de Caparica, Portugal

The cytochrome *c* peroxidase of *Paracoccus denitrificans* is similar to the well-studied enzyme from *Pseudomonas aeruginosa*. Like the *Pseudomonas* enzyme, the *Paracoccus* peroxidase contains two haem *c* groups, one high potential and one low potential. The high-potential haem acts as a source of the second electron for H_2O_2 reduction, and the low-potential haem acts as a peroxidatic centre. Reduction with ascorbate of the high-potential haem of the *Paracoccus* enzyme results in a switch of the low-potential haem to a high-spin state, as shown by visible and n.m.r. spectroscopy. This high-spin haem of the mixed-valence enzyme is accessible to ligands and binds CN^- with a K_D of 5 μM. The *Paracoccus* enzyme is significantly different from that from *Pseudomonas* in the time course of high-spin formation after reduction of the high-potential haem, and in the requirement for bivalent cations. Reduction with 1 mM ascorbate at pH 6 is complete within 2 min, and this is followed by a slow appearance of the high-spin state with a half-time of 10 min. Thus the process of reduction and spin state change can be easily separated in time and the intermediate form obtained. This separation is also evident in e.p.r. spectra, although the slow change involves an alteration in the low-spin ligation at this temperature rather than a change in spin state. The separation is even more striking at pH 7.5, where no high-spin form is obtained until 1 mM Ca^{2+} is added to the mixed-valence enzyme. The spin-state switch of the low-potential haem shifts the midpoint redox potential of the high-potential haem by 50 mV, a further indication of haem–haem interaction.

INTRODUCTION

H_2O_2 is formed as a result of incomplete reduction of O_2 to water. The toxicity of H_2O_2 arises from its ability to form free radicals, e.g. hydroxyl radicals, which are highly reactive and can result in cell damage or cell death (Halliwell and Gutteridge, 1989). H_2O_2 may be removed by catalase in a dismutation reaction or by peroxidase in a process of reduction to water.

The bacterial cytochrome *c* peroxidase of *Pseudomonas aeruginosa* has been extensively studied both spectrally and kinetically. The enzyme contains two haem *c* moieties covalently attached to a single polypeptide chain (Ellfolk and Soininen, 1970; Soininen et al. 1970). The midpoint oxidation–reduction potentials of the two haems are +320 mV and −330 mV (Ellfolk et al., 1983). The high-potential haem acts as an electron-transferring pole and can be reduced physiologically by azurin or cytochrome *c*-551, or non-physiologically by ascorbate. The low-potential haem acts as the peroxidatic centre. The fully oxidized enzyme does not bind added ligands (Ellfolk et al., 1984a) and only slowly reacts with H_2O_2 (Araiso et al., 1980). In contrast, the low-potential haem of the ascorbate-reduced enzyme will readily bind added ligands, including H_2O_2 (Ellfolk et al., 1984a; Araiso et al., 1980). Thus a haem–haem interaction appears to be important in this enzyme, by which reduction of the high-potential haem results in the low-potential haem adopting a more open conformation, allowing access of the substrate.

Various spectroscopic studies have shown the low-potential haem of the *Pseudomonas aeruginosa* peroxidase to be high spin in the mixed-valence enzyme (Ellfolk et al., 1983, 1984a; Ronnberg et al., 1980; Ellfolk et al., 1984b; Foote et al., 1984, 1985; Villalain et al., 1984). Ellfolk and co-workers concluded that this haem was also high-spin in the fully oxidized enzyme (Ronnberg et al., 1980; Ellfolk et al., 1984b). Similarly, a study of the spin states of a cytochrome *c* peroxidase from *Pseudomonas stutzeri* led Villalain and co-workers to assign the high-spin signal to the low-potential haem in both the fully oxidized and ascorbate-reduced enzyme (Villalain et al., 1984). In contrast, Foote and co-workers, using m.c.d. spectroscopy, proposed that the high-spin signal of the fully oxidized enzyme of the *Pseudomonas aeroginosa* peroxidase was due to a labile methionine co-ordination of the high-potential haem (Foote et al., 1984, 1985).

The amino acid sequence of the *Pseudomonas aeruginosa* peroxidase is known (Ronnberg et al., 1989). There is faint similarity (26 % identity) to *Pseudomonas aeruginosa* cytochrome *c*-551 in the C-terminal region of the molecule, and this area may form a class I domain with a Cys-Xaa-Yaa-Cys-His haem-binding site and extraplanar iron co-ordination by His-181 and Met-254. Ronnberg et al. (1989) have proposed that His-240 is the distal ligand of the peroxidatic haem which controls the access of ligands to the haem group. The close proximity of Met-254 to His-240 may provide the link through which the high-potential haem is able to alter the structure around the low-potential haem. Indeed, the residue in cytochrome *c*-551 (Gly-51) corresponding to His-240 in the peroxidase lies very close behind the methionine ligand at the left hand side of the molecule.

A cytochrome *c* peroxidase from *Paracoccus denitrificans* has recently been identified (Goodhew et al., 1990). The enzyme is a dihaem *c*-type cytochrome of M_r 42000 on SDS/PAGE. The physiological electron donor to the peroxidase is probably the

Abbreviations used: PMS, phenazine methosulphate; PES, phenazine ethosulphate; DAD, diaminodurol; HNQ, 2-hydroxy-1,4-naphthoquinone.

§ To whom correspondence should be sent.

Table 1 Amino acid composition of *P. denitrificans* cytochrome *c* peroxidase

The amino acid composition was determined as described in the Materials and methods section. The 'Average' is the average of 20 and 70 h values, except that 70 h values were taken for Ile, Val and Leu.

	Composition (mol/2 mol of haem)			
Amino acid	20 h	70 h	Average	Nearest integer
Asp	33.6	35.9	34.8	(35)
Thr	29.7	33.4	31.6	(32)
Ser	13.7	14.5	14.1	(14)
Glu	46.3	52.7	49.5	(50)
Pro	27.8	30.7	29.3	(29)
Gly	28.7	32.3	30.5	(31)
Ala	40.3	44.2	42.3	(42)
Val	13.1	19.5	19.5	(20)
Met	8.9	9.6	9.3	(9)
Ile	10.1	16.3	16.3	(16)
Leu	18.3	23.2	23.2	(23)
Tyr	4.1	5.1	4.6	(5)
Phe	16.3	20.1	18.2	(18)
His	7.1	7.1	7.1	(7)
Lys	10.7	12.7	11.7	(12)
Arg	10.0	11.3	10.7	(11)
Cys			[4]*	
Trp			[1]†	
Haem			[2]	
		Total M_r...	39565	

* Two haem-binding sites assumed, each containing two cysteine residues.

† Assumed value of 1 for tryptophan by analogy with *Ps. aeruginosa* cytochrome *c* peroxidase.

soluble cytochrome *c*-550 (Pettigrew, 1991). The present paper describes a spectroscopic characterization of the enzyme and proposes a mechanism for the haem–haem interaction.

MATERIALS AND METHODS

Growth of cells

Paracoccus denitrificans (A.T.C.C. 19367, N.C.I.B. 8944, L.M.D. 52.44) was grown as described by Goodhew et al. (1990).

Enzyme purification

Cytochrome *c* peroxidase was purified by the method of Goodhew et al. (1990). The pure enzyme had an A_{409}/A_{280} ratio of 5.6 and gave a single band on SDS/PAGE when converted into the apoprotein (see Goodhew et al., 1990).

Redox titration

Reductive and oxidative titrations were performed in an anaerobic cuvette constantly flushed with argon and magnetically stirred. The cuvette contained approx. 6 μM cytochrome *c* peroxidase in 5 mM Mes/5 mM Hepes (sodium salts), adjusted to pH 7.5 with HCl, and 17 μM phenazine methosulphate (PMS), phenazine ethosulphate (PES), diaminodurol (DAD), 2-hydroxy-1,4-naphthoquinone (HNQ) and FMN as redox mediators. Higher buffer concentrations were avoided in order to prevent Ca^{2+} contamination from buffer salts. The pH at the end of the redox titration was measured, and these values are given in the Figure legends.

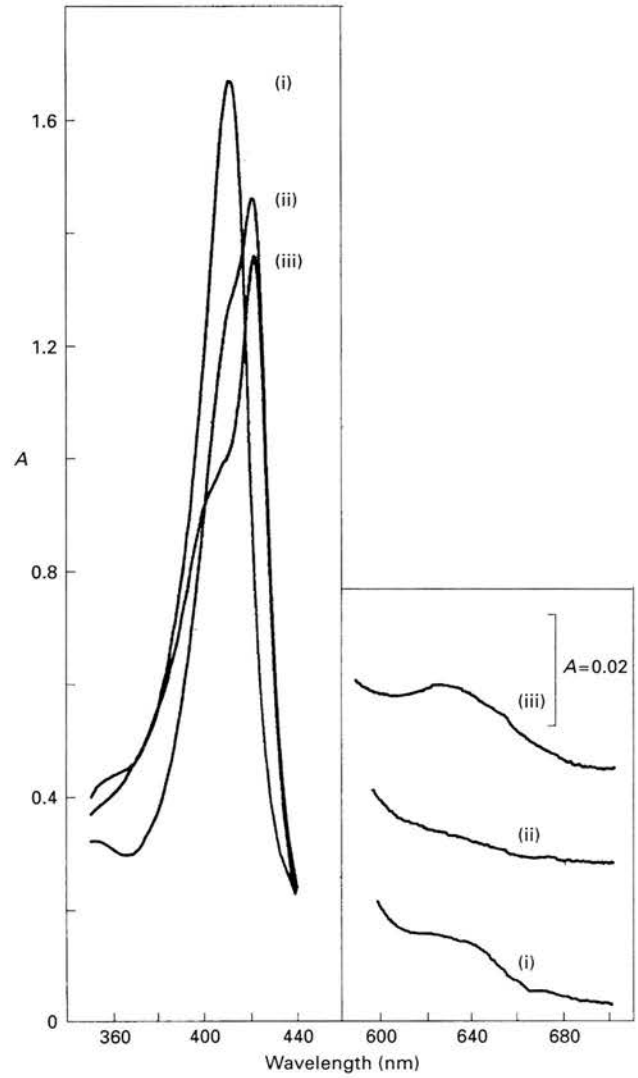

Figure 1 Visible absorption spectra of *P. denitrificans* cytochrome *c* peroxidase

The spectrum of oxidized cytochrome *c* peroxidase (i) was obtained from an untreated, 8 μM sample of enzyme in 5 mM Mes/5 mM Hepes, pH 6. Mixed-valence spectra were obtained by addition of 1 mM ascorbate and 5 μM DAD. (ii) Shows a spectrum of the peroxidase 2 min after ascorbate addition. The same sample is shown in (iii), 60 min after ascorbate addition in the presence of 1 mM $CaCl_2$.

The ambient redox potential ($E_{obs.}$) was monitored by a Pt pin electrode in combination with an Ag/AgCl reference (Russell pH Ltd.) and the potential, with reference to the standard hydrogen electrode, was obtained by adding 196 mV to $E_{obs.}$.

Reductive titrations were carried out by addition of anaerobic sodium dithionite (30 mM). Sodium dithionite stock solutions were prepared in anaerobic 100 mM Mes/100 mM Hepes (sodium salts) adjusted to pH 7.5 with HCl. Oxidative titrations were carried out using 30 mM potassium ferricyanide in the same buffer.

Amino acid composition and determination of haem content

The amino acid composition of the protein was determined on a Locarte analyser after hydrolysis in 6 M HCl/0.1 % phenol *in vacuo* for 20 or 70 h. The haem content of the same protein

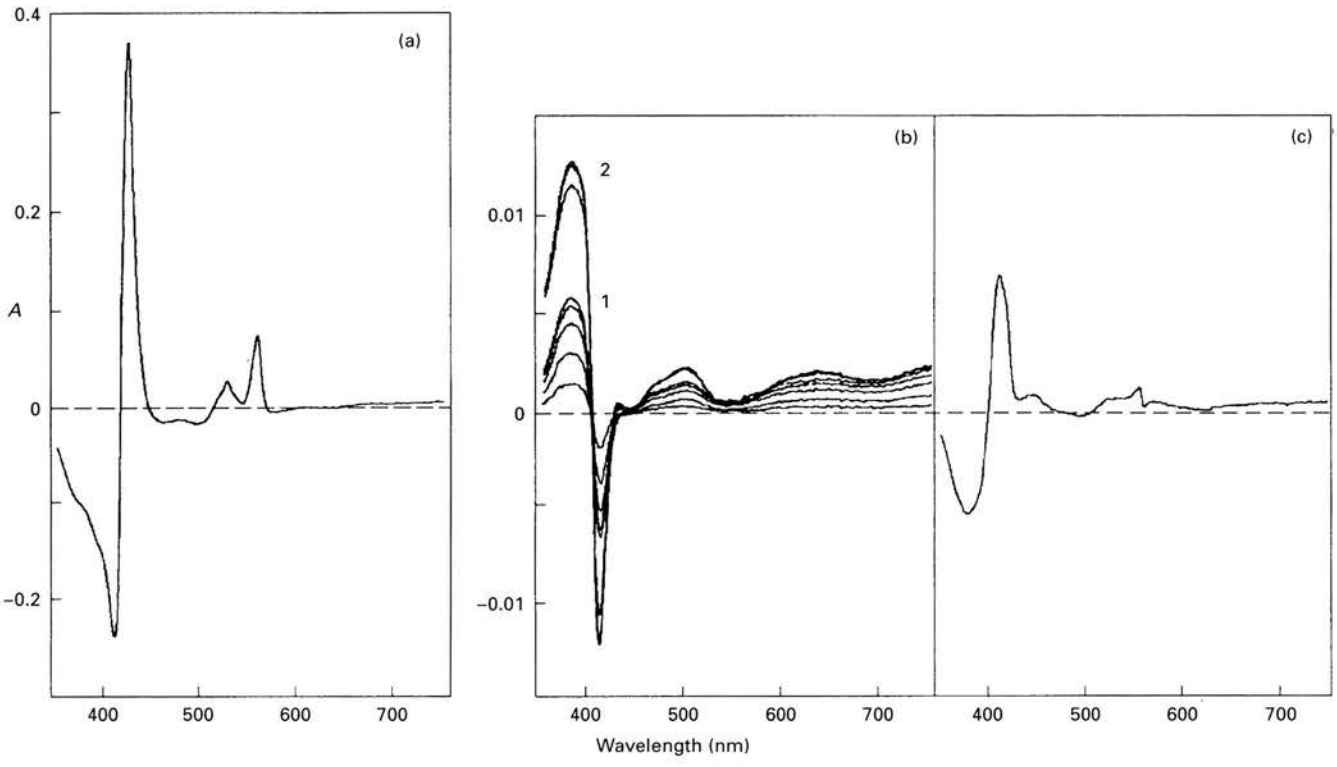

Figure 2 Appearance of a high-spin state after ascorbate reduction of cytochrome *c* peroxidase

A 4 μM solution of cytochrome *c* peroxidase in 5 mM Mes/5 mM Hepes, pH 6, was reduced with 1 mM ascorbate/5 μM DAD. (**a**) shows the difference spectrum of the enzyme 2 min after ascorbate addition minus that of the oxidized enzyme. Ascorbate reduction is complete within 2 min and is followed by the slow appearance of ferric high-spin signals. (**b**) Shows difference spectra with increasing time after ascorbate addition minus that of the enzyme 2 min after ascorbate addition. The high-spin state forms slowly over 30 min in the absence of added Ca^{2+} and reaches an initial end point (1). After addition of 1 mM $CaCl_2$ an enhanced high-spin state (2) forms within 15 min. The high-spin formation is temperature-dependent and can be reversed by cooling on ice. (**c**) Shows the difference spectrum of the ascorbate-reduced high-spin enzyme put on ice for 20 min minus that of the same sample at room temperature.

solution was determined by the pyridine ferrohaemochrome method (ϵ_{550} 29.1 $mM^{-1} \cdot cm^{-1}$) (Morton, 1958).

RESULTS AND DISCUSSION

Haem content and amino acid analysis

The amino acid composition of the *Paracoccus denitrificans* cytochrome *c* peroxidase is shown in Table 1, expressed as mol of amino acid per 2 mol of haem. Summation of this composition yields a relative molecular mass of 39565, in reasonable agreement with the value of 42000 obtained from SDS/PAGE (Goodhew et al., 1990). We conclude that the protein has two haem groups, as observed for the *Pseudomonas aeruginosa* peroxidase (Ellfolk and Soininen, 1970; Soininen et al., 1970).

Optical spectra of oxidized and ascorbate-reduced cytochrome *c* peroxidase

Figure 1 shows optical spectra of the oxidized and ascorbate-reduced peroxidase. The oxidized enzyme has a Soret maximum at 409 nm and possesses a weak absorption band at 640 nm [Figure 1, trace (i)]. The 640 nm signal indicates the presence of a ferric high-spin haem (Moore and Pettigrew, 1990). This signal is also observed in the *Pseudomonas* enzyme, but there is disagreement as to its origin (Ellfolk et al., 1984b; Foote et al., 1984). Reduction of the high-potential haem by ascorbate/DAD is complete within 2 min and results in a shift to 419 nm of the high-potential haem Soret and disappearance of the 640 nm band [Figure 1, trace (ii)]. The shoulder on the u.v. side of the high-potential haem Soret arises from the oxidized low-potential haem. The loss of the 640 nm band suggests that the high-spin signals of the fully oxidized enzyme arise from the high-potential haem. This assignment is in agreement with that of Foote et al. (1984) for the *Pseudomonas* enzyme. If the mixed-valence enzyme is aged for 60 min at room temperature in the presence of 1 mM $CaCl_2$, marked changes are seen to occur in the spectrum [Figure 1, trace (iii)]. The gain of absorbance at 380 nm with concomitant loss at 410 nm represents a blue shift in the Soret of the oxidized low-potential haem, which, in conjunction with the appearance of a band at 640 nm, represents a low-spin to high-spin transition in that haem.

The ascorbate reduction and subsequent spin-state changes can be seen more clearly using difference spectroscopy (Figure 2). At pH 6.0, the different spectrum of the enzyme 2 min after ascorbate addition versus the oxidized enzyme (Figure 2a) shows characteristic features of a reduced low-spin haem with maxima at 419, 525 and 557 nm. Difference spectra, recorded at various times after this, versus the enzyme 2 min after ascorbate addition (Figure 2b), show the slow appearance of ferric high-spin signals with maxima at 380, 500 and 640 nm. The level of high-spin state formed and the time for its formation varies from one enzyme preparation to the next and may be due to different amounts of residual $CaCl_2$ already on the enzyme. (After treatment of oxidized enzyme preparations with EGTA, no formation of the high-spin state is observed after ascorbate reduction.) Addition of 1 mM $CaCl_2$ after the partial high-spin state has formed leads

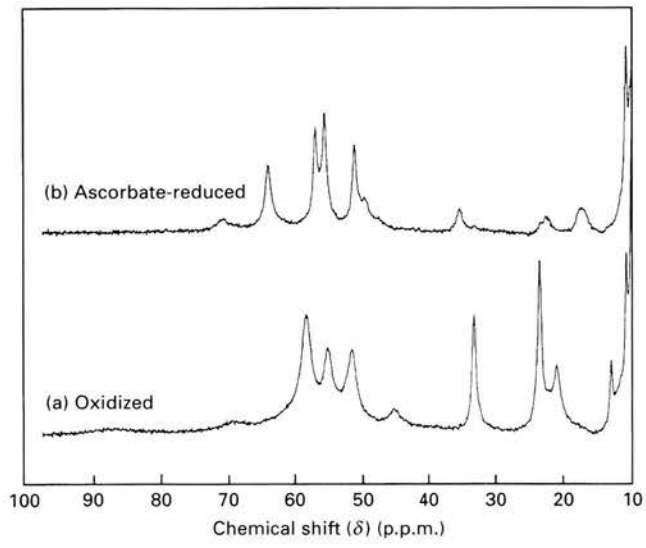

Figure 3 300 MHz ^{1}H n.m.r. spectroscopy of cytochrome *c* peroxidase

Spectra were recorded on a 1 mM sample of enzyme in 10 mM Mes/10 mM Hepes, pH 6 (99.8% ^2H_2O). The temperature was 303 K, and number of scans was 5000. The oxidized spectrum (**a**) was obtained from an untreated peroxidase sample. The ascorbate-reduced spectrum (**b**) was obtained 60 min after addition of 5 mM ascorbate/5 μM DAD.

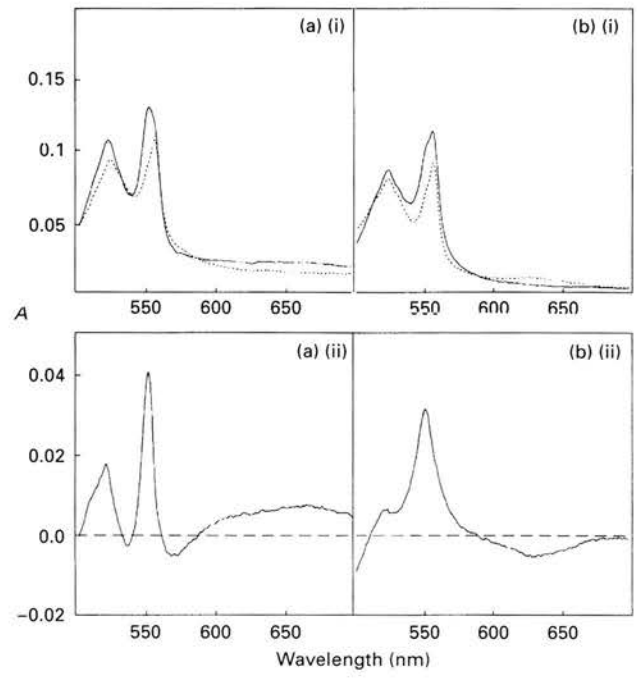

Figure 4 Spectral changes in the low-potential haem after ascorbate reduction of cytochrome *c* peroxidase

Anaerobic solutions of cytochrome *c* peroxidase (4 μM) in 5 mM Mes/5 mM Hepes, pH 7.5, in the absence (**a**) and presence (**b**) of 1 mM $CaCl_2$ were reduced by addition of 1 mM ascorbate and 5 μM DAD. Under these conditions the higher-potential haem is reduced ($HP_{red.}$) and the lower-potential haem remains oxidized ($LP_{ox.}$). This mixed-valence enzyme was incubated at room temperature for 30 min to allow any spin-state changes to occur. Small aliquots of a solution of anaerobic dithionite (50 mM) in 100 mM Mes/100 mM Hepes, pH 7.5, were added until full reduction of the enzyme was obtained ($LP_{red.}HP_{red.}$). The absolute spectra of $LP_{red.}HP_{red.}$ (——) and $LP_{ox.}HP_{red.}$ (----) forms are shown in (**a**)(i) and (**b**)(i). The difference spectra [(**a**)(ii), (**b**)(ii)] of the $LP_{red.}HP_{red.}$ minus $LP_{ox.}HP_{red.}$ is the redox difference spectrum of the low-potential haem and gives information on its spin state.

to an enhancement of the high-spin signals (from 1 to 2 in Figure 2b). The Ca^{2+} effect is rapid and complete within 15 min. The low-spin to high-spin transition can be reversed if the Ca^{2+}-treated, ascorbate-reduced sample is put on ice for 20 min (Figure 2c). Ca^{2+} ions can be replaced by Mg^{2+} ions with similar results being obtained (results not shown). The partial high-spin state in the absence of added Ca^{2+} is not observed at pH 7.5, although addition of 1 mM Ca^{2+} results in the full appearance of the high-spin form. Thus the residual Ca^{2+} on the enzyme seems to be more weakly bound at this higher pH. This convenient property was exploited in obtaining the spectra of Figure 4 (below) and in the redox titrations (Figure 5, below).

300 MHz ^{1}H n.m.r. spectroscopy of cytochrome *c* peroxidase

N.m.r. spectroscopy confirms the presence of a high-spin haem in the fully oxidized and mixed-valence enzyme. The fully oxidized enzyme shows two groups of haem methyl resonances (Figure 3a). The group of strongly downfield-shifted resonances at 58.2 (2 methyls), 55 and 51.5 p.p.m. arise from the partially high-spin, high-potential haem. The high-spin ferric cytochromes *c'* have been shown to have very large downfield-shifted haem methyl resonances, in the region 60–90 p.p.m. (Emptage et al., 1981). The group of resonances at 33.2 and 23.8 p.p.m. arise from the low-spin, low-potential haem. The observation of a broad resonance near 90 p.p.m., which we assign to the ϵ-CH_3 group of an axial methionine, suggests that the partially high-spin haem has methionine–histidine co-ordination.

A spectrum taken 60 min after ascorbate addition shows the disappearance of the signals seen in the oxidized enzyme, with a new set of resonances occurring between 51 and 64 p.p.m. (Figure 3b). The strong downfield shifts of these resonances arise from the oxidized low-potential haem being in a high-spin state.

N.m.r. spectroscopy has been applied to both the *Ps. aeruginosa* and the *Ps. stutzeri* cytochrome *c* peroxidases (Ellfolk et al., 1983, 1984a; Villalain et al., 1984). The results are summarized in Table 2. The fully oxidized enzymes all show two sets of resonances, one set strongly downfield-shifted, representing a high-spin haem, and another set, less shifted and representing a low-spin haem. The ascorbate-reduced enzymes all show a set of strongly downfield-shifted resonances indicative of a high-spin haem.

Ellfolk et al. (1984a) assigned the strongly downfield-shifted resonances seen in the *Ps. aeruginosa* enzyme to the low-potential haem in both the oxidized and ascorbate-reduced states. Villalain et al. (1984) made the same assignments for the *Ps. stutzeri* peroxidase. In contrast, we propose the strongly downfield-shifted resonances of the oxidized *Paracoccus denitrificans* enzyme to be due to the high-potential haem in a high-spin state, whereas the downfield-shifted resonances of the mixed-valence enzyme are those of the high-spin, low-potential haem. This is consistent with m.c.d. spectroscopy of *Ps. aeruginosa* peroxidase, which led Foote et al. (1984) to conclude that, in the fully oxidized enzyme, it was the high-potential haem that was high-spin.

Spectral features of the reduced low-potential haem

Figure 4 shows the effect of fully reducing the enzyme after ascorbate reduction in the presence and absence of Ca^{2+} at pH 7.5.

In the absence of added Ca^{2+}, the fully reduced spectrum has an α- and a β-band at 551 and 525 nm respectively [Figure 4a(i)]. The α-band has a shoulder on the long-wavelength side,

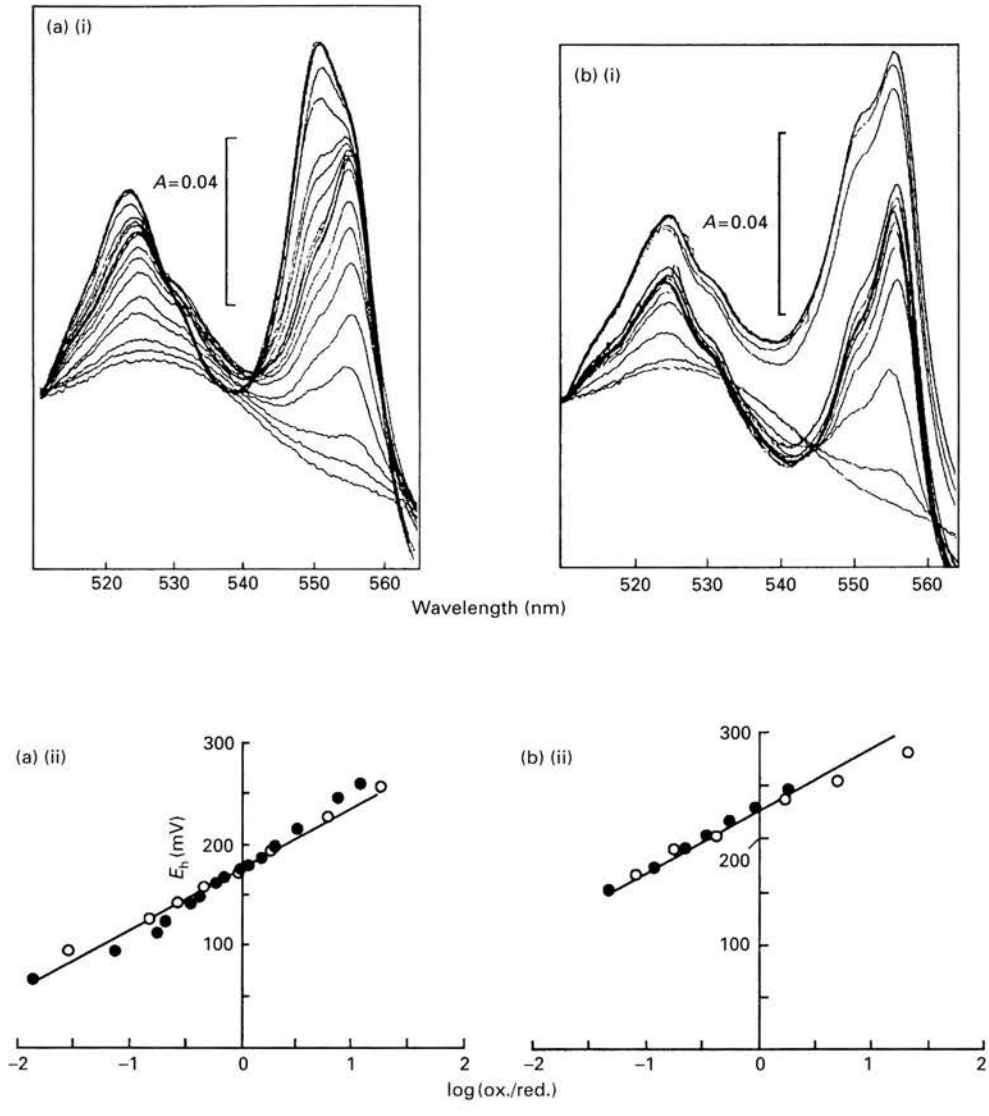

Figure 5 Potentiometric redox titration of cytochrome *c* peroxidase in the absence and presence of Ca^{2+}

The redox titration was performed as described in the Materials and methods section (**a**)(i) and (**b**)(i) show reductive titrations of the peroxidase, as followed in the region of the α- and β-bands, in the absence and presence of Ca^{2+} respectively. (**a**)(ii) and (**b**)(ii) are Nernst analyses of the high-potential component in the absence and presence of Ca^{2+} respectively. Closed circles are for oxidative titration. Open circles are for reductive titration. The pH values measured after titration were 7.35 and 7.32 in (**a**) and (**b**) respectively.

at 557 nm. The spectrum of the reduced low-potential haem can be obtained by subtracting the ascorbate-reduced spectrum from the fully reduced spectrum [Figure 4a(ii)]. This difference spectrum shows fully resolved α- and β-bands, indicative of a ferrous low-spin haem. The absence of a trough at 640 nm shows that the low-potential haem was not high-spin in the ascorbate-reduced enzyme.

In the presence of Ca^{2+}, the fully reduced spectrum has an α- and a β-band at 557 and 525 nm respectively [Figure 4b(i)]. The α-band has a shoulder on the short-wavelength side (551 nm). A fully reduced minus ascorbate-reduced spectrum shows the reduced low-potential haem to have a fused α/β band similar to that seen in ferrous high-spin cytochromes *c'* [Figure 4b(ii)] (Meyer and Kamen, 1982). The trough at 640 nm suggests that this haem was also high-spin in the ascorbate-reduced enzyme.

These results show that the position and shape of the fully reduced α-band of the *Paracoccus* peroxidase is dependent on the spin state of the low-potential haem. In the absence of Ca^{2+}, the fully reduced spectrum (with the low-potential haem in the low-spin state) has an α-band peak at 551 nm with a shoulder on the long-wavelength side. In the presence of Ca^{2+} (with the low-potential haem in the high-spin state) the α-band peak is at 557 nm with a shoulder at 551 nm.

Potentiometric redox titration of cytochrome *c* peroxidase

Oxidative and reductive titrations were carried out in the absence and presence of Ca^{2+} at pH 7.5. The respective reductive titrations are shown in Figure 5(a)(i) and 5(b)(i). In both cases, because of the large separation of midpoint potential (E_m) values, the contribution of a higher-potential haem could be easily separated from that of a lower-potential haem, and, in each case, the high-potential contribution is fitted to a Nernst plot with a slope of 59 mV (25 °C) [Figures 5a(ii) and 5b(ii)].

The redox titration establishes the presence of a high-potential and a low-potential haem as found in the pseudomonad cyto-

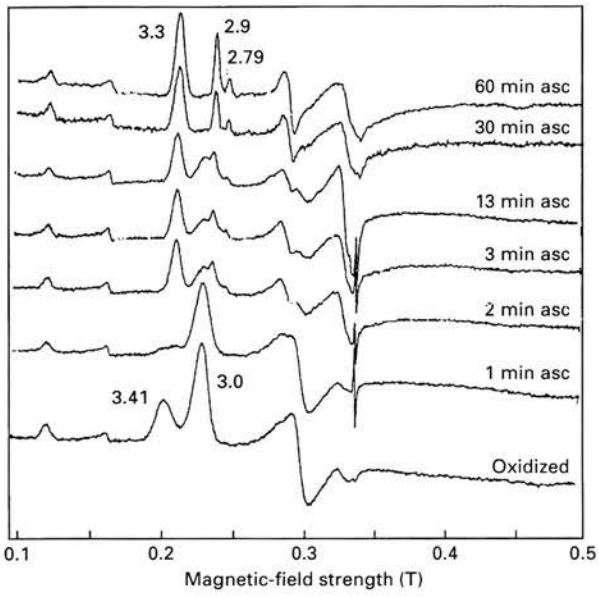

Figure 6 E.p.r. spectroscopy of cytochrome *c* peroxidase

Spectra were recorded from a 337 μM sample of enzyme in 10 mM NaCl/1 mM phosphate, pH 7. The temperature was 8 K, the microwave frequency was 9.45 GHz, the microwave power was 2 mW, the modulation was 10.39 and the gain was 1.6×10^5. The oxidized spectrum was obtained from an untreated sample of enzyme. Ascorbate (asc) was used to obtain the mixed-valence spectrum. *g* values for selected resonances are shown.

chrome *c* peroxidases (Ellfolk et al., 1983; Villalain et al., 1984). The high-potential haem has a midpoint potential of 176 mV in the absence of Ca^{2+} and 226 mV in its presence. The latter value is consistent with an approximately isopotential electron transfer from the proposed electron donor, cytochrome *c*-550 [$E_m = 0.25$ V, pH 7 (Kamen and Vernon, 1955)]. Non-concordance of the midpoint potential of the high-potential haem in the absence and presence of Ca^{2+} may reflect an influence of the spin state of the low-potential haem. When the high-potential haem is titrated in the presence of Ca^{2+}, the low-potential haem is high spin, but in the absence of Ca^{2+} it is low spin.

The low-potential haem was difficult to titrate accurately, with poor reversibility of spectroscopic changes and a midpoint potential in the range -100 to -200 mV. We suspect this difficulty may be due to spin-state changes in this haem during the titration, perhaps as a result of alternative haem ligands being generated from dithionite. The midpoint potentials for the peroxidatic haems of other peroxidases are: *Ps. aeruginosa* peroxidase, -330 mV (Ellfolk et al., 1983); horseradish peroxidase, -270 mV (Harbury, 1957); yeast cytochrome *c* peroxidase, -190 mV (Conroy et al., 1978).

E.p.r. spectroscopy of cytochrome *c* peroxidase

The high-to-low-spin transition seen upon cooling the enzyme from 20 to 0 °C (Figure 2c) means that, when the enzyme is subjected to e.p.r. spectroscopy, carried out at 8 K, very little in the way of high-spin features will be observed. The e.p.r. spectrum of the oxidized enzyme shown in Figure 6 indicates the presence of three spectral components. The signals at $g = 3.41$ and $g = 3.0$ are indicative of two haems in a low-spin state with the signal at $g = 6.0$ representing a minor high-spin component.

The relative intensity of the signal at $g = 3.41$ compared with that at $g = 3.0$ is less than 1. It is therefore possible that the signal at $g = 6.0$ represents a small proportion of the haem with $g = 3.41$ in a high-spin state even at very low temperature.

Ascorbate reduction of the enzyme results in the loss of the $g = 3.41$ signal with initially no change in the $g = 3.0$ signal. From this we conclude that the $g = 3.41$ signal is that of the high-potential haem, whereas the low-potential haem is represented by the $g = 3.0$ signal. This $g = 3.0$ signal disappears over a 60 min period as new spectral features appear at $g = 3.3$ (82%), $g = 2.9$ (16%) and $g = 2.79$ (2%). The alteration in the e.p.r. signal represents a change in the co-ordination structure around the haem. It is this same slow process that, at room temperature, gives rise to the high-spin state of that haem.

Interestingly, an inactive form of the *Ps. aeruginosa* peroxidase has been found in which no ferric high-spin state forms after ascorbate reduction (Foote et al., 1985). This inactive form has a $g = 3$ e.p.r. signal like the transient ascorbate-reduced form of the *Paracoccus* enzyme and may correspond in structure to this form.

A summary of e.p.r. data for the bacterial peroxidases is shown in Table 2. The signals for the individual peroxidases are similar, except for the signal arising from the low-potential haem

Table 2. N.m.r. and e.p.r. data for bacterial cytochrome *c* peroxidases

	Oxidized				Ascorbate-reduced‡		Spin-state assignments				
	High-potential haem		Low-potential haem		Low-potential haem		Oxidized		Ascorbate-reduced		
Organism	N.m.r.*	E.p.r.†	N.m.r.*	E.p.r.†	N.m.r.*	E.p.r.†	HP§ haem	LP‖ haem	HP haem	LP haem	Reference
Ps. aeruginosa	19.5, 21.5 p.p.m.	$g = 3.24$ $g = 3.3$	45–65 p.p.m.	$g = 2.93$ $g = 3.0$	45–65 p.p.m.	$g = 2.84$ $g = 2.85$	Low High	High Low	Low Low	High High	Ellfolk et al. (1984) Foote et al. (1984)
Ps. stutzeri	22.7, 32.0 p.p.m.	$g = 3.39$	69.3, 64.1, 57.3, 55.9 p.p.m.	$g = 3.01$	62.0, 55.9, 55.1, 53.5 p.p.m.	$g = 2.94$	Low	High	Low	High	Villalain et al. (1984)
P. denitrificans	58.2, 55.0, 51.5 p.p.m.	$g = 3.41$	23.8, 33.2 p.p.m.	$g = 3.0$	64.0, 57.0, 55.5, 51.0 p.p.m.	$g = 3.3$	High	Low	Low	High	The present study

* Position of resolved downfield-shifted haem methyl groups.
† $g_{max.}$ values.
‡ Ascorbate-reduced high-potential haem is e.p.r.-invisible and, owing to being much less strongly downfield-shifted, is not resolved in n.m.r.
§ HP, high-potential.
‖ LP, low-potential.

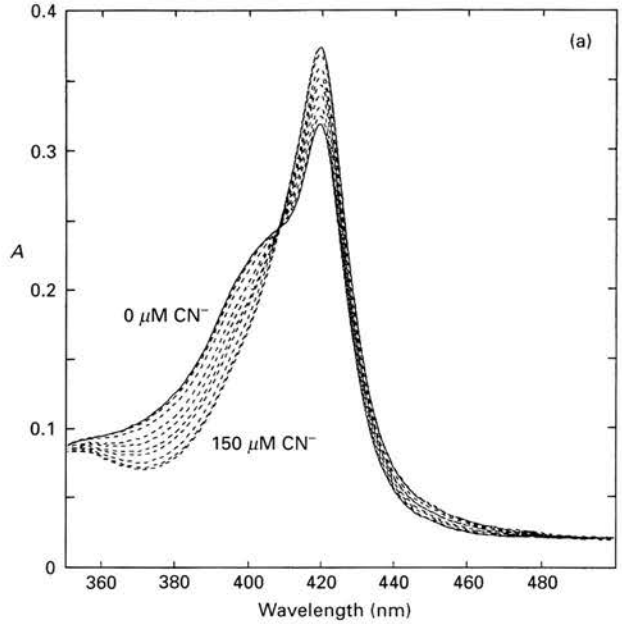

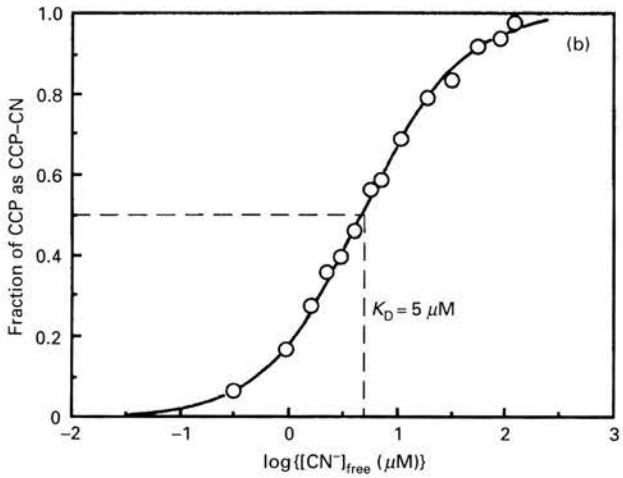

Figure 7 CN^- titration of the ascorbate-reduced form of cytochrome *c* peroxidase

A 1.76 μM solution of cytochrome *c* peroxidase (CCP) in 5 mM Mes/5 mM Hepes (pH 6)/1 mM $CaCl_2$ was reduced with 1 mM ascorbate/5 μM DAD. The sample was aged for 60 min at room temperature to allow formation of the high-spin state. A CN^- titration was performed using a stock neutralized NaCN solution. Selected spectra are shown at the following CN^- concentrations: 0, 0.5, 1.5, 3.5, 6.0, 10.0, 15.0, 40.0, 110.0, 150.0 μM (**a**). The dissociation constant for CN^- binding was calculated using the decrease in absorbance at 380 nm as an indicator of CN bound to the enzyme. (**b**) Shows a plot of CN^--bound peroxidase versus log $[CN^-]_{free}$. The experimental points are fitted to a theoretical curve for the titration of a single binding site with a K_D of 5 μM.

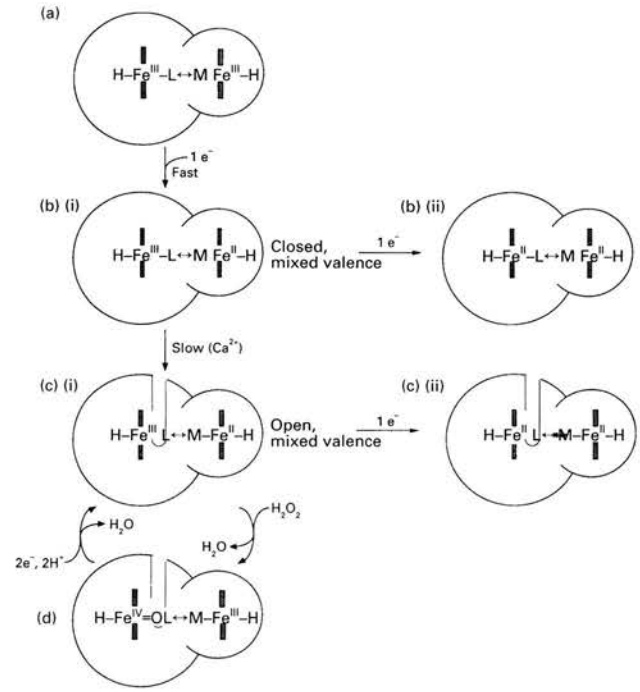

Scheme 1 Model of action for cytochrome *c* peroxidase of *P. denitrificans*

The diagram represents the cytochrome *c* peroxidase as a two-domain dihaem enzyme. We propose that the smaller domain is formed by a class I cytochrome *c* sequence with methionine–histidine co-ordination of one haem. This is based on the amino acid sequence of the *Ps. aeruginosa* enzyme (Ellfolk et al., 1991) and the same class I features are present in the amino acid sequence of the enzyme from *P. denitrificans* (J. van Beeumen, R. Gilmour, C. F. Goodhew and G. W. Pettigrew, unpublished work). In addition, the oxidized form has a weak absorption band at 695 nm indicative of methionine co-ordination (Moore and Pettigrew, 1990). Class I cytochromes tend to have positive redox potentials (Pettigrew and Moore, 1987) and we propose that this domain accepts the incoming electron to the oxidized enzyme (**a**). An intermediate mixed-valence state [(**b**)(i)] is formed in which the low-potential oxidized haem remains low-spin. Reduction of that haem with dithionite results in a low-spin bis-Fe^{II} enzyme [(**b**)(ii)]. In a slow phase, enhanced by Ca^{2+} the intermediate state [(**b**)(i)] is converted into a form [(**c**)(i)] which contains a high-spin low-potential Fe^{III} haem. A channel indicates ligand access to this haem. When this species [(**c**)(i)] is reduced with dithionite, a high-spin Fe^{II} haem is observed [(**c**)(ii)]. The enzyme cycle at the bottom of the diagram has not been studied directly in the present paper and is based on the model of Ellfolk et al. (1983) for the *Pseudomonas* enzyme. It shows the reduction of H_2O_2 using one electron from the methionine–histidine haem and a second from the Fe^{III} of the peroxidatic centre (Ellfolk et al., 1983). Although the amino acid sequence strongly suggests a methionine–histidine co-ordination for the high-potential domain, the co-ordination of the peroxidatic haem is speculative. The distal ligand to the peroxidatic haem (L) is thought to be either a histidine or lysine (Ellfolk et al., 1991). It should be noted that the evidence for the high-potential domain being the methionine–histidine haem is slight, and is based on the knowledge that the class I cytochromes tend to have positive potentials (Pettigrew and Moore, 1987). However, if the methionine is weakly bound, this haem could conceivably be low potential with the bis-histidine haem high potential. Thus an alternative model would have an electron entering the bis-histidine haem as a high-potential haem, followed by a fast switch in haem potentials so that the methionine–histidine haem becomes reduced by internal electron transfer. Such a model would retain the bis-histidine haem as the peroxidatic centre.

of the mixed-valence form of the *Paracoccus* enzyme. The *g*-value of 3.3 is a somewhat higher value than that observed for the other peroxidases.

CN^- titration of cytochrome *c* peroxidase

No change in the spectrum of the oxidized enzyme is observed upon addition of up to 150 μM CN^- (results not shown). This result indicates that the high-spin haem of the fully oxidized enzyme is not available for ligand binding, a result not surprising considering that the high-spin haem in this state is the high-potential, electron-transferring haem. The fully oxidized form of *Ps. aeruginosa* peroxidase is also unable to bind cyanide unless concentrations of over 4 mM are used, at which point reduction of the enzyme is also seen (Ellfolk et al., 1984a).

When the ascorbate-reduced aged enzyme (in 1 mM $CaCl_2$) is titrated with CN^-, marked spectral changes occur, representing a high-to-low-spin transition in the oxidized low-potential haem

(Figure 7a). The decrease in absorbance at 380 nm can be used as a measure of CN^- bound to the peroxidase. The experimental data fit a theoretical saturation curve created for the titration of a single binding site per protein molecule with a dissociation constant of 5 μM (Figure 7b), which is similar to the 23 μM found for the *Ps. aeruginosa* peroxidase (Ellfolk et al., 1984a). The Soret band of the low-potential haem with CN^- bound is more red-shifted than would be expected for a low-spin low-potential haem. This is a result of the CN^- ligation, and has also been observed in the CN^- adducts of *Ps. aeruginosa* (Ellfolk et al., 1984a), horseradish (Keilin and Hartree 1951) and yeast cytochrome *c* peroxidases (Sievers, 1978).

Conclusion

The cytochrome *c* peroxidase of *P. denitrificans* is a dihaem *c*-type cytochrome with high- and low-potential haems. The haems of the fully oxidized enzyme are unavailable for ligand binding, even though the high-potential haem is at least partly high-spin. Ascorbate reduction of the enzyme results in the rapid conversion of the high-potential haem from high-spin into low-spin, followed by a slow conversion of the low-potential haem from low-spin into high-spin. The high-spin formation in the low-potential haem is temperature-dependent and enhanced by the presence of bivalent cations. The high-spin low-potential haem will readily bind added ligands.

The spin state change seen in the high-potential haem when it becomes reduced may play a pivotal role in the haem–haem interaction in this enzyme. The stronger association of the methionine ligand to the reduced high-potential haem may be linked through the protein to the movement of a histidine away from the low-potential haem, ensuring that the substrate will only bind when the enzyme has the reducing power available to carry out the reaction. A model for the proposed activation of the enzyme is shown in Scheme 1. The reaction cycle shown is based upon the model proposed for the *Ps.* peroxidase (Ellfolk et al., 1983).

Received 19 February 1993/4 May 1993; accepted 8 May 1993

This work was supported by a Wellcome Trust Project Grant to G. W. P., a Science and Engineering Research Council studentship to R. G. and the Junta Nacional de Investigacao Cientifica e Tecnologica (grant no. PMCT/C/BIO/885 to I. M.) and grant no. STRDA/CEN/538/2 to J. M.

REFERENCES

Arasio, T., Ronnberg, M., Dunford, H. B. and Ellfolk, N. (1980) FEBS Lett. **118**, 99–102
Conroy, C. W., Tyma, P., Daum, P. H. and Erman, J. E. (1978) Biochim. Biophys. Acta **537**, 62–69
Ellfolk, N. and Soininen, R. (1970) Acta Chem. Scand. **24**, 2126–2136
Ellfolk, N., Ronnberg, M., Aasa, R., Andreasson, L.-E. and Vanngard, T. (1983) Biochim. Biophys. Acta **743**, 23–30
Ellfolk, N., Ronnberg, M., Aasa, R., Andreasson, L.-E. and Vanngard, T. (1984a) Biochim. Biophys. Acta **784**, 62–67
Ellfolk, N., Ronnberg, M., Aasa, R., Vanngard, T. and Ångstrom, J. (1984b) Biochim. Biophys. Acta **791**, 9–14
Ellfolk, N., Ronnberg, M. and Osterlund, K. (1991) Biochim. Biophys. Acta **1080**, 68–77
Emptage, M. H., Xavier, A. V., Wood, J. M., Alsaadi, B. M., Moore, G. R., Pitt, R. C., Williams, R. J. P., Ambler, R. P. and Bartsch, R. G. (1981) Biochemistry **20**, 58–64
Foote, N., Peterson, J., Gadsby, P. M. A., Greenwood, C. and Thomson, A. J. (1984) Biochem. J. **223**, 369–378
Foote, N., Peterson, J., Gadsby, P. M. A., Greenwood, C. and Thomson, A. N. (1985) Biochem. J. **230**, 227–237
Goodhew, C. F., Wilson, I. B. H., Hunter, D. J. B. and Pettigrew, G. W. (1990) Biochem. J. **271**, 707–712
Halliwell, B. and Gutteridge, J. M. C. (1989) Free Radicals in Biology and Medicine, Oxford Science Publications, Oxford
Harbury, H. A. (1957) J. Biol. Chem. **225**, 1009–1023
Kamen, M. D. and Vernon, L. P. (1955) Biochim. Biophys. Acta **17**, 10–22
Keilin, D. and Hartree, E. F. (1951) Biochem. J. **49**, 88–104
Meyer, T. E. and Kamen, M. D. (1982) Adv. Protein Chem. **35**, 105–212
Moore, G. E. and Pettigrew, G. W. (1990) Cytochromes *c* – Evolutionary, Structural and Physicochemical Aspects, Springer-Verlag, Heidelberg
Morton, R. K. (1958) Rev. Pure Appl. Chem. **8**, 161–220
Pettigrew, G. W. (1991) Biochim. Biophys. Acta **1058**, 25–27
Pettigrew, G. W. and Moore, G. E. (1987) Cytochromes *c* – Biological Aspects, Springer-Verlag, Heidelberg
Ronnberg, M., Osterlund, K. and Ellfolk, N. (1980) Biochim. Biophys. Acta **626**, 23–30
Ronnberg, M., Kalkinnen, N. and Ellfolk, N. (1989) FEBS Lett. **250**, 175–178
Sievers, G. (1978) Biochim. Biophys. Acta **536**, 212–225
Soininen, R., Sojonen, H. and Ellfolk, N. (1970) Acta Chem. Scand. **24**, 2314–2320
Villalain, J., Moura, I., Liu, M. C., Payne, W. J., LeGall, J., Xavier, A. V. and Moura, J. J. G. (1984) Eur. J. Biochem. **141**, 305–312